A shoot-derived micro RNA orchestrates root organ formation in response to nitrate

Dissertation

der Mathematisch-Naturwissenschaftlichen Fakultät

der Eberhard Karls Universität Tübingen

zur Erlangung des Grades eines

Doktors der Naturwissenschaften

(Dr. rer. nat.)

vorgelegt von

Moritz Sexauer

Aus Freiburg

Tübingen

2024

Gedruckt mit Genehmigung der Mathematisch-Naturwissenschaftlichen Fakultät der Eberhard Karls Universität Tübingen.

Tag der mündlichen Qualifikation:	02.12.2024
Dekan:	Prof. Dr. Thilo Stehle
1. Berichterstatter/-in:	Prof. Dr. Katharina Markmann
2. Berichterstatter/-in:	Prof. Dr. Klaus Harter
3. Berichterstatter/-in:	Prof. Dr. Martin Parniske

Table of content

Table of Figures

Abstract

In a natural soil environment, nitrogen availability is often limiting and not uniformly distributed. To ensure sufficient nitrogen supply, many seed plants adapt their root system architecture in response to nitrogen availability in the substrate, a process known as foraging response. Nitrogen-dependent root system architectural adaptations are shoot dependent and integrate the systemic nitrogen status of the plant. Similarly, the number of root symbiotic nodules in legumes is regulated according to nitrogen availability in a systemic process called Autoregulation of Nodulation (AON). We show that the shoot derived micro RNA miR2111 and its root expressed target *TOO MUCH LOVE* (*TML*) regulate both bacterial endosymbiosis and nitrogen-dependent root system adaptation. miR2111 acts as a mobile shoot signal translocating to the root in a nitrogen homeostasis-dependent manner to control lateral root initiation. Intriguingly, this miR2111-*TML* node is functionally conserved across plant lineages including the asymbiotic ruderal *Arabidopsis thaliana* and the legume model *Lotus japonicus*, identifying it as an essential, evolutionarily stable factor facilitating shoot dependent adaptation of root organ formation in response to nitrate availability in plants of divergent lifestyles.

Zusammenfassung

In einer natürlichen Bodenumgebung ist die Verfügbarkeit von Stickstoff oft limitiert und das Stickstoffvorkommen nicht gleichmäßig verteilt. Um eine ausreichende Versorgung zu gewährleisten, passen viele Samenpflanzen ihre Wurzelsystemarchitektur als Reaktion auf die lokale Stickstoffverfügbarkeit im Substrat an. Dieser Prozess ist auch als "foraging response" bekannt. Anpassungen des Wurzelsystems an die Verfügbarkeit von Stickstoff im Boden sind sprossabhängig und berücksichtigen den systemischen Stickstoffstatus der Pflanze. In ähnlicher Weise wird die Anzahl der symbiotischen Wurzelknöllchen in Leguminosen in Abhängigkeit von der Stickstoffverfügbarkeit durch einen systemischen Prozess reguliert, der auch als Autoregulation der Nodulation (AON) bezeichnet wird. Wir zeigen, dass die aus dem Spross stammende micro RNA miR2111 und ihr in der Wurzel exprimiertes Ziel *TOO MUCH LOVE* (*TML*) sowohl die bakterielle Endosymbiose als auch die Stickstoffabhängige Anpassung des Wurzelsystems regulieren. miR2111 fungiert hierbei als mobiles Sprosssignal, das in Abhängigkeit von der Stickstoffhomöostase in die Wurzel wandert, um die Bildung von Seitenwurzeln zu steuern. Erstaunlicherweise ist das miR2111-*TML*-Regulon in zweikeimblättrigen Pflanzen funktionell konserviert, so auch in der asymbiotischen Ruderalpflanze *Arabidopsis thaliana* und dem Leguminosen-Model *Lotus japonicus*. Dies identifiziert miR2111-*TML* als zentralen, evolutionär stabilen Faktor bei der sprossabhängigen Anpassung der Wurzelorganbildung als Reaktion auf die Nitratverfügbarkeit in Pflanzen mit unterschiedlichen Lebensweisen.

List of Manuscripts

Publications (peer-reviewed, published)

Moritz Sexauer, Hemal Bhasin, Maria Schoen, Elena Roitsch, Caroline Wall, Ulrike Herzog, Katharina Markmann (2023). A micro RNA mediates shoot control of root branching. Nature Communications 14:8083. doi: 10.1038/s41467-023-43738-6.

Moritz Sexauer, Defeng Shen, Maria Schön, Tonni Grube Andersen, Katharina Markmann (2021). Visualizing polymeric components that define distinct root barriers across plant lineages. Development 148. doi: 10.1242/dev.199820

Review article (peer-reviewed, published)

Marios I Valmas, **Moritz Sexauer**, Katharina Markmann, Daniela Tsikou (2023). Plants recruit peptides and micro RNAs to regulate nutrient acquisition from soil and symbiosis. Plants (Basel) 12:187. doi: 10.3390/plants12010187.

Manuscripts in preparation

Moritz Sexauer, Katharina Markmann (2024). To the roots of nodules: Nodule organogenesis utilizes lateral root development processes.

Participation in publications and manuscripts

Visualizing polymeric components that define distinct root barriers across plant lineages

Moritz Sexauer, Defeng Shen, Tonni G Andersen and Katharina Markmann conceptualized the manuscript. The methodology was established by **Moritz Sexauer** and Maria Schoen as part of her Bachelor thesis, in collaboration with Defeng Shen. **Moritz Sexauer**, Tonni G Andersen and Katharina Markmann wrote the manuscript. Moritz Sexauer prepared figures and acquired microscopy images, with exception of two photon microscopy images (Figure 2C, and Figure 3C,D), and spectral analysis (Figure S8), which was performed by Defeng Shen.

Plants recruit peptides and micro RNAs to regulate nutrient acquisition from soil and symbiosis

Daniela Tsikou conceptualized the manuscript. Marios I. Valmas and **Moritz Sexauer** wrote the original draft. Marios I. Valmas prepared the tables, **Moritz Sexauer** prepared the Figure. Daniela Tsikou and Katharina Markmann reviewed and edited the manuscript.

A micro RNA mediates shoot control of root branching

Katharina Markmann and **Moritz Sexauer** conceptualized and wrote the manuscript. **Moritz Sexauer** prepared all figures, curated and analyzed the data. Experiments presented in this manuscript have been performed by **Moritz Sexauer**, with the following exceptions:

- *Arabidopsis thaliana* lines were generated or isolated by Hemal Bhasin, who contributed to conceptualizing experiments involving *A. thaliana* and performed initial experiments in this species.
- Maria Schoen generated the split root plants.
- Maria Schoen and Elena Roitsch contributed to analysis of lateral root initiations in *Lotus japonicus* and *Arabidopsis thaliana* and to different phenotyping experiments.
- Caroline Wall performed aphid experiments.
- Ulrike Herzog analyzed *pMIR2111*-3:*GUS* lines.

To the roots of nodules: Nodule organogenesis utilizes lateral root development processes

Moritz Sexauer conceptualized the manuscript, wrote the original draft and prepared the figures. Katharina Markmann edited the manuscript and assisted in conceptualizing and writing of the original draft.

Introduction

Among the key inventions of civilization is the Haber-Bosch process, the dominant industrial mode of reducing aerial nitrogen to ammonia. Its invention enabled the production of synthetic nitrogen fertilizer, a crucial element of the "green revolution" aiming to feed a rapidly growing global population. Today roughly half of the world's population is estimated to be "fed" by the Haber-Bosch process (Erisman et al., 2008).

Regardless of its success, the use of Haber-Bosch derived nitrogen fertilizer harbors fundamental problems. Firstly, it tends to have a relatively low use efficiency, and runoff can lead to pollution and eutrophication of nearby waters, threatening biodiversity (Howarth, 2008; Oenema et al., 2009). Secondly, the Haber-Bosch process is very energy intense. It alone accounts for 1,4% of the annual global CO_2 emission, and 1% of global energy consumption (Capdevila-Cortada, 2019).

The implementation of plants able to utilize nitrogen with high efficiency, or to cover their nitrogen demand via root symbiosis, may be one way of reducing global fertilizer demand. So far, many commonly used crop varieties exhibit low nitrogen use or, with respect to legume crops, low fixation efficiency (Phillips, 1980; Liu et al., 2022b). Appropriate breeding strategies to combat these problems will require an understanding of how plants adapt to different nitrogen regimes, and what strategies they have evolved to optimize access to available nitrogen resources.

Nitrogen as a key resource of plant growth

Nitrogen is a macronutrient essential for plant development. Even though plants can use inorganic nitrogen compounds, and the atmosphere mainly consists of nitrogen, plants are not capable of using aerial di-nitrogen directly. Instead, they are limited to nitrogen compounds like nitrate, ammonia or urea (Vidal et al., 2020; Barłóg et al., 2022). Nitrogen is frequently the growth limiting nutrient in natural soil environments, and is extremely unevenly distributed (Jobbágy and Jackson, 2001).

To deal with these limitations, plants have evolved diverse strategies to optimize their nitrogen intake according to their demand and in balance with other nutrients (Vidal

et al., 2020). The two most common forms of bio available nitrogen are ammonia and nitrate. This thesis will focus on the latter (Barłóg et al., 2022).

The earliest adaptation to nitrogen availability in a plant's life might be the nitrate dependent promotion of germination by *NIN LIKE PROTEIN 8* (*NLP8*) (Yan et al., 2016). From germination on, most plants are dependent on nitrate uptake from soil. The uptake of nitrate and its cross-membrane transport inside the plant is achieved by a class of proteins called *NITRATE TRANPORTERs* (*NRTs*). They can be categorized into low, high, and dual affinity *NRTs* (Vidal et al., 2020).

NRT1.1 is a dual affinity *NRT* and can switch from high affinity under low nitrate conditions to low affinity at elevated nitrate supply, depending on its phosphorylation pattern(Liu and Tsay, 2003). To further optimize nitrate uptake, several *NRTs* are regulated by nitrate supply (Vidal et al., 2020).

NRT2.1, a high affinity *NRT* was shown to be regulated by nitrate availability both locally and systemically (Cerezo et al., 2001; Filleur et al., 2001; Ohkubo et al., 2021; Misawa et al., 2022). In addition, *NRT2.1* is regulated by light (Chen et al., 2016).

Apart from the direct regulation of nitrate transporter abundance and affinity, plants are able to regulate nutrient uptake via their root architecture. Plants can promote root growth systemically to enhance the overall root surface area and therefore the zone of nutrient accessibility, also termed the depletion zone (Giehl and von Wirén, 2014). Further, root growth is locally responsive to patches of enhanced nitrate concentrations, enabling the plant to preferentially grow into nitrate-rich soil patches (Oldroyd and Leyser, 2020). Such root adaption in response to nutrient limitation is termed foraging.

However, the most conspicuous adaptation to overcome nitrate limitation has evolved within a plant clade encompassing the dicotyledonous orders Fabales, Fagales, Cucurbitales and Rosales (FaFaCuRo) (Kistner and Parniske, 2002). Some members of the FaFaCuRo have evolved the ability to establish a nitrogen fixing endosymbiosis with bacterial symbionts, which are hosted in root nodules (Griesmann et al., 2018; Roy et al., 2019). Two forms of nitrogen fixing nodulation symbiosis can be distinguished: actinorhiza, a symbiosis between members of the Fagales, Cucurbitales or Rosales with gram-positive Frankia bacteria, and the more specialized rhizobia legume symbiosis

(RLS) (Griesmann et al., 2018) between members of the Fabales with gram-negative rhizobia.

The success of a plants' nitrogen uptake strategy and its overall nitrogen status influences multiple developmental and physiological parameters, such as secondary growth, production of secondary metabolites and, more importantly for agriculture, overall biomass production and yield. This makes nitrogen use efficiency a desired breeding goal (Vidal et al., 2020; Wang et al., 2022).

NRT2.1 – a central node in nitrate uptake

Nitrate supply can affect the expression of several *NRT* genes in *Arabidopsis thaliana* (Arabidopsis). A well-studied example is *NRT2.1* (Asim et al., 2020; Vidal et al., 2020), a high affinity nitrate transporter which is expressed in the root epidermis and is involved in nitrate uptake. *NRT2.1* is accountable for 75 % of high affinity nitrate uptake in Arabidopsis (Asim et al., 2020; Vidal et al., 2020).

In *Lotus japonicus* (Lotus) it was recently shown, that *NRT2.1* expression is directly regulated by *NLP1* in a nitrate-dependent manner (Misawa et al., 2022). Besides this direct regulation, *NRT2.1* is regulated by a systemic feedback loop involving *C-TERMINALLY ENCODED PEPTIDES* (*CEPs*), *CEP DOWNSTREAM* (*CEPD*) and *CEPD LIKE* (*CEPDL*) peptides (Tabata et al., 2014; Ohkubo et al., 2017; Oldroyd and Leyser, 2020; Ota et al., 2020). At the beginning of this feedback loop, *CEPs* are expressed in the root and translocate shootward (Tabata et al., 2014). In *Medicago truncatula*, *CEP* expression was shown to depend on *NLPs* and is negatively regulated by nitrate supply (Luo et al., 2022a). In the Arabidopsis shoot, interaction of *CEPs* and *CEP RECEPTOR 1* (*CEPR1*) activates the expression of *CEPDs* and *CEPDLs* (Ohkubo et al., 2017; Ota et al., 2020). These downstream peptides are mobile too and translocate from shoot to root (Ota et al., 2020). In the root, *CEPD1/2 and CEPDL2* positively regulate *NRT2.1* expression (Ota et al., 2020). Besides the transcriptional activation of *NRT2.1*, *CEPD1/2* and *CEPDL2* induce *CEPD-INDUCED PHOSPHATASE (CEPH)* expression (Ohkubo et al., 2021). CEPH, a type 2C protein phosphatase, activates NRT2.1 post-translationally by dephosphorylation (Ohkubo et al., 2021). In Lotus, *NRT2.1* was shown to be involved in *NLP* signaling, which could close the feedback loop (Misawa et al., 2022). Medicago

COMPACT ROOT ARCHITECTURE 2 (*CRA2*), the putative orthologue of *CEPR1*, can induce expression of *NRT2.1*, in a *CEP1* dependent manner, suggesting that the *CEP/CEPD* pathway might be conserved between dicot lineages (Luo et al., 2022b).

Apart from nitrate dependent regulation, *NRT2.1* transcription is controlled by light via shoot-derived, phloem-mobile transcription factor *ELONGATED HYPOCOTYL 5* (*HY5*) (Chen et al., 2016). Following translocation to the root, *HY5* induces its own expression in a positive feedback loop (Chen et al., 2016). The amplified *HY5* population then further activates *NRT2.1* expression (Chen et al., 2016).

In summary, *NRT2.1* and therefore nitrate uptake underlies a complex network of regulatory mechanisms, involving systemic nitrogen demand and local nitrate availability, but also illumination level translating into carbon (C) availability.

Apart from its role in nitrate uptake, *NRT2.1* also acts in regulating lateral root formation, but its exact function therein is not yet clear (Little et al., 2005; van Gelderen et al., 2021).

Root architecture and development

Angiosperm root architecture is distinct between monocots and dicots. Monocots develop multiple seminal roots (SR) and crown roots (CR), while the PR is often transient and difficult to identify at a later developmental stage (Hochholdinger and Zimmermann, 2008; Atkinson et al., 2014). In contrast, a dicot root system typically consists of a lasting primary root (PR) and lateral roots (LR)s emerging from it, alongside few stem-borne adventitious roots (AR) (Hochholdinger and Zimmermann, 2008; Atkinson et al., 2014). Furthermore, dicot roots show secondary growth and periderm formation, which is absent in monocots (Serra et al., 2022). This work focuses on dicot root systems. Dicot root architecture is mostly determined by PR elongation and LR formation. Three phases of LR formation can be distinguished: initiation, emergence, and elongation. Some authors include priming, which precedes initiation, as a fourth phase (De Smet, 2012; Du and Scheres, 2017a; Laskowski and Ten Tusscher, 2017). Dicot LRs arise from xylem pole pericycle cells (Lavenus et al., 2013).

LR priming determines the competence of so-called LR founder cells for LR initiation (Lavenus et al., 2013; Motte et al., 2019). Priming takes place at pre-branch sites inside the oscillation zone (Motte et al., 2019), in which auxin levels oscillate pre-branch sites

are determined by local auxin maxima (Moreno-Risueno et al., 2010; Hobecker et al., 2017; Motte et al., 2019), where auxin signaling relies on *INDOLE-3-ACETIC ACID INDUCIBLE 28* (*IAA28*) and multiple *AUXIN RESPONSE FACTORs* (*ARFs*). *IAA28* and *ARF5,6,7,8,19* activity leads to a founder cell specific expression of *GATA23* (De Rybel et al., 2010; Lavenus et al., 2013).

LR initiation starts with the asymmetric division of LR founder cells. This depends on polar auxin transport (Lavenus et al., 2013) as well as the transcription factors *LATERAL ORGAN BOUNDARIES DOMAIN16* (*LBD16*)/*ASYMMETRIC LEAVES2-LIKE18* (*ASL18*) and *LBD18*/*ASL20.* The expression of the latter is induced by *IAA14-ARF7-ARF19* dependent auxin signaling (Okushima et al., 2007; Goh et al., 2012; Lavenus et al., 2013). LR initiation in nearby cells is restricted by a pathway involving *TARGET OF LBD SIXTEEN 2*, *RECEPTOR-LIKE KINASE7* and *PUCHI* (Motte et al., 2019; Toyokura et al., 2019).

Further development of the LR primordia involves auxin signaling, and the activity of several transcriptions factor genes: *WUSCHEL-LIKE HOMEOBOX 5* (*WOX5*), *SCARECROW* (*SCR*), *SHORTROOT* (*SHR*) and several *PLETHORAs* (*PLTs*) (Ditengou et al., 2008; Della Rovere et al., 2013; Goh et al., 2016; Du and Scheres, 2017a; Motte et al., 2019). Auxin signaling during primordia outgrowth is regulated by the miR390 and miR390 derived trans-acting small interfering RNAs (tasiRNAs), negative regulators of *ARFs* including *ARF2-4* (Marin et al., 2010).

During LR emergence, primordia grow through the overlaying root cell layers, cortex and epidermis (Péret et al., 2009). The first cell layer that the growing primordium has to pierce is the endodermis, the innermost cortical cell layer which possesses a highly lignified cell wall fraction forming the casparian strip (Geldner, 2013). Primordial piercing of this cell layer is associated with the death of the respective overlaying cell. Cell death is thought to occur as a consequence of deformation and flattening of the overlaying cell and finally a fusion of its membranes, rather than by programmed cell death (Vermeer et al., 2014; Vilches-Barro and Maizel, 2015; Stoeckle et al., 2018). The remaining cortical and epidermal cell layers are less well interconnected than endodermal cells, making them easier to pass for the LR primordia (von Wangenheim et al., 2016; Stoeckle et al., 2018). To cross these cell layers, the primordium pushes apart the overlaying cells and finds a way through the tissue. This is preceded by cell

wall modifications in the overlaying tissue, following auxin dependent induction of cell wall remodeling enzymes (Swarup et al., 2008; Stoeckle et al., 2018).

After emergence, LR growth depends on continuous cell proliferation by the root meristem stem cell niche (SCN), analogous to PR growth (Yamoune et al., 2021).

Root architectural adaptation to nitrogen levels

For many plants, adaptation of root growth in response to nutrient supply was shown (Oldroyd and Leyser, 2020). It has been long known that local supply of the macronutrients phosphate, nitrate or ammonia can lead to a local induction of root growth (DREW, 1975). More recently deficiency in several macro- and micronutrients has been shown to impact root plasticity in Arabidopsis as well (Gruber et al., 2013). These changes in root plasticity have been assumed to depend on internal nutrient status, leading to a systemic root response (Giehl et al., 2013; Giehl and von Wirén, 2014).

Nutrient dependent adaptation of root architecture, also termed nutrient foraging, can be divided into a local and a systemic response, where similar concentrations of a respective nutrient can trigger different root morphological adaptations (Giehl et al., 2013; Giehl and von Wirén, 2014). This thesis focuses on nitrate. Nitrate is alongside ammonia, the most important component of nitrogen fertilizer used in agriculture, furthermore ammonia is reduced to nitrate in soil via a process called nitrification (Ward, 2013).

In a natural soil system, nutrients including nitrate are unevenly distributed (Podlasek et al., 2021). Split root growth systems can be used to simulate such conditions. Local and systemic nitrate responses have been intensively studied in Arabidopsis using split root setups, supplying high and low nitrate concentrations to separate parts of root systems, respectively. In such experiments, both local and systemic effects of nitrate on LR growth can be observed (Ruffel et al., 2011; Guan et al., 2014). Local nitrate supply induces a local promotion and a systemic restriction of LR growth, while partial nitrate starvation systemically promotes LR growth (Ruffel et al., 2011). This implies the existence of both a systemic nitrate demand as well as a systemic nitrate supply signal.

The promotion of LR growth in nitrate-rich soil patches was shown to be at least partially dependent on *ARABIDOPSIS NITRATE REGULATED 1* (*ANR1*) acting downstream of *NRT1.1* (Remans et al., 2006; Guan et al., 2014). Local control of nitrate dependent root growth was shown to depend on *NLP7*, while the systemic foraging response was dependent on *(TCP)-DOMAIN FAMILY PROTEIN 20* (*TCP20*) (Guan et al., 2014; Zhang et al., 2021). Further, *NRT2.1* was shown to restrict LR initiation in a nitrate dependent manner (Little et al., 2005). LR emergence is restricted by *CLAVATA3/EMBRYO SURROUNDING REGION-RELATED* (*CLE*)/*CLAVATA1* (*CLV1*) dependent signaling under nitrate starvation (Araya et al., 2014). Further factors regulating root growth at different nitrate regimes include *BT1/2* or *AGAMOUS-LIKE 44* (*AGL44*) (Giehl and von Wirén, 2014; Liu et al., 2019a).

Different phytohormones are involved in nitrate foraging. The promotion of LR growth under systemic nitrogen demand was shown to depend on cytokinin biosynthesis (Ruffel et al., 2011). Low nitrogen also leads to an accumulation of auxin at LR primordia, promoted by *TRYPTOPHAN AMINOTRANSFERASE RELATED 2* (*TAR2)* and resulting in enhanced LR emergence (Ma et al., 2014). Further, auxin plays a role in nitrate foraging, as *NAC DOMAIN CONTAINING PROTEIN 4* (*NAC4*) regulates LR density downstream of the auxin receptor *AUXIN SIGNALING F-BOX 3* (*AFB3)*. *AFB3* in turn is targeted by the miRNA miR393, which is induced by nitrate metabolites (Vidal et al., 2010; Vidal et al., 2013; Giehl and von Wirén, 2014). Mild nitrogen deficiency also induces brassinosteroid biosynthesis, leading to an activation of *BRI1-EMS-SUPPRESSOR 1* (*BES1*) (Chai et al., 2022). BES1 is then able to interact with the negative regulators of nitrate signaling LBD37/38/39 and prevent them from DNA binding. As a result, nitrogen responsive genes downstream of these transcriptional inhibitors can be activated, leading to LR foraging (Chai et al., 2022).

In legumes, the nitrate receptor *MtNRT1.3* and the transcription factor *MtNLP1* have been shown to be involved in nitrate foraging (Pellizzaro et al., 2014; Lin et al., 2018). Apart from local responses to nitrate availability, split root experiments have demonstrated that systemic factors exist that regulate both *NRT*-mediated uptake of nitrate (Gansel et al., 2001; Ota et al., 2020), as well as root growth responses triggered by nitrogen sufficiency or starvation conditions (Giehl et al., 2013; Gruber et al., 2013; Guan et al., 2014; Oldroyd and Leyser, 2020). Peptide hormones of the

CEPs/CEPDs/CEPDLs and *CLE* groups have been shown to be involved in systemic regulation of nitrate acquisition (Araya et al., 2014; Roberts et al., 2016; Gautrat et al., 2020; Ota et al., 2020). However, systemically mobile nitrogen demand- and -sufficiency signals inducing root architectural responses have yet to be identified (Oldroyd and Leyser, 2020). Both *CEPs/CEPDs/CEPDLs* (Gautrat et al., 2020; Ota et al., 2020; Luo et al., 2021) and *CLE* peptides (Tsikou et al., 2018; Gautrat et al., 2020; Moreau et al., 2021) represent promising candidates, as they are known to be nitrate responsive and involved in systemic signaling processes (Valmas et al., 2023). Apart from peptide signals, miRNAs represent attractive candidate molecules, as they act with a high degree of specificity and are capable of shoot-root mobility through the phloem (Pant et al., 2009; Skopelitis et al., 2018; Tsikou et al., 2018). miR2111, a conserved regulator of the F-box Kelch Repeat gene *TML*/*HOLT* (Tsikou et al., 2018; Okuma et al., 2020), shows nitrogen-dependent abundance shifts and systemically regulates nodulation symbiosis in the legume *Lotus japonicus* (Tsikou et al., 2018; Okuma et al., 2020). In this thesis we show that in addition, miR2111 has a conserved function as a systemic shoot-root signal restricting LR initiation in response to nitrate supply (Sexauer et al., 2023). The role of peptide hormones as well as miR2111 in symbiosis regulation is introduced in more detail below (section miR2111 is the shoot-derived signal in the Autoregulation of Nodulation).

Small RNA dependent gene silencing

RNA silencing is an important mechanism to regulate transcript levels in eukaryotic organisms. In plants, it is best understood in Arabidopsis, and unless stated otherwise the following paragraph will focus on sRNA biogenesis and function as described in this species. RNA silencing is important in many plant developmental processes and crucial for cell identity determination (Carlsbecker et al., 2010). It regulates hormonal responses (Fahlgren et al., 2006) and is a key mechanism in plant antiviral defense (Ding and Voinnet, 2007). Plant small RNA (sRNA) generation depends on *DICER-LIKE* (*DCL*) proteins. In Arabidopsis, four paralogs (*DCL1-DCL4*) exist (Bologna and Voinnet, 2014). The two most important classes of plant sRNAs involved in gene silencing are small interfering (si)RNAs and micro (mi)RNAs (Bologna and Voinnet, 2014).

siRNAs are derived from long dsRNAs of various sources and can be categorized by size. One class of siRNA are 24 nucleotide (nt) long, DCL3-derived siRNAs which are involved

in DNA methylation (Nagano et al., 2014; Xie and Yu, 2015). These siRNAs, which are also called heterochromatic siRNAs, were shown to bind to ARGONAUTE4 (AGO4), *AGO6* and *AGO9* and induce transcriptional gene silencing (Matzke et al., 2015). siRNAs produced by DCL4 and DCL2 are typically 21 nt and 22 nt long, respectively (Bouche et al., 2006; Deleris et al., 2006). In contrast to the majority of their 24 nt long relatives, they are involved in post-transcriptional gene silencing (Bologna and Voinnet, 2014).

Most plant miRNAs are transcribed from their own loci by RNA polymerase II (Lee et al., 2004). The primary transcripts (pri-miRNAs) contain one or multiple RNA stem-loops. During maturation, these pri-miRNAs are processed by *DCL1*, *SERRATE* (*SE*) and *HYPONASTIC LEAVES1* (*HYL1*) in a step where the pri-miRNA loses its 5' cap and polyA-tail and matures into a pre-miRNA (Kurihara et al., 2006; Dong et al., 2008; Achkar et al., 2016). In further *DCL1*-dependent processing, the mature miRNA/miRNA*-duplex is excised from its pre-miRNA stem-loop (Achkar et al., 2016). The miRNA/miRNA* duplex then undergoes 2'-O-methylation at its 3' ends (Yang et al., 2006). This modification is mediated by HUA ENHANCER1 (HEN1) and protects the miRNAs from degradation by exonucleases via poly-U tailing (Li et al., 2005; Yu et al., 2005; Baranauskė et al., 2015; Zhang et al., 2015). In plants, both miRNA transcription and processing are taking place in the nucleus (Achkar et al., 2016). After complete processing, the miRNA is exported from the nucleus into the cytosol, where it can serve its purpose in initiating post-transcriptional gene silencing (Achkar et al., 2016).

In mammalian cells, nuclear export of miRNAs is mediated by *EXPORTIN 5* (Lund et al., 2004). For a long time, it was assumed that the putative plant orthologue of *EXPORTIN 5*, *HASTY,* similarly mediates nuclear export. However more recently, a new model for nuclear export of plant miRNAs was proposed, including miRNA shuttling mediated by *AGO1* (Bologna et al., 2018). Unloaded AGO1 is translocated to the nucleus via its nuclear localization signal, where it can bind mature miRNAs. In its loaded form, AGO1 presents a nuclear export signal, which leads to an export of AGO1 and its bound miRNAs (Bologna et al., 2018).

In the cytosol, miRNAs can be bound by the RNA Induced Silencing Complex (RISC). The RISC consists of an ARGONAUTE (AGO) protein and multiple cofactors (Fang and Qi, 2016). ARGONAUTEs have differential affinity for different sRNAs and therefore mediate distinct biological functions (Liang et al., 2023). ARGONAUTEs selective sRNA

binding is dependent on sRNA length and 5’ nucleotide. AGO4 and AGO6 selectively load 24 nt siRNAs possessing a 5′ adenine (Liu et al., 2022c), while AGO1, AGO2 and AGO5 show affinity for 21nt sRNAs having an uridine (U), adenine (A), and cytosine (C) 5′ nucleotide, respectively(Mi et al., 2008), with AGO5 also being able to bind 22 & 24nt sRNAs (Mi et al., 2008). Recognition of the 5’ nucleotide by AGO1/2/5 was shown to depend on the MID-domain (Frank et al., 2012).

Most miRNAs associate with *AGO1* (Fang and Qi, 2016), where the miRNA guide strand selection is mediated by *HYL1* (Eamens et al., 2009). An active RISC can bind an mRNA possessing a sequence complementary to the miRNA. Silencing is achieved either by cleavage, leading to degradation of the target mRNA, or by translational repression (Brodersen et al., 2008; Fang and Qi, 2016).

In a process called transitivity, a cleaved mRNA can get stabilized at its cleaved ends by SUPPRESSOR OF GENE SILENCING 3 (SGS3) (Mourrain et al., 2000; Fukunaga and Doudna, 2009). RNA DEPENDENT RNAPOLYMERASE 6 (RDR6) is able to bind the stabilized, single stranded RNA and transcribe a complementary RNA strand (Dalmay et al., 2000; Fukunaga and Doudna, 2009). The resulting double stranded RNA gets released and cleaved by DCL4, which produces 21 nt siRNAs (Dunoyer et al., 2005). These secondary siRNAs are called trans-acting siRNAs (tasiRNAs) (Vazquez et al., 2004). tasiRNAs represent a class of secondary sRNAs which are able to silence whole gene families or act as signal amplifiers. However, the production of secondary siRNA, from miRNA target mRNA only rarely occurs in plants and its regulation is only poorly understood (Lu et al., 2005). Recently (Vigh et al., 2022) could show that both *PELOTA1* (*PEL1*) and *SUPERKILLER2* (*SKL2*) restrict generation of secondary siRNAs via distinct mechanisms. The authors propose a long RISC dwell time as a key factor in siRNA generation, and hypothesize that ribosome stalling in *pel1* mutants increases RISC dwell time while degradation of 5′-cleavage fragments by SKI2/3/8-exosome reduces it (Vigh et al., 2022).

One prominent example of tasiRNA generation is *TRANS-ACTING SIRNA3* (*TAS3*) which is targeted by miRNA390 and produces tasiRNAs regulating several *ARF* genes (Marin et al., 2010). *TAS3*-derived tasiRNAs are thus referred to as tasiR-ARFs (Marin et al., 2010).

Small RNA mobility

One important feature of miR390 dependent tasiR-ARFs is their non-cell-autonomous mode of action. tasiR-ARFs are able to move from cell to cell and establish a gradient, crucial for adaxial and abaxial identity (Chitwood et al., 2009). Small RNAs have been shown to be able to move from one cell to another and therefore act in short or long-range signaling (Skopelitis et al., 2018; Maizel et al., 2020; Chen and Rechavi, 2021). The cell-to-cell movement of sRNAs occurs via plasmodesmata (Voinnet, 2005). The exact mechanism of sRNA mobility has not been deciphered yet, however the movement of sRNAs through plasmodesmata seems to be regulated and polar (Skopelitis et al., 2018; Maizel et al., 2020). This polar gating of sRNA movement is independent of protein transport and creates unidirectional transport routes like the phloem, which only allows miRNA efflux, or mobility restricted zones like the quiescent center (QC) (Skopelitis et al., 2018; Maizel et al., 2020). For long-distance travel of sRNAs, plants make use of the phloem (Skopelitis et al., 2018; Li et al., 2021). Phloem sap was shown to be enriched with different species of RNA, including mRNAs and sRNAs (Buhtz et al., 2008; Notaguchi, 2015). In contrast, xylem fluid is devoid of RNA, as a result of which systemically mobile RNAs are predominantly transported from shoot to root (Buhtz et al., 2008; Kehr and Buhtz, 2008; Li et al., 2021). While root-to-shoot transport of mRNAs is weak but traceable, no evidence for a long-distance root to shoot transport of sRNAs has so far been found (Brioudes et al., 2021; Li et al., 2021). The phloem sap contains a multitude of mobile sRNAs (Buhtz et al., 2008; Pant et al., 2008; Pant et al., 2009; Tsikou et al., 2018; Okuma et al., 2020; Li et al., 2021; Valmas et al., 2023). Some of these mobile signals are nutrient responsive, like miR2111 or miR399 (Pant et al., 2008; Pant et al., 2009; Tsikou et al., 2018; Okuma et al., 2020; Valmas et al., 2023).

Movement of sRNA into the phloem from neighboring cell types is restricted, and it therefore seems necessary for a systemically mobile miRNA to be expressed in the phloem (Skopelitis et al., 2018). The mobile miRNA2111, which was shown to travel from shoot to root, is strongly and predominantly expressed in the phloem of leaf veins, which strengthens this hypothesis (Tsikou et al., 2018; Okuma et al., 2020). Unloading of sRNAs from the phloem is not restricted but depends on the LRR-receptor-like kinases *BARELY ANY MERISTEM 1* (*BAM1*) and *BAM2* (Rosas-Diaz et al., 2018; Skopelitis

et al., 2018). *BAM1 & BAM2*, targets of the viral protein C4, were more recently shown to mediate a miR166/165 gradient, which is directed inwards from the endodermis and crucial for correct xylem patterning (Rosas-Diaz et al., 2018; Fan et al., 2021). Expression of viral *C4* in the endodermis is sufficient for a disruption of the miR166 gradient, which results in impaired xylem development (Fan et al., 2021). These results hint at a more general role of *BAM1/2* in sRNA movement and therefore sRNA silencing and would thus explain the function of *C4* as suppressor of (antiviral) silencing (Rosas-Diaz et al., 2018; Fan et al., 2021). Another player involved in both cell-to-cell but also phloem transport of miRNAs is *HASTY* (Brioudes et al., 2021). *HASTY* was shown to regulate the unloading of phloem expressed miRNAs into the surrounding tissue, but also the long-distance transport into the root (Brioudes et al., 2021). Analysis of multiple miRNAs revealed a selective role of *HASTY* in sRNA mobility (Brioudes et al., 2021). Similar to *BAM1/2*, *HASTY* is involved in miR166 movement and xylem patterning (Brioudes et al., 2021). miRNAs and siRNAs are assumed to travel as AGO-free mature duplices in a sequence-independent manner, as it was shown for siRNA that their movement can be restricted by the viral silencing suppressor P19, which specifically binds 21-22 nt long sRNA duplices (Vargason et al., 2003; Devers et al., 2020). The establishment of sRNA gradients along their movement was shown to be dependent on consumption of siRNAs by AGOs in the traversed cells (Devers et al., 2020).

miRNA mobility has been shown to be involved in multiple developmental processes (Benkovics and Timmermans, 2014; Maizel et al., 2020). In some cases, not only translocation but also the concentration gradient of miRNAs is crucial for their function (Benkovics and Timmermans, 2014). One well-studied example is the definition of adaxial and abaxial cell identity in leaf development, which involves two sRNA gradients, namely those of tasiR-ARFs and of miR166 (Kuhlemeier and Timmermans, 2016). Although miRNA390 is expressed throughout the leaf, tasiR-ARF production is restricted to the adaxial leaf side, where *AGO7* and *TAS3A* are expressed (Chitwood et al., 2009). tasiR-ARFs can translocate cell autonomously, and travel to surrounding tissue, which results in a small RNA gradient, declining from adaxial to abaxial side (Chitwood et al., 2009; Benkovics and Timmermans, 2014). The second small RNA gradient involved in leaf polarity concerns miR166a, which is expressed on the abaxial and moves to the adaxial leaf side, creating a gradient inverse to that observed for tasiR-

ARFs (Juarez et al., 2004; Nogueira et al., 2009; Kuhlemeier and Timmermans, 2016). Interestingly, the mRNA targets of tasiR-ARFs and miR166a, *ARF2/3/4* and *CLASS III HOMEODOMAIN LEUCINE-ZIPPER* (*HD-ZIPIII*), respectively, don't show an abundance gradient opposed to that of the respective sRNAs. Instead, they show clear boundaries, defined by an sRNA threshold, a critical sRNA concentration which is sufficient to fully silence a mRNA population (Benkovics and Timmermans, 2014; Kuhlemeier and Timmermans, 2016; Skopelitis et al., 2017). As a result, activity of *HD-ZIPIII* is restricted to the adaxial, and that of *ARF3* to the abaxial leaf side in clear boundaries, assuring correct leaf polarity (Kuhlemeier and Timmermans, 2016; Skopelitis et al., 2017).

Beyond the establishment of leaf polarity, miR166 is involved in the radial symmetry and xylem cell-fate during root development. Again, this is achieved by a miR166 gradient originating from the endodermis, and an inverse *HD-ZIPIII* gradient (Miyashima et al., 2009; Carlsbecker et al., 2010; Benkovics and Timmermans, 2014). Apart from short-ranged miRNA gradients, miRNAs can act as long-range systemic signals. Multiple miRNAs have been proposed as long- or short-range signals in nutrient or symbiotic signaling processes, which we discussed in a review as part of this thesis (Valmas et al., 2023). One prominent example for this is miR2111, which was identified as a systemic activator of rhizobial symbiosis as discussed in detail in this thesis (Tsikou et al., 2018).

The endodermis as a transport barrier

After acquisition of solutes from the soil, a major fraction of these is transported towards the stele for further long-distance transport. The transport towards the stele can be separated into three different modes of transportation, the apoplastic, the symplastic and a coupled trans-cellular pathway (Barberon and Geldner, 2014; Andersen et al., 2015). In the apoplastic pathway, solutes diffuse through the apoplast without being taken up by cells of the traversed tissue. In contrast, in the symplastic pathway, solutes move from cell to cell through plasmodesmata (Barberon and Geldner, 2014; Andersen et al., 2015). The coupled trans-cellular pathway relies on repetitive influx into and efflux from cells in a polarized manner (Barberon and Geldner, 2014; Andersen et al., 2015). However, apoplastic movement of solutes from outer root layers into the central cylinder is restricted by chemical barriers in the endodermal cell walls, which are established as the endodermis, the innermost cortical cell layer, matures (Barberon and Geldner, 2014; Andersen et al., 2015).

Both endodermal and remaining cortex cells are derived of a common pool of cortex/endodermis initials (CEI), which produce CEI daughter cells (CEID) via anticlinal division (Di Mambro et al., 2019). The CEIDs undergo an asymmetric anticlinal division to produce endodermal and cortical cell layers, respectively. This asymmetric division and maintenance of endodermal activity is dependent on the SHR/SCR complex (Helariutta et al., 2000; Nakajima et al., 2001; Long et al., 2015; Di Mambro et al., 2019). The resulting endodermal cell initials undergo further cell divisions, before they start elongating and differentiating (Geldner, 2013). The onset of endodermal differentiation is marked by *MYB36* (*MYB transcription factor 36*) expression, which is induced by SCR/SHR (Liberman et al., 2015). In its undifferentiated state, transport through the endodermis is not restricted. During early differentiation, casparian bands are generated in the endodermal cell walls, blocking apoplastic transport. A second differentiation step involves deposition of a suberin lamella around the endodermal cells, additionally blocking the coupled trans-cellular pathway into the stele (Geldner, 2013; Andersen et al., 2015). The casparian bands deposited during the first differentiation phase span the endodermal cells longitudinally, and mainly consist of lignin (Naseer et al., 2012). The casparian bands grow via continuous lignin deposition until the bands of neighboring cells fuse, forming

the casparian strip, which renders the apoplast largely impenetrable at the endodermis (Geldner, 2013; Fujita et al., 2020). Casparian strip formation is orchestrated by the central transcription factor *MYB36* which induces *CASPARIAN STRIP DOMAIN PROTEINS 1–5* (*CASP1-5*) expression (Roppolo et al., 2011; Kamiya et al., 2015; Emonet and Hay, 2022).

CASPs localize to the site of casparian band formation in dependence of *EXO70A1* (Kalmbach et al., 2017; Emonet and Hay, 2022). Their correct localization is crucial for scaffolding the positioning and fusion of the casparian bands to a continuous casparian strip. Integrity of the casparian strip is assured by the Schengen signaling pathway (Emonet and Hay, 2022). The Schengen pathway, involves the production of CASPARIAN STRIP INTEGRITY FACTORS 1&2 (CIF1/2) in the stele (Doblas et al., 2017b). These are then sulphated by SCHENGEN2 (SGN2), which enables them to diffuse freely through the apoplast (Doblas et al., 2017b; Nakayama et al., 2017; Okuda et al., 2020). Once the casparian strip is closed, CIF1/2 cannot diffuse outside of the stele. If the casparian strip is not closed, CIF1/2 can diffuse towards the cortex and reach the SGN1 / SGN3 complex which is localized on the cortex sided cell walls of the endodermis (Alassimone et al., 2016; Emonet and Hay, 2022). CIF1/2 interaction with the SGN1/3 complex induces the formation of compensatory lignin, closing off the casparian strip (Fujita et al., 2020; Fujita, 2021; Emonet and Hay, 2022).

The second differentiation phase begins with a patchy deposition of suberin around individual cells, forming a secondary cell wall (Naseer et al., 2012; Geldner, 2013). As the endodermis matures, its suberization becomes more uniform, as all endodermal cells suberize with the exception of few cells located in the vicinity of xylem poles, termed passage cells. Suberin is a hydrophobic biopolymer which prevents trans-membrane transport into or out of the apoplast by the respective cell (Andersen et al., 2015; Andersen et al., 2018). Similar to its lignification during the first differentiation phase of the endodermis, suberization is controlled by *MYB* transcription factors (Kamiya et al., 2015; Shukla et al., 2021). So far, *MYB39, MYB41, MYB53, MYB92* and *MYB93* have been found to promote suberin formation (Kosma et al., 2014; Cohen et al., 2020; Wang et al., 2020; Shukla et al., 2021).

Passage cells, which are the only endodermal cells still able to conduct transmembrane transport in the mature stage II endodermis are assumed to play a role in nutrient

uptake (Holbein et al., 2021). Indeed it was shown that the expression of certain transporters like the phosphate efflux protein *PHOSPHATE 1* (*PHO1*) is associated with passage cells (Andersen et al., 2018). So far, a direct transport of nutrients through passage cells has not been shown. Interestingly, suberization itself is modulated by nutritional cues. In Arabidopsis, iron-, manganese- or zinc- deficiency lead to a reduction of suberization, while NaCl stress and potassium or sulfur starvation promotes suberization (Barberon et al., 2016; Barberon, 2017; Namyslov et al., 2020).

In barley, it was shown that nitrogen starvation leads to an increase in suberin deposition (Melino et al., 2021). These findings could imply the regulation of suberin deposition as an adaptation to nutrient availability, to balance uptake capability and stress resistance (Holbein et al., 2021).

Restriction of nutrient flow into the central cylinder might not sound beneficial for the plant, however the endodermal barriers not only restrict nutrient flow but also act as a physical barrier against abiotic and biotic stressors (Andersen et al., 2015; Holbein et al., 2021). In rice, for example, suberization was shown to mediate salt stress resistance (Vishal et al., 2019). In soybean and potato, suberization was associated with enhanced resistance towards pathogens (Lulai and Corsini, 1998; Thomas et al., 2007; Ranathunge et al., 2008; Buskila et al., 2011). However, plant roots are not only exposed to pathogens, but also to beneficial microbes or symbionts. In symbioses like arbuscular mycorrhiza (AM) or the rhizobium legume symbiosis (RLS) the respective symbionts colonize cortex or cortex-derived cells, but not the central cylinder (Oldroyd et al., 2011; Harrison, 2012). This raises the question how the bidirectional nutrient exchange across the differentiated endodermis is achieved during these interactions, and what role passage cells play in this process (Holbein et al., 2021).

Rhizobial symbiosis and early symbiotic signaling

The RLS is the best understood form of root nodulation symbiosis (RNS). RNS involves endosymbiotic associations of plant roots with frankia or rhizobia bacteria, where the microsymbionts fix aerial nitrogen, supplying the plant with ammonia (Roy et al., 2019). Nitrogen fixation takes place in specialized root organs, so-called nodules, which accommodate billions of bacteria. In return for fixed nitrogen, the bacteria are supplied with photosynthates and mineral nutrients (Roy et al., 2019). While AM symbiosis with fungi is ancient and widespread among plants, RNS is only found in certain species within the FaFaCuRo clade (Remy et al., 1994; Parniske, 2008; Griesmann et al., 2018). Notably, only a subset of FaFaCuRo species are able to establish RNS. It is hypothesized that RNS was lost multiple times during evolution, which implies a negative selection bias (Griesmann et al., 2018). This negative selection could be caused by opportunistic bacteria or ineffective regulation of symbiosis, as these factors can quickly turn a mutualistic symbiosis into parasitism (Sachs et al., 2018).

Within the FaFaCuRo, RLS is specific to legumes (Fabales), whereas actinorhiza is established by other members of the clade (Swensen and Benson, 2007; Griesmann et al., 2018). Apart from the bacterial symbionts involved, these two types of RNS differ in the respective infection processes and the structure of nodule organs formed. While actinorhiza plants have gram-positive Frankia bacteria as symbionts, legumes undergo a symbiotic relation with gram-negative rhizobia (MacGregor and Alexander, 1971; Berg, 1999). RLS is established by ecologically diverse, species-rich lineages and includes some agronomically important herbal crops such as soybean or chickpea, whereas actinorhiza is almost exclusively found in trees (Griesmann et al., 2018).

Like AM, RNS is a form of endosymbiosis, implying that the microsymbionts can enter the inside of host cells. Preceding bacterial infection, symbiotic signaling specifically identifies symbiont partners. Legumes secrete flavonoids, which are recognized by compatible rhizobia (Peters et al., 1986; Redmond et al., 1986; Lea et al., 2007). This triggers the production and release of so called Nod factors by the latter (Dénarié and Cullimore, 1993).

These chito-oligosaccharide compounds are specifically recognized by *NOD FACTOR RECEPTORs* (*NFRs*). In *Lotus,* NFR1 & NFR5 form heterodimers to recognize Nod factors of its symbiont *Mesorhizobium loti* (Madsen et al., 2003; Radutoiu et al., 2003). In

Medicago truncatula in contrast *LYSM-CONTAINING RECEPTOR-LIKE KINASE 3* (*LYK3*) and *NOD FACTOR PERCEPTION* (*NFP*) recognize Nod factors of *Synorhizobium meliloti* (Limpens et al., 2003; Arrighi et al., 2006; Smit et al., 2007). The correct pairing of Nod factors and *NFRs* is crucial for the selection of compatible symbiotic partners (Radutoiu et al., 2007). Further, NFR5 was shown to interact with the SYMBIOSIS RECEPTOR KINASE (SYMRK), which belongs to the group of common symbiosis genes, a set of genes involved in both AM and RLS (Stracke et al., 2002; Antolín-Llovera et al., 2014). In Medicago, the *SYMRK* putative orthologue DMI2 was shown to phosphorylate PLANT U-BOX PROTEIN1 (PUB1), which functions in Nod factor discrimination (Mbengue et al., 2010; Vernié et al., 2016). Several *SYMRK INTERACTING PROTEINS* (*SIPs*) have been identified in Lotus, whose knockout mutants were shown to be impaired in nodule development (Zhu et al., 2008; Chen et al., 2012; Yuan et al., 2012). Downstream of Nod factor perception, as well as of Myc factor perception in AM, periodic calcium oscillations ('spiking') can be traced in and around nuclei of epidermal cells (Ehrhardt et al., 1996; Walker et al., 2000; Kanamori et al., 2006; Kosuta et al., 2008; Charpentier and Oldroyd, 2013). A direct role in the generation of calcium spiking has been assigned to the calcium channels *CYCLIC NUCLEOTIDE GATED CHANNELS a/b/c* (*MtCNGC*) (Charpentier and Oldroyd, 2013; Charpentier et al., 2016).

Additionally, *MtDMI1* or its Lotus homologues *LjCASTOR* and *LjPOLLUX h*ave been shown to be crucial for calcium spiking *(Imaizumi-Anraku et al., 2005; Miwa et al., 2006; Charpentier et al., 2008)*. (Kim et al., 2019b) could demonstrate that CASTOR acts as a Ca^{2+}-regulated Ca^{2+} channel in vitro. Further they suggest that all three, *MtDMI1*, *LjCASTOR* and *LjPOLLUX*, primarily act as calcium channels rather than potassium channels (Kim et al., 2019b).

(Liu et al., 2022a) identified the Medicago mutant *spontaneous nodule development 1 (spd1*), to be a gain of function mutant of *DMI1*, which shows calcium spiking in the absence of rhizobia. Interestingly, the expression of the auto active *DMI1* alone was not sufficient for calcium spiking in HEK293 cells but required co expression with *CNGC15b/c* (Liu et al., 2022a).

Further the nucleoporin subunits *LjNUCLEOPORIN85* (*LjNUP85*) and *LjNUP133*, as well as nucleoporin-localized protein *LjNENA* are defective in calcium spiking and the

establishment of RLS or AM symbiosis (Kanamori et al., 2006; Saito et al., 2007; Groth et al., 2010).

The control of calcium influx into the nucleus is essential for the establishment of RLS. Consistently, *brush* a Lotus *CNGC* gain-of-function mutant, expressing a constitutive permeable CNGC complex (Chiasson et al., 2017), showed temperature dependent defects in nodule formation (Maekawa-Yoshikawa et al., 2009).

Calcium spiking leads to phosphorylation of LjCYCLOPS/INTERACTING PROTEIN OF DMI3 (MtIPD3) by the nuclear CALCIUM AND CALMODULIN-DEPENDENT KINASE (LjCCaMK)/DOES NOT MAKE INFECTIONS 3 (MtDMI3) (Gleason et al., 2006; Tirichine et al., 2006; Singh et al., 2014). *LjCYCLOPS/MtDMI3* is a transcription factor regulating the downstream expression of genes involved in infection and nodule organogenesis like *NODULATION SIGNALING PATHWAY1* (*NSP1*) and *NODULE INDUCTION* (*NIN*) (Delaux et al., 2013; Singh et al., 2014). *NIN* plays a key role in RLS establishment. It is sequentially required for infection thread (IT) formation, nodule formation and Autoregulation of Nodulation (AON) (Schauser et al., 1999), as discussed in more detail in (Sexauer and Markmann, 2024) and in the later chapter “Root nodule symbiosis adapted genes from AM and lateral root organogenesis”.

Infection thread formation and nodule organogenesis

Infection of legumes by rhizobial bacteria can be achieved by different mechanisms namely intercellular infection and intracellular infection via infection threads (ITs) (Tsyganova et al., 2021). The most evolutionarily derived and dominant form in terrestrial, herbaceous legumes is the IT-based infection process (Sprent and James, 2007). ITs are tubular, plasma membrane and cell wall lined structures reaching into and traversing the plant cells (Tsyganova et al., 2021).

In response to Nod factor signaling, and in dependence of the genes involved in it, root hairs start to curl around rhizobial microcolonies, forming an infection pocket (Sahlman and Fåhraeus, 1963). Following cell wall remodeling this pocket extends into a tubular IT inside the root hair and progressing towards the root as the bacteria divide (Fournier et al., 2015; Tsyganova et al., 2021). ITs growth is guided by the nucleus and paralleled by active cytoskeleton remodeling (Tsyganova et al., 2021). Correct

arrangement of the actin cytoskeleton has been shown to be crucial for IT formation and progression of intracellular infections (Yokota et al., 2009). In Lotus several members of the SUPPRESSOR OF CAMP RECEPTOR (SCAR)/ WASP FAMILY VERPROLIN HOMOLOGOUS PROTEIN (WAVE) complex, involved in nucleation of actin and cell morphology (Qian et al., 2009), like *NCK-ASSOCIATED PROTEIN 1* (*NAP1*), *121F-SPECIFIC P53 INDUCIBLE RNA* (*PIR1*) and *SCAR-Nodulation* (*SCARN*) have been identified (Yokota et al., 2009; Qiu et al., 2015). Mutants of the *SCAR/WAVE* complex like *nap1*, *pir1* and *scarn* all show reduced numbers of epidermal ITs, only rare cortical IT progression and uncolonized nodules (Yokota et al., 2009; Qiu et al., 2015). Upon reaching the inner host cell wall, cell walls and membranes fuse, releasing the rhizobia into the intercellular space, where growth of a cortical IT can be induced (Dixon, 1964; Fournier et al., 2015). Interestingly, the formation of endodermal and cortical ITs can be genetically uncoupled, as the cytokinin receptor *LOTUS HISTIDIN KINASE1 (LHK1)* is required for cortical, but not for epidermal IT development (Miri et al., 2019).

An additional factor having distinct roles in epidermal and cortical infection is *NIN.* The function of *NIN* can be differentiated between the cell types it is expressed in. In the epidermis, *NIN* mediates IT formation, while its cortical expression in response to cytokinin is required for the induction of nodule formation (Yoro et al., 2014; Liu et al., 2019b). In the cortex, *NIN* recruits various genes known from LR organogenesis or other developmental processes like *LBD16*, *STYLISH* (*STY*), *SHR* & *SCR* which induces cell division and formation of a nodule (Liu et al., 2019b; Schiessl et al., 2019; Soyano et al., 2019; Dong et al., 2020; Shrestha et al., 2021). The role of *NIN* and its downstream signaling in nodule formation is discussed in (Sexauer and Markmann, 2024) in more detail.

Several phytohormones are involved in infection and nodulation. Apart from cytokinin (Reid et al., 2017a; Miri et al., 2019; Lin et al., 2020; Triozzi et al., 2021), auxin plays multiple roles in rhizobial symbiosis (Lin et al., 2020). It was shown that auxin biosynthesis is already induced prior to and during IT formation (Breakspear et al., 2014; Nadzieja et al., 2018; Lin et al., 2020). Expression of *YUCCAS* during nodule organogenesis is important for proper nodule maturation (Schiessl et al., 2019; Lin et al., 2020; Shrestha et al., 2021). In Medicago a knockout of certain *PIN-FORMED* (*PIN*) genes led to a reduction in nodulation (Huo et al., 2006). In Lotus, Medicago and

soybean several *ARFs* were described as regulators of nodulation (Turner et al., 2013; Li et al., 2014; Nizampatnam et al., 2015; Wang et al., 2015; Hobecker et al., 2017). Interestingly, some of these act as positive, some as negative regulators. An example for this in Lotus are tasiR-ARFs targeting *LjARF3A*, *LjARF3B*, and *LjARF4* to induce nodulation (Li et al., 2014), whereas in Medicago tasiR-ARFs target *MtARF2*, *MtARF3* & *MtARF4* leading to a repression of nodulation (Hobecker et al., 2017).

Additionally, the phytohormone ethylene is known as a negative regulator of RLS. Mutants of *ETHYLENE INSENSITIVE 2 (EIN2)* show a "hypernodulation" phenotype, while exogenous application of the ethylene precursor ACC is able to restrict symbiotic signaling as early as calcium spiking (Oldroyd et al., 2001; Penmetsa et al., 2003; Reid et al., 2017b).

Finally, gibberellin biosynthesis is induced during nodule formation, promoting nodule development and restricting nodule numbers via induction of *CLEs* in a *NIN* dependent manner (Kim et al., 2019a; Akamatsu et al., 2021).

miR2111 is the shoot derived signal in the Autoregulation of Nodulation

This chapter includes parts of the following publications:

Marios I Valmas, **Moritz Sexauer**, Katharina Markmann, Daniela Tsikou

> Plants recruit peptides and micro RNAs to regulate nutrient acquisition from soil and symbiosis. Plants (Basel). 2023 Jan 2;12(1):187. doi: 10.3390/plants12010187.

Nodule number and infection is controlled in a systemic process, called the Autoregulation of Nodulation (AON) (Pierce and Bauer, 1983; Li et al., 2022).

AON is a systemic process regulating rhizobial infection and nodule formation in response to rhizobia and nitrate supply, to balance nitrogen demand and carbohydrate as well as mineral nutrient costs (Li et al., 2022). AON involves multiple *CEP* and *CLE* peptides, which are root derived peptides that translocate towards the shoot, where they are assumed to interact with their respective receptor reviewed in (Valmas et al., 2023) as part of this thesis.

In Medicago, accumulation of *MtCEP1,2,12* peptides has been shown to be enhanced under nitrogen starvation as well as upon rhizobial infection (Zhu et al., 2021). *MtCLE35*, *LjCLE-RS2* and *LjCLE-RS3* expression was shown to be induced by nitrate supply and rhizobia (Okamoto et al., 2009; Nishida et al., 2016; Mens et al., 2021; Moreau et al., 2021), while expression of *MtCLE12*, *MtCLE13* and *LjCLE-RS1* positively responded to rhizobia, but was independent of nitrate supply (Okamoto et al., 2009; Mortier et al., 2010; Laffont et al., 2020). Expression analysis revealed that accumulation of *LjCLE-RS1*, *LjCLE-RS2, MtCLE13* and *MtCEP7* transcripts upon rhizobial inoculation was impaired in *nin* mutants (Laffont et al., 2019; Yoro et al., 2020). For *LjCLE-RS2* and *MtCEP1* direct promotor binding by *Lj*NLP4 respectively *Mt*NLP1 was demonstrated (Nishida et al., 2018; Nishida et al., 2021; Luo et al., 2022a). Further, *CLE-ROOT SIGNAL 3* (*CLE-RS3*) expression regulation in response to rhizobial inoculation was shown depend on cytokinin perception by *LHK1 (Miri et al., 2019),* which is involved in local and systemic regulation of rhizobial symbiosis (Murray et al., 2007; Tirichine et al., 2007; Tsikou et al., 2018). For the systemic translocation of CLE-peptides through the xylem and their function in AON, prior tri-arabinosylation is a

prerequisite (Okamoto et al., 2013; Imin et al., 2018; Yoro et al., 2019). For CLE-RS3, this arabinosylation requires *PLENTY* (Yoro et al., 2019). Consistently, *plenty* loss-of-function mutants show enhanced nodule numbers (Yoro et al., 2019).

In the shoot, CLE-RS2 binds to the leucine-rich repeat-RLK HYPERNODULATION ABERRANT ROOT FORMATION1 (HAR1) (Krusell et al., 2002; Okamoto et al., 2009; Okamoto et al., 2013). So far, binding was demonstrated only for CLE-RS2-HAR1, but it is hypothesized that other CLEs likewise act as HAR1 ligands (Okamoto et al., 2013). *HAR1* was described as a negative regulator of symbiosis, with its autoregulatory activity linked the shoot (Krusell et al., 2002; Nishimura et al., 2002; Penmetsa et al., 2003). In contrast to symbiosis-related *CLE* peptides, *CEP* peptides can act as positive symbiosis regulators via a *HAR1* independent pathway that is instead mediated by the LRR-RLK *CRA2* (Mohd-Radzman et al., 2016; Laffont et al., 2019). Downstream of both *HAR1/SUNN* and *CRA2, TOO MUCH LOVE* (*TML*), encoding a Kelch repeat-containing F-box protein, was described as a negative regulator of symbiosis, restricting both infection and nodule formation in the root (Magori et al., 2009; Takahara et al., 2013; Gautrat et al., 2020).

It was proposed that shoot-root signaling downstream of CLE peptide perception by HAR1 and upstream of root *TML*-mediated restriction of infection and nodulation relies on shoot-derived mobile cytokinin (Sasaki et al., 2014). Indeed, the expression of *ISOPENTENYLTRANSFERASE 3* (*IPT3*) was upregulated upon activation of the *CLE-HAR1* signaling node leading to enhanced cytokinin biosynthesis in the leaves (Sasaki et al., 2014). As an essential mediator of specificity in AON shoot-root signaling, (Tsikou et al., 2018) identified the micro RNA miR2111 as a *HAR1*-dependent shoot-root mobile factor directly regulating root *TML* mRNA abundance and thereby systemically controlling symbiotic susceptibility.

miR2111 was shown to be repressed in both shoots and roots upon rhizobial infection (**Figure 1A**), as well as upon nitrate supply (Tsikou et al., 2018). Overexpression of miR2111 leads to an increase in both ITs and nodules (**Figure 1B-E**). As miR2111 targets *TML* mRNA for degradation, *TML* levels are enhanced after rhizobial infection, complementarily to miR2111 expression (**Figure 1F, G**). Using a Short Target Tandem Mimic (STTM) construct, miR2111 levels could be reduced in hairy roots, which resulted in enhanced *TML* levels and fewer nodules (**Figure 1H-J**).

In Lotus, there are seven *MIR2111* loci, three of which are polycistronic, expressing three isoforms of miR2111(a-c). Two loci, *MIR2111-3* and *MIR2111-5*, which are predominantly shoot-expressed, likely account for the bulk of mature miR2111 (Tsikou et al., 2018; Okuma et al., 2020).

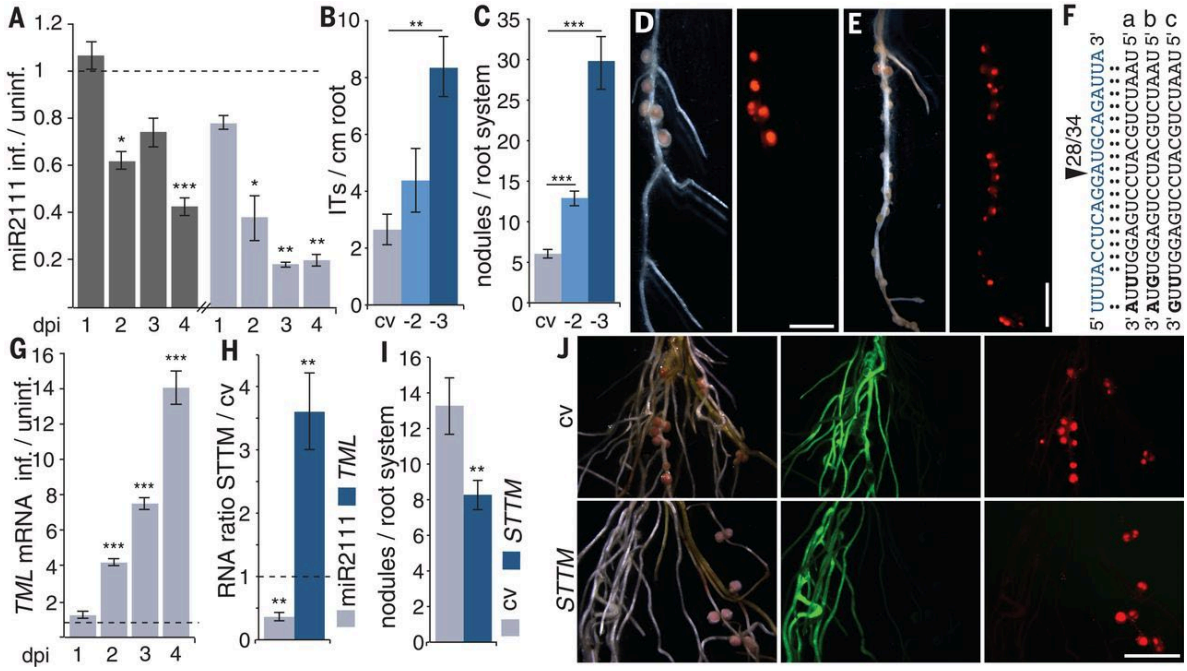

Figure 1. miR2111 regulates *TML* post-transcriptionally (Tsikou et al., 2018). A miR2111 abundance in Lotus leaves (dark bars) and roots (light bars) at 1 to 4 dpi with *M. loti*. Inf., infected; uninf., uninfected. **B** Infection thread (IT) (10 dpi) and **C** nodule (21 dpi) numbers in *pUBQ1:MIR2111-2* (-2) and *pUBQ1:MIR2111-3* (-3) roots compared to control (cv) roots. **D**, **E** Nodulation in control (**D**) and *pUBQ1:MIR2111-3* (**E**) roots (21 dpi). Right-hand panels visualize *M. loti DsRED* in nodules. Scale bars, 2 mm. **F** miR2111 directs *TML* cleavage. Bold font marks polymorphisms between miR2111 isoforms a to c (black). Numbers: degradome 5′ ends at arrowhead/total within *TML* target region (blue). **G** *TML* mRNA in *M. loti*–infected roots (1 to 4 dpi). **H**-**J** *miR2111STTM* (STTM) expression reduced miR2111, increased *TML* (**H**), and reduced nodulation (**I, J**) compared to those in control roots (cv). **I** n = 23/26 (*miR2111STTM* roots/control roots). Green fluorescence (**J**, center) shows co-transformation; red (**J**, right) indicates nodules with *M. loti DsRED*. Scale bar, 5 mm. Transgenic roots (**B-E** & **H**-**J**) were *A. rhizogenes* induced. **A**, **G** & **H** qRT-PCR analyses. RNA levels are relative to those for two reference genes. Dashed lines mark 1 as the reference value in ratio graphs. Error bars (**A**-**C** & **G**-**I**): SEM of at least three biological replicates. Student's t-test P values: *P ≤ 0.05; **P ≤ 0.01; ***P ≤ 0.001.

Using a *pMIR2111-3:GUS* reporter line, expression of mirR2111 from this locus was shown to be specific to the phloem of leaf veins and absent from roots (**Figure 2A-D**). In contrast, *TML* expression was previously shown to be limited to roots (Takahara et al., 2013), suggesting a long-distance transport of miR2111 to enable target regulation. In line with this hypothesis, roots of wild-type plants showed decreased miR2111 and complementarily increased *TML* levels 3 days after mechanical separation from shoots (**Figure 2E**).

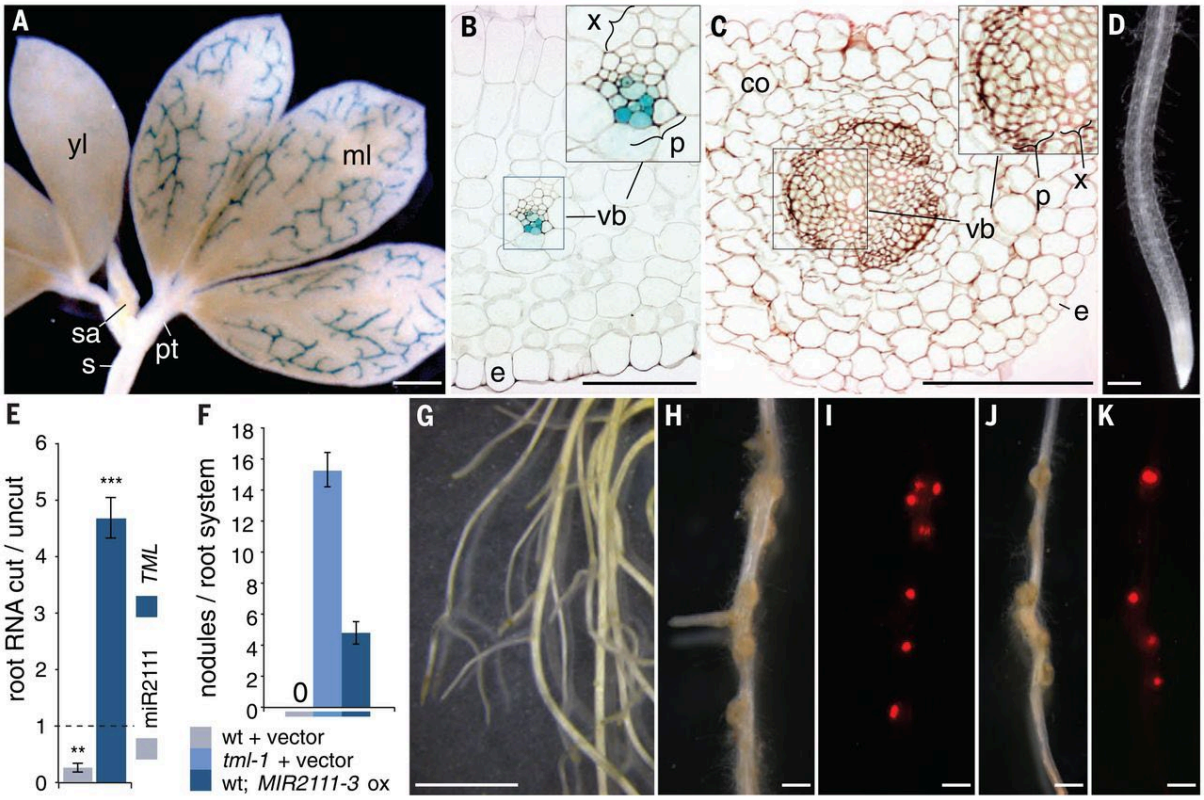

Figure 2. *MIR2111-3* expression and translocation to roots (Tsikou et al., 2018). A-D GUS activity in *pMIR2111-3*:*GUS*–expressing plants (2 weeks). **A**, **B** GUS activity in phloem (p) cells of higher-degree veins of mature leaves (**A**) and cotyledons (**B**). No GUS was detected in leaf xylem (x), shoot apices (sa), petioles (pt), and stems (s) (**A**) or roots (**C**, **D**). Co, cortex; e, epidermis; ml, mature leaflets; vb, vascular bundle; yl, young leaflets. Scale bars, 1 mm (**A**, **D**); 50 μm (**B**, **C**). **E** qRT-PCR analyses of miR2111 and *TML* levels in uninfected roots following root-shoot separation. Error bars: SEM of three biological replicates. $^{**}P \leq 0.01$; $^{***}P \leq 0.001$. **F-K** *TML* loss (**H**, **I**) or *pUBQ1*:*MIR2111-3* expression (**J**, **K**) rescues the asymbiotic phenotype of shoot-less wild-type roots (**G**). Nodule counts (**F**) were at 3 weeks post inoculation with *M. loti* expressing *DsRED* on *A. rhizogenes*–induced wild-type (wt) (**G**) or *tml-1* (**H**, **I**) roots (expressing control vector) and wild-type roots expressing *pUBQ*:*MIR2111-3* (**J**, **K**). **F** Error bars show SEM of two biological replicates (n = 12, 13, and 11 total root systems, respectively). Ox, *pUBQ1*-mediated overexpression. Scale bars, 1 cm (**G**); 1 mm (**H**-**K**).

To test whether the observed *TML* transcript accumulation is sufficient to restrict nodule formation, shoots from *tml-1* or wild-type roots expressing *pUBQ1:MIR2111-3* or an empty vector control, respectively, were removed. After inoculation with *M. loti*, shoot-less roots of *tml-1* or plants overexpressing miR2111 formed several small, infected nodules, while wild-type empty vector control roots remained devoid of nodules (**Figure 2F-K**). This confirms that the presence of shoot derived miR2111 and the coinciding downregulation of *TML* levels is required for nodule formation.

Shoot-root translocation of miR2111 was confirmed using grafting and split root experiments (Okuma et al., 2020; Sexauer et al., 2023). So far it could not be shown in which form miR2111 travels through the phloem, however it is assumed to be the mature miRNA duplex (Skopelitis et al., 2018; Devers et al., 2020; Brioudes et al., 2021). Downregulation of miR2111 upon rhizobial infection was lost in both *lhk1-1* and *har1-1* mutants (**Figure 3A**). Both *lhk1-1* and *har1-1* mutant plants showed increased infection thread numbers, in line with miR2111 deregulation in these lines (Tsikou et al., 2018). Interestingly, downregulation of infection was dependent on *LHK1* dependent cytokinin signaling in the root rather than in the shoot (**Figure 3B**). The dependence of miR2111 abundance regulation on *HAR1* and *LHK1* suggests the involvement of *CLE* peptides upstream of miR2111 regulation and activity. Indeed, infection- and nitrate-dependent downregulation of miR2111 is dependent on *CLE* signaling (Tsikou et al., 2018; Gautrat et al., 2020; Okuma et al., 2020; Moreau et al., 2021).

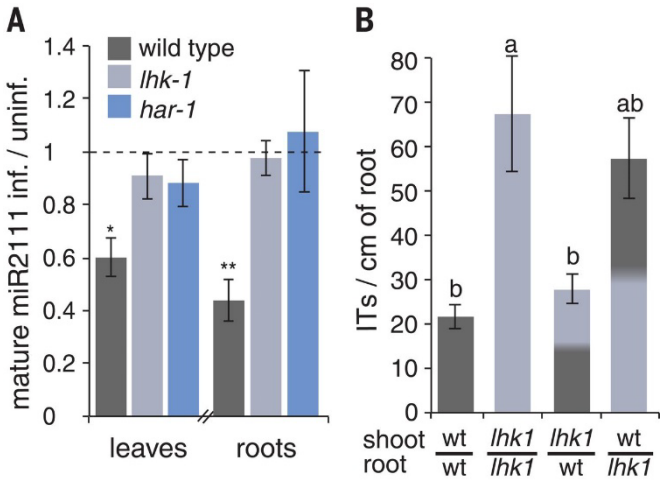

Figure 3. Systemic regulation of miR2111 (Tsikou et al., 2018). A Infection-dependent reduction of mature miR2111 levels in wild-type leaves and roots depends on *HAR1* and *LHK1*. Plants were harvested uninfected or 3 dpi with *M. loti* and were analyzed by qRT-PCR. **B** Infection thread (IT) counts on roots of grafted wild-type, *lhk1-1*, and chimeric plants. n = 3, 5, 6, 8 root systems (left to right). **A**, **B** Error bars show SEM of at least three biological replicates. Comparisons used Student's t test (infected versus uninfected; *P ≤ 0.05, **P ≤ 0.01) (**A**) or analysis of variance (ANOVA) and post hoc Tukey testing (**B**) (P = 0.011), with distinct letters indicating significant differences.

However, expression of miR2111 was shown to not only be regulated by *HAR1/SUNN* (Tsikou et al., 2018; Okuma et al., 2020; Moreau et al., 2021), but also *CRA2* (Gautrat et al., 2020). While *HAR1/SUNN* acts as a negative regulator of miR2111 in response to *CLE* peptides (Tsikou et al., 2018; Okuma et al., 2020; Moreau et al., 2021), *CRA2* functions as a positive regulator and induces miR2111 expression dependent on *CEP* peptides (Gautrat et al., 2020).

Both *CEPs* and *CLEs* involved in the AON are root derived peptides, which are responsive to various biotic and abiotic signals. Most of the peptides involved in AON are shown or assumed to translocate towards the shoot, where they interact with their respective receptor as we reviewed in (Valmas et al., 2023) (**Figure 4A-D**). Together they are proposed to balance miR2111 expression and therefore the amount of symbiosis according to rhizobial infection and nitrogen demand (Gautrat et al., 2020). Not only the initiation and thus number of nodules is negatively regulated by nitrate, but also their development is impaired under nitrate sufficiency (Lin et al., 2021). This process is assumed to be a locally regulated in the roots and depend on *NLPs* and cytokinin biosynthesis (Lin et al., 2021).

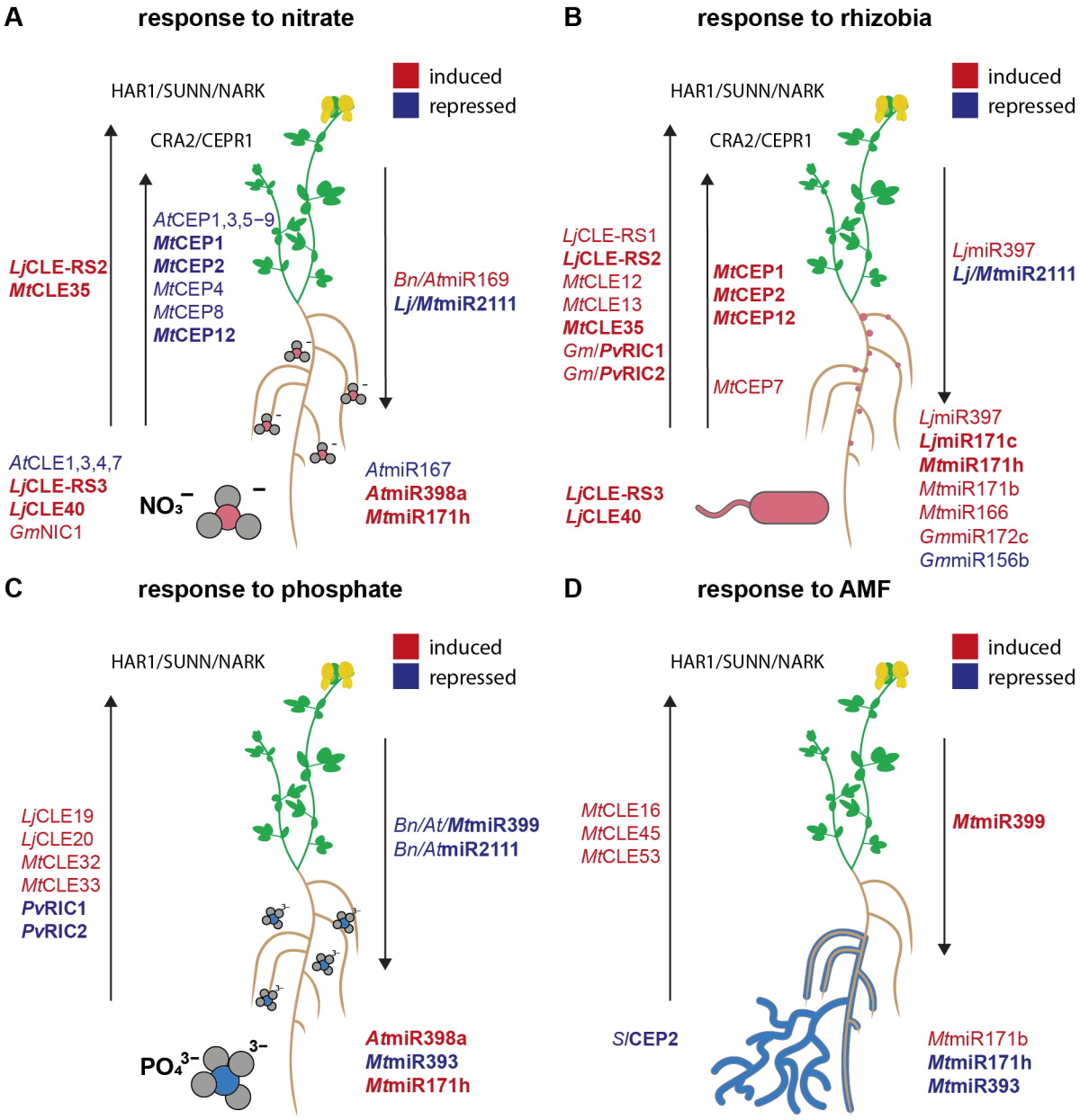

Figure 4. Nutrient homeostasis and acquisition mechanisms involve regulation by peptide hormones and miRNAs (Valmas et al., 2023). *CLE* and *CEP* peptides and miRNAs responding to (**A**) nitrogen availability, (**B**) rhizobia, (**C**) phosphorous availability and (**D**) arbuscular mycorrhizal fungi. Molecules that are induced or repressed by a respective stimulus are displayed in red or blue, respectively. Molecules that are responsive to more than one stimulus are in bold. Arrows indicate shoot-to-root or root-to-shoot translocation of mobile molecules. Specific responses are mediated by the shoot localized leucine-rich repeat receptor-like kinases *HAR1/SUNN/NARK* and *CRA2/CEPR1*. *Lj*, *Lotus japonicus*; *Mt*, *Medicago truncatula*; *At*, *A. thaliana*; *Bn*, *Brassica napus*; *Gm*, *Glycine max*; *Pv*, *Phaseolus vulgaris*; *Sl*, *Solanum lycopersicum*. *NIC*, *NITRATE INDUCED CLE*; *RIC*, *RHIZOBIA INDUCED CLE*

Apart from external nitrate supply, nodulation was shown to be regulated by light availability (Wang et al., 2021). In soybean it was shown that light exposure of the shoot leads to increased nodule numbers in the root compared to shaded plants (Wang et al., 2021). In this context homologs of *HY5* and *FLOWERING LOCUS T* are proposed to act as systemic signals, promoting *NIN* expression dependent on *CCaMK* in roots (Wang et al., 2021).

Interestingly, several mutants impaired in nitrogen fixation have been reported to have elevated nodule numbers (Suganuma et al., 2003; Krusell et al., 2005). The molecular basis for this is yet to be addressed.

In summary, legumes balance the number of nodules they establish according to nitrogen demand and supply as well as their photosynthetic productivity to maintain a beneficial carbon to nitrogen ratio for growth and development. This process requires systemic communication and accordingly involves mobile signals, including both peptides and RNAs. Of these, factors triggered by nitrate and rhizobia are discussed in more detail in (Valmas et al., 2023). The diversity of mobile signals involved in AON reflects the importance of a balanced nodule number, even in a complex soil environment. Interestingly, most of the genes involved in RLS regulation are widely conserved and have known functions in root development, as we reviewed in (Sexauer and Markmann, 2024).

Remarkably, the miR2111-*TML* regulon is conserved in dicot plants, including the non-symbiotic ruderal *Arabidopsis thaliana* (**Figure 5A-C**). In *Arabidopsis* no function of miR2111 and *TML* has yet been described, however miR2111 was already identified in sequencing approaches and shown to accumulate under phosphate starvation (Pant et al., 2009).

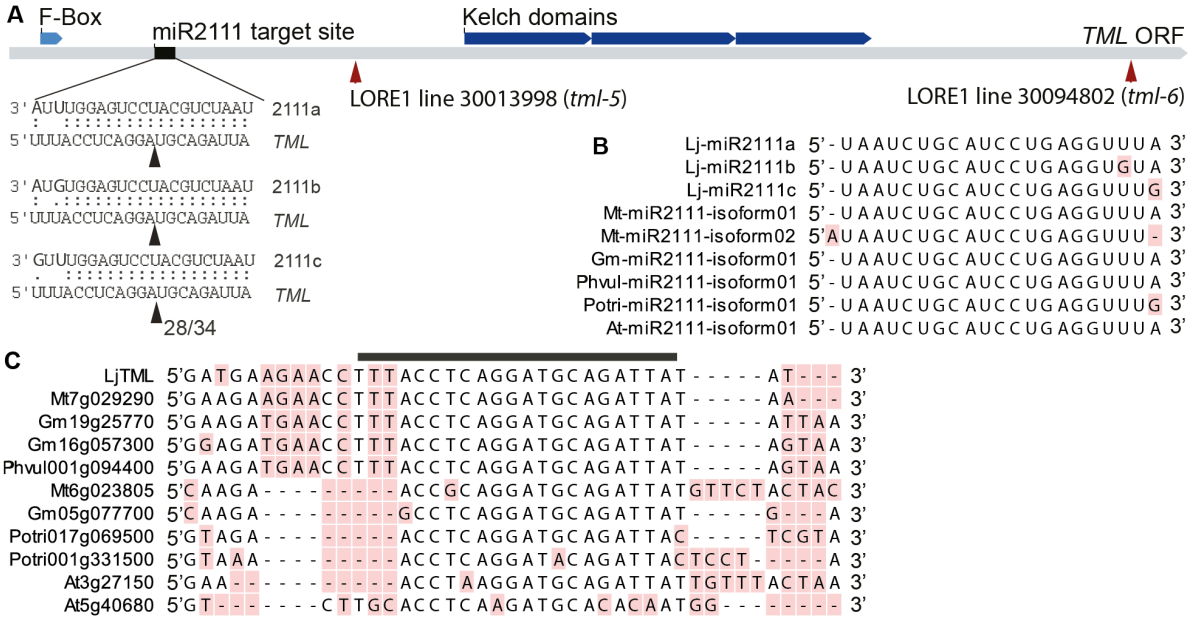

Figure 5 *TML* is a target of miR2111 (Tsikou et al., 2018), modified. **A** miR2111 directs endonucleolytic cleavage of *L. japonicus TML* in vivo. Bold font marks polymorphisms between miR2111 isoforms. Arrowheads: dominant cleavage site, numbers: cleavage events at this site/total degradome 5' ends within miR2111 target region. **B**, **C** Alignment of miR2111 isoforms (**B**) and miR2111 target sites in *TML* gene homologs (**C**, black bar) from selected legume (*Lj*, *Lotus japonicus*; *Mt*, *Medicago truncatula*; *Gm*, *Glycine max*; *Phvul*, *Phaseolus vulgaris*) and other (*Potri*, *Populus trichocarpa*; *At*, *Arabidopsis thaliana*) eudicotylodenous plants. Alignments were done using CLC Main Workbench (Qiagen) software and manually curated. Red background indicates less than 50 % conservation of a particular residue among aligned sequences.

Root nodule symbiosis adapted genes from AM and lateral root organogenesis

This chapter is based on the following manuscript in preparation:

Moritz Sexauer, Katharina Markmann

> To the roots of nodules: Nodule organogenesis utilizes lateral root development processes.

RNS and AM symbiosis share a common set of genes involved in early symbiosis signaling and establishment of endosymbiont accommodation. These dually required genes are referred to as common symbiosis (Common Sym) genes (Kistner and Parniske, 2002; Markmann and Parniske, 2009; Genre and Russo, 2016). Relatively seen, RNS is phylogenetically young and only found in certain members of the FaFaCuRo (Soltis et al., 1995; Griesmann et al., 2018), whereas AM likely arose among the first land plants and is widespread in the plant kingdom. It was thus suggested that during the evolution of RNS, pre-existing symbiosis genes were adapted to mediate the recognition and accommodation of bacterial symbionts in addition to fungal ones. The recruitment of these symbiotic genes from AM can therefore be seen as a key step in evolution of rhizobial symbiosis, allowing intracellular infection (Markmann et al., 2008). The Common Sym genes are active in the early stages of symbiotic signaling immediately downstream of Nod/Myc factor perception, triggering transcriptional responses specific to the respective type of symbiosis mediated by *CYCLOPS* (Yano et al., 2008; Genre and Russo, 2016).

A gene directly regulated by *CYCLOPS* is the transcription factor *NODULE INCEPTION* (*NIN*) which has been intensely studied in legumes (Singh et al., 2014; Lin et al., 2018; Liu et al., 2019b; Schiessl et al., 2019; Akamatsu et al., 2022; Cathebras et al., 2022). *NIN* is dually required for IT formation and nodule organogenesis during rhizobial infection. Interestingly, these functions can be linked to separate regulatory elements in the *NIN* promoter region and sequential, spatially distinct expression activities (Cathebras et al., 2022). IT formation depends on epidermal *NIN* expression (Schauser et al., 1999; Yoro et al., 2014; Akamatsu et al., 2022; Cathebras et al., 2022), whereas nodule organogenesis relies on the cortical and, in case of indetermined nodules, pericyclic expression of *NIN* (Yoro et al., 2014; Liu et al., 2019b).

While *NIN* is not exclusively present in the nitrogen fixing clade, the presence of an intact copy of the gene is crucial for successful RNS formation. Notably, the *NIN* promoter of RNS forming species features a *CYCLOPS* binding element (PACE), which is involved in *NIN* regulation following Nod factor signaling (Griesmann et al., 2018; Cathebras et al., 2022). *NIN* is a homologue of the widely conserved *NLPs*, which in contrast to *NIN* are regulated in a nitrate dependent manner (Suzuki et al., 2013).
NLPs have been described in species of several lineages and shown to be involved in adapting plant growth to nitrate availability, such as root development and architecture (Lin et al., 2018; Zhang et al., 2021), as well as nitrate uptake by regulation of *NRTs* (Zhao et al., 2018; Luo et al., 2022b) and control of nodulation via AON (Lin et al., 2018; Luo et al., 2021; Luo et al., 2022b). Both *NIN* and *NLPs* have further been shown to control the expression of *CLE* and *CEP* peptides, some of which are involved in systemic signaling during AON (Lin et al., 2018; Laffont et al., 2020; Luo et al., 2021; Nishida et al., 2021; Luo et al., 2022a). Besides their function in AON, *CLEs* and *CEPs* are involved in nitrogen foraging, via nitrate uptake control (Araya et al., 2014; Ohkubo et al., 2017; Ota et al., 2020). Interestingly, both these functions appear to be conserved between the asymbiotic Arabidopsis and legumes (Araya et al., 2014; Ohkubo et al., 2017; Ota et al., 2020; Hayashi-Tsugane and Kawaguchi, 2022; Luo et al., 2022b).

Much like during lateral root growth, nodule organogenesis follows a developmental chronology that in its early phase can be divided in the stages of priming, initiation, outgrowth and emergence. Legume root nodules which maintain a persistent apical meristem are termed indeterminate, while determinate nodules only have an active meristem during their early development (Hirsch, 1992). Like LRs, indeterminate nodules emerge from pericycle cells (Xiao et al., 2014), while determinate nodule initiation takes place in the root cortex (Hirsch, 1992). Cytokinin signaling and *NIN* expression precede and accompany nodule primordium initiation in either nodule type and may represent the onset of nodule initiation (Liu et al., 2019b; Miri et al., 2019; Cathebras et al., 2022) (**Figure 6A, B**). Recent transcriptome analyses suggest that during nodule organogenesis, *NIN* recruits various genes associated with lateral root development (Schiessl et al., 2019). This was experimentally verified for the transcription factor *LOB-DOMAIN PROTEIN 16* (*LBD16*)/*ASYMMETRIC LEAVES 2-LIKE 18* (*ASL18*), which is directly regulated by *NIN* through an intronic *NIN* responsive element (Schiessl et al., 2019; Soyano et al., 2019). In Arabidopsis, *LBD16* expression is

induced by *IAA14-ARF7-ARF19* dependent auxin signaling in LR founder cells (Okushima et al., 2007; Goh et al., 2012; Lavenus et al., 2013). The presence of a functional *LBD16* gene is required for both LR and adventious root initiation in this species (Goh et al., 2012; Lee et al., 2019), and was further shown to be involved in the initiation of other root-derived structures such as nematode feeding galls (Liu et al., 2018).

In both Medicago and Lotus, *LBD16/ASL18* was shown to be involved in nodule formation in addition to a conserved role in LR initiation (Schiessl et al., 2019; Soyano et al., 2019). In both legume species, *LBD16/ASL18* expression is enhanced upon infection and can be traced in both early stage LR- and nodule primordia (Schiessl et al., 2019; Soyano et al., 2019). *lbd16* mutants showed reduced and delayed formation of nodule primordia, suggesting a role during initiation of nodules (Schiessl et al., 2019; Soyano et al., 2019). In Lotus, this function was also dependent on *NF-YA* & *NF-YB* , while *LBD16s* function in LR initiation was not (Soyano et al., 2019). Like lateral root development, nodule organogenesis requires and is paralleled by auxin signaling (reviewed in (Du and Scheres, 2017a; Lin et al., 2020). The initiation of lateral roots was intensely studied in Arabidopsis and was shown to involve auxin maxima dependent priming of pericycle cells, which then develop into LR founder cells (De Smet et al., 2007; De Smet, 2012). In these cells, LR initiation can occur via asymmetric anticlinal cell division mediated by *LBD16*/*18* downstream of *ARF7*/*19* (Goh et al., 2012; Lee et al., 2017; Lee et al., 2019). After this initial cell division, the LRP grows by successive periclinal and anticlinal divisions of pericycle-derived cells. Likewise indetermined nodule primordium (NP) development is initiated with anticlinal divisions of the pericycle (Xiao et al., 2014). However, during NP development these are followed by further anticlinal and periclinal divisions in pericycle, inner cortex and the endodermis (Xiao et al., 2014).

The two transcription factors *SHORTROOT* (*SHR*) and *SCARECROW* (*SCR*) mediate the regulation of cell patterning and determination of endodermal identity in Arabidopsis (Helariutta et al., 2000; Nakajima et al., 2001; Cui et al., 2007). Notably, *SCR* is also active in LRPs, where it is proposed to induce periclinal cell divisions (Goh et al., 2016). Its expression focused in the outer layers of LRPs. This expression pattern was a prerequisite for the correct activity of the downstream acting transcription factor

WUSCHEL-RELATED HOMEOBOX 5 (*WOX5*), and specification of the QC during later stages of LRP development (Goh et al., 2016).

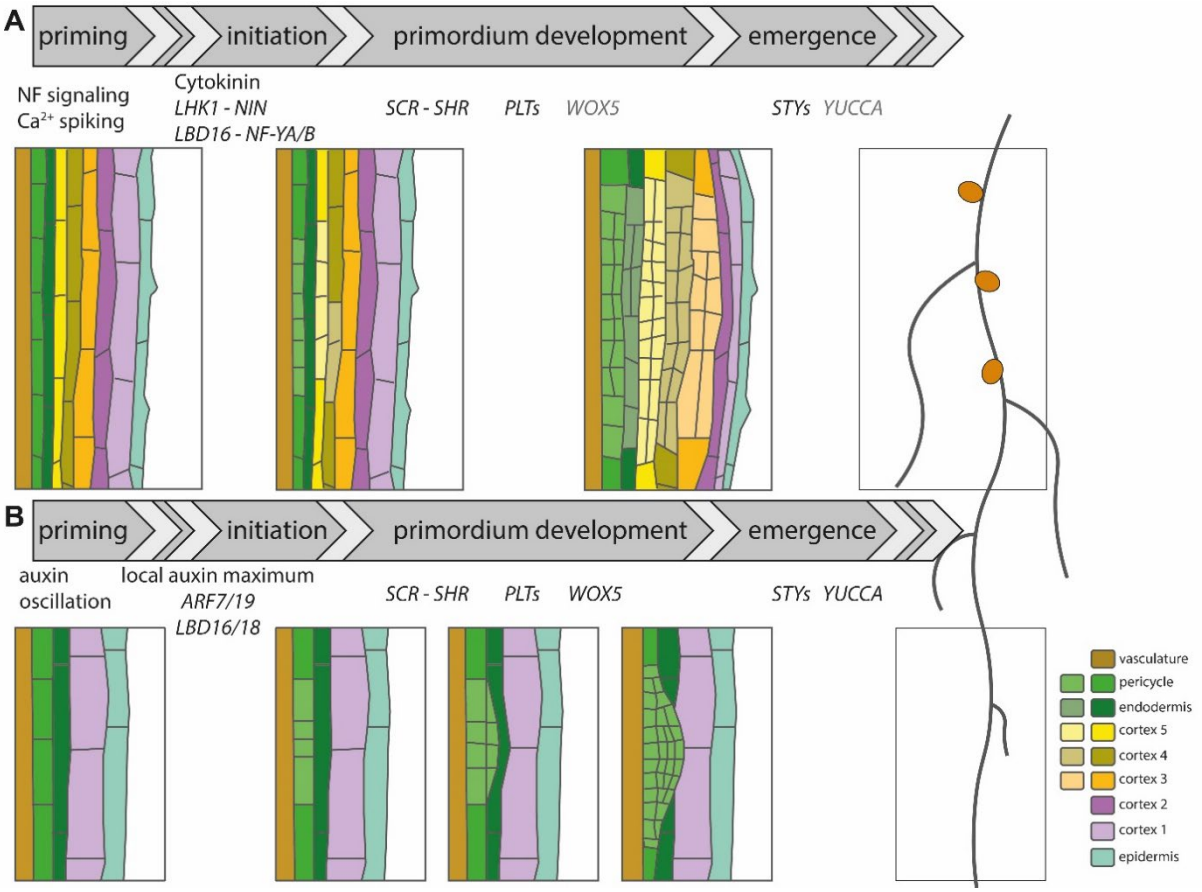

Figure 6 Nodule organogenesis and lateral root formation follow a similar pattern (Sexauer and Markmann, 2024). A scheme of nodule development in Medicago based on (Xiao et al., 2014). **B** scheme of LR development in Arabidopsis based on (Malamy and Benfey, 1997; Du and Scheres, 2017a). **A, B** The first step of both indeterminate nodule (**A**) and lateral root (**B**) organogenesis is priming, a transcriptional reprogramming of the founder cells, prior the first division. **B** In LR organogenesis, priming depends on auxin oscillation and downstream signaling. **A** As for nodule development, nod factor (NF) signaling and downstream Ca^{2+} spiking could be seen as priming step as they lead to transcriptional reprogramming of respective cells. **B** After priming, LR formation continues with *ARF7/19* and downstream *LBD16/18* dependent initiation, marked by the first asymmetric anticlinal division. Initiation is followed by primordial development involving further periclinal and anticlinal divisions. These following divisions and later primordium development depend on *SCR*, *SHR, PLTs* and *WOX5.* **A** Nodule initiation also starts with anticlinal divisions of pericycle cells followed by further divisions of the pericycle and cortex during NP development. **A** Initiation of primordia formation is dependent on cytokinin responsive *NIN* expression and downstream *LBD16* recruitment. *SHR*, *SCR* and *PLTs* appear to be involved during later cortical cell divisions. **A, B** The mature nodule and LR primordium emerge in a *STY* dependent manner. Black genes are placed based on functional data, grey genes are based on their expression and analogy to lateral development.

More recently, the *SHR-SCR* module was shown to mediate nodule organogenesis downstream of *NIN* in Medicago (Dong et al., 2020). The legume specific expression of *SCR* in cortical cells was shown to be crucial for cortical cell division during nodule primordia development (Dong et al., 2020). A role in LRP development in this species has not yet been described, yet *scr-1* mutants showed decreased LR density (Dong et al., 2020). Beyond *SCR*, *PLETHORA* (*PLT*) transcription factors have been shown to be involved in QC definition and maintenance of stem cell identity in the root apical meristem in Arabidopsis (Aida et al., 2004; Shimotohno et al., 2018), and *plt1 plt2* double mutants show abnormal meristem patterning (Aida et al., 2004). These plants formed more lateral roots than wild-type plants, but mutant roots displayed smaller apical meristems (Aida et al., 2004). *plt3 plt5 plt7* triple mutants showed delayed periclinal cell division during LR primordia development, which resulted in abnormal primordium patterning and reduced lateral root density (Du and Scheres, 2017b). Recently it was shown that during root stem cell maintenance, *PLTs* restrict *WOX5* expression to the QC while *WOX5* indirectly promotes *PLT* expression in surrounding cell layers (Burkart et al., 2022).

Differential expression of several *PLT* genes during LR and nodule formation in the legume Medicago (Franssen et al., 2015; Franssen et al., 2017) suggests a dual role in root lateral organ development. Indeed Medicago plants transiently expressing RNAi constructs targeting multiple *PLTs* showed, reduced nodule numbers and impaired nodule development (Franssen et al., 2015). Further, *WOX5* was also shown to be strongly expressed during early stages of Medicago nodule primordia development, however functional data of involvement in nodule formation is still lacking (Osipova et al., 2012).

The last step during both LR and nodule development is the emergence, a step which has been shown to be accompanied by auxin signaling (Ståldal et al., 2012; Singh et al., 2020; Shrestha et al., 2021).

In Arabidopsis, *STYLISH (STYs)/SHORT INTERNODES (SHIs)* regulate auxin biosynthesis (Sohlberg et al., 2006) which was shown for *STY1* to be achieved via YUCCA (*YUC)* induction (Eklund et al., 2010). *LATERAL ROOT PRIMORDIUM1 (LRP1),* a member of the *STY* family, was shown to be involved in lateral root emergence (Singh et al., 2020). In Lotus, plants stably expressing a dominant negative *STY3-SRDX*

(*SUBERMAN REPRESSION DOMAIN X*) (Hiratsu et al., 2003) construct showed a slightly reduced number of nodule primordia and failed to produce mature nodules (Shrestha et al., 2021). Furthermore, Lotus *YUCCA* expression was shown to be partially dependent on *STY3* (Shrestha et al., 2021), indicating a possible role of *STY-YUCCA* signaling in nodule emergence. Functional involvement of *STY3* or other *STY* genes as well as *STY*-dependent auxin signaling via *YUCCAs* in the regulation of lateral roots in legumes appears likely, as *STY* expression was shown for both nodule and LR primordia and plants transiently overexpressing *YUCCAs* show aberrant LR formation (Shrestha et al., 2021). However, a direct involvement of *STY* genes in LR formation in legumes has yet to be established.

Strikingly, the vast majority of previously discussed genes shows induced expression after inoculation with rhizobia, which was dependent on either *SCR*, or *LBD16* downstream of *NIN* (Schiessl et al., 2019; Dong et al., 2020). Transcriptome analysis by (Schiessl et al., 2019) revealed a major overlap of differentially regulated genes in *nin-1* and *lbd16-1* mutants compared to wild-type plants, including *STY, YUC* and *PLT* genes. In addition, cell cycle associated genes display similar regulation patterns in these two mutant backgrounds. These observations allow interesting insights into the subset of *NIN*-dependent genes requiring downstream factors potentially co-involved in RNS and root architecture control. Interestingly, (Dong et al., 2020) proposed a feedforward loop between *SCR* and *LBD16*, as their expression depends on each other.

Comparing the regulation and function of previously discussed genes during both LR and NP development, it appears that *LBD16* acts as a key transcription factor in lateral organ initiation and further recruits a common set of downstream genes involved in lateral organ development (**Figure 7A, B**). The transcriptional regulation of *LBD16*, however seems to differ between both functions, as during LR initiation *LBD16* expression is induced via the auxin dependent *IAA14-ARF7/ARF19* module (Okushima et al., 2007) (**Figure 7A**). During nodule formation *LBD16* expression is controlled via cytokinin induced *NIN* expression (Schiessl et al., 2019; Soyano et al., 2019) (**Figure 7B**). Whether an *ARF7/19* dependent recruitment of *LBD16* is also involved in nodulation is so far unknown.

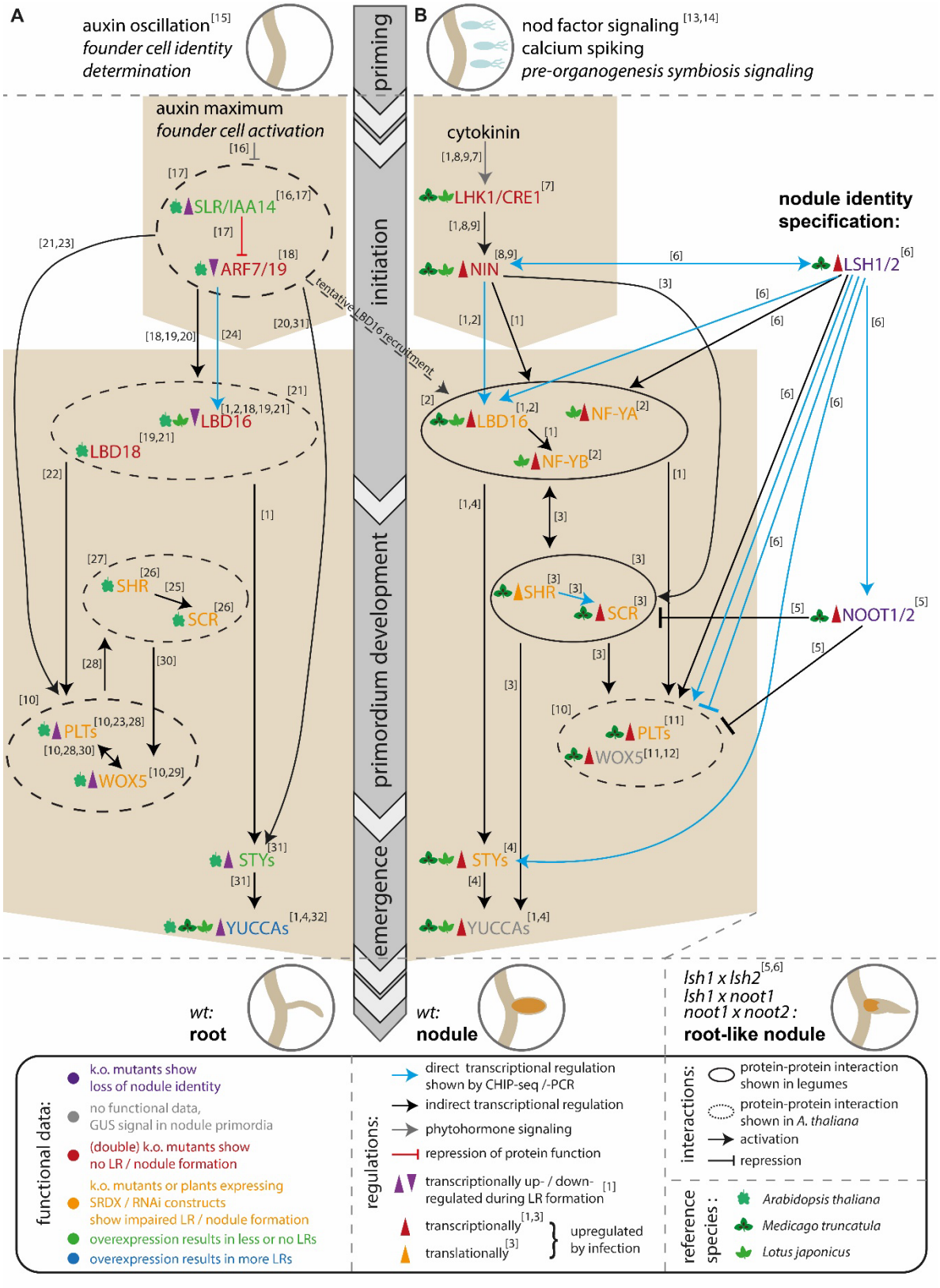

Figure 7 Genetic network involved in nodule and lateral root (LR) formation and nodule identity (Sexauer and Markmann, 2024). A, B schematic representation of dependencies between genes involved in nodule (**A**) and LR (**B**) formation. Circles indicate protein-protein interaction, gene color indicates functional data generated by mutant analysis. Arrows between genes indicate dependencies, colored triangles indicate transcriptional / translational regulation in response to rhizobial inoculation (**A**) or during LR formation (**B**). The Model is

based on data derived from *Medicago truncatula*, *Lotus japonicus* and *Arabidopsis thaliana*. leaves next to genes indicate species, in which analysis took place. Central arrow indicates during which stage of lateral organ formation each gene is active. Pictograms indicate which lateral organ is produced by the genetic network. **A** double knockout (k.o.) of the nodule identity genes *NOOT1/2* and *LSH1/2* leads to formation of root like nodules. Bracketed numbers indicate respective citations: [1](Schiessl et al., 2019),[2] (Soyano et al., 2019),[3](Dong et al., 2020),[4](Shrestha et al., 2021),[5](Magne et al., 2018),[6] (T. Lee et al., 2024),[7](Miri et al., 2019),[8](Yoro et al., 2014),[9](J. Liu et al., 2019),[10](Burkart et al., 2022),[11](Franssen et al., 2015),[12](Osipova et al., 2012),[13](Hayashi et al., 2010),[14](Liu et al., 2022a),[15](Laskowski and Ten Tusscher, 2017),[16](Fukaki et al., 2002),[17](Fukaki et al., 2005),[18](Okushima et al., 2007),[19](Lee et al., 2019),[20](Okushima et al., 2005)[21](Vanneste et al., 2005),[21](Lee et al., 2017)[22](Fan et al., 2012),[23](Hofhuis et al., 2013)[24] (Lavenus et al., 2015),[25](Levesque et al., 2006),[26](Goh et al., 2016),[27](Cui et al., 2007),[28](Du and Scheres, 2017b),[29](Tian et al., 2014),[30](Shimotohno et al., 2018),[31](Singh et al., 2020),[32](Munguía-Rodríguez et al., 2020).

Even though many similarities between lateral root and nodule development exist, they represent distinct organs. Lateral roots and actinorhiza nodules share the most features, as actinorhiza nodules resembling lateral root by both having a central vasculature as well as an apical meristem (Huss-Danell, 1997). Determined and indetermined nodules differ from LRs as they possess a peripheral vasculature and in case of determined nodules lack a persistent meristem (Hirsch, 1992). This raises the question how nodule identity is distinguished from LRs on a genetic basis. In Medicago *MtNODULE ROOT1* (*NOOT1*) and *NOOT2* were described as essential factors for maintaining nodule identity (Magne et al., 2018). Double mutants of *noot1 noot2* showed only few functional nodules, instead a high percentage of the nodules showed a root-like conversion (Magne et al., 2018). More recently in Medicago the expression of *LIGHT SENSITIVE HYPOCOTYL1/2* (*LSH1/2*) was shown to be strongly induced during nodule formation (Lee et al., 2024). (Lee et al., 2024) could further show that overexpression of *LSH1* lead to a reduction in LR numbers, while *lsh1* knockout plants showed less functional, and more deformed nodules than wt, which was at least partially dependent on *NOOT1*. Further they could show that induction of *NOOT1/2* expression upon rhizobial inoculation is impaired in *lsh1/2* mutants (Lee et al., 2024). In both *noot1/2* and *lsh1/2* mutants the expression of *PLTs* among other factors associated with nodule and or lateral root primordia development was deregulated (Magne et al., 2018; Lee et al., 2024). This suggests that *LSH1/2* may act as positive regulators of nodule identity by promoting the expression of *NOOT1/2* and downstream factors like *PLTs* (**Figure 7B**).

Comparing the genetic bases of nodule organogenesis and root branching reveals commonalities consistent with the hypothesis that during RLS evolution, existing genetic pathways of conserved developmental processes were co-opted. This hypothesis is further backed by a recent study which utilizes a comparative phylotranscriptomic approach to identify a set of differentially expressed orthogroups (DEOGs) shared by 9 species of the FaFaCuRo, in response to RLS or actinorhiza (Libourel et al., 2023). These DEOGs are hypothesized to have evolved RNS-dependent expression patterns in the most recent common ancestor of all RNS species (Libourel et al., 2023). Notably, these DEOGs include several genes showing activity patterns depending on AM or LR formation including *SHR*, *LBDs*, *STYs*, *ARFs*, *YUCCAs*, *PLTs* and *WOX* all of which are involved in LR formation (Libourel et al., 2023).

The successful establishment of RNS requires 4 major steps: 1. symbiont recognition 2. intracellular symbiont accommodation 3. lateral organ formation 4. autoregulation of nodulation. Taken together, it appears that during evolution of RNS, plants adapted genes for symbiont recognition and intracellular infection from AM (Markmann et al., 2008; Libourel et al., 2023), and further co-opted genes involved in LR development to establish a new lateral organ, the nodule (Schiessl et al., 2019; Libourel et al., 2023).

Regarding the 4. major step, the AON, a genetic basis was so far not discussed. However, many of the factors involved in AON show conserved functions involved in nitrate homeostasis. As the *CEP-CEPR1/CRA2* module is involved in regulation of nitrate uptake via *NRT2.1* (Ota et al., 2020; Luo et al., 2022b). While *CLV1*, the putative *HAR1* orthologue was proposed to steer local root adaptation to nitrate availability (Araya et al., 2014).

So far, miR2111 and its target *TML* have only be functionally characterized in the context of nodulation. Their wide conservation among dicots (Tsikou et al., 2018), however hints to an additional conserved function, which we hypothesize might also be associated with nitrogen homeostasis.

Aims

Previously, we identified miR2111 as a shoot derived signal regulating the nodule numbers and infection process in *Lotus japonicus.*

The wide conservation of the miR2111-*TML* regulon in dicot plants, including non-symbiotic species, suggests a conserved function of this node apart from its role in the Autoregulation of Nodulation. In this thesis we aim to unravel the non-symbiotic function of the miR2111-*TML* regulon.

We further want to decipher whether miR2111-*TML* has a function which is conserved between non-symbiotic plants and legumes.

For this we choose *Lotus japonicus*, a model legume species for RLS, where *TML* was first described and *Arabidopsis thaliana* as a non-symbiotic model organism for physiological experiments, utilizing a series of knockout mutant or overexpression lines.

Based on the previously described genetic overlaps between LR organogenesis and nodule development as well as nitrate homeostasis and AON, we hypothesized that miR2111-*TML* might be involved in adaptation of root traits to nitrogen availability. Along this line, we focused our work on root developmental traits such as root architecture or cell wall modifications.

An important aim is to determine whether AON-independent functions of the miR2111-*TML* node equally rely on systemic mobility of miR2111, and whether miR2111 might represent a postulated, so far unidentified morphogenic signal in systemic nitrate foraging.

Finally, we want to compare the role of the miR2111-*TML*/*HOLT* regulon in different plant lineages in order to understand its phylogenetic conservation and functional adaptation.

Results and Discussion

miR2111 mediates shoot control of root foraging.

This chapter is based on the following submitted manuscript and contains its main figures and selected supplementary figures:

Moritz Sexauer, Hemal Bhasin, Maria Schoen, Elena Roitsch, Caroline Wall, Ulrike Herzog, Katharina Markmann.

A micro RNA mediates shoot control of root branching

Nature Communications (2023), 14, 8083. doi:10.1038/s41467-023-43738-6

Remaining supplementary figures are attached in the manuscript in Appendix 3.4.
In addition, the chapter contains unpublished data, that were prepared by the author of this thesis.

To investigate whether miR2111 indeed has an impact on Lotus root architecture, we generated and characterized Lotus plants expressing a *pUBQ1:MIR2111-3* transgene (**Figure 8A-F**) resulting in overabundance of mature miR2111 (**Figure 8A**). Indeed, *pUBQ1:MIR2111-3* expressing plants developed less LRs than wild-type plants (**Figure 8B**).

miR2111 is primarily produced in shoots and is proposed to translocate to roots *via* the phloem (Tsikou et al., 2018; Okuma et al., 2020). Phloem-mobile miRNAs were recently suggested to translocate as fully processed duplices, rather than as pri- or pre-miRNA precursors (Devers et al., 2020; Brioudes et al., 2021). Consistently, we could trace plant specific mature miR2111 transcripts in aphids (*Planococcus citri*) feeding on Lotus, indicating its presence in the phloem sap (**Figure 9A-C**). To investigate whether shoot-derived miR2111 is indeed functional in Lotus roots and sufficient to regulate LR number, we grafted *pUBQ1:MIR2111-3* expressing shoots onto wild-type root stocks (**Figure 8C**). Roots of chimeric plants showed enhanced levels of miR2111 (**Figure 8D**), and fewer emerged LRs compared to control grafts (**Figure 8C, E**) confirming that shoot miR2111 indeed translocates to roots to steer LR numbers.

miR2111 was proposed to directly target *TML* for posttranscriptional regulation in Lotus as well as Medicago (Tsikou et al., 2018; Gautrat et al., 2020). Consistently, roots of *pUBQ1:MIR2111-3*/wild-type (shoot/root) grafts had significantly lower *TML* levels than wild-type/wild-type controls (**Figure 8F**).

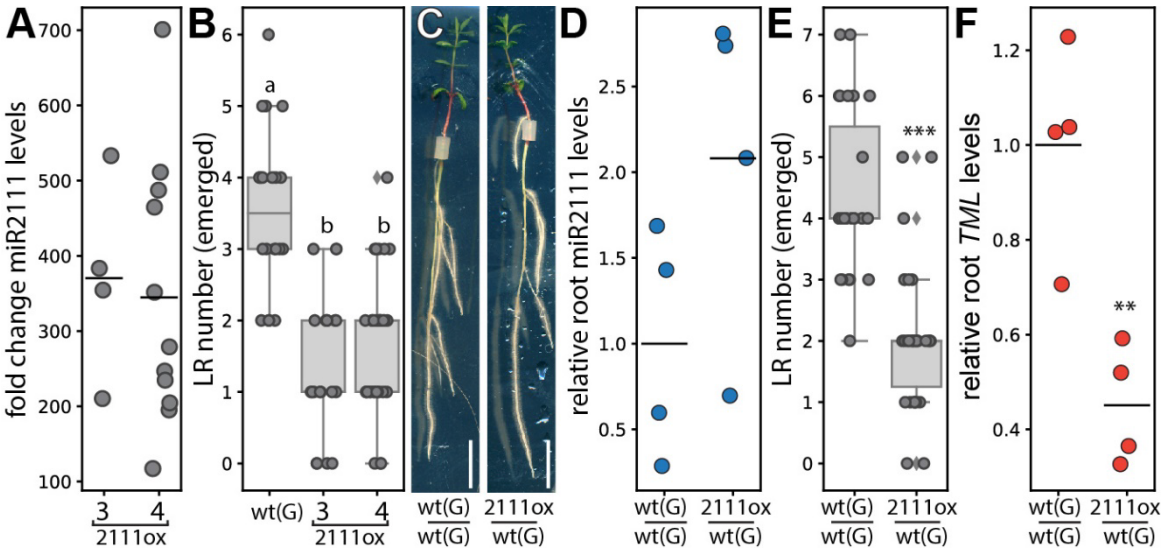

Figure 8 Shoot-derived miR2111 regulates lateral root (LR) numbers in *L. japonicus* (Lotus) (Sexauer et al., 2023), modified. A miR2111 abundance fold change compared to Gifu wild-type (wt(G)) plants, and **B** LR count in transgenic *pUBQ1:MIR2111-3* (2111ox) expressing lines (#3, 4) compared to wt(G). Line #3 was used for further analysis. **C-F** 2111ox / wt(G) (shoot / root) grafts compared to wt(G) / wt(G) control grafts. **c** Example of grafted plants. Scale bars equal 1 cm. **D** miR2111 levels, **E** LR numbers and **F** *TML* levels in roots of respective grafts. **A**, **F** and **f** qRT-PCR analyses. RNA levels are relative to those of two reference genes. RNA was extracted from root (**D**, **F**) or shoot samples (**A**). **A** Adult plants grown in soil. **B-G** Plants were grown at 0 mM nitrate and evaluated or harvested after two weeks of cultivation. Student's t-test (**=p≤0.01; ***=p≤0.001) (**D**-**F**) or analysis of variance (ANOVA) and post-hoc Tukey testing (p ≤ 0.05) (**B**), with distinct letters indicating significant differences. All experiments were in ecotype Gifu B-129 (wt(G)). Sample size, replicates and exact p-values are listed in Appendix Table 2. Dotplots show individual data points and a line indicating their average value. Boxplot central line shows median value, box limits indicate the 25 th and 75 th percentiles whiskers extend 1.5 times the interquartile range or to the last datapoint, data are represented by dots.

tml knockout mutants developed less LRs than wild-type plants (**Figure 10A, B**), and were phenotypically indistinguishable from *pUBQ1:MIR2111-3* plants (**Figure 10A, B**), suggesting that *TML* is the main target of miR2111 activity in LR control. Interestingly, this was equally the case when all initiated LRs, including pre-emergence root primordia and emerged lateral roots, were considered (**Figure 10C**) (Sexauer et al., 2023, Supplementary Fig. 2). The combined number of LR primordia and emerged LRs represents the total number of LR initiations, independent of LR emergence rates (Sexauer et al., 2023, Supplementary Fig. 2). LR initiations were also reduced in grafted plants expressing *pUBQ1:MIR2111-3* in their shoots compared to wild-type/wild-type control grafts (**Figure 10D**).

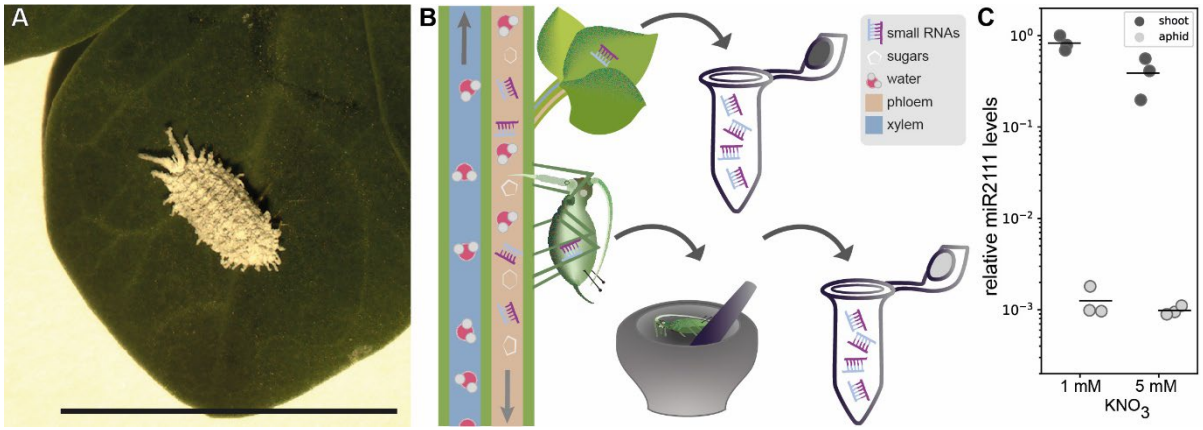

Figure 9 Mature miR2111 can be traced in aphids feeding on *L. japonicus* (Lotus) phloem sap (Sexauer et al., 2023), modified. A *Planococcus citri* on Lotus leaf, scalebar equals 1 cm. **B** Simplified sketch of experimental procedure of an aphid feeding experiment. Plants are grown for four weeks in absence of aphids, then colonized by a small aphid population, which propagates for two weeks while feeding on phloem sap. During feeding, aphids ingest mobile small RNAs, which have been suggested to travel through the phloem as mature duplices (Devers et al., 2020). Possible association of miRNAs with proteins during phloem transfer is not considered here. Aphids and plant material are harvested separately for RNA extraction and qRT-PCR based detection of mature plant miR2111. **C** miR2111 levels in shoot tissue of Lotus ecotype Gifu wild-type plants and aphids (*Planococcus citri*) after feeding on respective plants grown at indicated nitrate conditions. qRT-PCR analyses. miR2111 levels from Lotus shoot RNA extracts are relative to two endogenous reference genes, miR2111 levels from aphid RNA extracts are relative to one aphid reference gene. Host and aphid tissues were harvested after two weeks of aphid feeding and six weeks after plant germination. Dotplots show individual data points and a line indicating their average value.

Using CRISPR-Cas9 technology, we generated line *mir2111-3-1,* which possesses a 12 bp deletion in the stem-loop region of the *MIR2111-3* locus in immediate proximity to the mature miRNA2111a sequence (Sexauer et al., 2023, Supplementary Fig. 3a-c) (**Figure 10E, G**). *mir2111-3-1* plants showed significantly lower miR2111 abundance than wild-type plants (**Figure 11A**) and, consistently, higher *TML* transcript levels (**Figure 11B**). In line with the observed reduced primordium formation in miR2111 overexpressors (**Figure 10C, D**). LR initiation numbers were higher in *mir2111-3-1* plants compared to wild-type plants (**Figure 10E**), and grafts of *mir2111-3-1* shoots on wild-type root stocks equally showed an enhanced LR initiation compared to control grafts (**Figure 10F**). This is consistent with a shoot specific expression pattern of the *MIR2111-3* locus (**Figure 10G**) and confirms that shoot miR2111 is required for LR initiation control. Taken together, these data suggest a role of miR2111 in modulating LR initiations systemically *via* its target *TML* (**Figure 10C-G**) (Sexauer et al., 2023, Supplementary Fig. 3a-c) . Interestingly, this is in addition to the described function of shoot-derived miR2111 in systemic nodule number control in the context of symbiosis

autoregulation (**Figure 11C**) (Tsikou et al., 2018; Okuma et al., 2020). Since root nodulation symbiosis, a known activity context of miR2111-*TML*, is an adaptation to nitrogen limitation, we hypothesized that this regulon may also help to adapt root architecture to nitrogen availability (**Figure 12A-J**).

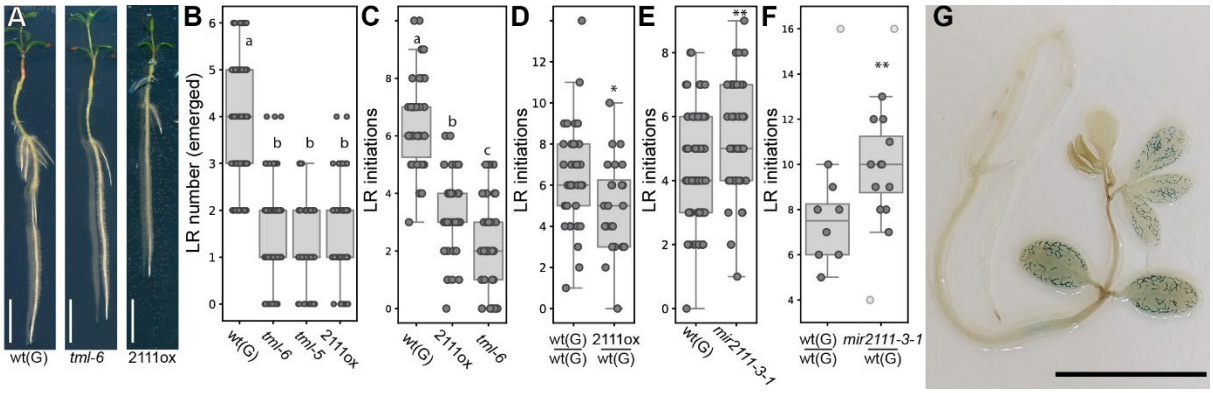

Figure 10 *TML* mediates miR2111 control of *L. japonicus* (Lotus) lateral root (LR) initiation (Sexauer et al., 2023), modified. A Root phenotype of Gifu wild-type (wt(G)), *tml-6* and *pUBQ1:MIR2111-3* plants (2111ox). Scale bars equal 1 cm. **B** Emerged LR numbers in wt(G), *tml-6*, *tml-5* and 2111ox plants. **C-E** Number of LR initiations (emerged and primordial stages combined) in wt(G), 2111ox and *tml-6* plants (**C**), on 2111ox / wt(G) (shoot / root) grafts compared to wt(G) / wt(G) control grafts (**D**), in *mir2111-3-1* compared to wt(G) plants (**E**) and on *mir2111-3-1* / wt(G) (shoot / root) grafts compared to wt(G) / wt(G) control grafts (**F**). **F** light grey dots represent data points not considered in the statistical analysis due to strong divergence of primary root length in the respective plants from the mean. **G** Plants expressing *pMIR2111-3:GUS* show pronounced GUS activity in leaf veins, while roots are free of visually traceable activity. Scale bar equals 1 cm. we tested 30 more plants with similar expression pattern. **B** Datapoints are identical to datapoints at 0 mM nitrate in Fig. 12A. **A-E** Plants grown at 0 mM nitrate. Comparisons used Student's t-test (*=p≤0.05; **=p≤0.01) (**D**, **E**) or analysis of variance (ANOVA) and post-hoc Tukey testing (p≤0.05) (**B**, **C**), with distinct letters indicating significant differences. All experiments were in ecotype Gifu B-129 (wt(G)). **A-G** Plants were evaluated or harvested after two weeks of cultivation (**A-C**, **E** & **G**) or grafting (**D, F**). Sample size, replicates and exact p-values are listed in Appendix Table 2. Boxplot central line shows median value, box limits indicate the 25 th and 75 th percentiles whiskers extend 1.5 times the interquartile range or to the last datapoint, data are represented by dots.

Lotus showed enhanced LR numbers under nitrogen starvation (**Figure 12A**). This was ecotype-independent (**Figure 12A, B**) and is consistent with the nitrate foraging responses reported in other plants (Oldroyd and Leyser, 2020). Notably, this trend was only apparent for emerged LRs. LR primordia, on the contrary, were more abundant under nitrate sufficient conditions compared to deficiency. This results in a positively nitrate-correlated (**Figure 12C, D**) or nitrate-independent (**Figure 13A**) sum of initiated roots. Following a likewise trend, mature miR2111 levels were negatively correlated with nitrate availability in a dosage-dependent manner in both shoots and

roots (**Figure 12E, F**), indicating an involvement in systemic nitrogen response signaling. The levels of *TML* transcripts, which were only detected in roots, showed a complementary, inverse pattern (**Figure 12G**), suggesting *TML* suppression by systemic miR2111 under nitrogen starvation conditions. Here, we could observe ecotype specific differences, as this pattern was particularly apparent in the Lotus ecotype MG-20, consistent with a more pronounced responsiveness of LR initiations to nitrate availability compared to Gifu B-129 (**Figure 13A-D**).

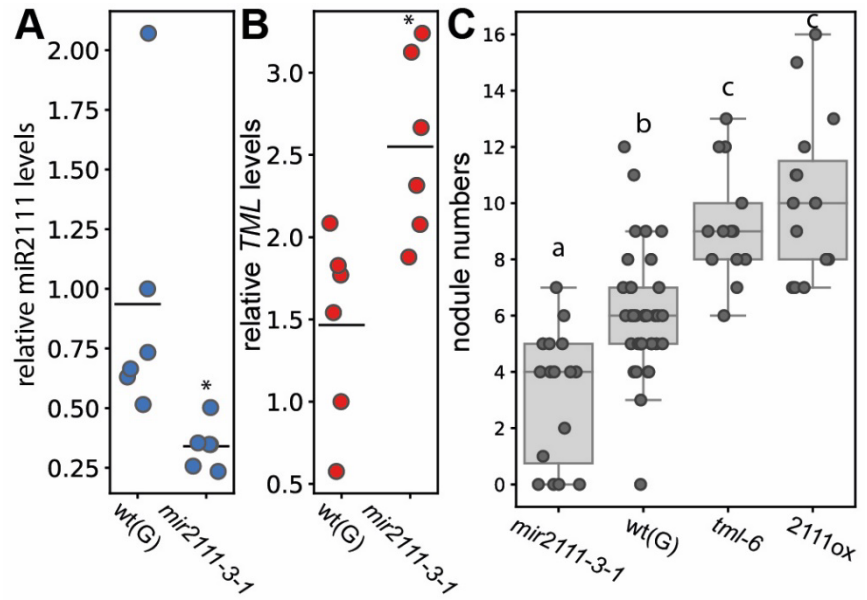

Figure 11 Alterations of miR2111 and *TML* levels influence nodule numbers in *L. japonicus* (Lotus) (Sexauer et al., 2023), modified. A, B miR2111 (**A**) and *TML* levels (**B**) in roots of Lotus ecotype Gifu wild-type (wt(G)) and *mir2111-3-1* plants. **c** Nodule numbers of wt(G), *tml-6*, *MIR2111-3* ox (2111ox) and *mir2111-3-1* mutants, *tml-6* and 2111ox plants. **A, B** qRT-PCR analyses. Root RNA levels are relative to those of two reference genes. Tissue was harvested 14 days after transfer. Plants were grown at 5 mM nitrate. **A-C** Comparisons used Student's *t*-test (*=p<0.05) (**A, B**) or (**C**) analysis of variance (ANOVA) and post-hoc Tukey testing (p≤0.05), with distinct letters indicating significant differences. **C** plants evaluated three weeks after inoculation with *M. loti*, plants grown at 0 mM nitrate. Sample size, replicates and exact p-values are listed in Appendix Table 2. Dotplots show individual data points and a line indicating their average value. Boxplot central line shows median value, box limits indicate the 25 th and 75 th percentiles whiskers extend 1.5 times the interquartile range or to the last datapoint, data are represented by dots.

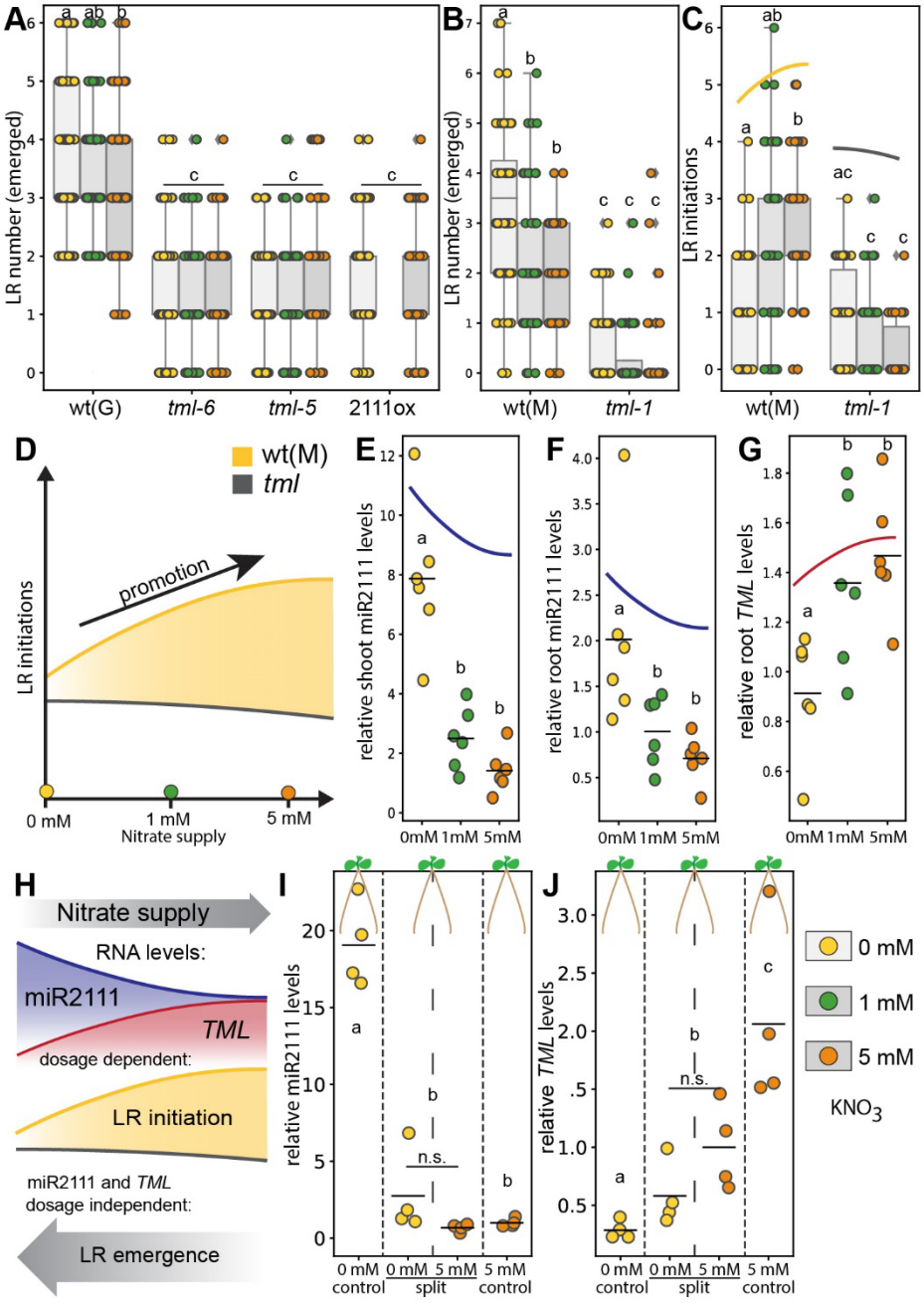

Figure 12 Systemic nitrogen status controls lateral root (LR) initiations *via* the miR2111-*TML* regulon in *L. japonicus* (Lotus) (Sexauer et al., 2023), modified. A-B Emerged LRs in (**A**) Gifu B-129 wild-type (wt(G)), *tml-6*, *tml-5* and *pUBQ1:MIR2111-3* (2111ox), and in (**B**) MG20 wild-type (wt(M)) and *tml-1* plants. **C** Number of LR initiations (emerged plus primordial stages) in wt(M) and *tml-1* plants. **D** Simplified model of nitrate dependency of LR initiations in wild-type and *tml* mutant plants. **E, F** Relative mature miR2111 levels in shoots (**E**) and roots (**F**). **G** Relative *TML* levels in same wild-type root systems as in **F**. **H** Simplified model outlining nitrate dependency of miR2111 and *TML* levels, and root architectural responses. **I, J** Split root experiments. Relative miR2111 (**I**) and *TML* (**J**) levels in secondary roots of wt(M) plants. **E-G, I, J** qRT-PCR analyses. RNA levels are relative to those of two reference genes. **A, B, E-G**, and **I, J** Tissue harvest / analysis after two weeks and **C** 10 days of cultivation. Comparisons used analysis of variance (ANOVA) and post-hoc Tukey. testing ($p \leq 0.05$), with distinct letters indicating significant differences and additional Student's *t*-test (**I-J**) comparing only the split roots (n.s.=$p > 0.05$). **C-H** Trendlines are simplified and not to scale. Plants grown at indicated nitrate concentrations. Sample size, replicates and exact p-values are listed in Appendix Table 2.

Compared to wild-type plants, both miR2111 overexpressors and *tml* mutants had a consistently lower number of LRs, and emerged LR number was independent of nitrate availability (**Figure 12A, B**). The same was true for LR initiation, not only in the ecotype Gifu B-129, but also in MG-20, where a nitrate-dependent increase in LR primordia is more strongly pronounced than in Gifu B-129 (**Figure 12C, D** and **Figure 13A**). Shoot specific overexpression of *MIR2111-3* using heterografting experiments induced a loss of nitrate responsive LR initiation in chimeric plants with MG-20 root stocks (**Figure 14A, B**), suggesting that shoot-derived miR2111 efficiently represses this response. On this basis, we predicted that nitrate-independent *TML* transcript levels in Gifu B-129 (**Figure 13D**) may prevent adaptive primordia formation in this ecotype. Indeed, increased *TML* transcript levels in *MIR2111-3* knockout compared to wild-type plants (**Figure 11B**) resulted in a positive nitrate response of LR initiation numbers in the ecotype Gifu B-129 as well (**Figure 14C**). This indicates that miR2111 mediated *TML* control is necessary for the ecotype-specific attenuation of root system response to nitrate observed in Gifu B-129.

The combined phenotypic and molecular data suggests a role of the miR2111-*TML* regulon in LR initiation and adaptive emergence in response to nitrate, with miR2111 systemically repressing *TML*. Contrasting with their respective roles in symbiosis, our data identify miR2111, a positive regulator of nodule numbers, as a repressor of root primordia, and *TML* as a root primordial activator (**Figure 12H**). The data further reveal that nitrate dependent regulation of primordia emergence into full LRs strictly requires the presence of functional *TML* (**Figure 12A-C**), but does not correlate with *TML* transcript abundance (**Figure 12G, H** and **Figure 13D**). This suggests involvement of additional factors in regulating nitrate responsive emergence of *TML*-dependent LR primordia.

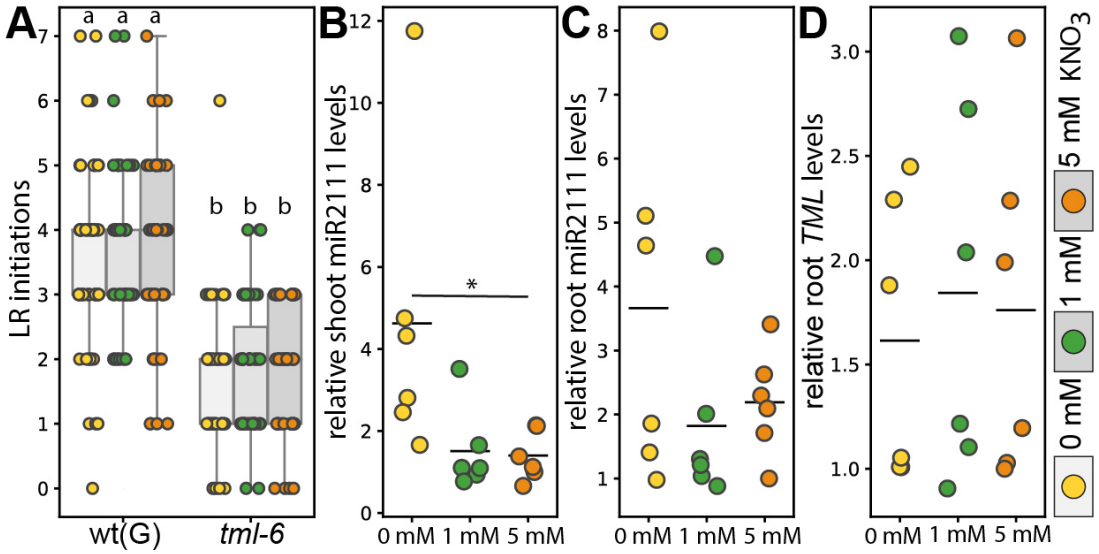

Figure 13 *L. japonicus* (Lotus) ecotype Gifu lateral root (LR) initiation numbers and *TML* levels are nitrate independent (Sexauer et al., 2023), modified. A LR initiations in wild-type Gifu (wt(G)) and *tml-6* plants 10 days post transfer. **B-D** Relative mature miR2111 levels in shoots (**B**) and roots (**C**) and relative *TML* levels in the same root systems (**D**) of ecotype Gifu B-129 wild-type plants after 14 days of cultivation. **B-D** qRT-PCR analyses. RNA levels are relative to those of two reference genes. Comparisons used analysis of variance (ANOVA) and post-hoc Tukey testing ($p \leq 0.05$), with distinct letters indicating significant differences (**A**) or Student's t-test (*=$p<0.05$) (**B**). Sample size, replicates and exact p-values are listed in Appendix Table 2. Dotplots show individual data points and a line indicating their average value. Boxplot central line shows median value, box limits indicate the 25 th and 75 th percentiles whiskers extend 1.5 times the interquartile range or to the last datapoint, data are represented by dots.

Nitrate perception and nitrogen starvation have been found to trigger local and systemic responses involving physiological and morphological adaptations (Oldroyd and Leyser, 2020). We thus performed split root assays to identify the trigger underlying miR2111 regulation under asymbiotic conditions. Roots growing on nitrogen starvation medium contained low miR2111 levels if other roots of the same plant experienced nitrate sufficiency (**Figure 12I**). This suggests that miR2111 accumulation is not triggered by roots experiencing nitrate starvation, but rather systemically repressed by roots experiencing nitrate sufficiency (**Figure 12I**), implying that miR2111 levels are regulated through nitrate supply rather than deficiency. *TML* levels in these roots were complementary yet intermediate (**Figure 12J**). Consistent with previous observations, *TML* abundance is thus likely subject to additional regulatory factors (Tsikou et al., 2018).

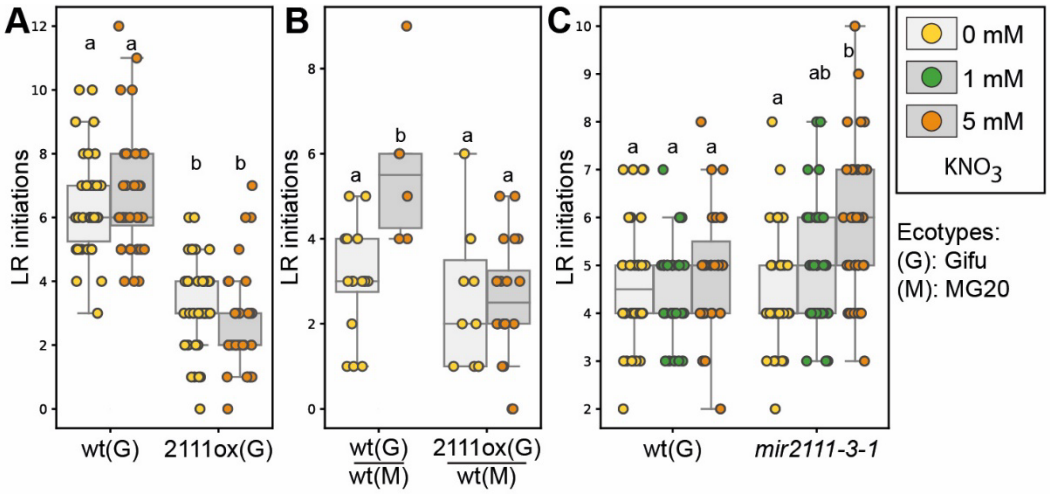

Figure 14 Low miR2111 levels are required and sufficient for enhanced lateral root (LR) initiation under high nitrate conditions in *L. japonicus* (Lotus) (Sexauer et al., 2023), modifed. A-C LR initiations of Lotus ecotype Gifu wild-type (wt(G)) and *mir2111-3-1* plants (**A**), heterografted plants assembled of Lotus ecotype MG20 wild-type (wt(M)) root stocks and ecotype Gifu wild-type or *MIR2111-3* overexpression (2111ox) shoots (**B**), and ecotype Gifu wild-type and *mir2111-3-1 plants* (**C**). **A, B** Plants were grown at indicated nitrate concentrations and analyzed after two weeks of cultivation (**A, B**) or graft regeneration (**C**), respectively. Comparisons used analysis of variance (ANOVA) and post-hoc Tukey testing ($p \leq 0.05$), with distinct letters indicating significant differences. Sample size, replicates and exact p-values are listed in Appendix Table 2. Boxplot central line shows median value, box limits indicate the 25 th and 75 th percentiles whiskers extend 1.5 times the interquartile range or to the last datapoint, data are represented by dots.

Root architecture adaptation to abiotic stimuli is an ancient necessity and a core developmental feature of land plants that is phylogenetically widespread (Oldroyd and Leyser, 2020) and thus precedes the evolution of nitrogen-fixing nodulation symbiosis. Consistently, the miR2111-*TML* regulon is conserved in non-nodulating plants, including the nonsymbiotic plant *Arabidopsis thaliana* (Arabidopsis) (Takahara et al., 2013; Tsikou et al., 2018). Arabidopsis possesses two *MIR2111* precursor loci generating a single isoform identical to *Lj*miR2111a (Sexauer et al., 2023, Supplementary Fig. 8a,b)(Tsikou et al., 2018). Phylogenetic analysis revealed one putative *TML* orthologue, which we named *HOMOLOGUE OF LEGUME TML (HOLT),* featuring a miR2111 complementary site in the coding sequence (Takahara et al., 2013; Tsikou et al., 2018) (Sexauer et al., 2023, Supplementary Fig. 9a,b). Thus, we wondered whether the function of miR2111 as systemic regulator of nitrate foraging is conserved in Arabidopsis (**Figure 15A-L**). Consistent with the expression pattern of *MIR2111* loci in Lotus, Arabidopsis *pMIR2111a/b:GUS* expressing lines showed predominant GUS activity in leaf vein phloem cells (**Figure 15A, B**) (Sexauer et al., 2023, Supplementary Fig. 10a,b), suggesting systemic mobility (Skopelitis et al., 2018). These observations

are in line with organ specific expression data (Sexauer et al., 2023, Supplementary Table 1). Similar to what has been previously observed for selected Lotus *MIR2111* precursor genes (Okuma et al., 2020), moderate *pMIR2111a/b:GUS* activity was evident in mature root parts of Arabidopsis as well (**Figure 15A**) (Sexauer et al., 2023, Supplementary Fig. 10a), although *MIR2111a/b* precursor transcripts were not traceable in publicly available RNAseq datasets (Sexauer et al., 2023, Supplementary Table 1).

Like in Lotus, Arabidopsis LR initiation depends on nitrogen supply, peaking around 1 mM KNO_3 under long day conditions in plate-grown wild-type plants (**Figure 15C**). In comparison, plants grown under starvation or saturating conditions show reduced numbers of LR initiations (**Figure 15C**). The observed increase of LR numbers under moderately deficient (1 mM KNO_3) as compared to sufficient nitrogen supply (10 mM KNO_3) has previously been associated with nitrogen dependent root architectural adaptations commonly referred to as foraging response (Giehl and von Wirén, 2014). To evaluate a possible role of the miR2111/*HOLT* regulon in nitrogen foraging related LR initiation in Arabidopsis, we generated transgenic lines overexpressing miR2111 under the control of a *35S* promoter, showing concomitant reduction in *HOLT* levels (Sexauer et al., 2023, Supplementary Fig. 11a,b). All tested lines showed reduced LR initiation compared to wild-type plants in the T2 generation (Sexauer et al., 2023, Supplementary Fig. 11c). We chose a representative line #3 for further propagation, as it showed stable overabundance of miR2111 and the corresponding reduction of *TML* transcript abundance in the T3 generation (**Figure 15D, E**). We further isolated Arabidopsis *holt-1* and *holt*-2 mutants lacking a traceable full-length *HOLT* transcript (Sexauer et al., 2023, Supplementary Fig. 12a,b). *holt-1*, *holt-2* and *p35s:MIR2111b* plants showed significantly reduced LR initiations at low and moderate nitrate concentrations compared to wild-type plants (**Figure 15F**). Notably, they failed to show a traceable foraging response (**Figure 15F, G**). Wild-type plants exposed to severe nitrogen limitation repress LR development, a response known as a survival strategy (Giehl and von Wirén, 2014), which is thought to involve the nitrate transporter *NRT1.1* (Krouk et al., 2010) as well as locally induced LR inhibition through the *CLAVATA3/CLAVATA1* signaling module (Araya et al., 2014). Transcript abundance of *NRT1.1* and other *NRTs* was not significantly altered in *holt-1* or *p35s:MIR2111b* as compared to wild-type plants (**Figure 16A-D**). Consistent with a

HOLT independent mechanism, a successive reduction in LR initiation numbers at nitrate levels <1 mM was retained in *holt-1*, *holt-2* and *p35s:MIR2111b* in a similar way as in wild-type plants (**Figure 15F, G**). In wild-type plants, miR2111 levels correlate positively with nitrate concentration (**Figure 15H**), consistent with low *HOLT* levels at high nitrate supply (**Figure 15I**). The integration of phenotypic and molecular data reveals that, in line with observations in Lotus, *HOLT* levels positively correlate with LR initiations (**Figure 15J**). To investigate whether shoot-derived miR2111 is sufficient to regulate root architecture in Arabidopsis as observed in Lotus, we analyzed *p35s:MIR2111b*/Col-0 (shoot/root) grafts. These had significantly less LR initiations than Col-0/Col-0 control grafts (**Figure 15K**), confirming miR2111 as a systemically acting, mobile regulator of LR initiation across dicot plant lineages.

In line with divergent habitat requirements and ecological strategies of the symbiotic Lotus (Szczyglowski and Stougaard, 2008; Shah et al., 2020) and the asymbiotic ruderal Arabidopsis (Pigliucci, 2002), abundance patterns of LR primordia with respect to external nitrogen supply were distinct in these two species (**Figure 15L**). Yet, consistent with a conserved positive role of *TML*/*HOLT* in nitrate-dependent LR initiation, *TML*/*HOLT* RNA levels were upregulated in both species under nitrate conditions triggering abundant LR primordia. Accordingly, in either species, miR2111 levels were low under such conditions, in line with a negative effect on *TML*/*HOLT* levels and LR initiation. The dynamic response pattern of the Arabidopsis root system reflected in integrating distinct and functionally overlapping regulatory nodes (Krouk et al., 2010; Araya et al., 2014; Sexauer et al., 2023) indicates its capacity to populate a wide variety of soils (Pigliucci, 2002).

Our data suggests that Lotus, as a pioneer lineage that is primarily competitive on nitrogen poor soils (Griesmann et al., 2018), lacks differentiation between starvation and foraging response, and initiates additional root primordia upon nitrate supply, lacking root system optimization at sufficient nitrate supply (**Figure 15L**). The lack of a strong nitrogen starvation response in Lotus could be explained by the nitrogen fixing symbiosis, which supplies nitrogen and prevents nitrogen-starvation even on N limited soils.

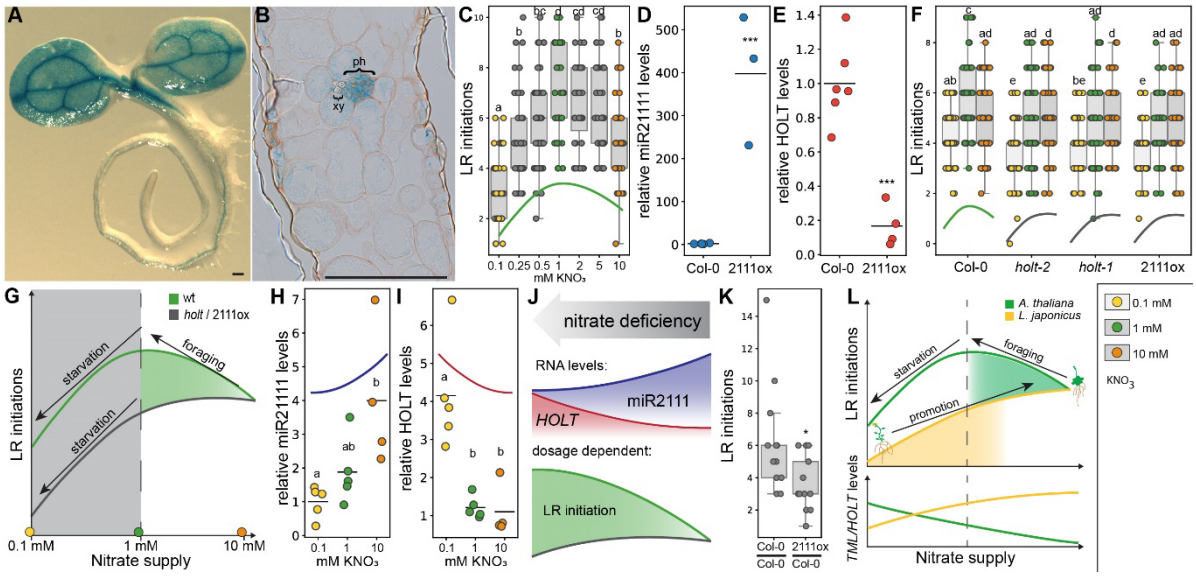

Figure 15 The *A. thaliana* (Arabidopsis) miR2111-*HOLT* regulon controls lateral root (LR) initiation at moderate nitrate starvation (Sexauer et al., 2023), modified. A-B Stably transformed *A. thaliana* (Arabidopsis) plants expressing *pMIR2111b:GUS* show predominant GUS activity in the phloem of leaf veins. **B** Leaf cross section of *pMIR2111b:GUS* plants. ph, phloem and xy, xylem. **C** Numbers of LR initiations at different nitrate concentration in Arabidopsis wild-type (Col-0) plants. **D-E** miR2111 (**D**) and *HOLT* (**E**) levels in Col-0 and *p35s:MIR2111b* expressing plants (2111ox) at 1 mM nitrate. **F** LR initiations in *holt-1*, *holt-2* and 2111ox plants compared to Col-0. **G** Schematic model of nitrate responsiveness of Arabidopsis lateral root initiations. *holt-1* and 2111ox plants lack a foraging response at moderate nitrate starvation. **H, I** miR2111 (**H**) and *HOLT* (**I**) levels of Col-0 at varying nitrate concentrations. **J** Simplified model outlining nitrate dependency of miR2111 and *HOLT* levels, and of root architectural responses in Arabidopsis between 1 and 10 mM nitrate. **K** Number of LR initiations on 2111ox / Col-0 (shoot / root) grafts compared to Col-0 / Col-0 control grafts at 1 mM KNO_3. **L** Combined simplified model of Arabidopsis and *L. japonicus* (Lotus) root responses to varying nitrate supply. *HOLT* positively correlates with LR initiations in both species, but nitrate dependent abundance patterns of both LR initiations and *TML*/*HOLT* levels are opposite. **D-E, H, I** qRT-PCR analyses. RNA levels are relative to those of two reference genes, whole plant tissue harvested 10 days after germination. **C, F, K** Analysis seven days after germination (**C, F**) or after graft regeneration (**K**). Comparisons used analysis of variance (ANOVA) and post-hoc Tukey testing ($p \leq 0.05$), with distinct letters indicating significant differences (**C, F, H, I**) or Student's t-test (*=$p \leq 0.05$) (**D, E, K**). **A, B** Scale bars equal 200 µm (**A**) or 100µm (**B**). **A**, **B** all 21 tested plants of 3 independent lines showed same expression pattern. Analysis of three independent lines showed similar results. **C**, **F**, **H, I** plants were grown at indicated nitrate concentrations using ½ strength MS media free of other nitrogen sources. **C, F-J, L** Trendlines are simplified and not to scale. Sample size, replicates and exact p-values are listed in Appendix Table 2.

An important role of the miR2111-*TML*/*HOLT* regulon in adapting plant root systems to their natural habitat is in line with the observed differences in LR abundance patterns between Lotus MG-20 and Gifu-129 ecotypes (**Figure 12A-C, Figure 13A** and **Figure 14A-C**). *Lotus japonicus* underwent intense diversification during evolution and encompasses more than 130 ecotypes that have adapted to a wide range of

environmental conditions on the Japanese Islands (Shah et al., 2020). A time course experiment revealed an increasing difference between wild type and *tml-1* in LR numbers over time. Here, *tml-1* plants showed significantly less biomass production in both below- and aboveground tissues compared to wild type (Sexauer et al., 2023, Supplementary Fig. 14a,b), suggesting that root architecture adaption plays an important role in plant productivity and fitness. We have no evidence for a direct involvement of the miR2111-*TML/HOLT* regulon in nitrate uptake or mRNA levels of nitrate transporter genes. *NRT1.1*, *NRT1.5*, *NRT2.1* and *NRT3.1* accumulation levels are unaltered in *holt-1* and *p35s:MIR2111b* lines compared to wild-type controls (**Figure 16A-D**). This is in contrast to *CEP*/*CEPD*/*CEPDL2* mediated regulation of nitrate uptake via *NRT2.1* (Ohkubo et al., 2017; Ota et al., 2020; Ohkubo et al., 2021), and suggests an indirect role of the miR2111-*TML*/*HOLT* regulon in nutrient uptake regulation by altering the extent of the root surface area (**Figure 16**).

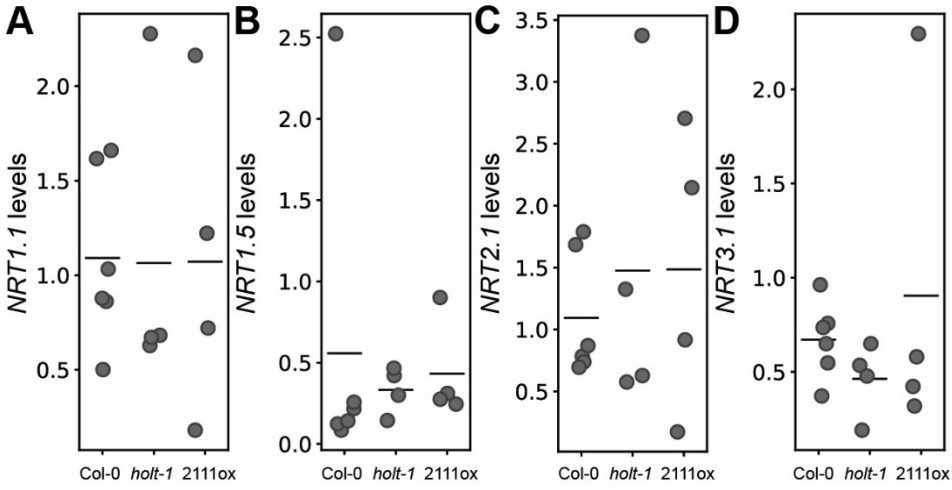

Figure 16 mRNA abundance of *A. thaliana NRT* genes is wild-type-like in *holt-1* or *MIR2111b* overexpression plants (Sexauer et al., 2023), modified. A-D Relative levels of *NRT1.1* (**A**), *NRT1.5* (**B**), *NRT2.1* (**C**) and *NRT3.1* (**D**) in *holt-1* and *p35s:MIR2111b* (2111ox) plants compared to ecotype col-0 wild-type plants. Plants grown for ten days on 1 mM nitrate. **A-D** qRT-PCR analyses. RNA levels are relative to those of two reference genes. Comparisons using analysis of variance (ANOVA) identified no significant differences of mRNA abundances between lines. Sample size, replicates and exact p-values are listed in Appendix Table 2. Dotplots show individual data points and a line indicating their average value.

In addition to quantitative evaluation of LR initiation and emergence, we analyzed the positioning of LRs along the primary root. We defined the LR zone as the relative position of the most distal LR along the primary root. The initiation zone was respectively defined as the relative position of the most distal initiated LR / LR (**Figure 17A**), and evaluated in *tml-6* and *pUBQ1:MIR2111-3* plants and *pUBQ1:MIR2111-3* grafts in comparison to wild type (**Figure 17B-D**). *tml-6* and *pUBQ1:MIR2111-3* expressing plants showed significantly reduced LR and initiation zones compared to wild-type plants (**Figure 17C, D**), indicating a role of the *TML*-miR2111 regulon in LR zone control. To test whether systemic miR2111 is sufficient to alter the LR zone, we generated *pUBQ1:MIR2111-3* / wild-type and wild-type / wild-type control grafts. Chimeric plants resulting from grafting of *pUBQ1:MIR2111-3* expressing shoots on wild-type root stocks (**Figure 8C**) showed a significantly shorter LR zone than wild-type / wild-type control grafts (**Figure 17B**). We hypothesized that the *TML*-miR2111 module regulates nitrate supply-triggered LR zone control. Indeed, wild-type plants showed a reduced LR zone upon nitrate supply, while *tml-6* and *pUBQ1:MIR2111-3* expressing plants showed a nitrate independent zone (**Figure 17C**). Similar tendencies were observed for the initiation zone (**Figure 17D**).

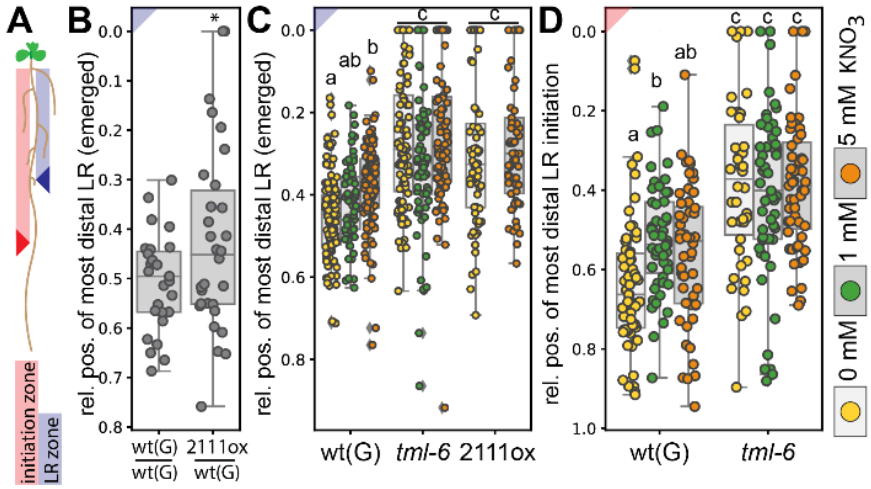

Figure 17. *TML* mediates miR2111 control of lateral root zonation. A Scheme of LR positioning; blue arrow indicates most distal emerged LR, red arrow indicates most distal initiated LR. **B**, **C** Relative position of most distal emerged LRs on 2111ox / wild-type (shoot / root) grafts compared to wild-type / wild-type control grafts (**B**) and wild-type, *tml-6* and *pUBQ1:MIR2111-3* plants (2111ox) (**C**). **D** Relative position of most distal initiated LRs of wild-type and *tml-6* plants. Comparison used Student's t-test (*=p≤0.05) (**B**) or analysis of variance (ANOVA) and post-hoc Tukey testing (p≤0.05) (**C**, **D**), with distinct letters indicating significant differences. Sample size, replicates and exact p-values are listed in Appendix Table 2. Boxplot central line shows median value, box limits indicate the 25 th and 75 th percentiles whiskers extend 1.5 times the interquartile range or to the last datapoint, data are represented by dots.

This suggests that functional *TML* is necessary for a nitrate responsive zonation control of LR initiation and emergence. However, there is no dose dependence between *TML* levels and LR (initiation) zone expansion (**Figure 12G, H** and **Figure 17C, D**). A quantification of Arabidopsis LR zones in Col-0 and *holt-1* mutants failed to produce consistent results.

The loss of zonation control in Lotus *tml-6* and *pUBQ1:MIR2111-3* expressing plants could thereby be explained by an indirect effect of the low numbers of LR initiations in these plants, which narrows the zone regardless of nitrate supply (**Figure 13A** and **Figure 14A**). Nevertheless, the function of *TML* proves to be an essential factor in determining the positioning of LR initiation and therefore also the location of the roots' depletion zone in the substrate.

Alteration of the root depletion zone also affects the uptake of other nutrients. Interestingly, in Arabidopsis, miR2111 was shown to be induced by phosphate starvation (Hsieh et al., 2009), and Arabidopsis is known to adapt its root architecture to phosphate availability (Williamson et al., 2001). This could hint to a more general role of miR2111 in adapting root architecture to nutrient availability.

Whether miR2111 functions in systemic foraging responses to further nutrients beyond nitrate is an interesting topic for further studies. An additional question is the molecular nature of miR2111 abundance and mobility regulation, which follows distinct patterns in Arabidopsis and Lotus. The differences of the function of the miR2111-*TML/HOLT* regulon between Lotus and Arabidopsis and their ecological relevance will be discussed in the later chapter "Nitrogen physiology – integrating different signals and responses.".

HAR1 controls LR emergence in nitrate response, independent of miR2111

In Lotus, genetic regulation of miR2111 expression was dissected in the context of symbiotic signaling during AON. We thus hypothesized that in Lotus, miR2111 regulation in the context of nitrate foraging may be dependent on the same genetic pathway known from miR2111 regulation in AON. miR2111 regulation in response to infection with rhizobial bacteria depends on *HAR1/SUNN* and *CRA2 (Gautrat et al., 2020)*. Apart from a hypernodulation phenotype resembling *tml* mutants (Krusell et al., 2002; Magori et al., 2009; Takahara et al., 2013), *har1* loss-of-function mutants show root architectural aberrations (Krusell et al., 2002). Interestingly, the putative *Arabidopsis thaliana HAR1* orthologue *CLAVATA1* (*CLV1*) (Clark et al., 1997; Krusell et al., 2002; Nishimura et al., 2002) is involved in adapting root architecture to the soil nitrogen regime (Araya et al., 2014; Araya et al., 2016).

We thus hypothesized that HAR1 may systemically regulate root system architecture through miR2111 and *TML*, possibly following perception of *CLV3*-like CLE-peptides regulated nitrogen homeostasis (**Figure 18A, B**) (Nishida et al., 2016). In contrast to *tml* and *pUBQ1:MIR2111-3* plants, *har1* mutants showed wild-type-like LR numbers (**Figure 18C**), but similarly failed to adapt these to nitrate levels (**Figure 18C**). Consistent with a stunted primary root phenotype (Krusell et al., 2002; Nishimura et al., 2002; Buzas and Gresshoff, 2007) (**Figure 18D**), LR density was higher than in wild-type plants (**Figure 18E**). Notably, *har1* mutants developed an expanded LR zone compared to wild-type controls (**Figure 18F**).

While both *tml-6* and *har1-3* mutants show no nitrate responsive LR emergence, the combined data suggest divergent roles of *HAR1* and *TML* in LR number control and zone definition. In line with this observation, LR zone adaptation to nitrate levels, which required *TML* (**Figure 17C-D**), was *HAR1* independent (**Figure 18F**).

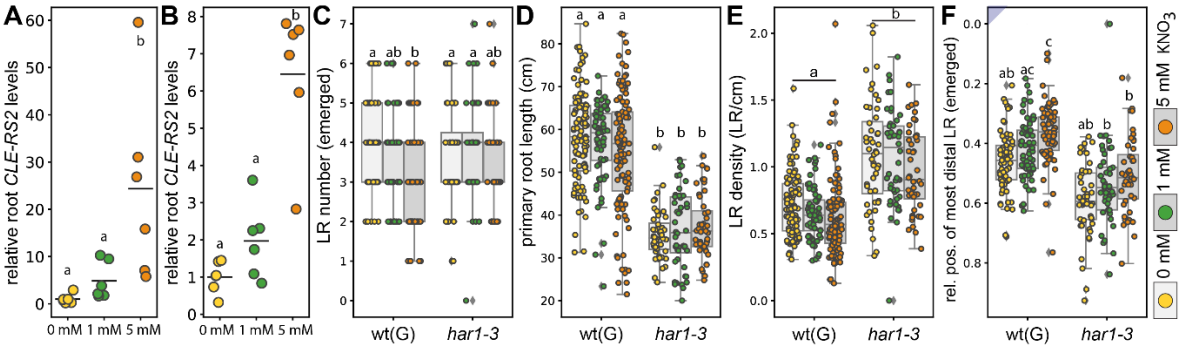

Figure 18 *HAR1* is involved in root architecture adaptation. Plants were grown on media with indicated concentrations of KNO_3 in the absence of other N sources. **A**-**B** transcript levels of *CLE-RS2* in roots of Gifu-B129 (**A**) and MG-20 (**B**) wild-type plants. **A**-**B** qRT-PCR analyses. RNA levels are relative to those of two reference genes. **C**-**F** Emerged LR numbers (**C**), primary root length (**D**), LR density (**E**) and relative position of most distal emerged LR along the primary root (**F**) in wild-type and *har1-3* plants. **A-F** All experiments were in ecotype Gifu B-129 (G). Comparisons used analysis of variance (ANOVA) and post-hoc Tukey testing ($p \leq 0.05$), with distinct letters indicating significant differences. Sample size, replicates and exact p-values are listed in Appendix Table 2. Dotplots show individual data points and a line indicating their average value. Boxplot central line shows median value, box limits indicate the 25 th and 75 th percentiles whiskers extend 1.5 times the interquartile range or to the last datapoint, data are represented by dots.

In contrast to *TML, HAR1* was involved in LR emergence rather than initiation, as *har1-3* showed wild-type-like LR initiations but no restriction of LR emergence at high nitrate supply (**Figure 19A, B**). Grafting experiments suggested a significant contribution of root *HAR1* to root growth control (Buzas and Gresshoff, 2007; Hayashi-Tsugane and Kawaguchi, 2022) (**Figure 19C**), and consistently, nitrate-triggered inhibition of shoot miR2111 levels was *HAR1* independent (**Figure 19D**). These data demonstrate that miR2111-*TML* and *HAR1*, that act in the same genetic pathway in infection-triggered AON (Krusell et al., 2002; Gautrat et al., 2020), have uncoupled functions in integrating local and systemic responses in the context of nitrogen-dependent root system control (**Figure 19E**) (Hayashi-Tsugane and Kawaguchi, 2022).

HAR1 independence of nitrate-triggered miR2111 abundance regulation implies that miR2111 abundance is controlled by distinct upstream factors in abiotic and biotic response contexts. The LRR-RLK *CRA2*/*CEPR1*, a second shoot regulator of miR2111 abundance in nodulation symbiosis, was similarly dispensable for nitrogen-triggered abundance limitation of miR2111 levels in *Medicago truncatula* (Gautrat et al., 2020). As for *HAR1*, *CRA2*/*CEPR1* impact on root development was locally determined and did not require shoot *CRA2*/*CEPR1* (Huault et al., 2014; Laffont et al., 2019). Putative shoot factors restricting miR2111 accumulation under nitrate sufficient conditions thus remain to be determined.

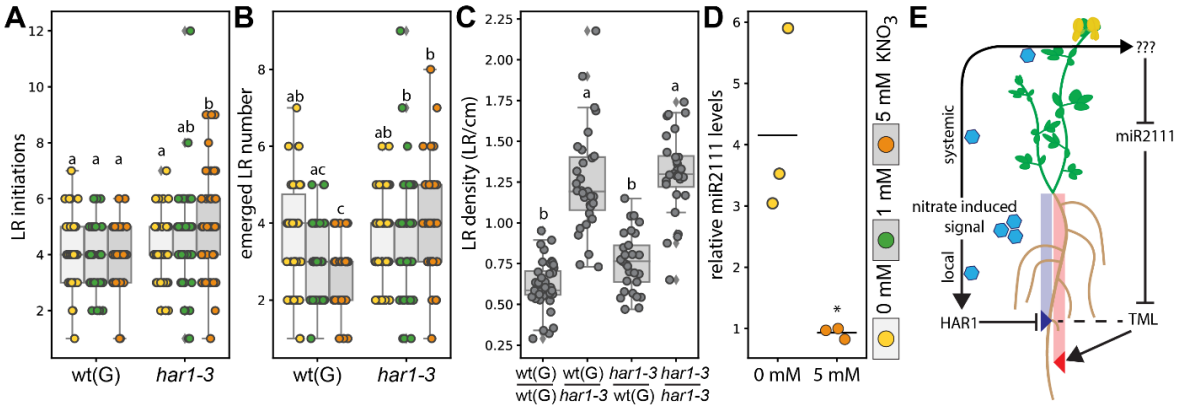

Figure 19. *HAR1* is involved in local LR emergence rather than systemic foraging. A LR initiations and **B** emerged LR numbers of wild-type and *har1-3* plants. Counts in (**A**) and (**B**) were on the same plants. **C** LR density in grafted plants of the genotypes Gifu and *har1-3*. **D** Relative mature miR2111 levels in shoots of *har1-3* plants. qRT-PCR analysis. RNA levels are relative to those of two reference genes. **E** Model of miR2111, *TML* and *HAR1* involvement in local and systemic LR control and adaptation to nitrate. Dotted line represents dosage independent effects. blue arrow indicates most distal emerged LR, red arrow indicates most distal initiated LR. **A**-**D** All experiments were in ecotype Gifu B-129 (G). Comparisons used analysis of variance (ANOVA) and post-hoc Tukey testing ($p \leq 0.05$), with distinct letters indicating significant differences (**A**-**C**), or Student's t-test (*=$p \leq 0.05$) (**D**). Sample size, replicates and exact p-values are listed in Appendix Table 2. Dotplots show individual data points and a line indicating their average value. Boxplot central line shows median value, box limits indicate the 25 th and 75 th percentiles whiskers extend 1.5 times the interquartile range or to the last datapoint, data are represented by dots.

The independence of *HAR1* and miR2111-*TML* in context of root adaptations is consistent with literature (Buzas and Gresshoff, 2007; Hayashi-Tsugane and Kawaguchi, 2022). (Hayashi-Tsugane and Kawaguchi, 2022) found that *HAR1* has a role in root architecture control, which functions independently of *TML*. However, they did not observe a function of *TML* in controlling LR foraging. This could be explained by a function of *TML* in LR initiation rather than emergence. In contrast to (Hayashi-Tsugane and Kawaguchi, 2022) we could not see significant effects of the shoot portion of *HAR1* on root architecture, which might be due to strong variations caused by graft recovery.

Interestingly, the functions of both the *CLE-HAR1* and miR2111-*TML* nodes in nitrate foraging appear to be conserved in Arabidopsis (Araya et al., 2014; Sexauer et al., 2023). This implies that during evolution of RLS, legumes adapted distinct pathways of nitrate foraging to a new function in the AON. This is consistent with recent observations of genes known from LR architecture and nitrate uptake homeostasis being active in nodule development or AON (Sexauer and Markmann, 2024).

TML/HOLT impact endodermal suberization

This chapter is based on the following publication:

Moritz Sexauer, Defeng Shen, Maria Schön, Tonni Grube Andersen, Katharina Markmann

> Visualizing polymeric components that define distinct root barriers across plant lineages. Development 2021 Dec 1;148(23):dev199820. doi: 10.1242/dev.199820

In addition, the chapter contains unpublished data, that were prepared by the author of this thesis.

Apart from genes shared between nodule organogenesis and LR development, several genes involved in developmental processes and cell identity determination in Arabidopsis roots have been found to also be active during nodule development (Osipova et al., 2012; Franssen et al., 2015; Dong et al., 2020). Examples include *SCR* and *SHR,* both involved in determining endodermal identity and maturation, including suberin deposition (Helariutta et al., 2000; Nakajima et al., 2001; Cui et al., 2007; Long et al., 2015; Dong et al., 2020; Wang et al., 2020). Suberin deposition in endodermis cells is influenced by nutritional cues, including nitrogen status, in several species (Barberon et al., 2016; Barberon, 2017; Namyslov et al., 2020; Melino et al., 2021).

In cooperation with Tonni G. Andersen, who hypothesized a role of *HOLT* in endodermal suberization in *Arabidopsis* based on expression data (T.G. Andersen, personal communication), we set out to investigate a possible involvement of the *L. japonicus TML*-miR2111 regulon in the nitrate adaptation of suberin deposition in the root endodermis.

Aiming to specifically visualize endodermal suberin depositions in roots of *Lotus* and *Arabidopsis* for comparative analysis, we initially used a well-established lactic acid-based protocol for fluorol yellow (FY) staining of suberin in *Arabidopsis* roots and semi-thin cuts (Lux et al., 2005). When applied to *Lotus* roots, which have a different internal structure and more cortical cell layers than *Arabidopsis* roots, this protocol did give rise to suberin associated signals (**Figure 20A, B**), but these were weak and difficult to image due to a low signal intensity in whole mount roots (**Figure 20A**).

To improve staining in deeper root tissues, we combined the lactic acid-based FY staining directly with a previously established ClearSee-based protocol (Kurihara et al., 2015), which has been successfully used together with other histochemical dyes (Ursache et al., 2018). However, this approach resulted in a precipitation of FY and almost complete loss of suberin associated signals. To solve this, we tested alternative solvents for FY, and found that the use of 96% ethanol rendered the staining solution compatible with ClearSee. A combined treatment with ethanol-dissolved FY and ClearSee yielded greatly enhanced signals from suberized endodermal cells in *Lotus* roots (**Figure 20C**) compared to the initially tested protocol (Lux et al., 2005) (**Figure 20A**). In contrast to the established lactic acid-based protocol, this procedure can be performed at room temperature, suggesting that it may be compatible with the imaging of fluorescent proteins.

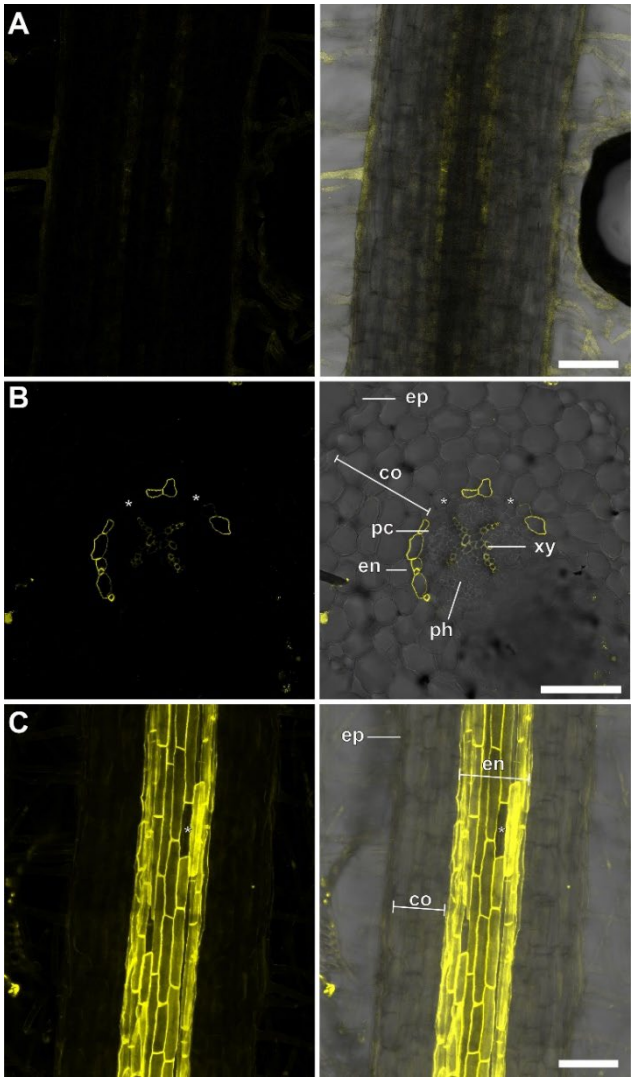

Figure 20. Staining of endodermal suberization in *L. japonicus* (Sexauer et al., 2021). Fluorol Yellow (FY)-stained *L. japonicus* whole mount roots (**A**) and semi-thin sections (**B**), using a lactic acid-based protocol. (**C**) *L. japonicus* roots stained by optimized ClearSee-based method. * indicate passage cells. **A-C** Left panel, FY channel and right panel, merged FY and transmission light channels. Plants grew for 10 days. Indicated cell types are co, parenchymatic cortex; en, endodermis ep, epidermis; pc, pericycle; ph, phloem and xy, xylem. Scale bars: 100 µm.

To test this, we employed a *DsRED* expressing strain of the rhizobacterium *Mesorhizobium loti*, which symbiotically infects *Lotus* roots. This setting further enabled us to evaluate whether these bacteria remained traceable in FY-stained roots, and to test the applicability of the protocol for analyzing barriers in a root endosymbiotic context (**Figure 21A, B**). Intriguingly, suberized endodermal cells and *DsRED*-labelled epidermal and cortical infection threads could be reliably visualized in the same samples (**Figure 21A**). Further, a suberized periderm-like layer in colonized nodules was apparent. In line with earlier observations in *Vicia faba* nodules (Hartmann et al., 2002), these suberized cells appeared to connect to the endodermis of the root tissue and of nodule vascular bundles (**Figure 21B**). This hints towards an important function of cell wall barriers in this plant-bacterial interaction and paves the way for in-depth visual analysis of suberin depositions in the context of nodulation symbiosis.

In *Arabidopsis*, endodermal suberization is assumed to be subsequent to lignification of the Casparian strip (Doblas et al., 2017a). To evaluate if our protocol could distinguish between these polymers, we combined it with basic fuchsin (BF) based lignin staining (Kurihara et al., 2015). In FY/BF co-stained roots, we were able to clearly identify the lignified Casparian strip and the suberin lamella as separate entities in the *Lotus* root endodermis (**Figure 21C**). The emission signals of both dyes were visually separable (**Figure 21C**) (Sexauer et al., 2021; Figure 3&4), and we rarely observed co-localization of FY-stained suberin and BF-labelled lignin in root samples. Moreover, FY signal was absent from the xylem, while BF stained meta- and protoxylem (Sexauer et al., 2021; Figure 3A). This implies specificity of the staining technique, confirms distinct accumulation patterns and is consistent with independent functions of suberin and lignin depositions (Barberon et al., 2016). Barrier deposition strategies in roots differ between plant lineages and species (Holbein et al., 2021). We thus extended the protocol to other species, aiming to cover a representative set of spermatophytic lineages (Sexauer et al., 2021; Figure 3&4, Supplementary Figure 1). Extension of the protocol is part of the manuscript (Sexauer et al., 2021), included in the Appendix 3.2.

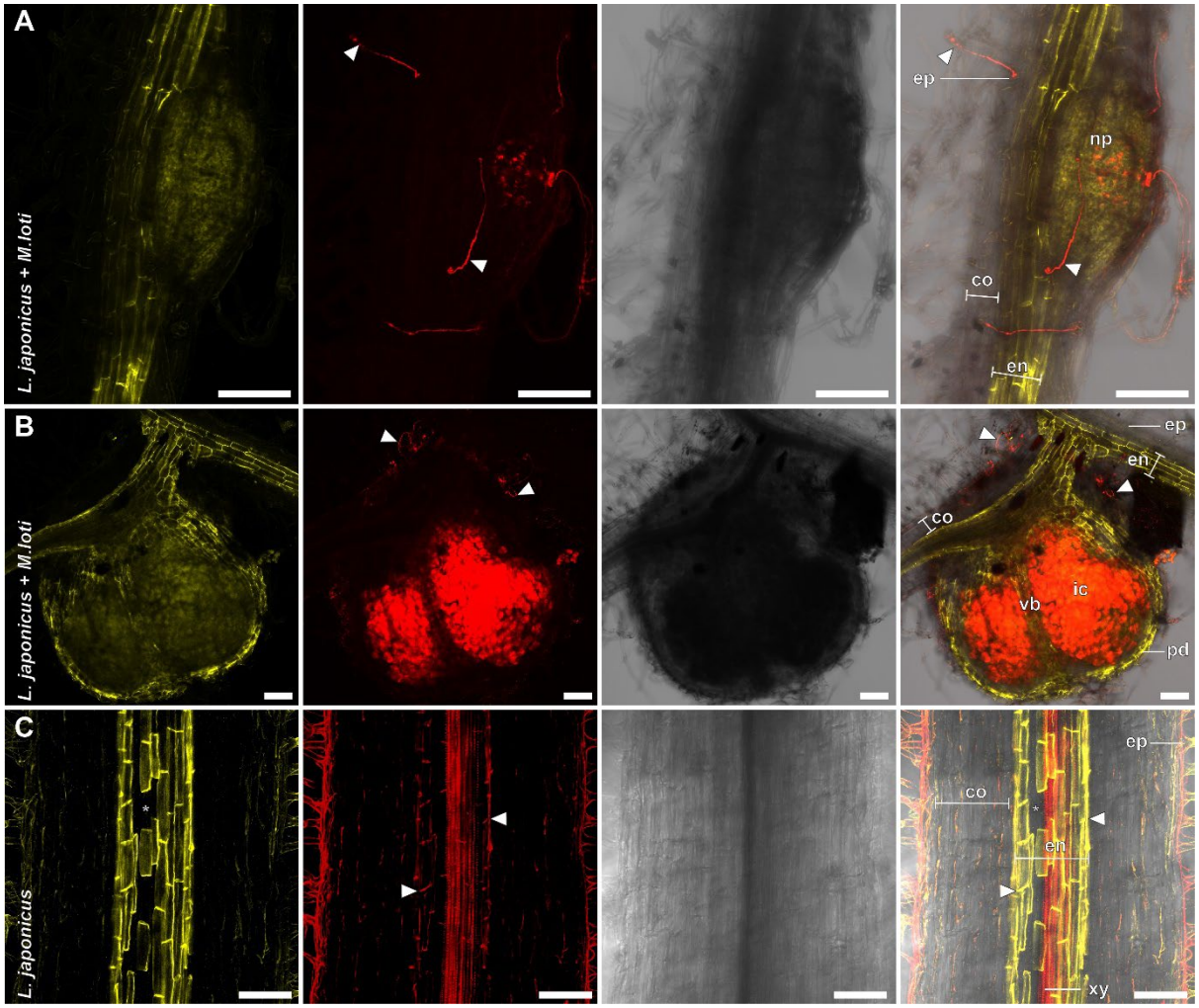

Figure 21. Fluorol Yellow (FY) based suberin staining is compatible with Basic Fuchsin (BF) staining of lignin and fluorescent protein imaging (Sexauer et al., 2021). A *L. japonicus* primordium showing nodule primordia prior to formation of a suberized periderm (10 days post inoculation), **B** mature nodule (21 days post inoculation) and (**C**) uninfected root 10 days post germination stained with FY (**A, B**) or double-stained with FY and BF (**C**) using an optimized ClearSee-based method. Panels (left to right) show FY, DsRED (**A, B**) or BF (**C**), transmission light and merged channel. **A, B** *L. japonicus* infected with *M. loti* expressing DsRED at 10 / 21 days post inoculation, respectively. (**C**) Root co-stained with BF. White arrowheads indicate **A, B** infection threads **C** Casparian strip, * indicate passage cells. Indicated cell types are: co, parenchymatic cortex; en, endodermis; ep, epidermis; xy, xylem; ic, infected nodule cortex and vb, vascular bundle. Scale bars: 100 µm.

Using the optimized protocol, we quantified suberization of *Lotus* wild-type plants and *tml-6* mutants (**Figure 22A**). In Gifu wild-type plants, suberization appeared uniform across different nitrate conditions, showing no significant differences for either patchy or continuous suberization (**Figure 22A**). *tml-6* in contrast showed reduced suberization at high nitrate supply (**Figure 22A**). This effect was significant for patchy and continuous suberization, albeit more pronounced for the latter (**Figure 22A**). Patchy suberization was significantly less in *tml-6* compared to Gifu at 5 mM nitrate

(**Figure 22A**). The continuous suberization was significantly reduced in *tml-6* at all concentrations compared to wild-type plants (**Figure 22A**).

Next, we wanted to see if this function is conserved in *Arabidopsis*. For this we quantified suberization of the *holt-1* mutant in comparison to Col-0 wild-type plants (**Figure 22B**). Col-0 shows a significant increased suberization at low nitrate supply, compared to sufficient nitrate (**Figure 22B**). Equally, *holt-1* shows a negative correlation of external nitrate supply and endodermal suberization. For both Col-0 and *holt-1* change in suberization is mainly mediated by an increase of continuous suberin, while the relative length of patchy suberization is constant (**Figure 22B**). Comparing *holt-1* to Col-0, there are no significant differences in suberization at moderate and high nitrate concentrations, however *holt-1* shows significant more suberin than Col-0 at 100 µM nitrate (**Figure 22B**).

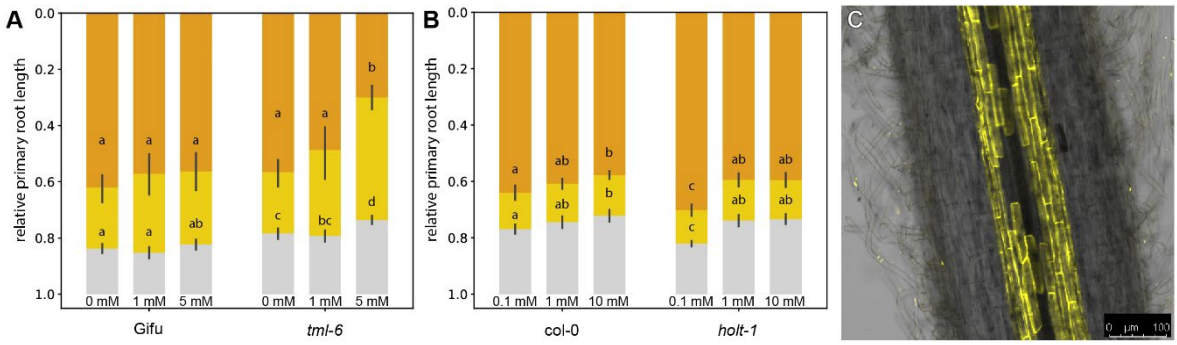

Figure 22. *tml* /*holt* mutants show altered suberization pattern. A-C show suberization of *L. japonicus* (**A, C**) and *A. thaliana* (**B**) roots. (**A, B**) relative position of fully suberized zone (orange) or patchy suberized zone (yellow) along the primary root (grey) of *tml-6* compared to Gifu (**A**) and *holt-1* compared to Col-0 (**B**) at different nitrate conditions. 0 marking the beginning of the root at the hypocotyl, and 1 marking the root tip. **C** Whole root mounts of *L. japonicus*, Fluorol Yellow stained, showing holes in continuous zone of endodermal suberization. Comparisons are based on the relative position of the distal end of the according zone and used analysis of variance (ANOVA) and post-hoc Tukey testing ($p \leq 0.05$), with distinct letters indicating significant differences.

Interestingly, in *Arabidopsis* the differences between *holt-1* and Col-0 in suberization were only present at low nitrate concentrations, while in *Lotus* the differences between *tml-6* and Gifu were more pronounced at high nitrate supply. In both *Arabidopsis* and *Lotus TML / HOLT* levels were increased at these conditions (**Figure 15G, H** and **Figure 12I, J**). Similarly, in context of LR initiations, enhanced *TML* levels were shown to promote LR initiation at high nitrate in *Lotus*, while in *Arabidopsis* increased *HOLT* levels promote LR initiation at low nitrate (**Figure 15H** and **Figure 12J**).

However, in case of suberization, *holt-1* shows increased suberization, while *tml-6* shows the opposite, a decrease of suberization compared to wild type (**Figure 22A, B**).

As TML was predicted to be an F-Box Kelch Repeat protein, assumed to target transcription factors for degradation (Takahara et al., 2013), this could be explained by a diversification of *TML* targets between species. However, this seems unlikely, as *TML* / *HOLT* is highly conserved in dicots. Moreover, its function in LR initiation is conserved between *Arabidopsis* and *Lotus* (Tsikou et al., 2018; Sexauer et al., 2023). A more likely scenario seems to be an indirect impact of *TML* / *HOLT* on suberization as consequence of its role in root system adaptation, which could explain the species-specific mutant phenotypes. To further evaluate this, additional experiments are necessary, including screenings for TML / HOLT targets and interactors, discussed in more detail in the outlook.

Interestingly, in Arabidopsis wild-type plants a correlation between nitrate supply and suberin deposition was apparent, whereas Lotus wild-type plants showed no differences in endodermal suberization between nitrate concentrations, but a larger and more variable patchy zone including "passage holes"(**Figure 22A, C**). This might reflect the symbiotic competence of Lotus, which under natural conditions renders the species independent of substrate-derived nitrogen supply.

Nitrogen physiology – integrating different signals and responses.

This chapter includes parts of the following manuscript:

Moritz Sexauer, Hemal Bhasin, Maria Schoen, Elena Roitsch, Caroline Wall, Ulrike Herzog, Katharina Markmann.

A micro RNA mediates shoot control of root branching

Nature Communications (2023), 14(1), 8083. doi:10.1038/s41467-023-43738-6

In addition, the chapter contains unpublished data, that were prepared by the author of this thesis.

In a natural soil environment, legumes like Lotus usually grow in symbiotic relationships, rarely relying on soil nitrate alone. However, as uptake of soil nitrate has a better energy and nutrient balance than the fixation of aerial nitrogen, symbiosis is strictly regulated by nitrate availability (Lin et al., 2018; Lin et al., 2021; Moreau et al., 2021; Misawa et al., 2022).

On the other hand, the symbiosis-essential transcription factor *NIN* represses *NRT2.1* expression and therefore nitrate uptake (Misawa et al., 2022). Since miR2111 and *TML* have dual functions in AON and in nitrate foraging, we wondered how these functions integrate.

Apart from nitrate, rhizobial infection triggers changes in miR2111 and *TML* transcript abundance (**Figure 23A-C**), and miR2111 acts as a positive regulator of nodule organogenesis by suppressing the nodulation inhibitor *TML* (Tsikou et al., 2018)(**Figure 11**). We thus wondered, how miR2111-*TML* dynamics affected LR formation under symbiotic conditions. Interestingly, in both wild-type and *tml-6* plants, symbiotic infection led to a decrease of LR initiations (**Figure 23D**), implying that an additional *TML*-independent regulation of LR initiation overlays miR2111-*TML* dependent primordium formation under symbiotic conditions.

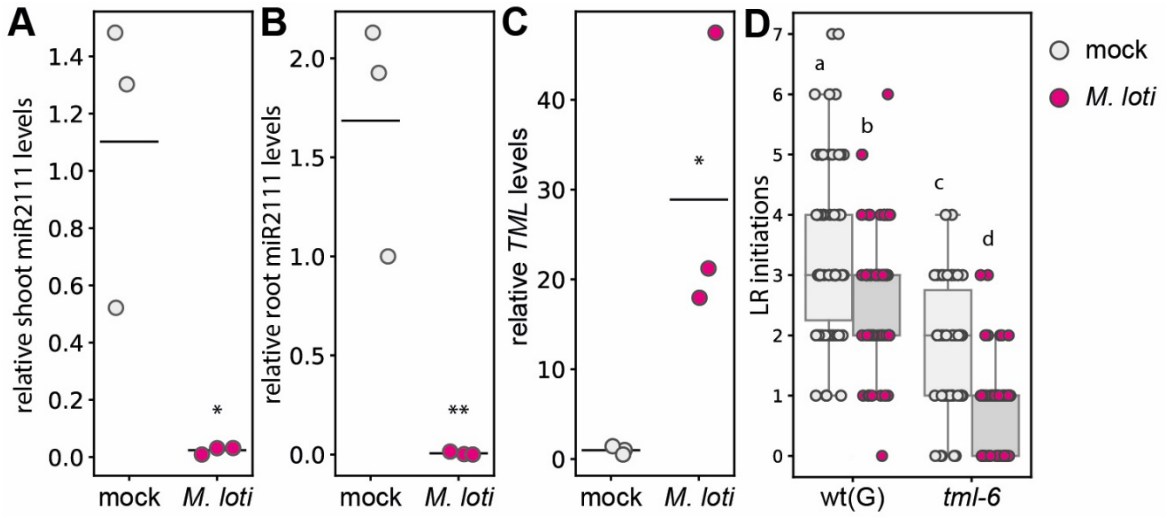

Figure 23 Symbiosis restricts lateral root initiation independent of *TML* (Sexauer et al., 2023), modified. A-C Relative mature miR2111 levels in shoots (**A**) and roots (**B**) and relative *TML* levels (**C**) in the same Lotus plants (ecotype Gifu wild type (wt(G))) at 21 days post inoculation. Plants were cultivated for 3 weeks. **D** LR initiations in symbiotic and non-symbiotic wild-type and *tml-6* plants at 10 days post inoculation. **A-C** qRT-PCR analyses. RNA levels are relative to those of two reference genes. Plants were inoculated with *Mesorhizobium loti* or treated with water (mock control). Comparisons used analysis of variance (ANOVA) and post-hoc Tukey testing ($p \leq 0.05$) (**D**), with distinct letters indicating significant differences or Student's *t*-test (*=$p < 0.05$) (**A-C**). Sample size, replicates and exact p-values are listed in Appendix Table 2. Dotplots show individual data points and a line indicating their average value. Boxplot central line shows median value, box limits indicate the 25 th and 75 th percentiles whiskers extend 1.5 times the interquartile range or to the last datapoint, data are represented by dots.

In symbiotic plants, *TML* is required for the regulation of nodule formation. At sufficient nitrate supply, increased *TML* levels lead to a decrease in nodulation in the wild type, while *tml-1* plants show unaffected, high nodule numbers (**Figure 12G** and **Figure 24A**). However, apart from quantitative regulation of nodulation by nitrate, nodule development is also qualitatively regulated by nitrate supply (Lin et al., 2021). This seemed to be *TML* independent, as we observed a decrease in nodule size in both MG20 wild-type and *tml-1* plants upon nitrate supply (**Figure 24B**). Interestingly, infection thread numbers were lower under high nitrate supply than under nitrogen-deficient conditions in both Gifu wild-type and *tml-6* mutants (**Figure 24C**), suggesting that at the stage of initial bacterial infection, nitrogen-triggered quantitative symbiosis regulation is *TML*-independent.

Over time, the phenotypic differences between *tml* mutants and wild-type plants result in lower biomass of *tml* mutants (Sexauer et al., 2023, Supplementary Fig. 14a,b). Consistent with an impaired resource balance of *tml* mutant plants, *tml-6* and *tml-1* to

produce seeds of significantly lower weight compared to wild-type plants of the respective ecotypes under standard greenhouse conditions **(Figure 24D, E**). As *TML* is only traceably expressed in roots (Takahara et al., 2013), decreased seed weight probably is an indirect effect of impaired nutrient homeostasis impacting plant growth and resource partitioning as a whole.

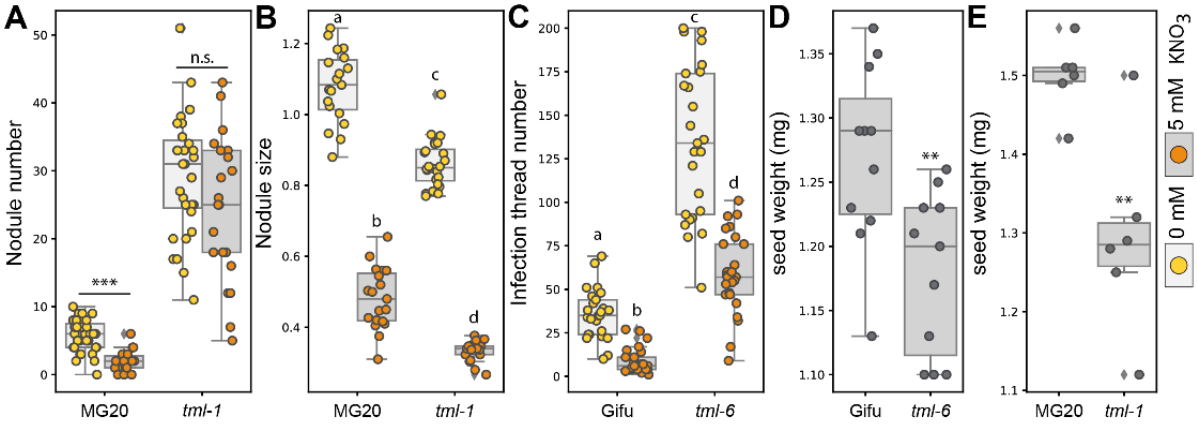

Figure 24. Nitrogen triggered regulation of symbiosis is only partially regulated by *TML*. **A** Nodule number and **B** nodule size of MG20 wild-type and *tml-1* plants. Counts in (**A**) and measurements in (**B**) were on the same plants 4 weeks post inoculation. **B** Shows average size of the three biggest nodules per plant in mm. **C** Number of total infection threads on Gifu wild-type and *tml-6* plants 10 dpi. **D-E** Seed weight of greenhouse grown plants, each datapoint equals the average of 100 seeds of individual mother plants. Comparisons used analysis of variance (ANOVA) and post-hoc Tukey testing ($p \leq 0.05$), with distinct letters indicating significant differences (**B-C**), or Student's t-test (*=$p \leq 0.05$; **=$p \leq 0.01$; ***=$p \leq 0.001$) (**A, D, E**). Sample size, replicates and exact p-values are listed in Appendix Table 2. Boxplot central line shows median value, box limits indicate the 25 th and 75 th percentiles whiskers extend 1.5 times the interquartile range or to the last datapoint, data are represented by dots.

Summarizing, we found that *TML/HOLT* serve multiple functions in the control of root architecture, and regulation of nitrogen fixing symbiosis. In *Lotus*, we observed a dose dependency between miR2111 expression and nodule numbers, indicating a positive regulatory role of miR2111 on nodule formation in response to infection and nitrate supply (**Figure 12**, **Figure 11** and **Figure 24**). Regarding early infection and nodule development, *tml* mutants show enhanced IT numbers and a decreased nodule diameter, however IT numbers and nodule development showed a wild-type-like restriction upon nitrate supply (**Figure 24B, C**). This implies a miR2111-*TML* independent mechanism in restriction of IT formation and nodule development upon nitrate supply.

With respect to endodermal suberization *holt-1* showed an enhanced nitrate responsive suberin deposition at low nitrate, compared to Col-0 wild-type plants, while

tml-6 showed a decreased suberin accumulation at high nitrate, compared to the nitrate unresponsive wild type Gifu. However, comparing the two species Arabidopsis and Lotus, the mutation in *TML* / *HOLT* led to opposed effects, most likely explained by indirect effects of the *TML* / *HOLT* knockout (**Figure 22**).

In *Lotus* the LR positioning varied with nitrate availability (**Figure 16C, D**). This nitrate dependence was lost in *tml-6* and miR2111 overexpression lines (**Figure 17C, D**). Nevertheless, there was no dosage dependance between *TML* levels and LR zonation, which counter indicates a direct control of LR positioning by the miR2111-*TML* regulon (**Figure 17**). Instead, the loss of the LR zonation response to nitrate conditions could reflect an indirect impact of the overall low numbers of LR initiations in plants with reduced *TML* levels. Similarly, the nitrate independency of emerged LR numbers in *tml* mutants may be due to low numbers of primordia in these plants, overlaying possible effects of nitrate dependent emergence (**Figure 12A, B**).

Our data reveal the miR2111-*TML*/*HOLT* regulon as a key factor in systemic control of LR numbers. In both *Arabidopsis* and *Lotus* miR2111 restricts LR initiation in response to nitrate supply via its target *TML* in a dose dependent manner (**Figure 15I**). This renders miR2111 a systemic signal in both the nitrate foraging response and the Autoregulation of Nodulation (**Figure 25A, B**).

Comparing the habitat of *Arabidopsis* and *Lotus*, it becomes apparent that regarding nitrogen availability these plant species tend to be competitive under quite divergent conditions. While *Lotus*, a perennial pioneer plant, thrives on soils poor in nutrients, *Arabidopsis* grows on nutrient rich, disturbed sites, relying on its short lifecycle. Therefore, it does not appear surprising that these plants show different responses to nitrate supply regarding their respective foraging responses (**Figure 15I**). In both species, the systemic control of nitrogen foraging depends on miR2111, the regulation of which in response to nitrate differs strongly between the species, enabling diverse nitrate foraging responses in plants of different lifestyles. Consistently, different *Lotus* ecotypes equally show distinct responses (**Figure 12A-C** and **Figure 13A**).

Interestingly, miR2111 regulation does not only differ between species, but also depends on its respective functional involvement. In rhizobial triggered AON, miR2111 expression regulation is *HAR1* dependent, whereas in nitrate foraging, miR2111 regulation is *HAR1* independent (**Figure 25A**). Indeed, both *HAR1* and *CLV1* appear to

be mainly involved in local rather than systemic nitrate foraging dynamics (**Figure 25A, B**) (Araya et al., 2014). In contrast, shoot localized CRA2 was suggested to regulate miR2111 expression upon rhizobial infection (Gautrat et al., 2020), although miR2111 expression maintained responsiveness to nitrate supply in *cra2* mutants (Gautrat et al., 2020), suggesting additional regulatory mechanisms. In *Medicago truncatula,* the *CRA2* root fraction was shown to inhibit LR formation at low nitrogen. In *Arabidopsis* the putative *CRA2* orthologue *CEPR1* was suggested to locally inhibit LR formation in dependence of *CEP5* as a putative peptide ligand of *CEPR1* (Roberts et al., 2016; Zhu et al., 2020). The combined data suggest that during the evolution of nodulation symbiosis, legumes adapted genes involved in local nitrate foraging for the systemic AON, thereby reutilizing pre-established nitrate responsive pathways. The integration of local and systemic regulatory mechanisms, as well as the factors involved in the genetic regulation of miR2111 in response to nitrate foraging remains to be elucidated (**Figure 25A, B**).

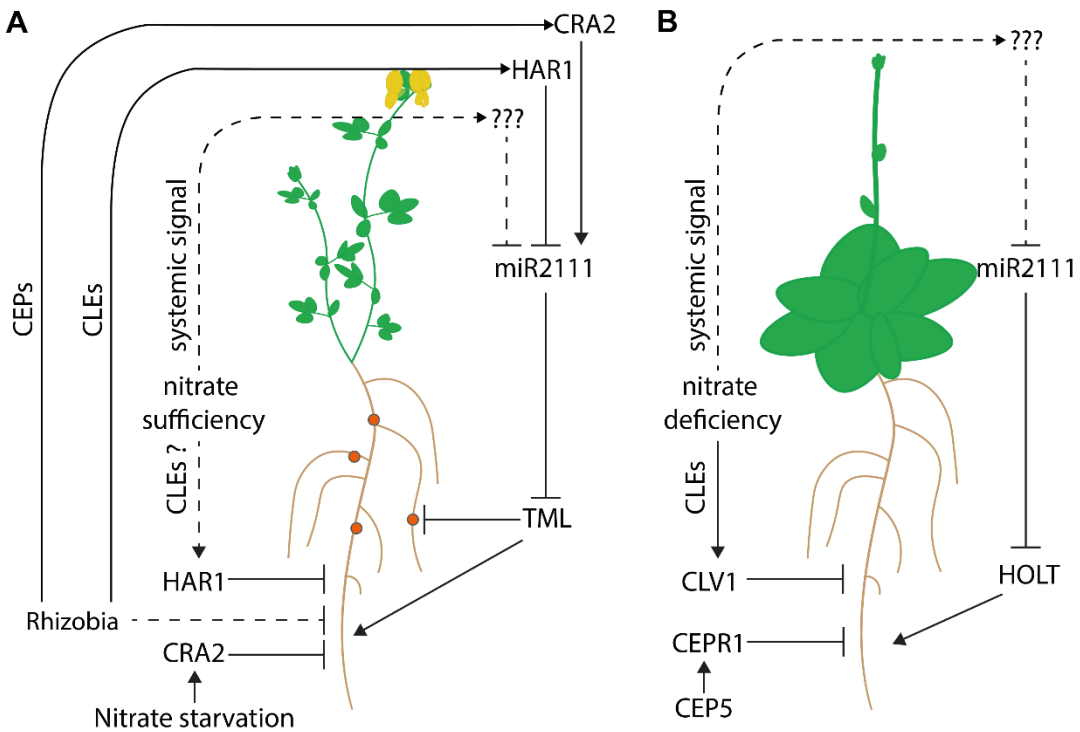

Figure 25 In context of nitrogen foraging, miR2111 is regulated independent of HAR1 and CRA2/ CEPR1. A Model of miR2111, *TML*, *HAR1* and *CRA2* involvement in local and systemic LR control and adaptation to nitrate and their function in the Autoregulation of Nodulation in legumes. **B** Model of miR2111, *HOLT*, *CLV1* and *CEPR1* involvement in local and systemic LR control and adaptation to nitrate, conserved in *A. thaliana.* Dotted lines resemble hypothetical pathways concluded from phenotypical observations, with so far unknown genetic basis.

Based on our observations, we propose miR2111 as one of the postulated systemic nitrogen signals in nitrate foraging (Alvarez et al., 2012; Guan et al., 2014; Oldroyd and Leyser, 2020). Interestingly, miR2111 can serve as either nitrate sufficiency or nitrate starvation signal, depending on the species (**Figure 15I** and **Figure 25A, B**).

Indeed, in Medicago it was shown that in context of AON miR2111 is regulated via *CEP* and *CLE* peptide signaling under nitrogen starvation as well as nitrate supply and rhizobial infection (Gautrat et al., 2020; Moreau et al., 2021). This defines miR2111 as an nitrogen homeostasis signal, which integrates multiple nitrogen signals. Further, in Arabidopsis, miR2111 was identified to be induced by phosphate starvation (Hsieh et al., 2009; Pant et al., 2009). If this regulation is conserved or has physiological relevance needs to be further elucidated.

The nitrate foraging behavior of Arabidopsis has been intensively studied in the past and was reviewed in (Oldroyd and Leyser, 2020). It was shown that while local supply of nitrate promotes root growth locally, nitrate sufficiency restricts root growth systemically, via an unknown systemic signal (Oldroyd and Leyser, 2020). In Arabidopsis, our findings match previous observations, and identify miR2111 as a systemic signal, restricting LR initiation at nitrate sufficiency. Systemic control of LR initiation instead of emergence hereby allows the plant to locally restrict the emergence of LR primordia at local low nitrate concentrations, a function which most likely depends on *CLV1* (**Figure 25A, B**) (Araya et al., 2014).

Lotus nitrate foraging has not been described in detail so far. Our data reveal an inverse foraging behavior, or a lack of strong foraging response (**Figure 12A-C, Figure 13A** and **Figure 14A-C**). Considering the second function of miR2111 in Lotus as a positive regulator of nodule formation, these findings indicate that in their natural habitat, Lotus plants may rely more on nitrogen supplied by symbiotic nitrogen fixation than on nitrate uptake by roots. In such a scenario, a tightly controlled AON is of higher fitness relevance than nitrate foraging.

The presented data identify miR2111 and *TML*/*HOLT* as conserved factors in root architectural control, suggesting that they were evolutionarily co-opted by rhizobial nodulation symbiosis to regulate root responses to symbiotic bacteria, and organogenesis of nodule organs (Tsikou et al., 2018). Consistent with this hypothesis, the transcription factors *SCARECROW* and *SHORTROOT (Dong et al., 2020)*, as well as

ASYMMETRIC LEAVES2-LIKE18 (Schiessl et al., 2019; Soyano et al., 2019) and *STYLISH* (Shrestha et al., 2021) mediating auxin signaling hold dual roles in nodule organogenesis and root development, and comparative transcriptome analysis of LR and nodule primordia further supports genetic ties between these organs (Schiessl et al., 2019; Libourel et al., 2023; Lee et al., 2024; Sexauer and Markmann, 2024).

A second pathway that was likely evolutionarily co-opted by RLS is the control of nitrate uptake via *CEP* peptides. At least the *CEP*/*CEPR1* regulon, known to regulate *NRT2.1* expression in response to nitrate availability, was adapted to regulate nodule formation via miR2111 (Gautrat et al., 2020; Ota et al., 2020; Luo et al., 2022b). In summary, it appears that the evolution of the RLS in legumes involved the adaptation of at least three nodes regulating different pathways of nitrate homeostasis, namely miR2111-*HOLT/TML*, CLE-*CLV1/HAR1* and CEP-*CEPR1/CRA2,* and their integration in AON. At the same time their ancestral function was conserved, but lost in relevance, as both nitrate uptake and LR formation are restricted by symbiosis (**Figure 23D** and **Figure 25A, B**) (Araya et al., 2014; Tsikou et al., 2018; Ota et al., 2020; Hayashi-Tsugane and Kawaguchi, 2022; Luo et al., 2022b; Misawa et al., 2022; Sexauer et al., 2023).

Outlook

Our data reveal the miR2111-*TML*/*HOLT* regulon as a key factor in systemic control of root system architecture and LR organ number. An exciting future challenge will be determining the molecular activity of the TML/HOLT protein, a proposed component of the E3 Ubiquitin ligase complex in Arabidopsis (Schumann et al., 2011) with a possible role in mediating degradation of the target transcription factors (Schumann et al., 2011). To this end, deciphering the downstream signaling of miR2111-*TML*/*HOLT* is a key next step. Determining downstream targets/ possible interactors of TML/HOLT will help us better understand how the miR2111-*TML*/*HOLT* regulon functionally integrates with hormonal networks and other regulators of root growth.

Addressing the question of downstream targets / possible interactors of TML/HOLT, we plan on combining targeted and untargeted approaches. For selection of possible candidates for a targeted approach, transcriptomic datasets published in (Schiessl et al., 2019) and (Lee et al., 2024) comparing root and nodule initiation could be utilized, as we expect TML targets to be involved in both. Testing protein-protein interaction for the chosen candidates could be done via co immunoprecipitation, FRET-FLIM (Förster Resonance Energy Transfer by Fluorescence Lifetime Imaging) or yeast two hybrid, using a F-BOX deletion version of *TML*/*HOLT* to circumvent proteasomal degradation. The targeted approach should be complemented by an unbiased approach for identifying *TML*/*HOLT* interactors using TurboID (Mair et al., 2019). This could identify additional potential interactors which are not differentially regulated during LR or nodule organogenesis. All identified candidates should be confirmed by two distinct methods at least.

Further, it will be interesting to determine whether there is a diversification between TML and HOLT targets, regarding both general differences between species, but also between functional context in Lotus or other nodulating legumes. This will elucidate whether the control of LR and nodule numbers are achieved by overlapping or by divergent downstream pathways. In addition, it will be exciting to decipher how regulation of LR and nodule organogenesis intertwine, how legumes achieve a functional nutrient foraging response while at the same time regulating their nodule numbers. Identification of TML targets could further lead to insights in control of

infection thread regulation and progression, as in *tml* mutants not only nodule numbers are deregulated, but also IT numbers.

Upstream of the miR2111-*TML*/*HOLT* regulon, the regulation of miR2111 remains to be investigated in more detail. It will be an interesting challenge to identify signaling components involved in regulating miR2111 expression downstream of *HAR1* and *CRA2,* and factors regulating miR2111 expression in response to nitrate supply. Several additional shoot expressed receptors like *CORYNE*, *CLAVATA2* or *KLAVIER* (Miyazawa et al., 2010; Krusell et al., 2011; Nowak et al., 2019) have been described to be involved in AON.

In respective mutant lines miR2111 expression in response to rhizobia or nitrate supply should be quantified using qRT-PCR, to test for a possible involvement in miR2111 expression regulation. Further, in collaboration with Dr. Manuel Frank we identified approximately 35 additional candidate genes for *HAR1* downstream signaling using comparative single cell sequencing data of Lotus wild-type and *har1-1* mutant plants. Complementary, to identify possible negative regulators of miR2111, we are conducting a *pMIR2111:GUS* activator screen. For this *pMIR2111:GUS* has been crossed into the active LORE1 line to generate mutagenized F3 seeds, homozygous for *pMIR2111:GUS* (Fukai et al., 2012; Urbanski et al., 2012; Malolepszy et al., 2016). Under symbiotic greenhouse conditions pMIR2111:GUS shows no signal, because miR2111 expression is suppressed by both nitrate supply and rhizobia (**Figure 25**). This will be used to screen for mutants in *MIR2111-3* suppressors which in theory should lead to a gain of signal under greenhouse conditions.

While comparing Arabidopsis and Lotus, the question arises how the divergent regulation of miR2111 is achieved. It would be interesting to see if miR2111 accumulation patterns are ecotype specific in Arabidopsis as well, and whether this results in differences in foraging behavior. In Arabidopsis, miR2111 was shown to be responsive to phosphate starvation. It will be interesting to see whether this regulation also results in a foraging response involving root system architectural adaptations and whether miR2111 is responsive to additional biotic or abiotic factors like nutrient levels or beneficial bacteria. Further the question arises whether the differences in miR2111 regulation between Arabidopsis and Lotus are a prerequisite for the

evolution of a beneficial RNS. To this end, it would be exciting to study the miR2111-*TML* regulon in additional nodulating and non-nodulating species of the FaFaCuRo.

Another important next step will be, the generation of so called “rescue constructs” for both *tml* and *holt* mutants, as overexpression of *TML* but also expression of *TML* under a native promotor fragment was not sufficient to reduce nodule numbers of *tml* mutants to wild-type-like levels. To tackle this problem, we plan to generate a construct expressing *TML* by a large promotor fragment, including predicted CIS-regulatory elements in the 20 kb upstream promotor region. If this approach will be successful, this promotor fragment could be used to study the expression pattern of *TML* and elucidate possible local effects on regulation of *TML* expression deduced from split root experiments (**Figure 12J**).

List of Abbreviations

AFB3	AUXIN SIGNALING F-BOX 3
AGL44	AGAMOUS-LIKE 44
AGO	ARGONAUT
AM	arbuscular mycorrhiza
ANR1	ARABIDOPSIS NITRATE REGULATED 1
AON	Autoregulation of Nodulation
AR	adventitious root
Arabidopsis	*Arabidopsis thaliana*
ARF	AUXIN RESPONSE FACTOR
ASL	ASYMMETRIC LEAVES2-LIKE
At	*Arabidopsis thaliana*
BAM	BARELY ANY MERISTEM
BES1	BRI1-EMS-SUPPRESSOR 1
BF	basic fuchsin
Bn	*Brassica napus*
C	carbon
CASP	CASPARIAN STRIPDOMAIN PROTEIN
CCaMK	CALCIUM AND CALMODULIN-DEPENDENT KINASE
CEI	cortex endodermis initial
CEID	cortex endodermis initial daughter
CEP	C-Terminally ENCODED Peptides
CEPD	CEP DOWNSTREAM
CEPDL	CEP DOWNSTREAM LIKE
CEPH	CEPD-INDUCED PHOSPHATASE
CEPR1	CEP RECEPTOR 1
CIF1/2	CASPARIAN STRIP INTEGRITY FACTOR 1/2
CLE	CLAVATA3/EMBRYO SURROUNDING REGION
CLE-RS	CLE-ROOT SIGNAL
CLV1	CLAVATA 1
CNGC	CYCLIC NUCLEOTIDE GATED CHANNELS
co	cortex
CR	crown root
CRA2	COMPACT ROOT ARCHITECTURE 2
CW	calcofluor white
DCL	DICER-LIKE
DEOG	differentially expressed orthogroups
DMI	DOES NOT MAKE INFECTIONS
DNA	deoxyribonucleic acid
dpi	days post inoculation
EIN2	ETHYLEN INSENSITIVE 2
en	endodermis
ep	epidermis
FaFaCuRo	Fabales, Fagales, Cucurbitales, Rosales
FY	fluorol yellow
Gm	*Glycine max*
HAR1	HYPERNODULATION ABERRANT ROOT FORMATION 1
HD-ZIPIII	CLASS III HOMEODOMAIN LEUCINE-ZIPPER

HEN1	HUA ENHANCER 1
HOLT	HOMOLOGUE OF LEGUME TML
HY5	ELONGATED HYPOCOTYL 5
HYL1	HYPONASTIC LEAVES 1
IAA28	INDOLE-3-ACETIC ACID INDUCIBLE 28
ic	infected cell
IT	infection thread
ko	knockout
LBD	LATERAL ORGAN BOUNDARIES DOMAIN
LHK	LOTUS HISTIDIN KINASE
Lj	*Lotus japonicus*
Lotus	*Lotus japonicus*
LR	lateral root
LRP	lateral root primordia
LRP1	LATERAL ROOT PRIMORDIUM1
LSH	LIGHT SENSITIVE HYPOCOTYL
LYK3	LYSM-CONTAINING RECEPTOR-LIKE KINASE 3
Medicago	*Medicago truncatula*
Mt	*Medicago truncatula*
miR	micro RNA
miRNA	micro RNA
Mt	*Medicago truncatula*
MYB	MYB transcription factor
N	nitrogen
NAC4	NAC DOMAIN CONTAINING PROTEIN 4
NFP	NOD FACTOR PERCEIPTION
NFR	NOD FACTOR RECEPTOR
NIC	NITRATE INDUCED CLE
NIN	NODULE INDUCTION
NOOT	NODULE ROOT
NLP	NIN LIKE PROTEIN
NRT	NITRATETRANSPORTER
NSP	NODULATION SIGNALING PATHWAY
nt	nucleotides
NUP	NUCLEOPORIN
ox	overexpression
PCR	Polymerase chain reaction
pd	periderm
ph	phloem
PHO1	PHOSPHATE 1
PIN	PIN-FORMED
PLT	PLETHORA
PR	primary root
PUB	PLANT U-BOX PROTEIN 1
Pv	*Phaseolus vulgaris*
QC	quiescent center
RDR6	RNA DEPENDENT RNA POLYMERASE 6
RIC	RHIZOBIA INDUCED CLE
RLS	rhizobia legume symbiosis
RNA	ribonucleic acid
RNS	root nodule symbiosis
RT-qPCR	real time quantitative PCR
SCN	stem cell niche

SCR	SCARECROW
SE	SERRATED
SGN	SCHENGEN
SGS3	SUPPRESSOR OF GENE SILENCING 3
SHR	SHORT ROOT
SIP	SYMRK INTERACTING PROTEINS
siRNA	small interfering RNA
Sl	*Solanum lycopersicum*
SR	seminal root
sRNA	small RNA
STY	STYLISH
SUNN	SUPER NUMERIC NODULES
TAR2	TRYPTOPHAN AMINOTRANSFERASE RELATED 2
TAS3	TRANS-ACTING SIRNA3
tasiR	trans acting small interfering RNA
TCP20	(TCP)-DOMAIN FAMILY PROTEIN 20
TML	TOO MUCH LOVE
vb	vascular bundle
WOX	WUSCHEL RELATED HOMEOBOX
wt	wild type
wt(G)	wild type (Gifu)
wt(M)	wild type (MG20)
xy	xylem

Acknowledgements

I want to thank Katharina Markmann for the opportunity to write this thesis in her supervision. I want to thank her for the opportunity to work quite autonomous and develop my own project. At the same time, she always supported and advised me.

I want to thank Uli for great experimental support and always cheering up the Lab.

I want to thank Caro for responsibly taking care of the aphids, and many nice discussions with or without an afterwork-beer.

I want to thank Max for support during acetylene reduction assays.

I want to thank Maria, Elena and Michael for support in the lab and staying well beyond handing in their thesis, in case of Elena even joining me in Halle again.

I want to thank Johanna Schröter and the gardening team for dedicated plant care, and Caterina Brancato for help with plant transformations.

I want to thank Dugald Reid for help with construct generation and I want to thank Laura Ragni, Toni G. Andersen, Farid El Kasmi and Üner Kulokisaoglu for discussions.

I want to thank Isabelle Monte for hosting me for final experiments in her lab and agreeing to be one of my examiners.

I want to thank Klaus Harter for support since my master thesis and enabling me to keep working in the ZMBP after the move to Halle – also for being reviewer of this thesis.

I want to thank Marja Timmermanns and Claudia Oecking for discussions and supervision.

I want to thank Martin, Merle, and Mars for taking me in as an occasional roommate.

I want to thank Peter Börkner, Bianca Rosinsky, Michael Röser, Juliane Werner, Ramona Abe and Andreas Fischer for supporting me during my short time in Halle.

I want to thank my parents Gabi and Stefan for supporting me during my whole studies and first enabling me my bachelor's and master's degree.

I want to thank the whole bot2 and the JvS institute, for a great welcome in Würzburg and a lot of support there and some distraction from writing.

Further I want to already thank all the people helping me in follow up projects, which are not part of this thesis. Namely: Ann-Kristin, Tine, Yvonne, Michael, Michael, Ulrich, Samuel, Katharina, Konstantin, Jutta, especially want to thank Philipp for proofreading.

Also, I want to thank Sonja and Melina for the great collaborative effort in organizing the JvS summer symposium.

Finally, I want to thank Angela for always supporting me, for moving with me to Halle, and FINALLY to Würzburg. I want to thank her for her support in graphical representations and for proofreading. All in all, I want to thank her for always having my back, also during difficult times.

Literature

Achkar, N.P., Cambiagno, D.A., and Manavella, P.A. (2016). miRNA biogenesis: A dynamic pathway. Trends in Plant Science **21,** 1034-1044.

Aida, M., Beis, D., Heidstra, R., Willemsen, V., Blilou, I., Galinha, C., Nussaume, L., Noh, Y.S., Amasino, R., and Scheres, B. (2004). The *PLETHORA* genes mediate patterning of the Arabidopsis root stem cell niche. Cell **119,** 109-120.

Akamatsu, A., Nagae, M., and Takeda, N. (2022). The CYCLOPS response element in the *NIN* promoter is important but not essential for infection thread formation during *Lotus japonicus*–rhizobia symbiosis. Molecular Plant-Microbe Interactions **35,** 650-658.

Akamatsu, A., Nagae, M., Nishimura, Y., Romero Montero, D., Ninomiya, S., Kojima, M., Takebayashi, Y., Sakakibara, H., Kawaguchi, M., and Takeda, N. (2021). Endogenous gibberellins affect root nodule symbiosis via transcriptional regulation of *NODULE INCEPTION* in *Lotus japonicus*. The Plant Journal **105,** 1507-1520.

Alassimone, J., Fujita, S., Doblas, V.G., van Dop, M., Barberon, M., Kalmbach, L., Vermeer, J.E., Rojas-Murcia, N., Santuari, L., Hardtke, C.S., and Geldner, N. (2016). Polarly localized kinase SGN1 is required for Casparian strip integrity and positioning. Nat Plants **2,** 16113.

Alvarez, J.M., Vidal, E.A., and Gutierrez, R.A. (2012). Integration of local and systemic signaling pathways for plant N responses. Current Opinion in Plant Biology **15,** 185-191.

Andersen, T.G., Barberon, M., and Geldner, N. (2015). Suberization—the second life of an endodermal cell. Current Opinion in Plant Biology **28,** 9-15.

Andersen, T.G., Naseer, S., Ursache, R., Wybouw, B., Smet, W., De Rybel, B., Vermeer, J.E.M., and Geldner, N. (2018). Diffusible repression of cytokinin signalling produces endodermal symmetry and passage cells. Nature **555,** 529-533.

Antolín-Llovera, M., Ried, Martina K., and Parniske, M. (2014). Cleavage of the SYMBIOSIS RECEPTOR-LIKE KINASE ectodomain promotes complex formation with Nod Factor Receptor 5. Current Biology **24,** 422-427.

Araya, T., von Wiren, N., and Takahashi, H. (2016). CLE peptide signaling and nitrogen interactions in plant root development. Plant Molecular Biology **91,** 607-615.

Araya, T., Miyamoto, M., Wibowo, J., Suzuki, A., Kojima, S., Tsuchiya, Y.N., Sawa, S., Fukuda, H., von Wiren, N., and Takahashi, H. (2014). CLE-CLAVATA1 peptide-receptor signaling module regulates the expansion of plant root systems in a nitrogen-dependent manner. Proceedings of the National Academy of Sciences **111,** 2029-2034.

Arrighi, J.-F.o., Barre, A., Ben Amor, B., Bersoult, A., Soriano, L.C., Mirabella, R., de Carvalho-Niebel, F., Journet, E.-P., Ghérardi, M.l., Huguet, T., Geurts, R., Dénarié, J., Rougé, P., and Gough, C. (2006). The *Medicago truncatula Lysine Motif-Receptor-Like Kinase* gene family includes *NFP* and new nodule-expressed genes. Plant Physiology **142,** 265-279.

Asim, M., Ullah, Z., Xu, F., An, L., Aluko, O.O., Wang, Q., and Liu, H. (2020). Nitrate signaling, functions, and regulation of root system architecture: Insights from *Arabidopsis thaliana*. Genes **11**.

Atkinson, J.A., Rasmussen, A., Traini, R., Voß, U., Sturrock, C., Mooney, S.J., Wells, D.M., and Bennett, M.J. (2014). Branching out in roots: uncovering form, function, and regulation. Plant Physiology **166,** 538-550.

Baranauskė, S., Mickutė, M., Plotnikova, A., Finke, A., Venclovas, Č., Klimašauskas, S., and Vilkaitis, G. (2015). Functional mapping of the plant small RNA methyltransferase: HEN1 physically interacts with HYL1 and DICER-LIKE 1 proteins. Nucleic Acids Research **43,** 2802-2812.

Barberon, M. (2017). The endodermis as a checkpoint for nutrients. New Phytologist **213,** 1604-1610.

Barberon, M., and Geldner, N. (2014). Radial transport of nutrients: The plant root as a polarized epithelium. Plant Physiology **166,** 528-537.

Barberon, M., Vermeer, Joop Engelbertus M., De Bellis, D., Wang, P., Naseer, S., Andersen, Tonni G., Humbel, Bruno M., Nawrath, C., Takano, J., Salt, David E., and Geldner, N. (2016). Adaptation of root function by nutrient-induced plasticity of endodermal differentiation. Cell **164,** 447-459.

Barłóg, P., Grzebisz, W., and Łukowiak, R. (2022). Fertilizers and fertilization strategies mitigating soil factors constraining efficiency of nitrogen in plant production. Plants (Basel, Switzerland) **11**.

Benkovics, A.H., and Timmermans, M.C.P. (2014). Developmental patterning by gradients of mobile small RNAs. Current Opinion in Genetics & Development **27,** 83-91.

Berg, R.H. (1999). *Frankia* forms infection threads. Canadian Journal of Botany **77,** 1327-1333.

Bologna, N.G., and Voinnet, O. (2014). The diversity, biogenesis, and activities of endogenous silencing small RNAs in Arabidopsis. Annual Review of Plant Biology **65,** 473-503.

Bologna, N.G., Iselin, R., Abriata, L.A., Sarazin, A., Pumplin, N., Jay, F., Grentzinger, T., Dal Peraro, M., and Voinnet, O. (2018). Nucleo-cytosolic shuttling of ARGONAUTE1 prompts a revised model of the plant MicroRNA pathway. Molecular Cell **69,** 709-719.e705.

Bouche, N., Lauressergues, D., Gasciolli, V., and Vaucheret, H. (2006). An antagonistic function for Arabidopsis *DCL2* in development and a new function for *DCL4* in generating viral siRNAs. The EMBO journal **25,** 3347-3356.

Breakspear, A., Liu, C., Roy, S., Stacey, N., Rogers, C., Trick, M., Morieri, G., Mysore, K.S., Wen, J., Oldroyd, G.E.D., Downie, J.A., and Murray, J.D. (2014). The root hair "infectome" of *Medicago truncatula* uncovers changes in cell cycle genes and reveals a requirement for auxin signaling in rhizobial infection The Plant Cell **26,** 4680-4701.

Brioudes, F., Jay, F., Sarazin, A., Grentzinger, T., Devers, E.A., and Voinnet, O. (2021). *HASTY,* the Arabidopsis *EXPORTIN5* ortholog, regulates cell-to-cell and vascular microRNA movement. The EMBO journal **40,** e107455-e107455.

Brodersen, P., Sakvarelidze-Achard, L., Bruun-Rasmussen, M., Dunoyer, P., Yamamoto, Y.Y., Sieburth, L., and Voinnet, O. (2008). Widespread translational inhibition by plant miRNAs and siRNAs. Science **320,** 1185-1190.

Buhtz, A., Springer, F., Chappell, L., Baulcombe, D.C., and Kehr, J. (2008). Identification and characterization of small RNAs from the phloem of *Brassica napus*. The Plant Journal **53,** 739-749.

Burkart, R.C., Strotmann, V.I., Kirschner, G.K., Akinci, A., Czempik, L., Dolata, A., Maizel, A., Weidtkamp-Peters, S., and Stahl, Y. (2022). PLETHORA-WOX5 interaction and subnuclear localization control *Arabidopsis* root stem cell maintenance. EMBO reports **23,** e54105.

Buskila, Y., Tsror Lahkim, L., Sharon, M., Teper-Bamnolker, P., Holczer-Erlich, O., Warshavsky, S., Ginzberg, I., Burdman, S., and Eshel, D. (2011). Postharvest dark skin spots in potato tubers are an oversuberization response to *Rhizoctonia solani* infection. Phytopathology **101,** 436-444.

Buzas, D.M., and Gresshoff, P.M. (2007). Short- and long-distance control of root development by *LjHAR1* during the juvenile stage of *Lotus japonicus*. Journal of Plant Physiology **164,** 452-459.

Capdevila-Cortada, M. (2019). Electrifying the Haber–Bosch. Nature Catalysis **2,** 1055-1055.

Carlsbecker, A., Lee, J.-Y., Roberts, C.J., Dettmer, J., Lehesranta, S., Zhou, J., Lindgren, O., Moreno-Risueno, M.A., Vatén, A., Thitamadee, S., Campilho, A., Sebastian, J., Bowman, J.L., Helariutta, Y., and Benfey, P.N. (2010). Cell signalling by microRNA165/6 directs gene dose-dependent root cell fate. Nature **465,** 316-321.

Cathebras, C., Gong, X., Andrade, R.E., Vondenhoff, K., Keller, J., Delaux, P.-M., Hayashi, M., Griesmann, M., and Parniske, M. (2022). A novel *cis*-element enabled bacterial uptake by plant cells. pre-print bioRxiv, 2022.2003.2028.486070.

Cerezo, M., Tillard, P., Filleur, S., Muños, S., Daniel-Vedele, F., and Gojon, A. (2001). Major alterations of the regulation of root NO^{3-}uptake are associated with the mutation of *NRT2.1* and *NRT2.2* genes in Arabidopsis. Plant Physiology **127,** 262-271.

Chai, S., Chen, J., Yue, X., Li, C., Zhang, Q., de Dios, V.R., Yao, Y., and Tan, W. (2022). Interaction of BES1 and LBD37 transcription factors modulates brassinosteroid-regulated root foraging response under low nitrogen in arabidopsis. Frontiers in plant science **13**.

Charpentier, M., and Oldroyd, G.E.D. (2013). Nuclear calcium signaling in plants. Plant Physiology **163,** 496-503.

Charpentier, M., Bredemeier, R., Wanner, G., Takeda, N., Schleiff, E., and Parniske, M. (2008). *Lotus japonicus* CASTOR and POLLUX are ion channels essential for perinuclear calcium spiking in legume root endosymbiosis. The Plant Cell **20,** 3467-3479.

Charpentier, M., Sun, J., Martins, T.V., Radhakrishnan, G.V., Findlay, K., Soumpourou, E., Thouin, J., Véry, A.-A., Sanders, D., Morris, R.J., and Oldroyd, G.E.D. (2016). Nuclear-localized cyclic nucleotide-gated channels mediate symbiotic calcium oscillations. Science **352,** 1102-1105.

Chen, T., Zhu, H., Ke, D., Cai, K., Wang, C., Gou, H., Hong, Z., and Zhang, Z. (2012). A MAP Kinase Kinase Interacts with SymRK and regulates nodule organogenesis in *Lotus japonicus* The Plant Cell **24,** 823-838.

Chen, X., and Rechavi, O. (2021). Plant and animal small RNA communications between cells and organisms. Nature Reviews Molecular Cell Biology.

Chen, X., Yao, Q., Gao, X., Jiang, C., Harberd, Nicholas P., and Fu, X. (2016). Shoot-to-Root mobile transcription factor *HY5* coordinates plant carbon and nitrogen acquisition. Current Biology **26,** 640-646.

Chiasson, D.M., Haage, K., Sollweck, K., Brachmann, A., Dietrich, P., and Parniske, M. (2017). A quantitative hypermorphic *CNGC* allele confers ectopic calcium flux and impairs cellular development. eLife **6,** e25012.

Chitwood, D.H., Nogueira, F.T.S., Howell, M.D., Montgomery, T.A., Carrington, J.C., and Timmermans, M.C.P. (2009). Pattern formation via small RNA mobility. Genes & development **23,** 549-554.

Clark, S.E., Williams, R.W., and Meyerowitz, E.M. (1997). The *CLAVATA1* gene encodes a putative receptor kinase that controls shoot and floral meristem size in Arabidopsis. Cell **89,** 575-585.

Cohen, H., Fedyuk, V., Wang, C., Wu, S., and Aharoni, A. (2020). *SUBERMAN* regulates developmental suberization of the Arabidopsis root endodermis. The Plant Journal **102,** 431-447.

Cui, H., Levesque, M.P., Vernoux, T., Jung, J.W., Paquette, A.J., Gallagher, K.L., Wang, J.Y., Blilou, I., Scheres, B., and Benfey, P.N. (2007). An evolutionarily conserved mechanism delimiting SHR movement defines a single layer of endodermis in plants. Science **316,** 421-425.

Dalmay, T., Hamilton, A., Rudd, S., Angell, S., and Baulcombe, D.C. (2000). An RNA-dependent rna polymerase gene in *Arabidopsis* is required for posttranscriptional gene silencing mediated by a transgene but not by a virus. Cell **101,** 543-553.

De Rybel, B., Vassileva, V., Parizot, B., Demeulenaere, M., Grunewald, W., Audenaert, D., Van Campenhout, J., Overvoorde, P., Jansen, L., Vanneste, S., Möller, B., Wilson, M., Holman, T., Van Isterdael, G., Brunoud, G., Vuylsteke, M., Vernoux, T., De Veylder, L., Inzé, D., Weijers, D., Bennett, M.J., and Beeckman, T. (2010). A novel *Aux/IAA28* signaling cascade activates *GATA23*-dependent specification of lateral root founder cell identity. Current Biology **20,** 1697-1706.

De Smet, I. (2012). Lateral root initiation: one step at a time. New Phytologist **193,** 867-873.

De Smet, I., Tetsumura, T., De Rybel, B., Frey, N.F.d., Laplaze, L., Casimiro, I., Swarup, R., Naudts, M., Vanneste, S., Audenaert, D., Inzé, D., Bennett, M.J., and Beeckman, T. (2007). Auxin-dependent regulation of lateral root positioning in the basal meristem of Arabidopsis. Development **134,** 681-690.

Delaux, P.-M., Bécard, G., and Combier, J.-P. (2013). *NSP1* is a component of the Myc signaling pathway. New Phytologist **199,** 59-65.

Deleris, A., Gallego-Bartolome, J., Bao, J., Kasschau Kristin, D., Carrington James, C., and Voinnet, O. (2006). Hierarchical action and inhibition of plant *Dicer-Like* proteins in antiviral defense. Science **313,** 68-71.

Della Rovere, F., Fattorini, L., D'Angeli, S., Veloccia, A., Falasca, G., and Altamura, M.M. (2013). Auxin and cytokinin control formation of the quiescent centre in the adventitious root apex of Arabidopsis. Annals of botany **112,** 1395-1407.

Dénarié, J., and Cullimore, J. (1993). Lipo-oligosaccharide nodulation factors: A new class of signaling molecules mediating recognition and morphogenesis. Cell **74,** 951-954.

Devers, E.A., Brosnan, C.A., Sarazin, A., Albertini, D., Amsler, A.C., Brioudes, F., Jullien, P.E., Lim, P., Schott, G., and Voinnet, O. (2020). Movement and differential consumption of short interfering RNA duplexes underlie mobile RNA interference. Nature Plants **6,** 789-799.

Di Mambro, R., Sabatini, S., and Dello Ioio, R. (2019). Patterning the axes: A lesson from the root. Plants (Basel, Switzerland) **8,** 8.

Ding, S.W., and Voinnet, O. (2007). Antiviral immunity directed by small RNAs. Cell **130,** 413-426.

Ditengou, F.A., Teale, W.D., Kochersperger, P., Flittner, K.A., Kneuper, I., van der Graaff, E., Nziengui, H., Pinosa, F., Li, X., Nitschke, R., Laux, T., and Palme, K. (2008). Mechanical induction of lateral root initiation in *Arabidopsis thaliana*. Proceedings of the National Academy of Sciences **105,** 18818-18823.

Dixon, R.O.D. (1964). The structure of infection threads, bacteria and bacteroids in pea and clover root nodules. Archiv für Mikrobiologie **48,** 166-178.

Doblas, V.G., Geldner, N., and Barberon, M. (2017a). The endodermis, a tightly controlled barrier for nutrients. Current Opinion in Plant Biology **39,** 136-143.

Doblas, V.G., Smakowska-Luzan, E., Fujita, S., Alassimone, J., Barberon, M., Madalinski, M., Belkhadir, Y., and Geldner, N. (2017b). Root diffusion barrier control by a vasculature-derived peptide binding to the SGN3 receptor. Science **355,** 280-284.

Dong, W., Zhu, Y., Chang, H., Wang, C., Yang, J., Shi, J., Gao, J., Yang, W., Lan, L., Wang, Y., Zhang, X., Dai, H., Miao, Y., Xu, L., He, Z., Song, C., Wu, S., Wang, D., Yu, N., and Wang, E. (2020). An SHR-SCR module specifies legume cortical cell fate to enable nodulation. Nature.

Dong, Z., Han, M.-H., and Fedoroff, N. (2008). The RNA-binding proteins HYL1 and SE promote accurate *in vitro* processing of pri-miRNA by DCL1. Proceedings of the National Academy of Sciences **105,** 9970-9975.

DREW, M.C. (1975). Comparison of the effects of a localised supply of phosphate, nitrate, ammonium and potassium on the growth of the seminal root system, and the shoot, in barley. New Phytologist **75,** 479-490.

Du, Y., and Scheres, B. (2017a). Lateral root formation and the multiple roles of auxin. J Exp Bot **69,** 155-167.

Du, Y., and Scheres, B. (2017b). PLETHORA transcription factors orchestrate de novo organ patterning during Arabidopsis lateral root outgrowth. Proc Natl Acad Sci U S A **114,** 11709-11714.

Dunoyer, P., Himber, C., and Voinnet, O. (2005). *DICER-LIKE 4* is required for RNA interference and produces the 21-nucleotide small interfering RNA component of the plant cell-to-cell silencing signal. Nature Genetics **37,** 1356.

Eamens, A.L., Smith, N.A., Curtin, S.J., Wang, M.-B., and Waterhouse, P.M. (2009). The *Arabidopsis thaliana* double-stranded RNA binding protein DRB1 directs guide strand selection from microRNA duplexes. RNA **15,** 2219-2235.

Ehrhardt, D.W., Wais, R., and Long, S.R. (1996). Calcium spiking in plant root hairs responding to *Rhizobium* nodulation signals. Cell **85,** 673-681.

Eklund, D.M., Ståldal, V., Valsecchi, I., Cierlik, I., Eriksson, C., Hiratsu, K., Ohme-Takagi, M., Sundström, J.F., Thelander, M., Ezcurra, I., and Sundberg, E. (2010). The *Arabidopsis thaliana* STYLISH1 protein acts as a transcriptional activator regulating auxin biosynthesis The Plant Cell **22,** 349-363.

Emonet, A., and Hay, A. (2022). Development and diversity of lignin patterns. Plant Physiology **190,** 31-43.

Erisman, J.W., Sutton, M.A., Galloway, J., Klimont, Z., and Winiwarter, W. (2008). How a century of ammonia synthesis changed the world. Nature Geoscience **1,** 636-639.

Fahlgren, N., Montgomery, T.A., Howell, M.D., Allen, E., Dvorak, S.K., Alexander, A.L., and Carrington, J.C. (2006). Regulation of *AUXIN RESPONSE FACTOR3* by *TAS3* ta-siRNA affects developmental timing and patterning in Arabidopsis. Current Biology **16,** 939-944.

Fan, M., Xu, C., Xu, K., and Hu, Y. (2012). *LATERAL ORGAN BOUNDARIES DOMAIN* transcription factors direct callus formation in Arabidopsis regeneration. Cell Research **22,** 1169-1180.

Fan, P., Aguilar, E., Bradai, M., Xue, H., Wang, H., Rosas-Diaz, T., Tang, W., Wolf, S., Zhang, H., Xu, L., and Lozano-Durán, R. (2021). The receptor-like kinases *BAM1* and *BAM2* are required for root xylem patterning. Proc Natl Acad Sci U S A **118,** e2022547118.

Fang, X., and Qi, Y. (2016). RNAi in plants: An argonaute-centered view. The Plant cell **28,** 272-285.

Filleur, S., Dorbe, M.F., Cerezo, M., Orsel, M., Granier, F., Gojon, A., and Daniel-Vedele, F. (2001). An Arabidopsis T-DNA mutant affected in *NRT2* genes is impaired in nitrate uptake. FEBS Letters **489,** 220-224.

Fournier, J., Teillet, A., Chabaud, M., Ivanov, S., Genre, A., Limpens, E., de Carvalho-Niebel, F., and Barker, D.G. (2015). Remodeling of the infection chamber before infection thread formation reveals a two-step mechanism for rhizobial entry into the host legume root hair. Plant Physiology **167,** 1233-1242.

Frank, F., Hauver, J., Sonenberg, N., and Nagar, B. (2012). *Arabidopsis* Argonaute MID domains use their nucleotide specificity loop to sort small RNAs. The EMBO Journal **31,** 3588-3595.

Franssen, H.J., Kulikova, O., Willemsen, V., and Heidstra, R. (2017). Cis-regulatory *PLETHORA* promoter elements directing root and nodule expression are conserved between *Arabidopsis thaliana* and *Medicago truncatula*. Plant Signal Behav **12,** e1278102.

Franssen, H.J., Xiao, T.T., Kulikova, O., Wan, X., Bisseling, T., Scheres, B., and Heidstra, R. (2015). Root developmental programs shape the *Medicago truncatula* nodule meristem. Development **142,** 2941-2950.

Fujita, S. (2021). CASPARIAN STRIP INTEGRITY FACTOR (CIF) family peptides - regulator of plant extracellular barriers. Peptides **143,** 170599.

Fujita, S., De Bellis, D., Edel, K.H., Köster, P., Andersen, T.G., Schmid-Siegert, E., Dénervaud Tendon, V., Pfister, A., Marhavý, P., Ursache, R., Doblas, V.G., Barberon, M., Daraspe, J., Creff, A., Ingram, G., Kudla, J., and Geldner, N. (2020). SCHENGEN receptor module drives localized ROS production and lignification in plant roots. The EMBO journal **39,** e103894.

Fukai, E., Soyano, T., Umehara, Y., Nakayama, S., Hirakawa, H., Tabata, S., Sato, S., and Hayashi, M. (2012). Establishment of a *Lotus japonicus* gene tagging population using the exon-targeting endogenous retrotransposon LORE1. The Plant Journal **69,** 720-730.

Fukaki, H., Tameda, S., Masuda, H., and Tasaka, M. (2002). Lateral root formation is blocked by a gain-of-function mutation in the *SOLITARY-ROOT/IAA14* gene of Arabidopsis. The Plant Journal **29,** 153-168.

Fukaki, H., Nakao, Y., Okushima, Y., Theologis, A., and Tasaka, M. (2005). Tissue-specific expression of stabilized *SOLITARY-ROOT/IAA14* alters lateral root development in Arabidopsis. The Plant Journal **44,** 382-395.

Fukunaga, R., and Doudna, J.A. (2009). dsRNA with 5' overhangs contributes to endogenous and antiviral RNA silencing pathways in plants. The EMBO journal **28,** 545-555.

Gansel, X., Muños, S., Tillard, P., and Gojon, A. (2001). Differential regulation of the NO^{3-} and NH^{4+} transporter genes *AtNRT2.1* and *AtAMT1.1* in Arabidopsis: relation with long-distance and local controls by N status of the plant. The Plant Journal **26,** 143-155.

Gautrat, P., Laffont, C., and Frugier, F. (2020). *Compact Root Architecture 2* promotes root competence for nodulation through the miR2111 systemic effector. Current Biology **30,** 1339-1345.e1333.

Geldner, N. (2013). The endodermis. Annual Review of Plant Biology **64,** 531-558.

Genre, A., and Russo, G. (2016). Does a common pathway transduce symbiotic signals in plant-microbe interactions? Frontiers in plant science **7,** 96.

Giehl, R.F.H., and von Wirén, N. (2014). Root nutrient foraging. Plant Physiology **166,** 509-517.

Giehl, R.F.H., Gruber, B.D., and von Wirén, N. (2013). It's time to make changes: modulation of root system architecture by nutrient signals. J Exp Bot **65,** 769-778.

Gleason, C., Chaudhuri, S., Yang, T., Muñoz, A., Poovaiah, B.W., and Oldroyd, G.E.D. (2006). Nodulation independent of rhizobia induced by a calcium-activated kinase lacking autoinhibition. Nature **441,** 1149-1152.

Goh, T., Joi, S., Mimura, T., and Fukaki, H. (2012). The establishment of asymmetry in Arabidopsis lateral root founder cells is regulated by LBD16/ASL18 and related LBD/ASL proteins. Development **139,** 883-893.

Goh, T., Toyokura, K., Wells, D.M., Swarup, K., Yamamoto, M., Mimura, T., Weijers, D., Fukaki, H., Laplaze, L., Bennett, M.J., and Guyomarc'h, S. (2016). Quiescent center initiation in the Arabidopsis lateral root primordia is dependent on the SCARECROW transcription factor. Development **143,** 3363-3371.

Griesmann, M., Chang, Y., Liu, X., Song, Y., Haberer, G., Crook, M.B., Billault-Penneteau, B., Lauressergues, D., Keller, J., Imanishi, L., Roswanjaya, Y.P., Kohlen, W., Pujic, P., Battenberg, K., Alloisio, N., Liang, Y., Hilhorst, H., Salgado, M.G., Hocher, V., Gherbi, H., Svistoonoff, S., Doyle, J.J., He, S., Xu, Y., Xu, S., Qu, J., Gao, Q., Fang, X., Fu, Y., Normand, P., Berry, A.M., Wall, L.G., Ané, J.-M., Pawlowski, K., Xu, X., Yang, H., Spannagl, M., Mayer, K.F.X., Wong, G.K.-S., Parniske, M., Delaux, P.-M., and Cheng, S. (2018). Phylogenomics reveals multiple losses of nitrogen-fixing root nodule symbiosis. Science **361,** eaat1743.

Groth, M., Takeda, N., Perry, J., Uchida, H., Dräxl, S., Brachmann, A., Sato, S., Tabata, S., Kawaguchi, M., Wang, T.L., and Parniske, M. (2010). *NENA*, a *Lotus japonicus* homolog of *Sec13*, is required for rhizodermal infection by arbuscular mycorrhiza fungi and rhizobia but dispensable for cortical endosymbiotic development The Plant Cell **22,** 2509-2526.

Gruber, B.D., Giehl, R.F.H., Friedel, S., and von Wirén, N. (2013). Plasticity of the Arabidopsis root system under nutrient deficiencies Plant Physiology **163,** 161-179.

Guan, P., Wang, R., Nacry, P., Breton, G., Kay, S.A., Pruneda-Paz, J.L., Davani, A., and Crawford, N.M. (2014). Nitrate foraging by Arabidopsis roots is mediated by the transcription factor *TCP20* through the systemic signaling pathway. Proc Natl Acad Sci U S A **111,** 15267-15272.

Handberg, K., and Stougaard, J. (1992). *Lotus japonicus*, an autogamous, diploid legume species for classical and molecular genetics. The Plant Journal **2,** 487-496.

Harrison, M.J. (2012). Cellular programs for arbuscular mycorrhizal symbiosis. Current Opinion in Plant Biology **15,** 691-698.

Hartmann, K., Peiter, E., Koch, K., Schubert, S., and Schreiber, L. (2002). Chemical composition and ultrastructure of broad bean (*Vicia faba*) nodule endodermis in comparison to the root endodermis. Planta **215,** 14-25.

Hayashi-Tsugane, M., and Kawaguchi, M. (2022). *Lotus japonicus HAR1* regulates root morphology locally and systemically under a moderate nitrate condition in the absence of rhizobia. Planta **255,** 95.

Hayashi, T., Banba, M., Shimoda, Y., Kouchi, H., Hayashi, M., and Imaizumi-Anraku, H. (2010). A dominant function of *CCaMK* in intracellular accommodation of bacterial and fungal endosymbionts. The Plant Journal **63,** 141-154.

Helariutta, Y., Fukaki, H., Wysocka-Diller, J., Nakajima, K., Jung, J., Sena, G., Hauser, M.-T., and Benfey, P.N. (2000). The *SHORT-ROOT* gene controls radial patterning of the Arabidopsis root through radial signaling. Cell **101,** 555-567.

Hiratsu, K., Matsui, K., Koyama, T., and Ohme-Takagi, M. (2003). Dominant repression of target genes by chimeric repressors that include the EAR motif, a repression domain, in Arabidopsis. The Plant Journal **34,** 733-739.

Hirsch, A. (1992). Developmental biology of legume nodulation. New Phytologist **122,** 211-237.

Hobecker, K.V., Reynoso, M.A., Bustos-Sanmamed, P., Wen, J., Mysore, K.S., Crespi, M., Blanco, F.A., and Zanetti, M.E. (2017). The MicroRNA390/*TAS3* pathway mediates symbiotic nodulation and lateral root growth. Plant physiology **174,** 2469-2486.

Hochholdinger, F., and Zimmermann, R. (2008). Conserved and diverse mechanisms in root development. Current Opinion in Plant Biology **11,** 70-74.

Hofhuis, H., Laskowski, M., Du, Y., Prasad, K., Grigg, S., Pinon, V., and Scheres, B. (2013). Phyllotaxis and rhizotaxis in Arabidopsis are modified by three *PLETHORA* transcription factors. Current Biology **23,** 956-962.

Holbein, J., Shen, D., and Andersen, T.G. (2021). The endodermal passage cell – just another brick in the wall? New Phytologist **230,** 1321-1328.

Howarth, R.W. (2008). Coastal nitrogen pollution: A review of sources and trends globally and regionally. Harmful Algae **8,** 14-20.

Hsieh, L.-C., Lin, S.-I., Shih, A.C.-C., Chen, J.-W., Lin, W.-Y., Tseng, C.-Y., Li, W.-H., and Chiou, T.-J. (2009). Uncovering small RNA-mediated responses to phosphate deficiency in Arabidopsis by deep sequencing. Plant Physiology **151,** 2120-2132.

Huault, E., Laffont, C., Wen, J., Mysore, K.S., Ratet, P., Duc, G., and Frugier, F. (2014). Local and systemic regulation of plant root system architecture and symbiotic nodulation by a receptor-like kinase. PLoS genetics **10,** e1004891.

Huo, X., Schnabel, E., Hughes, K., and Frugoli, J. (2006). RNAi phenotypes and the localization of a *protein:GUS* fusion imply a role for *Medicago truncatula PIN* genes in nodulation. Journal of Plant Growth Regulation **25,** 156-165.

Huss-Danell, K. (1997). Actinorhizal symbioses and their N_2 fixation. New Phytologist **136,** 375-405.

Imaizumi-Anraku, H., Takeda, N., Charpentier, M., Perry, J., Miwa, H., Umehara, Y., Kouchi, H., Murakami, Y., Mulder, L., Vickers, K., Pike, J., Allan Downie, J., Wang, T., Sato, S., Asamizu, E., Tabata, S., Yoshikawa, M., Murooka, Y., Wu, G.-J., Kawaguchi, M., Kawasaki, S., Parniske, M., and Hayashi, M. (2005). Plastid proteins crucial for symbiotic fungal and bacterial entry into plant roots. Nature **433,** 527-531.

Imin, N., Patel, N., Corcilius, L., Payne, R.J., and Djordjevic, M.A. (2018). CLE peptide tri-arabinosylation and peptide domain sequence composition are essential for SUNN-dependent autoregulation of nodulation in *Medicago truncatula*. New Phytologist **218,** 73-80.

Jobbágy, E.G., and Jackson, R.B. (2001). The distribution of soil nutrients with depth: Global patterns and the imprint of plants. Biogeochemistry **53,** 51-77.

Juarez, M.T., Kui, J.S., Thomas, J., Heller, B.A., and Timmermans, M.C.J.N. (2004). microRNA-mediated repression of *Rolled Leaf1* specifies maize leaf polarity. Nature **428**.

Kalmbach, L., Hématy, K., De Bellis, D., Barberon, M., Fujita, S., Ursache, R., Daraspe, J., and Geldner, N. (2017). Transient cell-specific *EXO70A1* activity in the CASP domain and Casparian strip localization. Nature Plants **3,** 17058.

Kamiya, T., Borghi, M., Wang, P., Danku, J.M.C., Kalmbach, L., Hosmani, P.S., Naseer, S., Fujiwara, T., Geldner, N., and Salt, D.E. (2015). The MYB36 transcription factor orchestrates Casparian strip formation. Proc Natl Acad Sci U S A **112,** 10533-10538.

Kanamori, N., Madsen, L.H., Radutoiu, S., Frantescu, M., Quistgaard, E.M.H., Miwa, H., Downie, J.A., James, E.K., Felle, H.H., Haaning, L.L., Jensen, T.H., Sato, S., Nakamura, Y., Tabata, S., Sandal, N., and Stougaard, J. (2006). A nucleoporin is required for induction of Ca^{2+} spiking in legume nodule development and essential for rhizobial and fungal symbiosis. Proc Natl Acad Sci U S A **103,** 359-364.

Kawaguchi, M. (2000). *Lotus japonicus* `Miyakojima' MG-20: An early-flowering accession suitable for indoor handling. Journal of Plant Research **113,** 507-509.

Kehr, J., and Buhtz, A. (2008). Long distance transport and movement of RNA through the phloem. J Exp Bot **59,** 85-92.

Kim, G.-B., Son, S.-U., Yu, H.-J., and Mun, J.-H. (2019a). *MtGA2ox10* encoding C20-GA2-oxidase regulates rhizobial infection and nodule development in *Medicago truncatula*. Scientific Reports **9,** 5952.

Kim, S., Zeng, W., Bernard, S., Liao, J., Venkateshwaran, M., Ane, J.M., and Jiang, Y. (2019b). Ca^{2+}-regulated Ca^{2+}channels with an RCK gating ring control plant symbiotic associations. Nature communications **10,** 3703.

Kistner, C., and Parniske, M. (2002). Evolution of signal transduction in intracellular symbiosis. Trends in Plant Science **7,** 511-518.

Kosma, D.K., Murmu, J., Razeq, F.M., Santos, P., Bourgault, R., Molina, I., and Rowland, O. (2014). AtMYB41 activates ectopic suberin synthesis and assembly in multiple plant species and cell types. The Plant Journal **80,** 216-229.

Kosuta, S., Hazledine, S., Sun, J., Miwa, H., Morris, R.J., Downie, J.A., and Oldroyd, G.E.D. (2008). Differential and chaotic calcium signatures in the symbiosis signaling pathway of legumes. Proc Natl Acad Sci U S A **105,** 9823-9828.

Krouk, G., Lacombe, B., Bielach, A., Perrine-Walker, F., Malinska, K., Mounier, E., Hoyerova, K., Tillard, P., Leon, S., Ljung, K., Zazimalova, E., Benkova, E., Nacry, P., and Gojon, A. (2010). Nitrate-regulated auxin transport by *NRT1.1* defines a mechanism for nutrient sensing in plants. Developmental Cell **18,** 927-937.

Krusell, L., Madsen, L.H., Sato, S., Aubert, G., Genua, A., Szczyglowski, K., Duc, G., Kaneko, T., Tabata, S., Bruijn, F., Pajuelo, E., Sandal, N., and Stougaard, J. (2002). Shoot control of root development and nodulation is mediated by a receptor-like kinase. Nature **420,** 422–426.

Krusell, L., Krause, K., Ott, T., Desbrosses, G., Krämer, U., Sato, S., Nakamura, Y., Tabata, S., James, E.K., Sandal, N., Stougaard, J., Kawaguchi, M., Miyamoto, A., Suganuma, N., and Udvardi, M.K. (2005). The sulfate transporter *SST1* is crucial for symbiotic nitrogen fixation in *Lotus japonicus* root nodules. The Plant Cell **17,** 1625-1636.

Krusell, L., Sato, N., Fukuhara, I., Koch, B.E., Grossmann, C., Okamoto, S., Oka-Kira, E., Otsubo, Y., Aubert, G., Nakagawa, T., Sato, S., Tabata, S., Duc, G., Parniske, M., Wang, T.L., Kawaguchi, M., and Stougaard, J. (2011). The *Clavata2* genes of pea and *Lotus japonicus* affect autoregulation of nodulation. The Plant Journal **65,** 861-871.

Kuhlemeier, C., and Timmermans, M.C.P. (2016). The Sussex signal: insights into leaf dorsiventrality. Development **143,** 3230-3237.

Kurihara, D., Mizuta, Y., Sato, Y., and Higashiyama, T. (2015). ClearSee: a rapid optical clearing reagent for whole-plant fluorescence imaging. Development **142,** 4168-4179.

Kurihara, Y., Takashi, Y., and Watanabe, Y. (2006). The interaction between DCL1 and HYL1 is important for efficient and precise processing of pri-miRNA in plant microRNA biogenesis. RNA **12,** 206-212.

Laffont, C., Ivanovici, A., Gautrat, P., Brault, M., Djordjevic, M.A., and Frugier, F. (2020). The *NIN* transcription factor coordinates *CEP* and *CLE* signaling peptides that regulate nodulation antagonistically. Nature communications **11,** 3167-3167.

Laffont, C., Huault, E., Gautrat, P., Endre, G., Kalo, P., Bourion, V., Duc, G., and Frugier, F. (2019). Independent regulation of symbiotic nodulation by the *SUNN* negative and *CRA2* positive systemic pathways. Plant Physiology **180,** 559-570.

Laskowski, M., and Ten Tusscher, K.H. (2017). Periodic lateral root priming: What makes it tick? The Plant Cell **29,** 432-444.

Lavenus, J., Goh, T., Roberts, I., Guyomarc'h, S., Lucas, M., De Smet, I., Fukaki, H., Beeckman, T., Bennett, M., and Laplaze, L. (2013). Lateral root development in Arabidopsis: fifty shades of auxin. Trends in Plant Science **18,** 450-458.

Lavenus, J., Goh, T., Guyomarc'h, S., Hill, K., Lucas, M., Voß, U., Kenobi, K., Wilson, M.H., Farcot, E., Hagen, G., Guilfoyle, T.J., Fukaki, H., Laplaze, L., and Bennett, M.J. (2015). Inference of the Arabidopsis lateral root gene regulatory network suggests a bifurcation mechanism that defines primordia flanking and central zones. The Plant Cell **27,** 1368-1388.

Lea, U.S., Slimestad, R., Smedvig, P., and Lillo, C. (2007). Nitrogen deficiency enhances expression of specific *MYB* and *bHLH* transcription factors and accumulation of end products in the flavonoid pathway. Planta **225,** 1245-1253.

Lee, H.W., Kang, N.Y., Pandey, S.K., Cho, C., Lee, S.H., and Kim, J. (2017). Dimerization in LBD16 and LBD18 transcription factors is critical for lateral root formation. Plant Physiology **174,** 301-311.

Lee, H.W., Cho, C., Pandey, S.K., Park, Y., Kim, M.-J., and Kim, J. (2019). *LBD16* and *LBD18* acting downstream of *ARF7* and *ARF19* are involved in adventitious root formation in Arabidopsis. BMC Plant Biology **19,** 46.

Lee, T., Orvosova, M., Batzenschlager, M., Bueno Batista, M., Bailey, P.C., Mohd-Radzman, N.A., Gurzadyan, A., Stuer, N., Mysore, K.S., Wen, J., Ott, T., Oldroyd, G.E.D., and Schiessl, K. (2024). *Light-sensitive short hypocotyl* genes confer symbiotic nodule identity in the legume *Medicago truncatula*. Current Biology **34,** 825-840.e827.

Lee, Y., Kim, M., Han, J., Yeom, K.-H., Lee, S., Baek, S.H., and Kim, V.N. (2004). MicroRNA genes are transcribed by RNA polymerase II. The EMBO Journal **23,** 4051-4060.

Levesque, M.P., Vernoux, T., Busch, W., Cui, H., Wang, J.Y., Blilou, I., Hassan, H., Nakajima, K., Matsumoto, N., Lohmann, J.U., Scheres, B., and Benfey, P.N. (2006). Whole-genome analysis of the *SHORT-ROOT* developmental pathway in Arabidopsis. PLOS Biology **4,** e143.

Li, J., Yang, Z., Yu, B., Liu, J., and Chen, X. (2005). Methylation protects miRNAs and siRNAs from a 3'-end uridylation activity in Arabidopsis. Current Biology **15,** 1501-1507.

Li, S., Wang, X., Xu, W., Liu, T., Cai, C., Chen, L., Clark, C.B., and Ma, J. (2021). Unidirectional movement of small RNAs from shoots to roots in interspecific heterografts. Nature Plants **7,** 50-59.

Li, X., Lei, M., Yan, Z., Wang, Q., Chen, A., Sun, J., Luo, D., and Wang, Y. (2014). The *REL3*-mediated *TAS3* ta-siRNA pathway integrates auxin and ethylene signaling to regulate nodulation in *Lotus japonicus*. New Phytologist **201,** 531-544.

Li, Y., Pei, Y., Shen, Y., Zhang, R., Kang, M., Ma, Y., Li, D., and Chen, Y. (2022). Progress in the self-regulation system in legume nodule development-AON (Autoregulation of Nodulation). International journal of molecular sciences **23**.

Liang, C., Wang, X., He, H., Xu, C., and Cui, J. (2023). Beyond loading: Functions of plant ARGONAUTE proteins. International journal of molecular sciences **24,** 16054.

Liberman, L.M., Sparks, E.E., Moreno-Risueno, M.A., Petricka, J.J., and Benfey, P.N. (2015). MYB36 regulates the transition from proliferation to differentiation in the Arabidopsis root. Proceedings of the National Academy of Sciences **112,** 12099-12104.

Libourel, C., Keller, J., Brichet, L., Cazalé, A.-C., Carrère, S., Vernié, T., Couzigou, J.-M., Callot, C., Dufau, I., Cauet, S., Marande, W., Bulach, T., Suin, A., Masson-Boivin, C., Remigi, P., Delaux, P.-M., and Capela, D. (2023). Comparative phylotranscriptomics reveals ancestral and derived root nodule symbiosis programmes. Nature Plants.

Limpens, E., Franken, C., Smit, P., Willemse, J., Bisseling, T., and Geurts, R. (2003). LysM domain receptor kinases regulating rhizobial nod factor-induced infection. Science **302,** 630-633.

Lin, J.-s., Li, X., Luo, Z., Mysore, K.S., Wen, J., and Xie, F. (2018). NIN interacts with NLPs to mediate nitrate inhibition of nodulation in *Medicago truncatula*. Nature Plants **4,** 942-952.

Lin, J., Frank, M., and Reid, D. (2020). No home without hormones: How plant hormones control legume nodule organogenesis. Plant Communications **1,** 100104.

Lin, J., Roswanjaya, Y.P., Kohlen, W., Stougaard, J., and Reid, D. (2021). Nitrate restricts nodule organogenesis through inhibition of cytokinin biosynthesis in *Lotus japonicus*. Nature communications **12,** 6544-6544.

Little, D.Y., Rao, H., Oliva, S., Daniel-Vedele, F., Krapp, A., and Malamy, J.E. (2005). The putative high-affinity nitrate transporter *NRT2.1* represses lateral root initiation in response to nutritional cues. Proceedings of the National Academy of Sciences **102,** 13693-13698.

Liu, B., Wu, J., Yang, S., Schiefelbein, J., and Gan, Y. (2019a). Nitrate regulation of lateral root and root hair development in plants. J Exp Bot **71,** 4405-4414.

Liu, H., Lin, J.S., Luo, Z., Sun, J., Huang, X., Yang, Y., Xu, J., Wang, Y.F., Zhang, P., Oldroyd, G.E.D., and Xie, F. (2022a). Constitutive activation of a nuclear-localized calcium channel complex in *Medicago truncatula*. Proceedings of the National Academy of Sciences **119,** e2205920119.

Liu, J., Rutten, L., Limpens, E., van der Molen, T., van Velzen, R., Chen, R., Chen, Y., Geurts, R., Kohlen, W., Kulikova, O., and Bisseling, T. (2019b). A remote cis-regulatory region is required for *NIN* expression in the pericycle to initiate nodule primordium formation in *Medicago truncatula*. The Plant Cell **31,** 68-83.

Liu, K.H., and Tsay, Y.F. (2003). Switching between the two action modes of the dual-affinity nitrate transporter *CHL1* by phosphorylation. The EMBO journal **22,** 1005-1013.

Liu, Q., Wu, K., Song, W., Zhong, N., Wu, Y., and Fu, X. (2022b). Improving crop nitrogen use efficiency toward sustainable green revolution. Annual Review of Plant Biology **73,** 523-551.

Liu, W., Yu, J., Ge, Y., Qin, P., and Xu, L. (2018). Pivotal role of LBD16 in root and root-like organ initiation. Cellular and molecular life sciences **75,** 3329-3338.

Liu, W., Shoji, K., Naganuma, M., Tomari, Y., and Iwakawa, H.-o. (2022c). The mechanisms of siRNA selection by plant Argonaute proteins triggering DNA methylation. Nucleic Acids Research **50,** 12997-13010.

Long, Y., Goedhart, J., Schneijderberg, M., Terpstra, I., Shimotohno, A., Bouchet, B.P., Akhmanova, A., Gadella Jr, T.W.J., Heidstra, R., Scheres, B., and Blilou, I. (2015). SCARECROW-LIKE23 and SCARECROW jointly specify endodermal cell fate but distinctly control SHORT-ROOT movement. The Plant Journal **84,** 773-784.

Lu, C., Tej, S.S., Luo, S., Haudenschild, C.D., Meyers, B.C., and Green, P.J. (2005). Elucidation of the small RNA component of the transcriptome. Science **309,** 1567-1569.

Lulai, E.C., and Corsini, D.L. (1998). Differential deposition of suberin phenolic and aliphatic domains and their roles in resistance to infection during potato tuber (*Solanum tuberosum*) wound-healing. Physiological and Molecular Plant Pathology **53,** 209-222.

Lund, E., Güttinger, S., Calado, A., Dahlberg, J.E., and Kutay, U. (2004). Nuclear export of microRNA precursors. Science **303,** 95-98.

Luo, Z., Moreau, C., Wang, J., Frugier, F., and Xie, F. (2022a). NLP1 binds the *CEP1* signaling peptide promoter to repress its expression in response to nitrate. New Phytologist **n/a**.

Luo, Z., Lin, J.-s., Zhu, Y., Fu, M., Li, X., and Xie, F. (2021). *NLP1* reciprocally regulates nitrate inhibition of nodulation through *SUNN-CRA2* signaling in *Medicago truncatula*. Plant Communications **2,** 100183.

Luo, Z., Wang, J., Li, F., Lu, Y., Fang, Z., Fu, M., Mysore, K.S., Wen, J., Gong, J., Murray, J.D., and Xie, F. (2022b). The small peptide CEP1 and the NIN-like protein NLP1 regulate *NRT2.1* to mediate root nodule formation across nitrate concentrations. The Plant Cell.

Lux, A., Morita, S., Abe, J., and Ito, K. (2005). An improved method for clearing and staining free-hand sections and whole-mount samples. Annals of botany **96,** 989-996.

Ma, W., Li, J., Qu, B., He, X., Zhao, X., Li, B., Fu, X., and Tong, Y. (2014). Auxin biosynthetic gene TAR2 is involved in low nitrogen-mediated reprogramming of root architecture in Arabidopsis. The Plant Journal **78,** 70-79.

MacGregor, A.N., and Alexander, M. (1971). Formation of tumor-like structures on legume roots by *Rhizobium*. Journal of bacteriology **105,** 728-732.

Madsen, E.B., Madsen, L.H., Radutoiu, S., Olbryt, M., Rakwalska, M., Szczyglowski, K., Sato, S., Kaneko, T., Tabata, S., Sandal, N., and Stougaard, J. (2003). A receptor kinase gene of the LysM type is involved in legumeperception of rhizobial signals. Nature **425,** 637-640.

Maekawa-Yoshikawa, M., Müller, J., Takeda, N., Maekawa, T., Sato, S., Tabata, S., Perry, J., Wang, T.L., Groth, M., Brachmann, A., and Parniske, M. (2009). The temperature-sensitive *brush* mutant of the legume *Lotus japonicus* reveals a link between root development and nodule infection by rhizobia. Plant Physiology **149,** 1785-1796.

Maekawa, T., Maekawa-Yoshikawa, M., Takeda, N., Imaizumi-Anraku, H., Murooka, Y., and Hayashi, M. (2009). Gibberellin controls the nodulation signaling pathway in *Lotus japonicus*. The Plant Journal **58,** 183-194.

Magne, K., Couzigou, J.M., Schiessl, K., Liu, S., George, J., Zhukov, V., Sahl, L., Boyer, F., Iantcheva, A., Mysore, K.S., Wen, J., Citerne, S., Oldroyd, G.E.D., and Ratet, P. (2018). *MtNODULE ROOT1* and *MtNODULE ROOT2* are essential for indeterminate nodule identity. Plant Physiology **178,** 295-316.

Magori, S., Oka-Kira, E., Shibata, S., Umehara, Y., Kouchi, H., Hase, Y., Tanaka, A., Sato, S., Tabata, S., and Kawaguchi, M. (2009). *Too Much Love*, a root regulator associated with the long-distance control of nodulation in *Lotus japonicus*. Mol Plant Microbe Interact **22,** 259-268.

Mair, A., Xu, S.-L., Branon, T.C., Ting, A.Y., and Bergmann, D.C. (2019). Proximity labeling of protein complexes and cell-type-specific organellar proteomes in Arabidopsis enabled by TurboID. eLife **8,** e47864.

Maizel, A., Markmann, K., Timmermans, M., and Wachter, A. (2020). To move or not to move: roles and specificity of plant RNA mobility. Current Opinion in Plant Biology **57,** 52-60.

Malamy, J.E., and Benfey, P.N. (1997). Organization and cell differentiation in lateral roots of *Arabidopsis thaliana*. Development **124,** 33-44.

Malolepszy, A., Mun, T., Sandal, N., Gupta, V., Dubin, M., Urbanski, D., Shah, N., Bachmann, A., Fukai, E., Hirakawa, H., Tabata, S., Nadzieja, M., Markmann, K., Su, J., Umehara, Y., Soyano, T., Miyahara, A., Sato, S., Hayashi, M., Stougaard, J., and Andersen, S.U. (2016). The LORE1 insertion mutant resource. The Plant Journal **88,** 306-317.

Marin, E., Jouannet, V., Herz, A., Lokerse, A.S., Weijers, D., Vaucheret, H., Nussaume, L., Crespi, M.D., and Maizel, A. (2010). miR390, Arabidopsis *TAS3* tasiRNAs, and their A*UXIN RESPONSE FACTOR* targets define an autoregulatory network quantitatively regulating lateral root growth. The Plant Cell **22,** 1104-1117.

Markmann, K., and Parniske, M. (2009). Evolution of root endosymbiosis with bacteria: how novel are nodules? Trends in Plant Science **14,** 77-86.

Markmann, K., Giczey, G., and Parniske, M. (2008). Functional adaptation of a plant receptor-kinase paved the way for the evolution of intracellular root symbioses with bacteria. PLoS biology **6,** e68.

Matzke, M.A., Kanno, T., and Matzke, A.J. (2015). RNA-directed DNA methylation: The evolution of a complex epigenetic pathway in flowering plants. Annual Review of Plant Biology **66,** 243-267.

Mbengue, M., Camut, S., de Carvalho-Niebel, F., Deslandes, L., Froidure, S., Klaus-Heisen, D., Moreau, S., Rivas, S., Timmers, T., Hervé, C., Cullimore, J., and Lefebvre, B. (2010). The *Medicago truncatula* E3 ubiquitin ligase PUB1 nteracts with the LYK3 symbiotic receptor and negatively regulates infection and nodulation. The Plant Cell **22,** 3474-3488.

Melino, V.J., Plett, D.C., Bendre, P., Thomsen, H.C., Zeisler-Diehl, V.V., Schreiber, L., and Kronzucker, H.J. (2021). Nitrogen depletion enhances endodermal suberization without restricting transporter-mediated root NO^{3-} influx. Journal of Plant Physiology **257,** 153334.

Mens, C., Hastwell, A.H., Su, H., Gresshoff, P.M., Mathesius, U., and Ferguson, B.J. (2021). Characterisation of *Medicago truncatula CLE34* and *CLE35* in nitrate and rhizobia regulation of nodulation. New Phytologist **229,** 2525-2534.

Mi, S., Cai, T., Hu, Y., Chen, Y., Hodges, E., Ni, F., Wu, L., Li, S., Zhou, H., Long, C., Chen, S., Hannon, G.J., and Qi, Y. (2008). Sorting of small RNAs into *Arabidopsis* Argonaute complexes is directed by the 5' terminal nucleotide. Cell **133,** 116-127.

Miri, M., Janakirama, P., Huebert, T., Ross, L., McDowell, T., Orosz, K., Markmann, K., and Szczyglowski, K. (2019). Inside out: root cortex-localized LHK1 cytokinin receptor limits epidermal infection of *Lotus japonicus* roots by *Mesorhizobium loti*. New Phytologist **0**.

Misawa, F., Ito, M., Nosaki, S., Nishida, H., Watanabe, M., Suzuki, T., Miura, K., Kawaguchi, M., and Suzaki, T. (2022). Nitrate transport via NRT2.1 mediates NIN-LIKE PROTEIN-dependent suppression of root nodulation in *Lotus japonicus*. The Plant Cell.

Miwa, H., Sun, J., Oldroyd, G.E.D., and Downie, J.A. (2006). Analysis of nod-factor-induced calcium signaling in root hairs of symbiotically defective mutants of *Lotus japonicus*. Molecular Plant-Microbe Interactions **19,** 914-923.

Miyashima, S., Hashimoto, T., and Nakajima, K. (2009). *ARGONAUTE1* acts in Arabidopsis root radial pattern formation independently of the *SHR/SCR* pathway. Plant and Cell Physiology **50,** 626-634.

Miyazawa, H., Oka-Kira, E., Sato, N., Takahashi, H., Wu, G.J., Sato, S., Hayashi, M., Betsuyaku, S., Nakazono, M., Tabata, S., Harada, K., Sawa, S., Fukuda, H., and Kawaguchi, M. (2010). The receptor-like kinase *KLAVIER* mediates systemic regulation of nodulation and non-symbiotic shoot development in *Lotus japonicus*. Development **137,** 4317-4325.

Mohd-Radzman, N.A., Laffont, C., Ivanovici, A., Patel, N., Reid, D., Stougaard, J., Frugier, F., Imin, N., and Djordjevic, M.A. (2016). Different pathways act downstream of the CEP peptide receptor *CRA2* to regulate lateral root and nodule development. Plant Physiology **171,** 2536-2548.

Moreau, C., Gautrat, P., and Frugier, F. (2021). Nitrate-induced CLE35 signaling peptides inhibit nodulation through the SUNN receptor and miR2111 repression. Plant Physiology.

Moreno-Risueno, M.A., Norman, J.M.V., Moreno, A., Zhang, J., Ahnert, S.E., and Benfey, P.N. (2010). Oscillating gene expression determines competence for periodic *Arabidopsis* root branching. Science **329,** 1306-1311.

Mortier, V., Den Herder, G., Whitford, R., Van de Velde, W., Rombauts, S., D'haeseleer, K., Holsters, M., and Goormachtig, S. (2010). CLE peptides control *Medicago truncatula* nodulation locally and systemically. Plant Physiology **153,** 222-237.

Motte, H., Vanneste, S., and Beeckman, T. (2019). Molecular and environmental regulation of root development. Annual Review of Plant Biology **70,** 465-488.

Mourrain, P., Béclin, C., Elmayan, T., Feuerbach, F., Godon, C., Morel, J.-B., Jouette, D., Lacombe, A.-M., Nikic, S., Picault, N., Rémoué, K., Sanial, M., Vo, T.-A., and Vaucheret, H. (2000). *Arabidopsis SGS2* and *SGS3* genes are required for posttranscriptional gene silencing and natural virus resistance. Cell **101,** 533-542.

Munguía-Rodríguez, A.G., López-Bucio, J.S., Ruiz-Herrera, L.F., Ortiz-Castro, R., Guevara-García Á, A., Marsch-Martínez, N., Carreón-Abud, Y., López-Bucio, J., and Martínez-Trujillo, M. (2020). *YUCCA4* overexpression modulates auxin biosynthesis and transport and influences plant growth and development via crosstalk with abscisic acid in *Arabidopsis thaliana*. Genetics and molecular biology **43,** e20190221.

Murray, J.D., Karas, B.J., Sato, S., Tabata, S., Amyot, L., and Szczyglowski, K. (2007). A cytokinin perception mutant colonized by *Rhizobium* in the absence of nodule organogenesis. Science **315,** 101-104.

Nadzieja, M., Kelly, S., Stougaard, J., and Reid, D. (2018). Epidermal auxin biosynthesis facilitates rhizobial infection in *Lotus japonicus*. The Plant Journal **95,** 101-111.

Nagano, H., Fukudome, A., Hiraguri, A., Moriyama, H., and Fukuhara, T. (2014). Distinct substrate specificities of Arabidopsis DCL3 and DCL4. Nucleic Acids Res **42,** 1845-1856.

Nakajima, K., Sena, G., Nawy, T., and Benfey, P.N. (2001). Intercellular movement of the putative transcription factor *SHR* in root patterning. Nature **413,** 307-311.

Nakayama, T., Shinohara, H., Tanaka, M., Baba, K., Ogawa-Ohnishi, M., and Matsubayashi, Y. (2017). A peptide hormone required for Casparian strip diffusion barrier formation in *Arabidopsis* roots. Science **355,** 284-286.

Namyslov, J., Bauriedlová, Z., Janoušková, J., Soukup, A., and Tylová, E. (2020). Exodermis and endodermis respond to nutrient deficiency in nutrient-specific and localized manner. Plants (Basel, Switzerland) **9**.

Naseer, S., Lee, Y., Lapierre, C., Franke, R., Nawrath, C., and Geldner, N. (2012). Casparian strip diffusion barrier in *Arabidopsis* is made of a lignin polymer without suberin. Proc Natl Acad Sci U S A **109,** 10101-10106.

Nishida, H., Handa, Y., Tanaka, S., Suzaki, T., and Kawaguchi, M. (2016). Expression of the *CLE-RS3* gene suppresses root nodulation in *Lotus japonicus*. Journal of plant research **129,** 909-919.

Nishida, H., Tanaka, S., Handa, Y., Ito, M., Sakamoto, Y., Matsunaga, S., Betsuyaku, S., Miura, K., Soyano, T., Kawaguchi, M., and Suzaki, T. (2018). A NIN-LIKE PROTEIN mediates nitrate-induced control of root nodule symbiosis in *Lotus japonicus*. Nature communications **9,** 499.

Nishida, H., Nosaki, S., Suzuki, T., Ito, M., Miyakawa, T., Nomoto, M., Tada, Y., Miura, K., Tanokura, M., Kawaguchi, M., and Suzaki, T. (2021). Different DNA-binding specificities of NLP and NIN transcription factors underlie nitrate-induced control of root nodulation. The Plant cell **33,** 2340-2359.

Nishimura, R., Hayashi, M., Wu, G.-J., Kouchi, H., Imaizumi-Anraku, H., Murakami, Y., Kawasaki, S., Akao, S., Ohmori, M., Nagasawa, M., Harada, K., and Kawaguchi, M. (2002). *HAR1* mediates systemic regulation of symbiotic organ development. Nature **420,** 426.

Nizampatnam, N.R., Schreier, S.J., Damodaran, S., Adhikari, S., and Subramanian, S. (2015). microRNA160 dictates stage-specific auxin and cytokinin sensitivities and directs soybean nodule development. The Plant Journal **84,** 140-153.

Nogueira, F.T., Chitwood, D.H., Madi, S., Ohtsu, K., Schnable, P.S., Scanlon, M.J., and Timmermans, M.C. (2009). Regulation of small RNA accumulation in the maize shoot apex. PLoS genetics **5,** e1000320.

Notaguchi, M. (2015). Identification of phloem-mobile mRNA. Journal of Plant Research **128,** 27-35.

Nowak, S., Schnabel, E., and Frugoli, J. (2019). The *Medicago truncatula* CLAVATA3-LIKE CLE12/13 signaling peptides regulate nodule number depending on the *CORYNE* but not the *COMPACT ROOT ARCHITECTURE2* receptor. Plant Signal Behav **14,** 1598730-1598730.

Oenema, O., Witzke, H.P., Klimont, Z., Lesschen, J.P., and Velthof, G.L. (2009). Integrated assessment of promising measures to decrease nitrogen losses from agriculture in EU-27. Agriculture, Ecosystems & Environment **133,** 280-288.

Ohkubo, Y., Kuwata, K., and Matsubayashi, Y. (2021). A type 2C protein phosphatase activates high-affinity nitrate uptake by dephosphorylating NRT2.1. Nature Plants **7,** 310-316.

Ohkubo, Y., Tanaka, M., Tabata, R., Ogawa-Ohnishi, M., and Matsubayashi, Y. (2017). Shoot-to-root mobile polypeptides involved in systemic regulation of nitrogen acquisition. Nature Plants **3,** 17029.

Okamoto, S., Shinohara, H., Mori, T., Matsubayashi, Y., and Kawaguchi, M. (2013). Root-derived CLE glycopeptides control nodulation by direct binding to HAR1 receptor kinase. Nature communications **4,** 2191.

Okamoto, S., Ohnishi, E., Sato, S., Takahashi, H., Nakazono, M., Tabata, S., and Kawaguchi, M. (2009). Nod factor/nitrate-induced *CLE* genes that drive *HAR1*-mediated systemic regulation of nodulation. Plant Cell Physiol **50,** 67-77.

Okuda, S., Fujita, S., Moretti, A., Hohmann, U., Doblas, V.G., Ma, Y., Pfister, A., Brandt, B., Geldner, N., and Hothorn, M. (2020). Molecular mechanism for the recognition of sequence-divergent CIF peptides by the plant receptor kinases GSO1/SGN3 and GSO2. Proceedings of the National Academy of Sciences **117,** 2693-2703.

Okuma, N., Soyano, T., Suzaki, T., and Kawaguchi, M. (2020). MIR2111-5 locus and shoot-accumulated mature miR2111 systemically enhance nodulation depending on *HAR1* in *Lotus japonicus*. Nature communications **11,** 5192-5192.

Okushima, Y., Fukaki, H., Onoda, M., Theologis, A., and Tasaka, M. (2007). ARF7 and ARF19 regulate lateral root formation via direct activation of *LBD/ASL* genes in Arabidopsis. The Plant Cell **19,** 118-130.

Okushima, Y., Overvoorde, P.J., Arima, K., Alonso, J.M., Chan, A., Chang, C., Ecker, J.R., Hughes, B., Lui, A., Nguyen, D., Onodera, C., Quach, H., Smith, A., Yu, G., and Theologis, A. (2005). Functional genomic analysis of the *AUXIN RESPONSE FACTOR* gene family members in *Arabidopsis thaliana*: Unique and overlapping functions of *ARF7* and *ARF19* The Plant Cell **17,** 444-463.

Oldroyd, G.E.D., and Leyser, O. (2020). A plant's diet, surviving in a variable nutrient environment. Science **368**.

Oldroyd, G.E.D., Engstrom, E.M., and Long, S.R. (2001). Ethylene inhibits the nod factor signal transduction pathway of *Medicago truncatula*. The Plant Cell **13,** 1835-1849.

Oldroyd, G.E.D., Murray, J.D., Poole, P.S., and Downie, J.A. (2011). The rules of engagement in the legume-rhizobial symbiosis. Annual Review of Genetics **45,** 119-144.

Osipova, M.A., Mortier, V., Demchenko, K.N., Tsyganov, V.E., Tikhonovich, I.A., Lutova, L.A., Dolgikh, E.A., and Goormachtig, S. (2012). *Wuschel-related homeobox5* gene expression and interaction of CLE peptides with components of the systemic control add two pieces to the puzzle of Autoregulation of Nodulation. Plant physiology **158,** 1329-1341.

Ota, R., Ohkubo, Y., Yamashita, Y., Ogawa-Ohnishi, M., and Matsubayashi, Y. (2020). Shoot-to-root mobile CEPD-like 2 integrates shoot nitrogen status to systemically regulate nitrate uptake in Arabidopsis. Nature communications **11,** 641.

Pant, B.D., Buhtz, A., Kehr, J., and Scheible, W.R. (2008). MicroRNA399 is a long-distance signal for the regulation of plant phosphate homeostasis. The Plant Journal **53,** 731-738.

Pant, B.D., Musialak-Lange, M., Nuc, P., May, P., Buhtz, A., Kehr, J., Walther, D., and Scheible, W.-R. (2009). Identification of nutrient-responsive Arabidopsis and rapeseed MicroRNAs by comprehensive real-time polymerase chain reaction profiling and small RNA sequencing. Plant Physiology **150,** 1541-1555.

Parniske, M. (2008). Arbuscular mycorrhiza: the mother of plant root endosymbioses. Nature reviews. Microbiology **6,** 763–775.

Pellizzaro, A., Clochard, T., Cukier, C., Bourdin, C., Juchaux, M., Montrichard, F., Thany, S., Raymond, V., Planchet, E., Limami, A.M., and Morère-Le Paven, M.C. (2014). The nitrate transporter MtNPF6.8 (MtNRT1.3) transports abscisic acid and mediates nitrate regulation of primary root growth in *Medicago truncatula*. Plant Physiology **166,** 2152-2165.

Penmetsa, R.V., Frugoli, J.A., Smith, L.S., Long, S.R., and Cook, D.R. (2003). Dual genetic pathways controlling nodule number in *Medicago truncatula* Plant Physiology **131,** 998-1008.

Péret, B., Larrieu, A., and Bennett, M.J. (2009). Lateral root emergence: a difficult birth. J Exp Bot **60,** 3637-3643.

Peters, N.K., Frost, J.W., and Long, S.R. (1986). A plant flavone, luteolin, induces expression of *Rhizobium meliloti* nodulation genes. Science **233,** 977-980.

Phillips, D.A. (1980). Efficiency of symbiotic nitrogen fixation in legumes. Annual Review of Plant Biology **31,** 29-49.

Pierce, M., and Bauer, W.D. (1983). A rapid regulatory response governing nodulation in soybean. Plant Physiology **73,** 286-290.

Pigliucci, M. (2002). Ecology and evolutionary biology of Arabidopsis. Arabidopsis Book **1,** e0003.

Podlasek, A., Koda, E., and Vaverková, M.D. (2021). The variability of nitrogen forms in soils due to traditional and precision agriculture: Case studies in poland. International journal of environmental research and public health **18**.

Qian, P., Hou, S., and Guo, G. (2009). Molecular mechanisms controlling pavement cell shape in Arabidopsis leaves. Plant Cell Reports **28,** 1147-1157.

Qiu, L., Lin, J.S., Xu, J., Sato, S., Parniske, M., Wang, T.L., Downie, J.A., and Xie, F. (2015). SCARN a novel class of SCAR protein that is required for root-hair infection during legume nodulation. PLoS genetics **11,** e1005623.

Radutoiu, S., Madsen, L.H., Madsen, E.B., Jurkiewicz, A., Fukai, E., Quistgaard, E.M., Albrektsen, A.S., James, E.K., Thirup, S., and Stougaard, J. (2007). LysM domains mediate lipochitin–oligosaccharide recognition and *NFR* genes extend the symbiotic host range. The EMBO Journal **26,** 3923-3935.

Radutoiu, S., Madsen, L.H., Madsen, E.B., Felle, H.H., Umehara, Y., Grønlund, M., Sato, S., Nakamura, Y., Tabata, S., Sandal, N., and Stougaard, J. (2003). Plant recognition of symbiotic bacteria requires two LysM receptor-like kinases. Nature **425,** 585-592.

Ranathunge, K., Thomas, R.H., Fang, X., Peterson, C.A., Gijzen, M., and Bernards, M.A. (2008). Soybean root suberin and partial resistance to root rot caused by *Phytophthora sojae*. Phytopathology **98,** 1179-1189.

Rédei, G.P. (1992). A heuristic glance at the past of *Arabidopsis* genetics. In Methods in *Arabidopsis* Research, pp. 1-15.

Redmond, J.W., Batley, M., Djordjevic, M.A., Innes, R.W., Kuempel, P.L., and Rolfe, B.G. (1986). Flavones induce expression of nodulation genes in *Rhizobium*. Nature **323,** 632-635.

Reid, D., Nadzieja, M., Novak, O., Heckmann, A.B., Sandal, N., and Stougaard, J. (2017a). Cytokinin biosynthesis promotes cortical cell responses during nodule development. Plant Physiology **175,** 361-375.

Reid, D., Liu, H., Kelly, S., Kawaharada, Y., Mun, T., Andersen, S.U., Desbrosses, G., and Stougaard, J. (2017b). Dynamics of ethylene production in response to compatible nod factor. Plant Physiology **176,** 1764-1772.

Remans, T., Nacry, P., Pervent, M., Filleur, S., Diatloff, E., Mounier, E., Tillard, P., Forde, B.G., and Gojon, A. (2006). The *Arabidopsis NRT1.1* transporter participates in the signaling pathway triggering root colonization of nitrate-rich patches. Proc Natl Acad Sci U S A **103,** 19206-19211.

Remy, W., Taylor, T.N., Hass, H., and Kerp, H. (1994). Four hundred-million-year-old vesicular arbuscular mycorrhizae. Proc Natl Acad Sci U S A **91,** 11841-11843.

Roberts, I., Smith, S., Stes, E., De Rybel, B., Staes, A., van de Cotte, B., Njo, M.F., Dedeyne, L., Demol, H., Lavenus, J., Audenaert, D., Gevaert, K., Beeckman, T., and De Smet, I. (2016). *CEP5* and *XIP1/CEPR1* regulate lateral root initiation in Arabidopsis. J Exp Bot **67,** 4889-4899.

Roppolo, D., De Rybel, B., Tendon, V.D., Pfister, A., Alassimone, J., Vermeer, J.E.M., Yamazaki, M., Stierhof, Y.-D., Beeckman, T., and Geldner, N. (2011). A novel protein family mediates Casparian strip formation in the endodermis. Nature **473,** 380-383.

Rosas-Diaz, T., Zhang, D., Fan, P., Wang, L., Ding, X., Jiang, Y., Jimenez-Gongora, T., Medina-Puche, L., Zhao, X., Feng, Z., Zhang, G., Liu, X., Bejarano, E.R., Tan, L., Zhang, H., Zhu, J.-K., Xing, W., Faulkner, C., Nagawa, S., and Lozano-Duran, R. (2018). A virus-targeted plant receptor-like kinase promotes cell-to-cell spread of RNAi. Proc Natl Acad Sci U S A **115,** 1388-1393.

Roy, S., Liu, W., Nandety, R.S., Crook, A., Mysore, K.S., Pislariu, C.I., Frugoli, J., Dickstein, R., and Udvardi, M.K. (2019). Celebrating 20 years of genetic discoveries in legume nodulation and symbiotic nitrogen fixation. The Plant Cell **32,** 15-41.

Ruffel, S., Krouk, G., Ristova, D., Shasha, D., Birnbaum, K.D., and Coruzzi, G.M. (2011). Nitrogen economics of root foraging: Transitive closure of the nitrate–cytokinin relay and distinct systemic signaling for N supply vs. demand. Proc Natl Acad Sci U S A **108,** 18524-18529.

Sachs, J.L., Quides, K.W., and Wendlandt, C.E. (2018). Legumes versus rhizobia: a model for ongoing conflict in symbiosis. New Phytologist **219,** 1199-1206.

Sahlman, K., and Fåhraeus, G. (1963). An electron microscope study of root-hair infection by *Rhizobium*. Journal of General Microbiology **33,** 425-427.

Saito, K., Yoshikawa, M., Yano, K., Miwa, H., Uchida, H., Asamizu, E., Sato, S., Tabata, S., Imaizumi-Anraku, H., Umehara, Y., Kouchi, H., Murooka, Y., Szczyglowski, K., Downie, J.A., Parniske,

M., Hayashi, M., and Kawaguchi, M. (2007). *NUCLEOPORIN85* is required for calcium spiking, fungal and bacterial symbioses, and seed production in *Lotus japonicus*. The Plant Cell **19,** 610-624.

Sasaki, T., Suzaki, T., Soyano, T., Kojima, M., Sakakibara, H., and Kawaguchi, M. (2014). Shoot-derived cytokinins systemically regulate root nodulation. Nature communications **5,** 4983.

Schauser, L., Roussis, A., Stiller, J., and Stougaard, J. (1999). A plant regulator controlling development of symbiotic root nodules. Nature **402,** 191-195.

Schiessl, K., Lilley, J.L.S., Lee, T., Tamvakis, I., Kohlen, W., Bailey, P.C., Thomas, A., Luptak, J., Ramakrishnan, K., Carpenter, M.D., Mysore, K.S., Wen, J., Ahnert, S., Grieneisen, V.A., and Oldroyd, G.E.D. (2019). *NODULE INCEPTION* recruits the lateral root developmental program for symbiotic nodule organogenesis in *Medicago truncatula*. Current Biology **29,** 3657-3668.e3655.

Schumann, N., Navarro-Quezada, A., Ullrich, K., Kuhl, C., and Quint, M. (2011). Molecular evolution and selection patterns of plant F-box proteins with C-terminal kelch repeats. Plant Physiology **155,** 835-850.

Serra, O., Mähönen, A.P., Hetherington, A.J., and Ragni, L. (2022). The making of plant armor: The periderm. Annual Review of Plant Biology **73,** 405-432.

Sexauer, M., and Markmann, K. (2024). To the roots of nodules: Nodule organogenesis utilizes lateral root development processes. . Manuscript in preparation.

Sexauer, M., Shen, D., Schön, M., Andersen, T.G., and Markmann, K. (2021). Visualizing polymeric components that define distinct root barriers across plant lineages. Development **148**.

Sexauer, M., Bhasin, H., Schön, M., Roitsch, E., Wall, C., Herzog, U., and Markmann, K. (2023). A micro RNA mediates shoot control of root branching. Nature Communications **14,** 8083.

Shah, N., Wakabayashi, T., Kawamura, Y., Skovbjerg, C.K., Wang, M.Z., Mustamin, Y., Isomura, Y., Gupta, V., Jin, H., Mun, T., Sandal, N., Azuma, F., Fukai, E., Seren, U., Kusakabe, S., Kikuchi, Y., Nitanda, S., Kumaki, T., Hashiguchi, M., Tanaka, H., Hayashi, A., Sonderkaer, M., Nielsen, K.L., Schneeberger, K., Vilhjalmsson, B., Akashi, R., Stougaard, J., Sato, S., Schierup, M.H., and Andersen, S.U. (2020). Extreme genetic signatures of local adaptation during *Lotus japonicus* colonization of Japan. Nature communications **11,** 253.

Shimotohno, A., Heidstra, R., Blilou, I., and Scheres, B. (2018). Root stem cell niche organizer specification by molecular convergence of *PLETHORA* and *SCARECROW* transcription factor modules. Genes & development **32,** 1085-1100.

Shrestha, A., Zhong, S., Therrien, J., Huebert, T., Sato, S., Mun, T., Andersen, S.U., Stougaard, J., Lepage, A., Niebel, A., Ross, L., and Szczyglowski, K. (2021). *Lotus japonicus Nuclear Factor YA1,* a nodule emergence stage-specific regulator of auxin signalling. New Phytologist **229,** 1535-1552.

Shukla, V., Han, J.-P., Cléard, F., Lefebvre-Legendre, L., Gully, K., Flis, P., Berhin, A., Andersen, T.G., Salt, D.E., Nawrath, C., and Barberon, M. (2021). Suberin plasticity to developmental and exogenous cues is regulated by a set of MYB transcription factors. Proc Natl Acad Sci U S A **118,** e2101730118.

Singh, S., Katzer, K., Lambert, J., Cerri, M., and Parniske, M. (2014). CYCLOPS, a DNA-binding transcriptional activator, orchestrates symbiotic root nodule development. Cell Host & Microbe **15,** 139-152.

Singh, S., Yadav, S., Singh, A., Mahima, M., Singh, A., Gautam, V., and Sarkar, A.K. (2020). Auxin signaling modulates *LATERAL ROOT PRIMORDIUM1* (*LRP1*) expression during lateral root development in Arabidopsis. The Plant Journal **101,** 87-100.

Skopelitis, D.S., Benkovics, A.H., Husbands, A.Y., and Timmermans, M.C.P. (2017). Boundary formation through a direct threshold-based readout of mobile small RNA gradients. Developmental Cell **43,** 265-273.e266.

Skopelitis, D.S., Hill, K., Klesen, S., Marco, C.F., von Born, P., Chitwood, D.H., and Timmermans, M.C.P. (2018). Gating of miRNA movement at defined cell-cell interfaces governs their impact as positional signals. Nature Communications **9,** 3107.

Smit, P., Limpens, E., Geurts, R., Fedorova, E., Dolgikh, E., Gough, C., and Bisseling, T. (2007). Medicago LYK3, an entry receptor in rhizobial nodulation factor signaling. Plant Physiology **145,** 183-191.

Sohlberg, J.J., Myrenås, M., Kuusk, S., Lagercrantz, U., Kowalczyk, M., Sandberg, G., and Sundberg, E. (2006). *STY1* regulates auxin homeostasis and affects apical–basal patterning of the Arabidopsis gynoecium. The Plant Journal **47,** 112-123.

Soltis, D.E., Soltis, P.S., Morgan, D.R., Swensen, S.M., Mullin, B.C., Dowd, J.M., and Martin, P.G. (1995). Chloroplast gene sequence data suggest a single origin of the predisposition for symbiotic nitrogen fixation in angiosperms. Proc Natl Acad Sci U S A **92,** 2647-2651.

Soyano, T., Shimoda, Y., Kawaguchi, M., and Hayashi, M. (2019). A shared gene drives lateral root development and root nodule symbiosis pathways in *Lotus*. Science **366,** 1021-1023.

Sprent, J.I., and James, E.K. (2007). Legume evolution: where do nodules and mycorrhizas fit in? Plant Physiology **144,** 575-581.

Ståldal, V., Cierlik, I., Chen, S., Landberg, K., Baylis, T., Myrenås, M., Sundström, J.F., Eklund, D.M., Ljung, K., and Sundberg, E. (2012). The *Arabidopsis thaliana* transcriptional activator *STYLISH1* regulates genes affecting stamen development, cell expansion and timing of flowering. Plant Molecular Biology **78,** 545-559.

Stoeckle, D., Thellmann, M., and Vermeer, J.E.M. (2018). Breakout—lateral root emergence in *Arabidopsis thaliana*. Current Opinion in Plant Biology **41,** 67-72.

Stracke, S., Kistner, C., Yoshida, S., Mulder, L., Sato, S., Kaneko, T., Tabata, S., Sandal, N., Stougaard, J., Szczyglowski, K., and Parniske, M. (2002). A plant receptor-like kinase required for both bacterial and fungal symbiosis. Nature **417,** 959-962.

Suganuma, N., Nakamura, Y., Yamamoto, M., Ohta, T., Koiwa, H., Akao, S., and Kawaguchi, M. (2003). The *Lotus japonicus SEN1* gene controls rhizobial differentiation into nitrogen-fixing bacteroids in nodules. Molecular Genetics and Genomics **269,** 312-320.

Suzuki, W., Konishi, M., and Yanagisawa, S. (2013). The evolutionary events necessary for the emergence of symbiotic nitrogen fixation in legumes may involve a loss of nitrate responsiveness of the *NIN* transcription factor. Plant Signal Behav **8**.

Swarup, K., Benková, E., Swarup, R., Casimiro, I., Péret, B., Yang, Y., Parry, G., Nielsen, E., De Smet, I., Vanneste, S., Levesque, M.P., Carrier, D., James, N., Calvo, V., Ljung, K., Kramer, E., Roberts, R., Graham, N., Marillonnet, S., Patel, K., Jones, J.D.G., Taylor, C.G., Schachtman, D.P., May, S., Sandberg, G., Benfey, P., Friml, J., Kerr, I., Beeckman, T., Laplaze, L., and Bennett, M.J. (2008). The auxin influx carrier *LAX3* promotes lateral root emergence. Nature Cell Biology **10,** 946-954.

Swensen, S.M., and Benson, D.R. (2007). Evolution of actinorhizal host plants frankia endosymbionts. In Nitrogen-fixing actinorhizal symbioses (vol 6. Springer), pp. 73-104.

Szczyglowski, K., and Stougaard, J. (2008). *Lotus* genome: pod of gold for legume research. Trends in Plant Science **13,** 515-517.

Tabata, R., Sumida, K., Yoshii, T., Ohyama, K., Shinohara, H., and Matsubayashi, Y. (2014). Perception of root-derived peptides by shoot LRR-RKs mediates systemic N-demand signaling. Science **346,** 343-346.

Takahara, M., Magori, S., Soyano, T., Okamoto, S., Yoshida, C., Yano, K., Sato, S., Tabata, S., Yamaguchi, K., Shigenobu, S., Takeda, N., Suzaki, T., and Kawaguchi, M. (2013). TOO MUCH LOVE, a novel kelch repeat-containing f-box protein, functions in the long-distance regulation of the legume–rhizobium symbiosis. Plant and Cell Physiology **54,** 433-447.

Thomas, R., Fang, X., Ranathunge, K., Anderson, T.R., Peterson, C.A., and Bernards, M.A. (2007). Soybean root suberin: Anatomical distribution, chemical composition, and relationship to partial resistance to *Phytophthora sojae*. Plant Physiology **144,** 299-311.

Tian, H., Jia, Y., Niu, T., Yu, Q., and Ding, Z. (2014). The key players of the primary root growth and development also function in lateral roots in Arabidopsis. Plant Cell Reports **33,** 745-753.

Tirichine, L., Sandal, N., Madsen, L.H., Radutoiu, S., Albrektsen, A.S., Sato, S., Asamizu, E., Tabata, S., and Stougaard, J. (2007). A gain-of-function mutation in a cytokinin receptor triggers spontaneous root nodule organogenesis. Science **315,** 104-107.

Tirichine, L., Imaizumi-Anraku, H., Yoshida, S., Murakami, Y., Madsen, L.H., Miwa, H., Nakagawa, T., Sandal, N., Albrektsen, A.S., Kawaguchi, M., Downie, A., Sato, S., Tabata, S., Kouchi, H., Parniske, M., Kawasaki, S., and Stougaard, J. (2006). Deregulation of a Ca^{2+}/calmodulin-dependent kinase leads to spontaneous nodule development. Nature **441,** 1153-1156.

Toyokura, K., Goh, T., Shinohara, H., Shinoda, A., Kondo, Y., Okamoto, Y., Uehara, T., Fujimoto, K., Okushima, Y., Ikeyama, Y., Nakajima, K., Mimura, T., Tasaka, M., Matsubayashi, Y., and Fukaki, H. (2019). Lateral inhibition by a peptide hormone-receptor cascade during *Arabidopsis* lateral root founder cell formation. Developmental Cell **48,** 64-75.e65.

Triozzi, P.M., Irving, T.B., Schmidt, H.W., Keyser, Z.P., Chakraborty, S., Balmant, K., Pereira, W.J., Dervinis, C., Mysore, K.S., Wen, J., Ané, J.-M., Kirst, M., and Conde, D. (2021). Spatiotemporal cytokinin response imaging and *ISOPENTENYLTRANSFERASE 3* function in Medicago nodule development. Plant Physiology.

Tsikou, D., Yan, Z., Holt, D.B., Abel, N.B., Reid, D.E., Madsen, L.H., Bhasin, H., Sexauer, M., Stougaard, J., and Markmann, K. (2018). Systemic control of legume susceptibility to rhizobial infection by a mobile microRNA. Science **362,** 233-236.

Tsyganova, A.V., Brewin, N.J., and Tsyganov, V.E. (2021). Structure and development of the legume-rhizobial symbiotic interface in infection threads. Cells **10**.

Turner, M., Nizampatnam, N.R., Baron, M., Coppin, S., Damodaran, S., Adhikari, S., Arunachalam, S.P., Yu, O., and Subramanian, S. (2013). Ectopic expression of miR160 results in auxin hypersensitivity, cytokinin hyposensitivity, and inhibition of symbiotic nodule development in soybean. Plant Physiology **162,** 2042-2055.

Urbanski, D.F., Malolepszy, A., Stougaard, J., and Andersen, S.U. (2012). Genome-wide LORE1 retrotransposon mutagenesis and high-throughput insertion detection in *Lotus japonicus*. The Plant Journal **69,** 731-741.

Ursache, R., Andersen, T.G., Marhavy, P., and Geldner, N. (2018). A protocol for combining fluorescent proteins with histological stains for diverse cell wall components. The Plant Journal **93,** 399-412.

Valmas, M.I., Sexauer, M., Markmann, K., and Tsikou, D. (2023). Plants recruit peptides and micro RNAs to regulate nutrient acquisition from soil and symbiosis. Plants (Basel, Switzerland) **12**.

van Gelderen, K., Kang, C., Li, P., and Pierik, R. (2021). Regulation of lateral root development by shoot-sensed far-red light via *HY5* is nitrate-dependent and involves the *NRT2.1* nitrate transporter. Frontiers in plant science **12,** 660870.

Vanneste, S., De Rybel, B., Beemster, G.T.S., Ljung, K., De Smet, I., Van Isterdael, G., Naudts, M., Iida, R., Gruissem, W., Tasaka, M., Inzé, D., Fukaki, H., and Beeckman, T. (2005). Cell cycle progression in the pericycle is not sufficient for *SOLITARY ROOT/IAA14*-mediated lateral root initiation in *Arabidopsis thaliana*. The Plant Cell **17,** 3035-3050.

Vargason, J.M., Szittya, G., Burgyán, J., and Hall, T.M.T. (2003). Size selective recognition of siRNA by an RNA silencing suppressor. Cell **115,** 799-811.

Vazquez, F., Vaucheret, H., Rajagopalan, R., Lepers, C., Gasciolli, V., Mallory, A.C., Hilbert, J.-L., Bartel, D.P., and Crété, P. (2004). Endogenous trans-acting siRNAs regulate the accumulation of Arabidopsis mRNAs. Molecular Cell **16,** 69-79.

Vermeer, J.E.M., von Wangenheim, D., Barberon, M., Lee, Y., Stelzer, E.H.K., Maizel, A., and Geldner, N. (2014). A spatial accommodation by neighboring cells is required for organ initiation in *Arabidopsis*. Science **343,** 178-183.

Vernié, T., Camut, S., Camps, C., Rembliere, C., de Carvalho-Niebel, F., Mbengue, M., Timmers, T., Gasciolli, V., Thompson, R., le Signor, C., Lefebvre, B., Cullimore, J., and Hervé, C. (2016).

PUB1 interacts with the receptor kinase DMI2 and negatively regulates rhizobial and arbuscular mycorrhizal symbioses through its ubiquitination activity in *Medicago truncatula*. Plant Physiology **170,** 2312-2324.

Vidal, E.A., Moyano, T.C., Riveras, E., Contreras-López, O., and Gutiérrez, R.A. (2013). Systems approaches map regulatory networks downstream of the auxin receptor AFB3 in the nitrate response of *Arabidopsis thaliana* roots. Proc Natl Acad Sci U S A **110,** 12840-12845.

Vidal, E.A., Araus, V., Lu, C., Parry, G., Green, P.J., Coruzzi, G.M., and Gutiérrez, R.A. (2010). Nitrate-responsive miR393/*AFB3* regulatory module controls root system architecture in *Arabidopsis thaliana*. Proc Natl Acad Sci U S A **107,** 4477-4482.

Vidal, E.A., Alvarez, J.M., Araus, V., Riveras, E., Brooks, M.D., Krouk, G., Ruffel, S., Lejay, L., Crawford, N.M., Coruzzi, G.M., and Gutiérrez, R.A. (2020). Nitrate in 2020: Thirty years from transport to signaling networks. The Plant Cell **32,** 2094-2119.

Vigh, M.L., Bressendorff, S., Thieffry, A., Arribas-Hernández, L., and Brodersen, P. (2022). Nuclear and cytoplasmic RNA exosomes and PELOTA1 prevent miRNA-induced secondary siRNA production in Arabidopsis. Nucleic Acids Research **50,** 1396-1415.

Vilches-Barro, A., and Maizel, A. (2015). Talking through walls: mechanisms of lateral root emergence in *Arabidopsis thaliana*. Current Opinion in Plant Biology **23,** 31-38.

Vishal, B., Krishnamurthy, P., Ramamoorthy, R., and Kumar, P.P. (2019). *OsTPS8* controls yield-related traits and confers salt stress tolerance in rice by enhancing suberin deposition. New Phytologist **221,** 1369-1386.

Voinnet, O. (2005). Non-cell autonomous RNA silencing. FEBS Letters **579,** 5858-5871.

von Wangenheim, D., Fangerau, J., Schmitz, A., Smith, R.S., Leitte, H., Stelzer, E.H.K., and Maizel, A. (2016). Rules and self-organizing properties of post-embryonic plant organ cell division patterns. Current Biology **26,** 439-449.

Walker, S.A., Viprey, V., and Downie, J.A. (2000). Dissection of nodulation signaling using pea mutants defective for calcium spiking induced by nod factors and chitin oligomers. Proceedings of the National Academy of Sciences **97,** 13413-13418.

Wang, B., Zhou, G., Guo, S., Li, X., Yuan, J., and Hu, A. (2022). Improving nitrogen use efficiency in rice for sustainable agriculture: Strategies and future perspectives. Life (Basel, Switzerland) **12**.

Wang, C., Wang, H., Li, P., Li, H., Xu, C., Cohen, H., Aharoni, A., and Wu, S. (2020). Developmental programs interact with abscisic acid to coordinate root suberization in Arabidopsis. The Plant journal **104,** 241-251.

Wang, T., Guo, J., Peng, Y., Lyu, X., Liu, B., Sun, S., and Wang, X. (2021). Light-induced mobile factors from shoots regulate rhizobium-triggered soybean root nodulation. Science **374,** 65-71.

Wang, Y., Li, K., Chen, L., Zou, Y., Liu, H., Tian, Y., Li, D., Wang, R., Zhao, F., Ferguson, B.J., Gresshoff, P.M., and Li, X. (2015). MicroRNA167-directed regulation of the auxin response factors *GmARF8a* and *GmARF8b* is required for soybean nodulation and lateral root development. Plant Physiology **168,** 984-999.

Ward, B.B. (2013). Nitrification. In Encyclopedia of Ecology (Second Edition), B. Fath, ed (Oxford: Elsevier), pp. 351-358.

Williamson, L.C., Ribrioux, S.P., Fitter, A.H., and Leyser, H.M. (2001). Phosphate availability regulates root system architecture in Arabidopsis. Plant Physiology **126,** 875-882.

Xiao, T.T., Schilderink, S., Moling, S., Deinum, E.E., Kondorosi, E., Franssen, H., Kulikova, O., Niebel, A., and Bisseling, T. (2014). Fate map of *Medicago truncatula* root nodules. Development **141,** 3517-3528.

Xie, M., and Yu, B. (2015). siRNA-directed DNA methylation in plants. Current Genomics **16,** 23-31.

Yamoune, A., Cuyacot, A.R., Zdarska, M., and Hejatko, J. (2021). Hormonal orchestration of root apical meristem formation and maintenance in Arabidopsis. J Exp Bot **72,** 6768-6788.

Yan, D., Easwaran, V., Chau, V., Okamoto, M., Ierullo, M., Kimura, M., Endo, A., Yano, R., Pasha, A., Gong, Y., Bi, Y.-M., Provart, N., Guttman, D., Krapp, A., Rothstein, S.J., and Nambara, E. (2016). NIN-like protein 8 is a master regulator of nitrate-promoted seed germination in Arabidopsis. Nature Communications **7,** 13179.

Yang, Z., Ebright, Y.W., Yu, B., and Chen, X. (2006). HEN1 recognizes 21–24 nt small RNA duplexes and deposits a methyl group onto the 2′ OH of the 3′ terminal nucleotide. Nucleic Acids Research **34,** 667-675.

Yano, K., Yoshida, S., Müller, J., Singh, S., Banba, M., Vickers, K., Markmann, K., White, C., Schuller, B., Sato, S., Asamizu, E., Tabata, S., Murooka, Y., Perry, J., Wang, T.L., Kawaguchi, M., Imaizumi-Anraku, H., Hayashi, M., and Parniske, M. (2008). *CYCLOPS,* a mediator of symbiotic intracellular accommodation. Proc Natl Acad Sci U S A **105,** 20540-20545.

Yokota, K., Fukai, E., Madsen, L.H., Jurkiewicz, A., Rueda, P., Radutoiu, S., Held, M., Hossain, M.S., Szczyglowski, K., Morieri, G., Oldroyd, G.E., Downie, J.A., Nielsen, M.W., Rusek, A.M., Sato, S., Tabata, S., James, E.K., Oyaizu, H., Sandal, N., and Stougaard, J. (2009). Rearrangement of actin cytoskeleton mediates invasion of *Lotus japonicus* roots by *Mesorhizobium loti*. The Plant Cell **21,** 267-284.

Yoro, E., Suzaki, T., and Kawaguchi, M. (2020). *CLE-HAR1* systemic signaling and *NIN*-mediated local signaling suppress the increased rhizobial infection in the *daphne* mutant of *Lotus japonicus*. Molecular Plant-Microbe Interactions **33,** 320-327.

Yoro, E., Suzaki, T., Toyokura, K., Miyazawa, H., Fukaki, H., and Kawaguchi, M. (2014). A positive regulator of nodule organogenesis, *NODULE INCEPTION*, acts as a negative regulator of rhizobial infection in *Lotus japonicus*. Plant physiology **165,** 747-758.

Yoro, E., Nishida, H., Ogawa-Ohnishi, M., Yoshida, C., Suzaki, T., Matsubayashi, Y., and Kawaguchi, M. (2019). PLENTY, a hydroxyproline O-arabinosyltransferase, negatively regulates root nodule symbiosis in *Lotus japonicus*. J Exp Bot **70,** 507-517.

Yu, B., Yang, Z., Li, J., Minakhina, S., Yang, M., Padgett, R.W., Steward, R., and Chen, X. (2005). Methylation as a crucial step in plant microRNA biogenesis. Science **307,** 932-935.

Yuan, S., Zhu, H., Gou, H., Fu, W., Liu, L., Chen, T., Ke, D., Kang, H., Xie, Q., Hong, Z., and Zhang, Z. (2012). A ubiquitin ligase of symbiosis receptor kinase involved in nodule organogenesis. Plant Physiology **160,** 106-117.

Zhang, S., Liu, Y., and Yu, B. (2015). New insights into pri-miRNA processing and accumulation in plants. WIREs RNA **6,** 533-545.

Zhang, T.-T., Kang, H., Fu, L.-L., Sun, W.-J., Gao, W.-S., You, C.-X., Wang, X.-F., and Hao, Y.-J. (2021). NIN-like protein 7 promotes nitrate-mediated lateral root development by activating transcription of *TRYPTOPHAN AMINOTRANSFERASE RELATED 2*. Plant Science **303,** 110771.

Zhao, L., Zhang, W., Yang, Y., Li, Z., Li, N., Qi, S., Crawford, N.M., and Wang, Y. (2018). The Arabidopsis *NLP7* gene regulates nitrate signaling via *NRT1.1*-dependent pathway in the presence of ammonium. Scientific reports **8,** 1487.

Zhu, F., Ye, Q., Chen, H., Dong, J., and Wang, T. (2021). Multigene editing reveals that *MtCEP1/2/12* redundantly control lateral root and nodule number in *Medicago truncatula*. J Exp Bot **72,** 3661-3676.

Zhu, F., Deng, J., Chen, H., Liu, P., Zheng, L., Ye, Q., Li, R., Brault, M., Wen, J., Frugier, F., Dong, J., and Wang, T. (2020). A CEP peptide receptor-like kinase regulates auxin biosynthesis and ethylene signaling to coordinate root growth and symbiotic nodulation in *Medicago truncatula*. The Plant Cell **32,** 2855-2877.

Zhu, H., Chen, T., Zhu, M., Fang, Q., Kang, H., Hong, Z., and Zhang, Z. (2008). A novel ARID DNA-binding protein interacts with SymRK and is expressed during early nodule development in *Lotus japonicus*. Plant Physiology **148,** 337-347.

Appendix

Appendix 1 Material and Methods

Plant and bacterial resources.

Plants used in this thesis are listed in (**Appendix Table 1**). For infection *Mesorhizobium loti* strain MAFF303099 expressing *DsRED* was used (Maekawa et al., 2009). Generation of transgenic lines and prior cloning procedure were described in (Sexauer et al., 2023).

Plant growth procedure.

Plant growth conditions and experimental setup for root phenotyping, including grafting and split root experiments were described in (Sexauer et al., 2023). Growth conditions and procedure for analysis of endodermal suberization was described in (Sexauer et al., 2021). For assessment of nodule numbers, nodule size and It numbers, plants were pre germinated as described in (Sexauer et al., 2023). After transfer to plates for growing, plants were inoculated with a fresh *M. loti* culture OD_{600} = 0.01. Procedure of *M. loti* culture and infection was described in (Tsikou et al., 2018). Plants grew for 10 days for IT analysis, 3 weeks for molecular analysis and 4 weeks for analysis of nodule number and size.

Analysis of transcript levels

Analysis of transcript levels was done via qRT-PCR. cDNA was prepared using a pulsed RT protocol, RNA was prior DNAse treated. RNA extraction was done using a trizol-chloroform-RNA extraction protocol. Description of individual steps and a list of primers used during qRT-PCR and RT reaction can be found in (Sexauer et al., 2023).

Staining, microscopy, and data analysis

For analysis of Its and endodermal suberization, plants were fixed as described in (Sexauer et al., 2021). ITs were quantified using the fluorescence of MAFF303099 expressing *DsRED.* Analysis of endodermal suberization used the fluorescent dye FY. The staining procedure was as described in (Sexauer et al., 2021). Suberization was quantified by the proportion of the root showing suberin stained endodermis. Patchy zone is defined by the distal position of the first suberized endodermal cell and the beginning of the continuous zone, which begins at the first complete suberization of the endodermis and ends at the hypocotyl. GUS staining was carried out as described in (Sexauer et al., 2023), cell walls of semi-thin sectioned samples were stained using

0.1% ruthenium red. Microscopy procedure and data analysis was as described in (Sexauer et al., 2021; Sexauer et al., 2023).

Appendix 2 Tables

Appendix Table 1 Plant resources used in this thesis.

Line name	Ecotype	Species	ID / description	Reference
Gifu	Gifu B-129	*Lotus japonicus*		(Handberg and Stougaard, 1992)
MG20	MG-20	*Lotus japonicus*		(Kawaguchi, 2000)
tml-1	MG-20	*Lotus japonicus*		(Magori et al., 2009)
tml-5	Gifu B-129	*Lotus japonicus*	line ID 30013998	(Tsikou et al., 2018)
tml-6	Gifu B-129	*Lotus japonicus*	line ID 30094802	(Tsikou et al., 2018)
har1-3	Gifu B-129	*Lotus japonicus*		(Krusell et al., 2002)
MIR2111-3-1	Gifu B-129	*Lotus japonicus*	CRISPR/CAS *MIR2111-3*	(Sexauer et al., 2023)
miR2111ox	Gifu B-129	*Lotus japonicus*	*pUBQ1:MiR2111-3*	(Sexauer et al., 2023)
nfr1-1	Gifu B-129	*Lotus japonicus*		(Radutoiu et al., 2003)
nfr5-1	Gifu B-129	*Lotus japonicus*		(Madsen et al., 2003)
lhk1-1	Gifu B-129	*Lotus japonicus*	formerly *hit1-1*	(Murray et al., 2007)
lhk1-1 har1-1	Gifu B-129	*Lotus japonicus*		(Murray et al., 2007)
Col-0	Columbia-0	*Arabidopsis thaliana*		(Rédei)
holt-1	Columbia-0	*Arabidopsis thaliana*	SALK_044075.49.80	(Sexauer et al., 2023)
holt-2	Columbia-0	*Arabidopsis thaliana*	SALK_140092.27.55	(Sexauer et al., 2023)
miR2111ox	Columbia-0	*Arabidopsis thaliana*	*p35:MiR2111b*	(Sexauer et al., 2023)

Appendix Table 2 Sample size, number of biological replicates and results of statistical tests. Samples = biological replicates, individual cDNA samples derived from individual RNA extracts of pools of 4-8 plants. Samples derived of x individual independent experiments.

Figure 7							**test**	**p-value**	x =
Figure 7a									
Genotype / condition	2111ox-3	2111ox-4					n.a.	n.a.	1
individual plants n=	4	11							
Figure 7b									
Genotype / condition	Gifu	2111ox-3	2111ox-4				Anova	7.99757 E-10	1
individual plants n=	20	20	35						
Figure 7d									
Genotype / condition	Gifu/Gifu	2111ox/Gifu					t-test	0.11748 6351	2
individual samples n=	4	4							
Figure 7e									
Genotype / condition	Gifu/Gifu	2111ox/Gifu					t-test	3.49E-09	3
individual plants n=	27	30							
Figure 7f									
Genotype / condition	Gifu/Gifu	2111ox/Gifu					t-test	0.00463 528	2
individual samples n=	4	4							
Figure 9							**test**	**p-value**	x =
Figure 9b									
Genotype / condition	Gifu	tml-6	tml-5	2111ox			Anova	2.02958 E-64	>=3
individual plants n=	127	128	62	64					
Figure 9c									
Genotype / condition	Gifu	2111ox	tml-6				Anova	1.74951 E-23	2
individual plants n=	42	40	35						
Figure 9d									
Genotype / condition	Gifu/Gifu	2111ox/Gifu					t-test	0.01767 4657	3
individual plants n=	40	24							
Figure 9e									

Genotype / condition	Gifu	2111ko					t-test	0.002794132	3
individual plants n=	91	51							
Figure 9f									
Genotype / condition	Gifu/Gifu	mir2111-3-1/Gifu					t-test	0.005674273	1
individual plants n=	8	12							
Figure 10							**test**	**p-value**	x =
Figure 10a									
Genotype / condition	Gifu	2111ko					t-test	0.032299453	3
individual samples n=	6	6							
Figure 10b									
Genotype / condition	Gifu	2111ko					t-test	0.007565588	3
individual samples n=	6	6							
Figure 10c									
Genotype / condition	miR2111-3-1	Gifu	tml-6	2111ox			Anova	5.23827E-13	>=2
individual plants n=	16	37	13	15					
Figure 11							**test**	**p-value**	x =
Figure 11a									
Genotype / condition	Gifu_0 mM	Gifu_1 mM	Gifu_5 mM	tml-6_0 mM	tml-6_1 mM	tml-6_5 mM	Anova	1.4491E-141	>=3
individual plants n=	127	89	133	128	90	119			
Genotype / condition	tml-5_0 mM	tml-5_1 mM	tml-5_5 mM	2111ox_0 mM	2111ox_5 mM				
individual plants n=	62	63	70	64	61				
Figure 11b									
Genotype / condition	MG20_0 mM	MG20_1 mM	MG20_5 mM	tml-1_0 mM	tml-1_1 mM	tml-1_5 mM	Anova	6.11022E-57	3
individual plants n=	68	52	48	69	48	56			
Figure 11c									
Genotype / condition	MG20_0 mM	MG20_1 mM	MG20_5 mM	tml-1_0 mM	tml-1_1 mM	tml-1_5 mM	Anova	2.57473E-21	3

individual plants n=	36	41	42	38	47	34			
Figure 11e									
Genotype / condition	0 mM_MG20	1 mM_MG20	5 mM_MG20				Anova	9.04041E-06	3
individual samples n=	6	6	6						
Figure 11f									
Genotype / condition	0 mM_MG20	1 mM_MG20	5 mM_MG20				Anova	0.009584308	3
individual samples n=	6	6	6						
Figure 11g									
Genotype / condition	0 mM_MG20	1 mM_MG20	5 mM_MG20				Anova	0.009671809	3
individual samples n=	6	6	6						
Figure 11i									
Genotype / condition	0 mM control	0 mM split	5 mM split	5 mM control			Anova	3.00208E-08	2
individual samples n=	4	4	4	4			t-test (split)	0.18103262	
Figure 11j									
Genotype / condition	0 mM control	0 mM split	5 mM split	5 mM control			Anova	0.000789706	2
individual samples n=	4	4	4	4			t-test (split)	0.12232 2684	
Figure 12							**test**	**p-value**	x =
Figure 12a									
Genotype / condition	0 mM_Gifu	0 mM_tml-6	1 mM_Gifu	1 mM_tml-6	5 mM_Gifu	5 mM_tml-6	Anova	1.68147E-29	3
individual plants n=	62	42	52	55	53	55			
Figure 12b									
Genotype / condition	0 mM_Gifu	1 mM_Gifu	5 mM_Gifu				Anova	0.039826296	3
individual samples n=	6	6	6						
Figure 12c									
Genotype / condition	0 mM_Gifu	1 mM_Gifu	5 mM_Gifu				Anova	0.213193428	3
individual samples n=	6	6	6						

Figure 12d									
Genotype / condition	0 mM_Gifu	1 mM_Gifu	5 mM_Gifu				Anova	0.88568917	3
individual samples n=	6	6	6						
Figure 13							**test**	**p-value**	x =
Figure 13a									
Genotype / condition	Gifu_0 mM	2111ox_0 mM	Gifu_5 mM	2111ox_5 mM			Anova	9.26682E-27	>=2
individual plants n=	42	40	40	31					
Figure 13b									
Genotype / condition	Gifu/MG20_0 mM	2111ox/MG20_0 mM	Gifu/MG20_5 mM	2111ox/MG20_5 mM			Anova	0.000326578	>=2
individual plants n=	16	11	6	20					
Figure 13c									
Genotype / condition	Gifu_0 mM	Gifu_1 mM	Gifu_5 mM	2111-3 ko_0 mM	2111-3 ko_1 mM	2111-3 ko_5 mM	Anova	0.000111039	>=3
individual plants n=	38	34	35	35	36	39			
Figure 14							**test**	**p-value**	x =
Figure 14c									
Genotype / condition	100 uM	250 uM	500 uM	1 mM			Anova	1.96601E-25	2
individual plants n=	46	45	46	42					
Genotype / condition	2 mM	5 mM	10 mM						
individual plants n=	39	44	36						
Figure 14d									
Genotype / condition	Col-0	2111ox					t-test	0.000827479	>=3
individual samples n=	5	3							
Figure 14e									
Genotype / condition	Col-0	2111ox					t-test	0.000204175	>=3
individual samples n=	6	4							
Figure 14f									
Genotype / condition	0.1 mM_Col-0	1 mM_Col-0	10 mM_Col-0	0.1 mM_holt-2	1 mM_holt-2	10 mM_holt-2	Anova	5.46513E-38	>=3

individual plants n=	65	73	68	76	77	70			
Genotype / condition	0.1 mM_holt-1	1 mM_holt-1	10 mM_holt-1	0.1 mM_2111ox	1 mM_2111ox	10 mM_2111ox			
individual plants n=	70	75	64	71	61	68			
Figure 14h									
Genotype / condition	0.1 mM_Col-0	1 mM_Col-0	10 mM_Col-0				Anova	0.015192322	>=3
individual samples n=	4	5	5						
Figure 14i									
Genotype / condition	0.1 mM_Col-0	1 mM_Col-0	10 mM_Col-0				Anova	0.00029702	>=3
individual samples n=	5	5	5						
Figure 14j									
Genotype / condition	Gifu/Gifu	2111ox/Gifu					t-test	0.016751599	3
individual plants n=	13	13							
Figure 15							**test**	**p-value**	x =
Figure 15a									
Genotype / condition	col-0	holt-1	2111ox				Anova	0.997886527	>=3
individual samples n=	6	4	4						
Figure 15b									
Genotype / condition	col-0	holt-1	2111ox				Anova	0.873205604	>=3
individual samples n=	6	4	4						
Figure 15c									
Genotype / condition	col-0	holt-1	2111ox				Anova	0.76687568	>=3
individual samples n=	6	4	4						
Figure 15d									
Genotype / condition	col-0	holt-1	2111ox				Anova	0.503454319	>=3
individual samples n=	6	4	4						
Figure 16							**test**	**p-value**	x =
Figure 16B									

Genotype / condition	Gifu/Gifu	2111OX/Gifu					t-test	0.04514559	3
individual plants n=	27	30							
Figure 16C									
Genotype / condition	Gifu_0 mM	Gifu_1 mM	Gifu_5 mM	tml-6_0 mM	tml-6_1 mM	tml-6_5 mM	Anova	2.92973E-28	3
individual plants n=	103	65	110	104	69	95			
Genotype / condition	2111ox_0 mM	2111ox_5mM							
individual plants n=	64	61							
Figure 16D									
Genotype / condition	Gifu_0 mM	Gifu_1 mM	Gifu_5 mM	tml-6_0 mM	tml-6_1 mM	tml-6_5 mM	Anova	1.27908E-16	3
individual plants n=	60	51	52	42	55	55			
Figure 17							**test**	**p-value**	x =
Figure 17A									
Genotype / condition	0 mM_Gifu	1 mM_Gifu	5 mM_Gifu				Anova	0.008125689	2
individual samples n=	6	6	6						
Figure 17B									
Genotype / condition	0 mM_MG20	1 mM_MG20	5 mM_MG20				Anova	4.0078E-06	2
individual samples n=	6	6	6						
Figure 17C									
Genotype / condition	Gifu_0 mM	Gifu_1 mM	Gifu_5 mM	har1-3_0 mM	har1-3_1 mM	har1-3_5 mM	Anova	0.000174994	3
individual plants n=	65	65	65	48	48	44			
Figure 17D									
Genotype / condition	Gifu_0 mM	Gifu_1 mM	Gifu_5 mM	har1-3_0 mM	har1-3_1 mM	har1-3_5 mM	Anova	9.45881E-05	3
individual plants n=	103	65	110	48	48	44			
Figure 17E									
Genotype / condition	Gifu_0 mM	Gifu_1 mM	Gifu_5 mM	har1-3_0 mM	har1-3_1 mM	har1-3_5 mM	Anova	2.1548E-29	3
individual plants n=	103	65	110	48	48	44			
Figure 17F									

Genotype / condition	Gifu_0 mM	Gifu_1 mM	Gifu_5 mM	har1-3_0 mM	har1-3_1 mM	har1-3_5 mM	Anova	4.82973 E-29	3
individual plants n=	ab	ac	c	d	de	be			
Figure 18							**test**	**p-value**	x =
Figure 18A									
Genotype / condition	0 mM_Gifu	0 mM_har1-3	1 mM_Gifu	1 mM_har1-3	5 mM_Gifu	5 mM_har1-3	Anova	2.77647 E-51	3
individual plants n=	42	57	42	54	40	55			
Figure 18B									
Genotype / condition	0 mM_Gifu	0 mM_har1-3	1 mM_Gifu	1 mM_har1-3	5 mM_Gifu	5 mM_har1-3	Anova	4.98583 E-07	3
individual plants n=	42	57	42	54	40	55			
Figure 18C									
Genotype / condition	Gifu/Gifu	Gifu/har1-3	har1-3/Gifu	har1-3/har1-3			Anova	2.28942 E-27	2
individual plants n=	40	31	29	28					
Figure 18D									
Genotype / condition	0 mM_har1-3	5 mM_har1-3					t-test	0.02187 0782	2
individual samples n=	3	3							
Figure 21							**test**	**p-value**	x =
Figure 21a									
Genotype / condition	Gifu_0mM	Gifu_1mM	Gifu_5mM	tml-6_0mM	tml-6_1mM	tml-6_5mM	Anova	1.07118 E-16	3
individual plants n=	39	28	34	33	33	36	Anova	1.22169 E-09	
Figure 21b									
Genotype / condition	col-0_100 µM	col-0_1 mM	col-0_10 mM	holt-1_100 µM	holt-1_1 mM	holt-1_10 mM	Anova	6.65347 E-15	2
individual plants n=	45	44	36	53	37	35	Anova	1.31397 E-15	
Figure 22							**test**	**p-value**	x =
Figure 22a									
Genotype / condition	mock	M. loti					t-test	0.02169 6605	1
individual samples n=	3	3							

Figure 22b									
Genotype / condition	mock	M. loti					t-test	0.04052 0139	1
individual samples n=	3	3							
Figure 22c									
Genotype / condition	mock	M. loti					t-test	0.04052 0139	1
individual samples n=	3	3							
Figure 22d									
Genotype / condition	Gifu_mock	tml-6_mock	Gifu_M. loti	tml-6_M. loti			Anova	2.90646 E-32	3
individual plants n=	66	50	67	65					
Figure 23							**test**	**p-value**	x =
Figure 23A									
Genotype / condition	MG20_0 uM	tml-1_0 uM	MG20_5 mM	tml-1_5 mM			Anova	7.84085 E-30	2
individual plants n=	35	31	18	21					
Figure 23B									
Genotype / condition	MG20_0 uM	tml-1_0 uM	MG20_5 mM	tml-1_5 mM			Anova	1.35725 E-47	2
individual plants n=	19	24	19	20					
Figure 23C									
Genotype / condition	Gifu_0mM	Gifu_5mM	tml-6_0mM	tml-6_5mM			Anova	1.96442 E-30	2
individual plants n=	25	25	25	25					
Figure 23D									
Genotype / condition	Gifu	tml-6					t-test	0.00459 156	>3
individual plants n=	11	11							
Figure 23E									
Genotype / condition	MG20	tml-1					t-test	0.00330 3115	>3
individual plants n=	6	6							

Appendix 3 Accepted Manuscripts

Appendix 3.1 Visualizing polymeric components that define distinct root barriers across plant lineages.

© 2021. Published by The Company of Biologists Ltd | Development (2021) 148, dev199820. doi:10.1242/dev.199820

TECHNIQUES AND RESOURCES

RESEARCH REPORT

Visualizing polymeric components that define distinct root barriers across plant lineages

Moritz Sexauer[1], Defeng Shen[2], Maria Schön[1], Tonni Grube Andersen[2,‡] and Katharina Markmann[1,*,‡]

ABSTRACT

Hydrophobic cell wall depositions in roots play a key role in plant development and interaction with the soil environment, as they generate barriers that regulate bidirectional nutrient flux. Techniques to label the respective polymers are emerging, but are efficient only in thin roots or sections. Moreover, simultaneous imaging of the barrier constituents lignin and suberin remains problematic owing to their similar chemical compositions. Here, we describe a staining method compatible with single- and multiphoton confocal microscopy that allows for concurrent visualization of primary cell walls and distinct secondary depositions in one workflow. This protocol permits efficient separation of suberin- and lignin-specific signals with high resolution, enabling precise dissection of barrier constituents. Our approach is compatible with imaging of fluorescent proteins, and can thus complement genetic markers or aid the dissection of barriers in biotic root interactions. We further demonstrate applicability in deep root tissues of plant models and crops across phylogenetic lineages. Our optimized toolset will significantly advance our understanding of root barrier dynamics and function, and of their role in plant interactions with the rhizospheric environment.

KEY WORDS: Suberin, Lignin, Endodermis, Periderm, ClearSee, Fluorol Yellow, Basic Fuchsin, Symbiosis

INTRODUCTION

Roots are complex, dynamic organs that facilitate the extraction of solutes from their surroundings and mediate plant interactions with the biotic soil environment. In contrast to above-ground plant organs of most vascular plants, roots feature a central vascular cylinder known as the stele, which contains conductive xylem and phloem tissue responsible for bidirectional long-distance transport of water, minerals and assimilated solutes. The stele is surrounded and protected by concentric cell files including a highly specialized cell layer known as the endodermis, as well as outer cortical cell layers that vary in number between plant lineages. The endodermis directly surrounds the stele and serves as a dynamic filter, providing control over radial transport of solutes to and from the vascular tissues (Barberon and Geldner, 2014; Geldner, 2013). This sophisticated function is facilitated by the establishment of diverse polymeric secondary cell wall depositions. At the periphery of the cortex, often right underneath the outermost root epidermis, certain plant lineages feature a cell layer termed the exodermis, which is reminiscent of the endodermis in structure and function (Enstone et al., 2002). Arguably, the best-known endodermal barrier is the Casparian strip, which consists of defined, ring-shaped cell wall depositions of lignin synthesized autonomously in the endodermis (Andersen et al., 2021; Naseer et al., 2012). The Casparian strip blocks apoplastic diffusion to and from the rhizosphere in a manner that is remarkably similar to tight junctions in animals (Doblas et al., 2017), providing control of radial flow of water and solutes. As the endodermis matures in older root parts, hydrophobic suberin is deposited on the entire surface of most endodermal cell walls, blocking transcellular transport across the endodermal plasma membrane. In contrast to the Casparian strip, which consists of phenylpropanoid-derived lignin monomers (Naseer et al., 2012), suberin contains both aromatic and aliphatic constituents (Schreiber, 2010).

The deposition of lignin- or suberin-containing barriers in roots is not limited to the endodermis, they can also be found in the exodermis or in the periderm. The periderm is a frontier tissue developed during secondary growth of most eudicots and gymnosperms (Ragni and Greb, 2018). After it replaces the epidermis as the outermost tissue, the periderm restricts water and gas exchange (Lendzian, 2006), and grants resistance to pathogens (Lulai and Freeman, 2001). The patterning of lignin- or suberin-containing barriers, in terms of design and extent, is dynamic and varies between tissues, as well as between lineages and species. Although much remains to be understood about the genetic control and dynamics of barriers in roots, emerging evidence suggests that they play a key role in defining molecular communication with the underground environment, and also in shaping associated microbial communities (Salas-González et al., 2021).

The spatiotemporal differences in suberin and lignin deposits suggest that their roles in plant development and adaptation to environmental factors differ. To investigate this at a functional level, it is thus fundamental to visualize the individual barrier components differentially. Currently established methods rely on either autofluorescence, Raman signal or histochemical dyes (Rydahl et al., 2018; Wallace and Anderson, 2012) that can specifically highlight lignin or suberin, such as Basic Fuchsin (BF) and Fluorol Yellow (FY), respectively. One key limitation is that neither of these tools allows simultaneous visualization of lignin and suberin because of overlap in their emission spectra (DeVree et al., 2021) or incompatibility of the respective histochemical procedures (Ursache et al., 2018). Approaches based on genetically encoded fluorescent transcriptional reporters (Andersen et al., 2018; Barberon et al., 2016) have partially overcome this, but are limited to the underlying

[1]Department of Plant Physiology, Zentrum für Molekularbiologie der Pflanzen, Tübingen University, 72076 Tübingen, Germany. [2]Department of Plant Microbe Interactions, Max Planck Institute for Plant Breeding Research, 50829 Cologne, Germany.
*Present address: Genetics Institute, Martin Luther-University Halle-Wittenberg, 06120 Halle (Saale), Germany.

‡Authors for correspondence (katharina.markmann@zmbp.uni-tuebingen.de; tandersen@mpipz.mpg.de)

M. Sexauer, 0000-0003-1475-5167; D.S., 0000-0002-6530-8837; T.G.A., 0000-0002-8905-0850; K.M., 0000-0003-1257-3490

Handling Editor: Yka Helariutta
Received 20 May 2021; Accepted 11 October 2021

Development (2021) 148, dev199820. doi:10.1242/dev.199820

machinery and to genetically tractable models such as *Arabidopsis thaliana*. Moreover, although *A. thaliana* indeed is an outstanding model for image analysis and root developmental biology research, it lacks endosymbiotic associations, such as fungal arbuscular mycorrhiza formation or nitrogen-fixing nodulation with bacteria. As the vast majority of land plants form either fungal or bacterial root symbioses, such interactions are of extensive ecological and economical significance, and the current limitations therefore hinder the detailed study of the role of barriers in a biotic context.

Here, we present an improved histochemical staining technique that can distinguish lignin from suberin with subcellular resolution and a high degree of specificity. Our method is compatible with fluorescent markers and widely applicable to roots of varying thickness and complexity. We use this to highlight differences in barrier-associated lignin and suberin depositions in roots across diverse phylogenetic lineages, including both model and crop species. Compatibility of the toolset with imaging of fluorescent dyes and microbial markers make it a prime tool for hydrophobic barrier analysis also in root symbiotic contexts.

RESULTS AND DISCUSSION

Aiming to visualize specifically endodermal suberin depositions in roots of different model and crop plants for comparative analysis, we initially used a well-established lactic acid-based protocol for FY staining of suberin in *Arabidopsis thaliana* roots and semi-thin cuts (Lux et al., 2005). When applied to *Lotus japonicus* roots, which have a different internal structure and more cortical cell layers than *A. thaliana* roots, this protocol did give rise to suberin-associated signals (Fig. 1A,B), but these were weak and difficult to image owing low signal intensity in whole-mount roots (Fig. 1A). To improve staining in deeper root tissues, we combined the lactic acid-based FY staining directly with a previously established ClearSee-based protocol (Kurihara et al., 2015), which has been successfully used together with other histochemical dyes (Ursache et al., 2018). However, this approach resulted in a precipitation of FY and almost complete loss of suberin-associated signals. To solve this, we tested alternative solvents for FY, and found that the use of 96% ethanol rendered the staining solution compatible with ClearSee. A combined treatment with ethanol-dissolved FY and ClearSee yielded greatly enhanced signals from suberized endodermal cells in *L. japonicus* roots (Fig. 1C) compared with the initially tested protocol (Lux et al., 2005) (Fig. 1A).

In contrast to the established lactic acid-based protocol, this procedure can be performed at room temperature, suggesting that it may be compatible with imaging of fluorescent proteins. To test this, we employed a *DsRED*-expressing strain of the rhizobacterium *Mesorhizobium loti*, which symbiotically infects *L. japonicus* roots. This setting further enabled us to evaluate whether these bacteria remained traceable in FY-stained roots, and to test the applicability of the protocol for analyzing barriers in a root endosymbiotic context (Fig. 2A,B). Intriguingly, suberized endodermal cells and *DsRED*-labelled epidermal and cortical infection threads could be reliably visualized in the same samples (Fig. 2A). Furthermore, a suberized periderm-like layer in colonized nodules was apparent. In line with earlier observations in *Vicia faba* nodules (Hartmann et al., 2002), these suberized cells appeared to connect to the endodermis of the root tissue and of nodule vascular bundles (Fig. 2B). This hints towards an important function of cell wall barriers in this plant-bacterial interaction, and paves the way for in-depth visual analysis of suberin depositions in the context of nodulation symbiosis.

In *A. thaliana*, endodermal suberization is assumed to be subsequent to lignification of the Casparian strip (Doblas et al., 2017). To evaluate whether our protocol could distinguish between these polymers, we combined it with BF-based lignin staining (Kurihara et al., 2015). In FY/BF co-stained roots, we were able to clearly identify the lignified Casparian strip and the suberin lamella as separate entities in the *L. japonicus* root endodermis (Fig. 2C). The emission signals of both dyes were visually separable (Figs 3 and 4), and we rarely observed colocalization of FY-stained suberin and BF-labelled lignin in root samples. Moreover, FY signal was absent from the xylem, whereas BF stained meta- and protoxylem (Fig. 4A). This implies specificity of the staining technique, confirms distinct accumulation patterns and is consistent with independent functions of suberin and lignin depositions (Barberon et al., 2016). Barrier deposition strategies in roots differ between plant lineages and species (Holbein et al., 2021). We thus extended the protocol to other species, aiming to cover a representative set of spermatophytic lineages (The Angiosperm Phylogeny Group, 2016) (Fig. S1; Fig. 3A-E). To enhance visualization of cell structures inside roots, we further implemented concurrent cellulose staining using

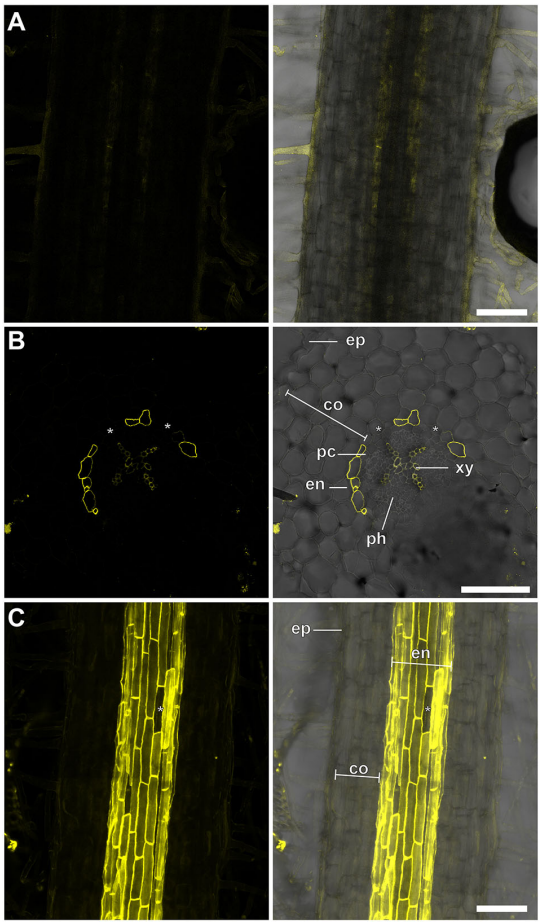

Fig. 1. Staining of endodermal suberization in *L. japonicus*. (A,B) FY-stained *L. japonicus* whole-mount roots (A) and semi-thin sections (B) using a lactic acid-based protocol. (C) *L. japonicus* roots stained using the optimized ClearSee-based method. Asterisks indicate passage cells. Left panels: FY channel. Right panels: merged FY and transmission light channels. Plants grew for 10 days. co, parenchymatic cortex; en, endodermis ep, epidermis; pc, pericycle; ph, phloem; xy, xylem. Scale bars: 100 µm.

Development (2021) 148, dev199820. doi:10.1242/dev.199820

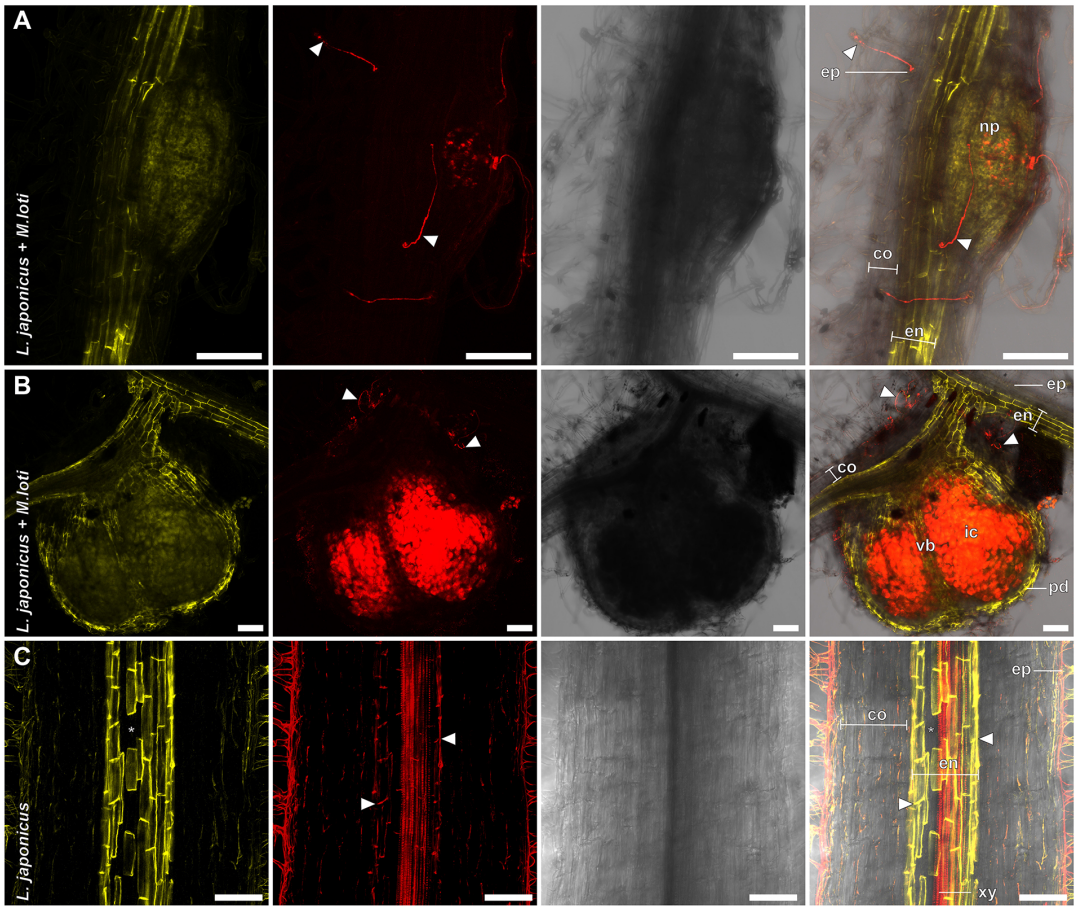

Fig. 2. FY-based suberin staining is compatible with BF staining of lignin and fluorescent protein imaging. (A-C) *L. japonicus* root showing nodule primordia prior to formation of a suberized periderm (10 days post-inoculation), (B) mature nodule (21 days post-inoculation) and (C) uninfected root 10 days post-germination stained with FY (A,B) or double-stained with FY and BF (C) using an optimized ClearSee-based method. Panels (left to right) show FY; DsRED (A,B) or BF (C); transmission light; and merged channel. (A,B) *L. japonicus* infected with *M. loti* expressing DsRED at 10 and 21 days post-inoculation, respectively. (C) Root co-stained with BF. White arrowheads indicate infection threads (A,B) or Casparian strip (C). Asterisks indicate passage cells. co, parenchymatic cortex; en, endodermis; ep, epidermis; ic, infected nodule cortex; np, nodule primordia; pd, periderm; xy, xylem; vb, vascular bundle. Scale bars: 100 µm.

Calcofluor White (CW) into the protocol. This allowed for simultaneous visualization of the primary cell wall of non-lignified, unsuberized cells, and, in line with the spectral properties of CW, CW staining did not interfere with suberin and lignin signals (Figs 3 and 4). For most of the tested species, triple staining with CW, FY and BF allowed a clear differentiation between primary and suberized, or lignified secondary cell walls such as the Casparian strip (Figs 3 and 4A-F). Standard single-photon confocal imaging techniques were sufficient to resolve root barrier features in most cases. However, to increase the depth of imaging in thick roots, we employed a multiphoton setup in *Solanum lycopersicum* (Fig. 3C) and *Brachypodium distachyon* (Fig. 3D). For a better understanding of the root cell wall composition, and to evaluate imaging limitations associated with whole-mount analyses, we performed triple CW, BF and FY staining on root cross-sections of the same species (Fig. 4A-E). Apart from xylem cell walls within the stele, *L. japonicus* (Figs 2C, 3A and 4A) and *A. thaliana* (Figs 3B and 4B) roots both possessed lignin depositions mainly in form of classical endodermal Casparian strips, and displayed endodermal suberin lamellae. The crop tomato (*S. lycopersicum* ecotype Moneymaker) showed no suberin deposition in the endodermis and only hardly detectable Casparian strips (Figs 3C and 4C). The establishment of a suberized exodermis was only sparsely observed in both *L. japonicus* and *S. lycopersicum* (Figs 3A,C and 4A,C). Whereas *L. japonicus* seems to have no continuous exodermis at all (Figs 3A and 4A), *S. lycopersicum* showed only rare and weak suberization but, in line with previous reports (Li et al., 2018), lignification of the exodermis (Fig. 4C). In the monocot *B. distachyon*, structures comparable to Casparian strips were rarely observed and only evident near the meristematic zone. This suggests that Casparian strips might be weakly pronounced or absent in these species, or that its chemical constituents are distinct, and not stainable by BF. In older developmental regions of *B. distachyon* roots, lignification encompassed entire endodermal cells (Figs 3D and 4D; Fig. S2A-D), indicating that lignin or lignin-based barriers may be serving distinct roles in this species. Strikingly, in cross-sections of *B. distachyon* roots (Fig. 4D), endodermal lignin depositions were mainly found on inner periclinal cell walls, whereas suberin predominantly lined outer periclinal cell walls, suggesting a polarity of lignin and suberin depositions. As in other species, the *B.*

Development (2021) 148, dev199820. doi:10.1242/dev.199820

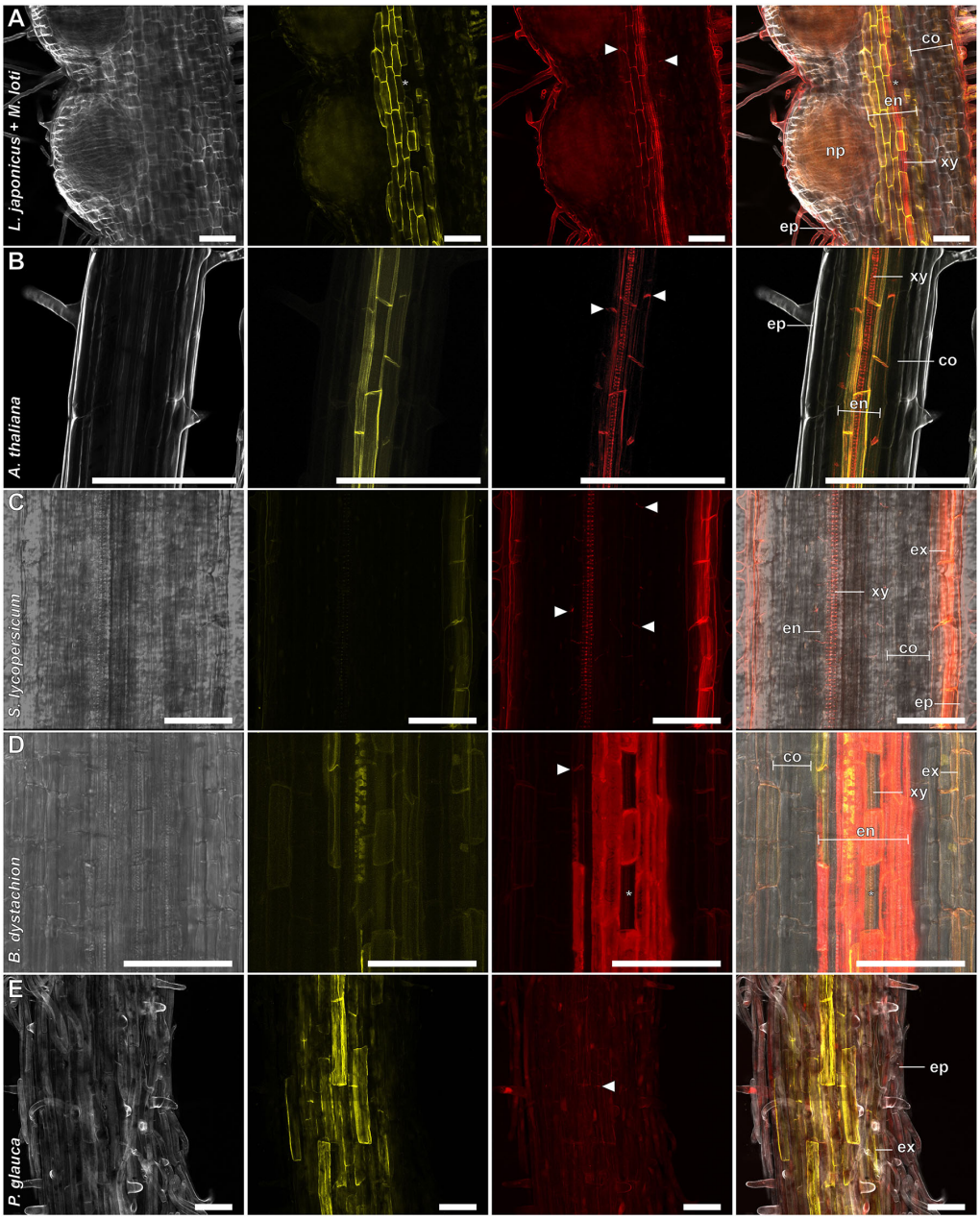

Fig. 3. Visualization of root barriers in a broad range of seed plants. (A-E) Whole-root mounts of *L. japonicus* infected with *M. loti* showing pre-peridermal nodule primordia (10 days post-inoculation) (A), *A. thaliana* (B), *S. lycopersicum* (C), *B. distachyon* (D) and *P. glauca* (E). Roots were stained with BF, FY and CW (A,B,E only). Panels (left to right) show CW (A,B,E) or transmission light (C,D); FY; BF; and merged channels. White arrowheads indicate Casparian strip. Asterisks indicate passage cells. Plants grew for 14 (A,E) or 10 (B,C,D) days. co, parenchymatic cortex; en, endodermis; ep, epidermis; ex, exodermis; np, nodule primordia; xy, xylem. Scale bars: 100 µm.

distachyon endodermis contained unsuberized passage cells (Fig. S2B,C), and, interestingly, cells lacking lignification were also observed (Fig. 3D; Fig. S2C). A further remarkable feature of *B. distachyon* roots was the existence of an exodermis with lignin and weak suberin depositions following a pattern reminiscent of Casparian strips (Fig. 4D; Fig. S2A). Among the species examined here, roots of the gymnosperm tree *Picea glauca* showed the highest degree of both suberin and lignin deposition (Figs 3E and 4E), with most cortical cell walls of 14-day-old treelets, including those of the endodermis, lignified and suberized. Notably, *P. glauca* showed high variability in cell wall composition depending on the developmental stage (Fig. S3A,B).

Development (2021) 148, dev199820. doi:10.1242/dev.199820

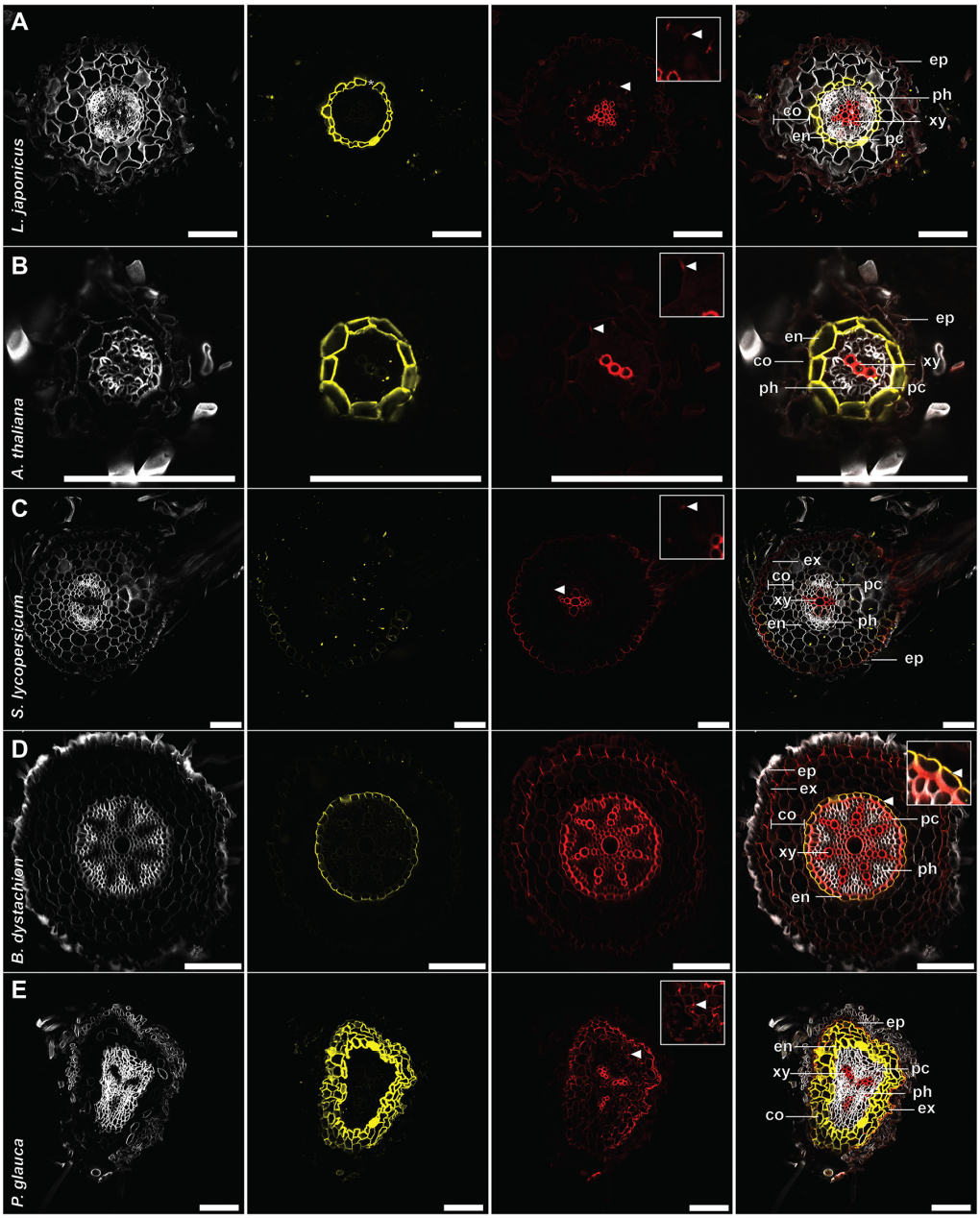

Fig. 4. Triple staining of cell wall components in semi-thin cross-sections of seed plant roots. (A-E) BF, FY and CW triple-stained cross-sections of *L. japonicus* (A), *A. thaliana* (B), *S. lycopersicum* (C), *B. distachyon* (D) and *P. glauca* roots (E). Panels (left to right) show CW; FY; BF; and merged channels. White arrowheads indicate Casparian strip in original image and corresponding magnification of the endodermal region (insets). Asterisks indicate passage cells. Plants grew for 14 (A,E) or 10 (B,C,D) days. co, parenchymatic cortex; en, endodermis; ep, epidermis; ex, exodermis; pc, pericycle; ph, phloem; xy, xylem. Scale bars: 100 µm.

In summary, different plant species displayed distinct barrier patterns, ranging from defined endodermal Casparian strips with or without accompanying suberin lamellae, to near universal lignification and suberization of the root cortex. The presented protocol allows qualitative imaging of diverse root barriers, including both inner (endodermis with Casparian strip) and peripheral barrier types such as exodermal (Figs 3D,E and 4D,E; Figs S2A,D and S3B) and peridermal suberization (Figs 2B; Figs S4 and S5). However, reliable quantitative visualization of suberin seems not to be feasible using FY owing to fast bleaching of this dye under laser exposure. Further limiting quantitative evaluation of both lignin and suberin depositions in inner root tissues of whole

Development (2021) 148, dev199820. doi:10.1242/dev.199820

mounts is the clearing efficiency, as in whole-mount tissue, incomplete clearing will result in compromised signal intensity. In cross-sections, we did not observe differences in staining efficiency between previously cleared and fresh tissue (Fig. S6A,B). We also observed that CW-based staining of primary cell walls in deeper tissue layers was of limited efficiency in whole-mount samples, but uncompromised when root sections were stained. Using properly cleared samples, a 3D reconstruction of endodermal cell wall modification can be achieved using this protocol (Fig. S7). To identify optimal settings for specific staining signals, we determined the multiphoton excitation and emission spectra of FY and BF (Fig. S8A,B).

How these different strategies respond to environmental triggers and what their effects are on biotic interactions in the rhizosphere are exciting questions. We tested our protocol on a broad phylogenetic range of species inhabiting diverse ecological niches, including non-models and cultivated crops. In *L. japonicus*, nodulation symbiosis triggers the *de novo* formation of bacteria-filled nodule organs. This process is accompanied by the establishment of novel barrier types, such as a suberized periderm surrounding the entire nodule organ (Fig. 2B; Fig. S5). It will be interesting to examine further these symbiosis-related barrier structures and their biological roles. Allowing for co-observation of multiple cell wall components and fluorescent proteins in the same samples, the presented toolset represents a valuable advance towards addressing these questions, and provides an exciting handle for comparative exploration of the interplay between polymeric root barriers and rhizospheric composition and interactions.

MATERIALS AND METHODS

Plant and bacterial resources

Plants used in this study were *Lotus japonicus* ecotype Gifu B-129 (Handberg and Stougaard, 1992), *Arabidopsis thaliana* ecotype Col-0, *Solanum lycopersicum* ecotype Moneymaker (Dörffling, 1970), *Brachypodium distachyon* ecotype BD-21 (Garvin et al., 2008) and *Picea glauca* (1a Saatgut; http://www.1a-saatgut.de/). For analysis of symbiotic roots, *L. japonicus* plants were inoculated with *M. loti* MAFF303099 expressing *DsRED* (Maekawa et al., 2009).

Plant growth and infection

All plants used in this study, except those shown in Fig. S4, were grown under sterile culture conditions. *A. thaliana* seeds were sterilized by 30 min incubation in a solution of 70% ethanol and 0.05% Triton X-100. Seeds of other species used in this study were sterilized by incubation in sodium hypochlorite solution containing 10 g/l Cl, then washed six times and incubated on a shaker in sterile ddH_2O at room temperature until imbibed. Seeds were transferred to sterile growth media on square plastic dishes and stratified at 4°C in darkness. Following cold treatment, seeds were pre-germinated at 22°C in darkness, or directly transferred to growing conditions at 21°C in the light/17°C in the dark (16 h light, 8 h dark). Detailed growth conditions of individual species are listed in Table S1. For infection of *L. japonicus* with *M. loti*, liquid bacterial cultures were grown for 2 days at 28°C and pelleted for 10 min at 3000 ***g***. The bacterial pellet was washed twice and resuspended in quarter-strength B&D (Broughton and Dilworth, 1971) medium. For inoculations, the optical density at λ=600 was adjusted to 0.01 and 20 µl bacterial suspension were applied to each root. Roots were harvested after 10-21 days depending on the species (Table S1) for fixation, cuts or direct staining.

Semi-thin sections of roots and nodules

Sectioning was conducted on either fresh, or previously fixed and cleared, primary root or nodule tissue. For sectioning, roots were cut into pieces of about 1 cm length, which contained the region of interest. These root fragments were embedded in 5-7% agarose. After hardening, small blocks of agarose including the sample fragments were sectioned by hand using a fresh razorblade.

Confocal microscopy

Roots were analysed with Leica SP8 inverted (Figs 1 and 2A,B), Zeiss LSM 880 (Figs 3A,B,E and 4; Figs S2-S7) or Leica SP8 FALCON-DIVE (Figs 2C and 3C,D) confocal microscopes. 2D and 3D reconstructions were created using Leica LAS X or ZEN Blue software. For single-photon microscopy, settings for visualization of dyes were: objectives 10×/0.3 dry or 20×/0.8 dry; excitation (EX) 405 nm, emission (EM) 425-475 nm for CW; EX 488 nm, EM 520-550 nm for FY; EX 561 nm, EM 600-700 nm for BF in sequential scans. For multi-photon microscopy, settings for visualization of dyes were: objective 25×/0.95, water immersion; MP set at 1045 nm, MP2 (output power 2.24 W) set at 977 nm; fluorescence collected at 500-535 nm for FY, and 585-605 nm for BF.

Fixation procedure

For fixation, root tissue was immersed in 4% paraformaldehyde in 1× PBS and gently shaken overnight at 4°C. Alternatively, tissue was immersed in 4% paraformaldehyde in 1× PBS and vacuum infiltrated for 1 h. After fixation, samples were washed three times in 1× PBS. Fixed samples were directly used for clearing.

Clearing of fixed samples

We cleared the samples using a ClearSee-based protocol (Kurihara et al., 2015). ClearSee solution was prepared by dissolving xylitol powder (10% w/v), sodium deoxycholate (15% w/v) and urea (25% w/v) in water, without heating the solution. Previously fixed tissue was incubated in ClearSee at room temperature for 1-14 days until clear. To improve the clearing, the tissue was gently shaken and the ClearSee solution was regularly exchanged when discoloured. Clearing duration was highly dependent on plant species, age and tissue (for details, see Table S1).

Staining procedure

For staining using dye combinations, best results were obtained when dyes were applied in the order BF, FY and CW. All dyes were successfully used either directly on thin cuts of fresh tissue, or on whole roots following clearing. For lignin staining, tissue was immersed in 0.2% BF in ClearSee for at least 1 h, rinsed once in fresh ClearSee and incubated in a second rinse for 30 min or longer. For suberin staining, a working solution of 0.01% FY in ethanol was prepared using a stock of 1% FY in DMSO. Tissue was rinsed once in ddH_2O and immersed in FY working solution for 30 min at room temperature. For basic staining of cell walls, tissue was immersed in 0.1% aqueous solution of CW and incubated for 15 min. If thin cuts were used as starting material, incubation times for all staining and washing steps were reduced to 10 min.

If only FY staining was applied, roots were optionally counterstained using 0.5% (w/v) Aniline Blue in ddH_2O for 20 min. Counterstaining of FY-stained samples with Aniline Blue improves contrast in thin samples and cuts, but is not recommended for imaging of deep tissue such as *L. japonicus* nodules to achieve higher signal intensity in optical sections.

Following the final staining, the tissue was washed once in 50% ethanol, twice in ddH_2O and stored in 50% glycerol. When stored cool and dark, samples could be imaged for up to 3 weeks without significant signal loss. Note that counterstaining with Aniline Blue is not recommended when FY staining is combined with BF and/or CW. FY solutions and FY-stained tissue must be kept in darkness to prevent bleaching.

For a short guide to the triple-staining procedure, see supplementary Materials and Methods.

Determination of dye spectra

Excitation and emission spectra for BF and FY were determined separately using a Leica SP8 FALCON-DIVE confocal microscope. *L. japonicus* Gifu nodules (21 days post-infection) were fixed, cleared, stained and sectioned as described. For both dyes, multi-photon excitation spectra were determined between λ=800 nm and 1265 nm, with stepwise increase of 15 nm; emission λ=500-550 nm for FY, λ=600-650 nm for BF. Emission

was measured from λ=380 nm to 750 nm, at a 10 nm step size. For excitation, previously determined excitation maxima (λ=935 nm for FY, 1055 nm for BF) were used. For each of two independent replicates using sections of different nodules, five regions of interest at the nodule vascular endodermis were selected to quantify BF or FY signals.

Acknowledgements
We thank Angela M. Fischer for drawing Fig. S1B, Ulrike Herzog for technical support, Johanna Schröter and the gardening team for dedicated plant care, and Laura Ragni for discussions. We apologize to authors whose work could not be cited owing to space limitations. The Leica SP8 and Zeiss LSM 880 confocal microscopes used in this study were funded by the German Research Foundation (INST 37/819-1 FUGG and INST 37/965-1 FUGG, respectively).

Competing interests
The authors declare no competing or financial interests.

Author contributions
Conceptualization: M. Sexauer, K.M., T.G.A., D.S.; Methodology: M. Sexauer, D.S., M. Schoen; Validation: M. Sexauer, D.S., M. Schoen; Formal analysis: M. Sexauer, D.S., M. Schoen; Investigation: M. Sexauer, D.S., M. Schoen; Resources: K.M., T.G.A.; Data curation: M. Sexauer, D.S., M. Schoen; Writing - original draft: M. Sexauer, K.M., T.G.A.; Writing - review & editing: K.M., T.G.A., D.S.; Visualization: M. Sexauer, D.S., M. Schoen; Supervision: K.M., T.G.A.; Project administration: K.M., T.G.A.; Funding acquisition: K.M., T.G.A.

Funding
This work was supported by the German Research Foundation (Deutsche Forschungsgemeinschaft; grant CRC1101, project C07) and the Ministry of Science, Research and Art of Baden-Wuerttemberg (Ministerium für Wissenschaft, Forschung und Kunst Baden-Württemberg; Az:7533-30-20/1) (K.M., M. Sexauer and M. Schoen), as well as the Alexander von Humboldt-Stiftung foundation and Max Planck Society (Max-Planck-Gesellschaft; T.G.A. and D.S.). Open access funding provided by Eberhard Karls Universität Tübingen. Deposited in PMC for immediate release.

Peer review history
The peer review history is available online at https://journals.biologists.com/dev/article-lookup/doi/10.1242/dev.199820.

References
Andersen, T. G., Naseer, S., Ursache, R., Wybouw, B., Smet, W., De Rybel, B., Vermeer, J. E. M. and Geldner, N. (2018). Diffusible repression of cytokinin signalling produces endodermal symmetry and passage cells. *Nature* **555**, 529-533. doi:10.1038/nature25976

Andersen, T. G., Molina, D., Kilian, J., Franke, R. B., Ragni, L. and Geldner, N. (2021). Tissue-autonomous phenylpropanoid production is essential for establishment of root barriers. *Curr. Biol.* **31**, 965-977.e5. doi:10.1016/j.cub.2020.11.070

Barberon, M. and Geldner, N. (2014). Radial transport of nutrients: the plant root as a polarized epithelium. *Plant Physiol.* **166**, 528-537. doi:10.1104/pp.114.246124

Barberon, M., Vermeer, J. E. M., De Bellis, D., Wang, P., Naseer, S., Andersen, T. G., Humbel, B. M., Nawrath, C., Takano, J., Salt, D. E. et al. (2016). Adaptation of root function by nutrient-induced plasticity of endodermal differentiation. *Cell* **164**, 447-459. doi:10.1016/j.cell.2015.12.021

Broughton, W. J. and Dilworth, M. J. (1971). Control of leghaemoglobin synthesis in snake beans. *Biochem. J.* **125**, 1075-1080. doi:10.1042/bj1251075

DeVree, B. T., Steiner, L. M., Głazowska, S., Ruhnow, F., Herburger, K., Persson, S. and Mravec, J. (2021). Current and future advances in fluorescence-based visualization of plant cell wall components and cell wall biosynthetic machineries. *Biotechnol. Biofuels* **14**, 78. doi:10.1186/s13068-021-01922-0

Doblas, V. G., Geldner, N. and Barberon, M. (2017). The endodermis, a tightly controlled barrier for nutrients. *Curr. Opin. Plant Biol.* **39**, 136-143. doi:10.1016/j.pbi.2017.06.010

Dörffling, K. (1970). Quantitative Veränderungen des Abscisinsäuregehaltes während der Fruchtentwicklung von Solanum lycopersicum L.. *Planta* **93**, 233-242. doi:10.1007/BF00387644

Enstone, D. E., Peterson, C. A. and Ma, F. (2002). Root endodermis and exodermis: Structure, function, and responses to the environment. *J. Plant Growth Regul.* **21**, 335-351. doi:10.1007/s00344-003-0002-2

Garvin, D. F., Gu, Y.-Q., Hasterok, R., Hazen, S. P., Jenkins, G., Mockler, T. C., Mur, L. A. J. and Vogel, J. P. (2008). Development of genetic and genomic research resources for *Brachypodium distachyon*, a new model system for grass crop research. *Crop Sci.* **48**, S-69-S-84. doi:10.2135/cropsci2007.06.0332tpg

Geldner, N. (2013). The endodermis. *Annu. Rev. Plant Biol.* **64**, 531-558. doi:10.1146/annurev-arplant-050312-120050

Handberg, K. and Stougaard, J. (1992). *Lotus japonicus*, an autogamous, diploid legume species for classical and molecular genetics. *Plant J.* **2**, 487-496. doi:10.1111/j.1365-313X.1992.00487.x

Hartmann, K., Peiter, E., Koch, K., Schubert, S. and Schreiber, L. (2002). Chemical composition and ultrastructure of broad bean (Vicia faba L.) nodule endodermis in comparison to the root endodermis. *Planta* **215**, 14-25. doi:10.1007/s00425-001-0715-z

Holbein, J., Shen, D. and Andersen, T. G. (2021). The endodermal passage cell - just another brick in the wall? *New Phytol.* **230**, 1321-1328. doi:10.1111/nph.17182

Kurihara, D., Mizuta, Y., Sato, Y. and Higashiyama, T. (2015). ClearSee: a rapid optical clearing reagent for whole-plant fluorescence imaging. *Development* **142**, 4168-4179. doi:10.1242/dev.127613

Lendzian, K. J. (2006). Survival strategies of plants during secondary growth: barrier properties of phellems and lenticels towards water, oxygen, and carbon dioxide. *J. Exp. Bot.* **57**, 2535-2546. doi:10.1093/jxb/erl014

Li, P., Yang, M., Chang, J., Wu, J., Zhong, F., Rahman, A., Qin, H. and Wu, S. (2018). Spatial expression and functional analysis of casparian strip regulatory genes in endodermis reveals the conserved mechanism in tomato. *Front. Plant Sci.* **9**, 832. doi:10.3389/fpls.2018.00832

Lulai, E. C. and Freeman, T. P. (2001). The importance of phellogen cells and their structural characteristics in susceptibility and resistance to excoriation in immature and mature potato tuber (*Solanum tuberosum* L.) periderm. *Ann. Bot.* **88**, 555-561. doi:10.1006/anbo.2001.1497

Lux, A., Morita, S., Abe, J. and Ito, K. (2005). An improved method for clearing and staining free-hand sections and whole-mount samples. *Ann. Bot.* **96**, 989-996. doi:10.1093/aob/mci266

Maekawa, T., Maekawa-Yoshikawa, M., Takeda, N., Imaizumi-Anraku, H., Murooka, Y. and Hayashi, M. (2009). Gibberellin controls the nodulation signaling pathway in *Lotus japonicus*. *Plant J.* **58**, 183-194. doi:10.1111/j.1365-313X.2008.03774.x

Naseer, S., Lee, Y., Lapierre, C., Franke, R., Nawrath, C. and Geldner, N. (2012). Casparian strip diffusion barrier in Arabidopsis is made of a lignin polymer without suberin. *Proc. Natl. Acad. Sci. USA* **109**, 10101-10106. doi:10.1073/pnas.1205726109

Ragni, L. and Greb, T. (2018). Secondary growth as a determinant of plant shape and form. *Semin. Cell Dev. Biol.* **79**, 58-67. doi:10.1016/j.semcdb.2017.08.050

Rydahl, M. G., Hansen, A. R., Kračun, S. K. and Mravec, J. (2018). Report on the current inventory of the toolbox for plant cell wall analysis: proteinaceous and small molecular probes. *Front. Plant Sci.* **9**, 581. doi:10.3389/fpls.2018.00581

Salas-González, I., Reyt, G., Flis, P., Custódio, V., Gopaulchan, D., Bakhoum, N., Dew, T. P., Suresh, K., Franke, R. B., Dangl, J. L. et al. (2021). Coordination between microbiota and root endodermis supports plant mineral nutrient homeostasis. *Science* **371**, eabd0695. doi:10.1126/science.abd0695

Schreiber, L. (2010). Transport barriers made of cutin, suberin and associated waxes. *Trends Plant Sci.* **15**, 546-553. doi:10.1016/j.tplants.2010.06.004

The Angiosperm Phylogeny Group, **Chase, M. W., Christenhusz, M. J. M., Fay, M. F., Byng, J. W., Judd, W. S., Soltis, D. E., Mabberley, D. J., Sennikov, A. N., Soltis, P. S. et al.** (2016). An update of the Angiosperm Phylogeny Group classification for the orders and families of flowering plants: APG IV. *Bot. J. Linn. Soc.* **181**, 1-20. doi:10.1111/boj.12385

Ursache, R., Andersen, T. G., Marhavý, P. and Geldner, N. (2018). A protocol for combining fluorescent proteins with histological stains for diverse cell wall components. *Plant J.* **93**, 399-412. doi:10.1111/tpj.13784

Wallace, I. S. and Anderson, C. T. (2012). Small molecule probes for plant cell wall polysaccharide imaging. *Front. Plant Sci.* **3**, 89. doi:10.3389/fpls.2012.00089

Supplementary Materials and Methods

Short Guide: Triple staining of cell wall components

This protocol is optimized for fixed and cleared tissue (steps 1-4). Thin samples and tissue cuts can be stained directly without prior fixation or clearing. In this case start at step 5 of the protocol.

The procedure is optimized for triple staining of root tissue using Fluorol Yellow (FY), Basic Fuchsin (BF) and Calcofluor White (CW). If not all three dyes are needed, the respective steps can be skipped. Additional ClearSee-compatible dyes can potentially be implemented.

The procedure is compatible with imaging of fluorescet proteins and fluorescently labelled microorganisms.

For more details, see Methods section of the associated manuscript.

Buffers and solutions

A. 1x PBS: Dissolve NaCl [137 mM], KCl [2.7 mM], Na_2HPO_4 [10 mM] and KH_2PO_4 [1.8 mM] in ddH_2O. Adjust pH to 7,4 using 1 M HCl.
Note: Can be prepared as 10x stock.

B. Fixation buffer: Dissolve 4 % (w/v) PFA in 1x PBS, adjust pH to 6.9. Store at -20°C.

C. ClearSee solution: Dissolve xylitol powder [10% (w/v)], sodium deoxycholate [15% (w/v)] and urea [25% (w/v)] in ddH_2O. Do not heat. Store at room temperature.
Note: It can take several hours until components are fully dissolved. Best prepare the solution in a fume hood using a capped bottle.

D. FY stock solution: 1% FY in DMSO. Store at 4°C in darkness.
Note: Careful heating to 60°C may be required to aid dissolution.

E. FY working solution: Use the FY stock solution (D) to prepare a 0.01% FY solution in EtOH (96%). Store at 4°C in darkness.

F. BF working solution: Dissolve 0,2% Basic Fuchsin in ClearSee. Store in darkness.

G. CW working solution: Dissolve 0.1% CW in ddH_2O. Alternatively, commercially available staining solutions can be used directly. Store in darkness.

Staining procedure

1. Fix samples by 1h of vacuum infiltration in fixation buffer.
   Alternatively, incubate samples overnight at 4°C in fixation buffer.
2. Discard the fixation buffer and wash 3 times in 1x PBS.
3. Transfer fixed tissue to ClearSee solution, incubate by gently shaking at room temperature.
4. Exchange ClearSee solution regularly, until solution remains clear.
   Note: The Clearing process is highly dependent on the sample properties, and can take several days to weeks.
5. Lignin staining: Immerse tissue in BF working solution for at least 1h.
   Discard solution rinse twice in ClearSee. Keep in the second wash for at least 30 minutes. Tissue can be stored in ClearSee at this stage.
6. Suberin staining: Briefly rinse tissue once in ddH2O, then immerse in FY working solution and incubate 30 minutes at room temperature, discard FY solution.
   Optional: Incubate tissue in 0,5% Aniline Blue in ddH_2O for 20 min, discard solution.
   Note: Aniline Blue stains cell walls and can be used in combination with FY, to enhance contrast. It is not recommended to combine it with CW and BF staining, or for staining of deep tissue layers.
7. Cell wall staining: Immerse tissue in CW working solution and incubate for 15 minutes at room temperature, discard solution.
8. Quickly wash once in 50% EtOH and twice in ddH_2O.
9. Store at 4°C in darkness. For optimal signal intensity, image within three weeks.
   Mount tissue on slides using 50%-70 % glycerol to prevent drying.
   Note: To avoid bleaching, store FY-stained tissue in darkness whenever possible. Imaging of cuts should be done using low laser intensity, or fast scanning modes.

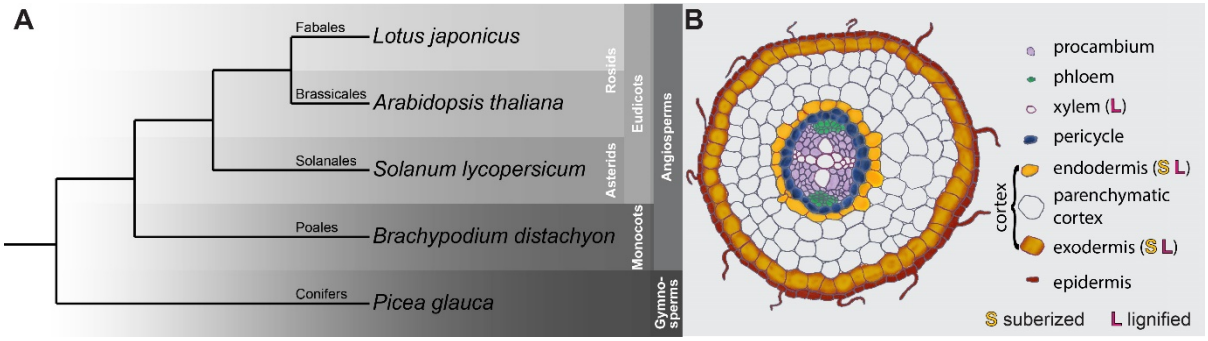

Fig. S1. Phylogenetic context of tested species and cell types visible in representative mature root section. (A) Phylogenetic relationships are based on the Angiosperm Phylogeny Group (APGIV, 2016). (B) Sketch of a root section showing commonly present cell types of a mature *A. thaliana* root. (B) shows a basic cell structure of a root during primary growth with two xylem poles and an established exodermis. The number of xylem poles varies between species and even within. Also not every species develops an exodermis. Common suberin and lignin depositions are indicated next to the cell types.

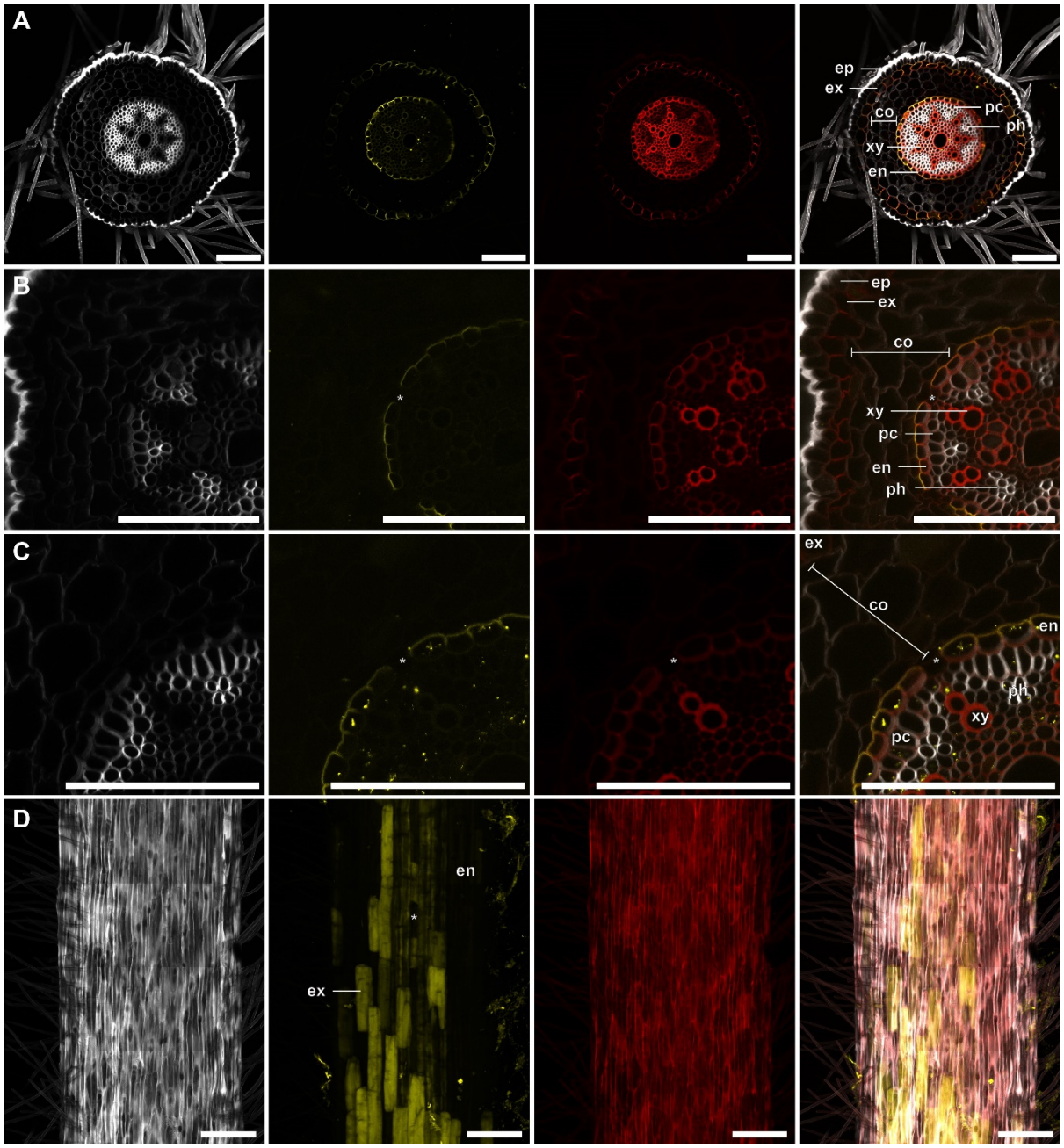

Fig. S2. Triple staining of cell wall components in *Brachypodium distachyon.* (A-D) Basic Fuchsin (BF), Fluorol Yellow (FY) and Calcofluor-white (CW) triple-stained semi-thin cross sections (A-C) and whole root mounts (D) of *B. distachyon* 10 days post germination. Panels (left to right) show CW, FY, BF and merged channels. (B-D) * indicate passage cells. Cell types indicated are co, parenchymatic cortex; en, endodermis; ep, epidermis; pc, pericycle; ph, phloem; xy, xylem and ex, exodermis. Scale bars: 100 µm.

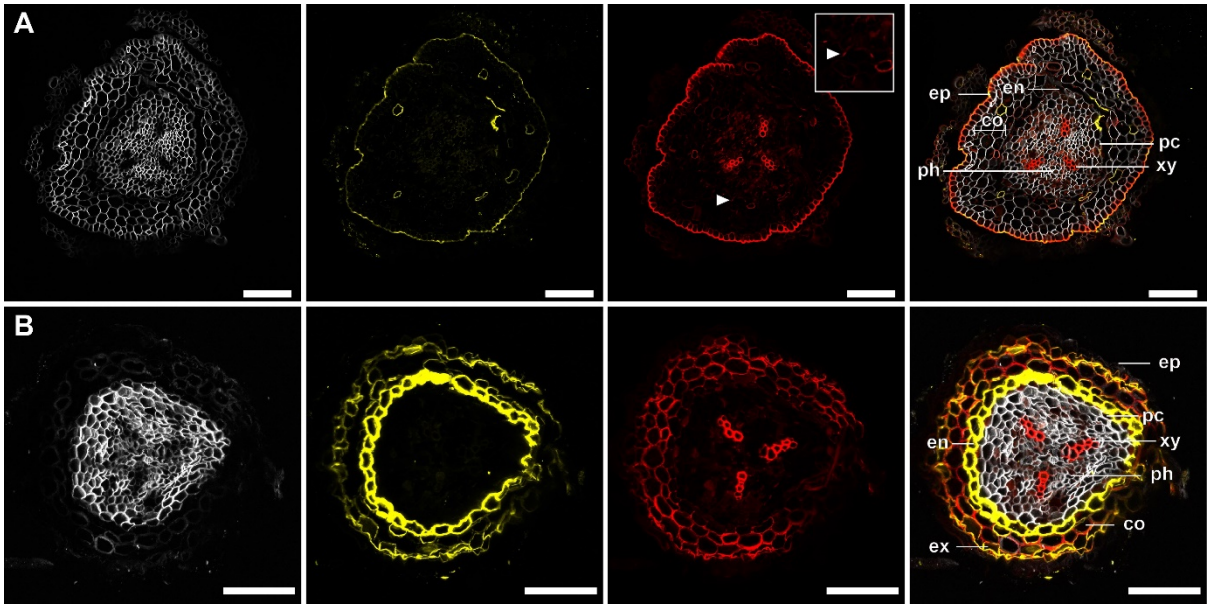

Fig. S3. Triple staining of cell wall components in *Picea glauca* cross sections (manual). (A-B) Basic Fuchsin (BF), Fluorol Yellow (FY) and Calcofluor-white (CW) triple-stained cross sections of *P. glauca* (A) 10 days and (B) 14 days post germination. Panels (left to right) show CW, FY, BF and merged channels. White arrowheads indicate Casparian strip in original image and corresponding magnification. Indicated cell types are co, parenchymatic cortex; en, endodermis; ep, epidermis; pc, pericycle; ph, phloem; xy, xylem; ex, exodermis. Scale bars: 100 µm.

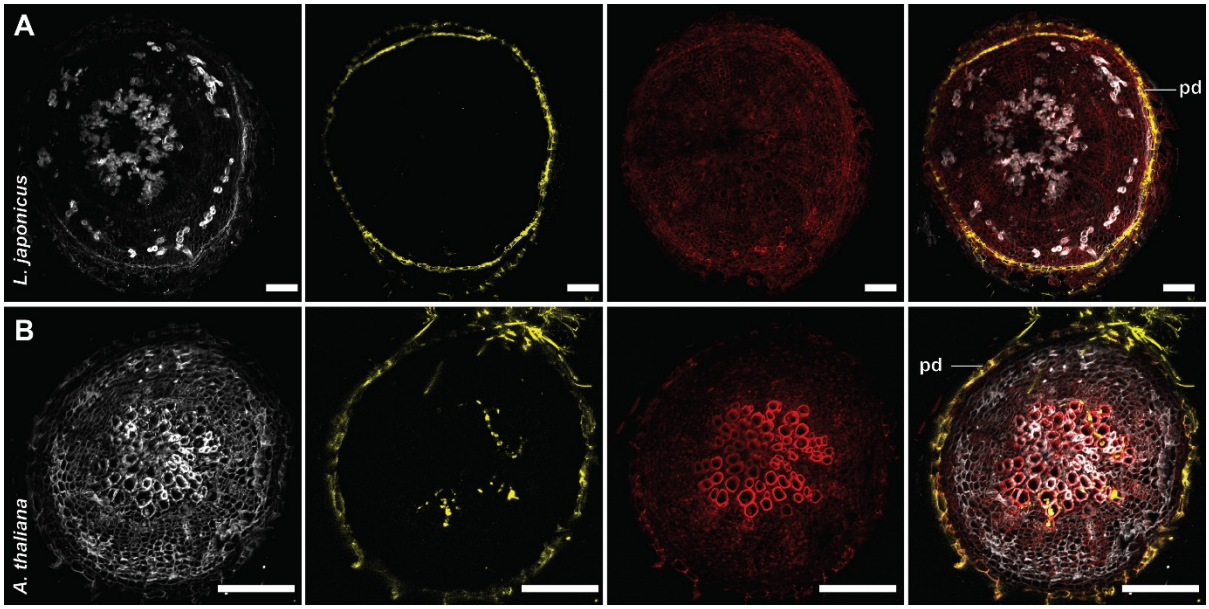

Fig. S4. Triple staining of cell wall components in semi-thin cross sections after secondary root growth. (A-B) Basic Fuchsin (BF), Fluorol Yellow (FY) and Calcofluor-white (CW) triple-stained cross sections of (A) *L. japonicus* and (B) *A. thaliana*. (A-B) cross sections of adult plants grown in pots. (A-B) Panels (left to right) show CW, FY, BF and merged channels. Suberized periderm (pd) stained by FY. Scale bars: 100 µm.

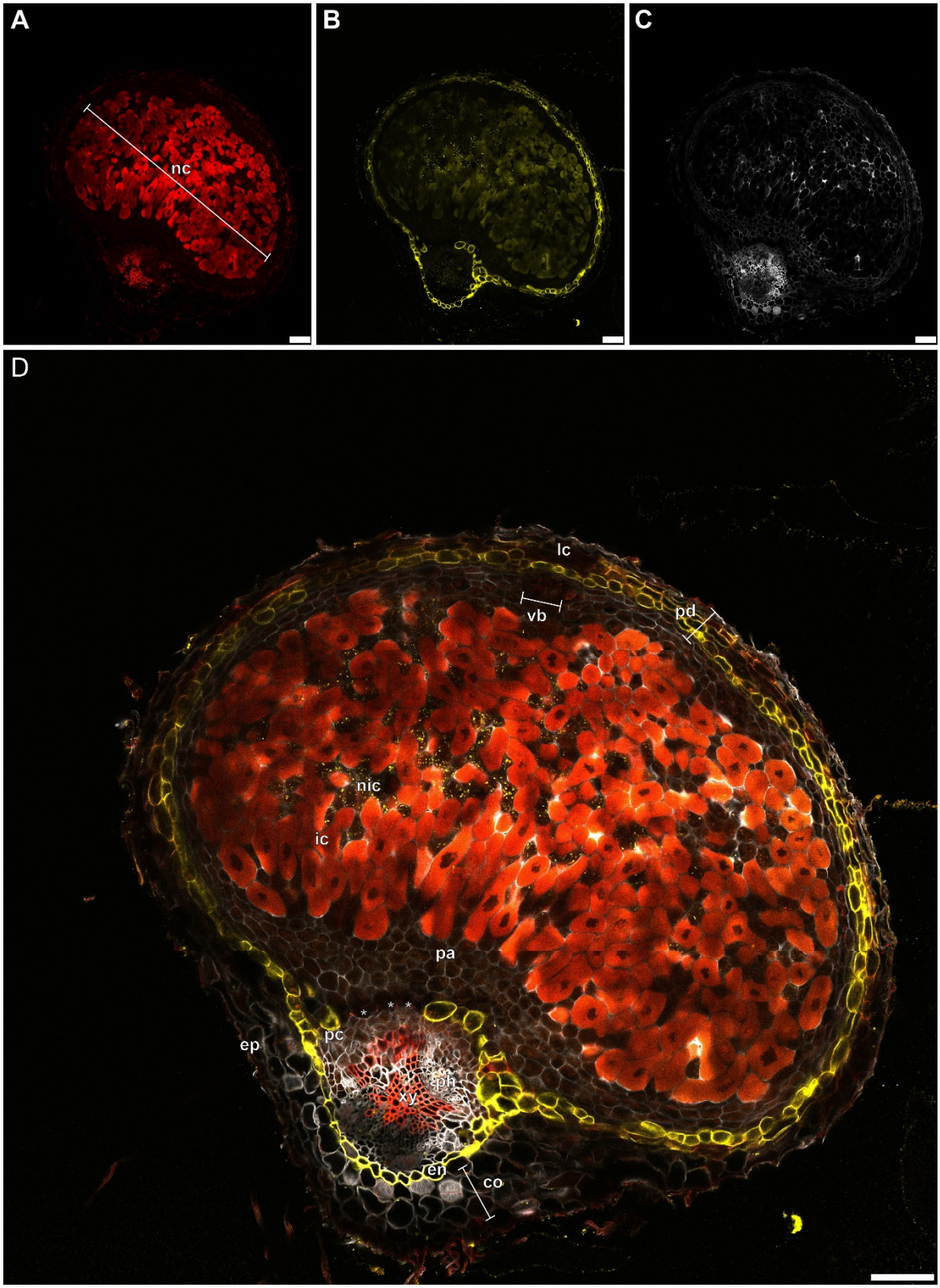

Fig. S5. Triple staining of nodule cross section. (A-B) Basic Fuchsin (BF), Fluorol Yellow (FY) and Calcofluor-white (CW) triple-stained cross section of a *L. japonicus* nodule (21 days post infection). (A) CW, (B) FY, (C) BF and *DsRED* expressed by *M. loti* and (D) merged channels. Cell types indicated are co, parenchymatic cortex; en, endodermis; ep, epidermis; pc, pericycle; ph, phloem; xy, xylem; pd, periderm; pa, nodule parenchyma; ic, infected cells; nic, non-infected cells; lc, lenticels; nc, nodule cortex and vb, vascular bundle. * indicate passage cells. Scale bar: 100 µm.

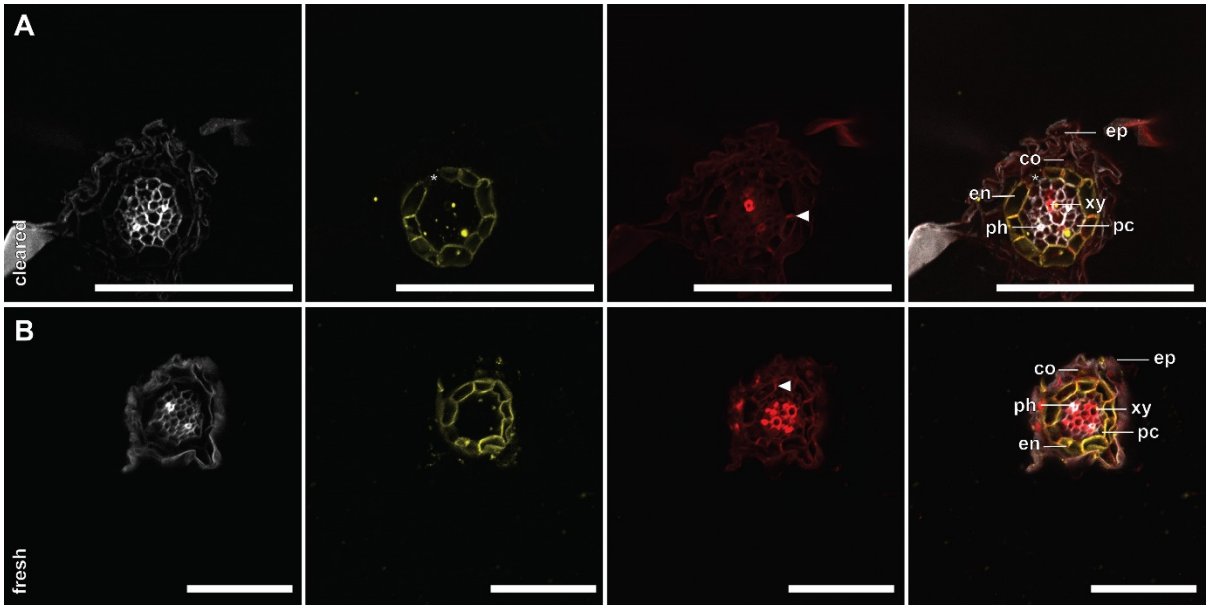

Fig. S6. ClearSee treatment does not compromise integrity and visualization of secondary cell wall components. (A-B) Basic Fuchsin (BF), Fluorol Yellow (FY) and Calcofluor-white (CW) triple-stained cross sections of (A) previously cleared and (B) fresh *A. thaliana* root cross sections (manual cuts), 10 days post germination. (A-B) Panels (left to right) show CW, FY, BF and merged channels. White arrowheads indicate Casparian strips, * indicate passage cells. Indicated cell types are co, parenchymatic cortex; en, endodermis; ep, epidermis; pc, pericycle; ph, phloem; xy, xylem. Scale bars: 50 µm.

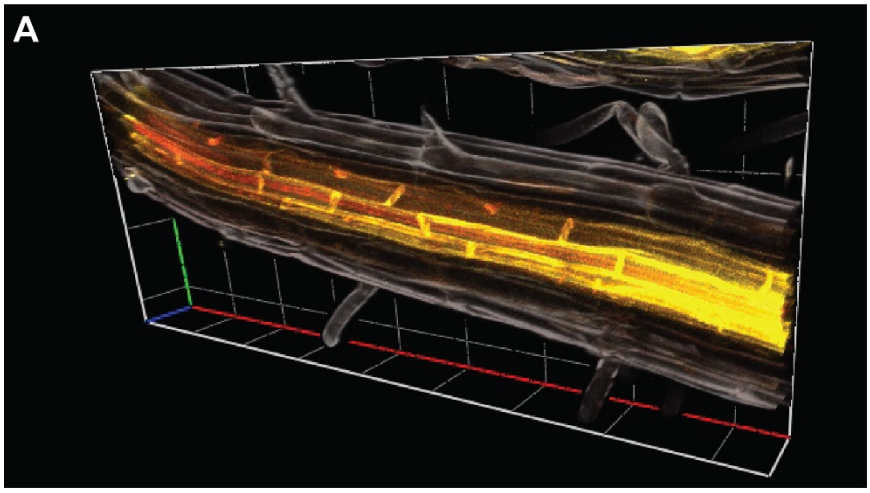

Fig. S7. 3D reconstruction of triple stained *A. thaliana* root. Computational 3D reconstruction of Basic Fuchsin, red; Fluorol Yellow, yellow; and Calcofluor-white, grey triple-stained *A. thaliana* root 10 days post germination. 3D-image reconstructed using Zen Blue 3.4 and 49 single images.

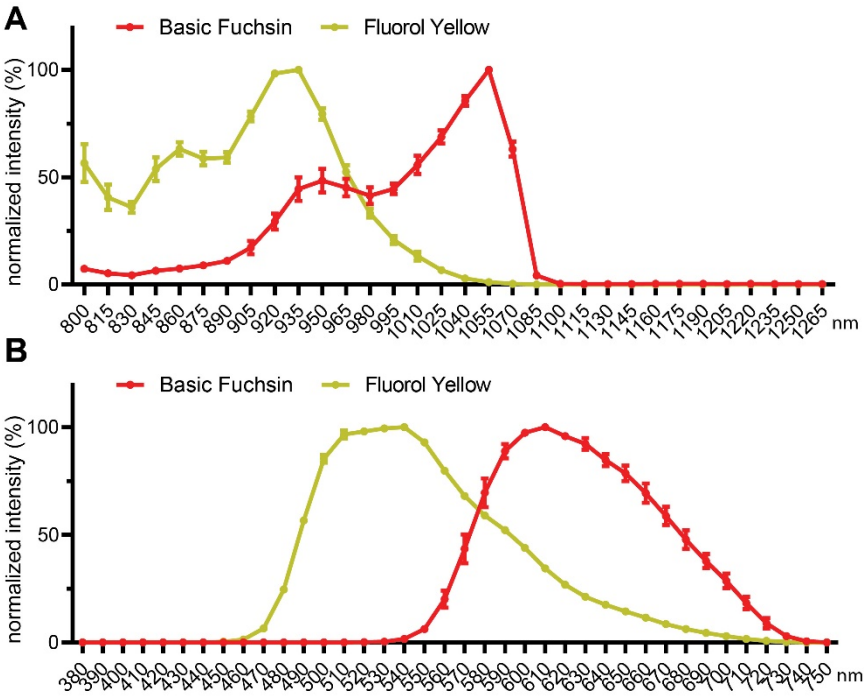

Fig. S8. Emission and excitation spectra of Fluorol Yellow (FY) and Basic Fuchsin (BF). (A) Multi photon excitation and (B) emission spectra of BF and FY in a stained *L. japonicus* nodule section. (A,B) The wavelength showing the highest intensity was set as 100%. Dots represent mean intensities at a given wavelength, error bars show standard deviation. n = 5 independent measurements on different regions near the nodule vasculature of the same nodule section. Similar results were acquired from two independent spectrum analyses, each measuring five spots, performed on two different nodules.

Table S1. Plant Cultivation Procedure. Cultivation procedure of different plant species used in this study.

Plant species	***Lotus japonicus***	***Arabidopsis thaliana***	***Solanum lycopersicum***	***Brachypodium dystachion***	***Picea glauca***
Ecotype or source	Gifu B-129	col-0	Money Maker	BD-21	1a seeds
pre treatment	scarification*	-	-	removal of husk and lemma**	-
Sterilization Method and Duration	Bleach treatment 10 min	Ethanol treatment 30 min	Bleach treatment 20 min	Bleach treatment 20 min	Bleach treatment 20 min
Stratification at 4°C	3 days	2 days	3 days	3 days	4 weeks
pre germination* **	Yes, 3 days	No	No	No	Yes, 1 week
growth medium	1/4 B&D****	1/2 MS	1/4 B&D****	1/4 B&D****	1/4 B&D****
growth duration	10-21 Days	10 Days	10 Days	10 Days	10-14 Days
recommended clearing duration	> 3days for roots; >1 week for nodules	> 1 day	>3 days	>1 week	>2 weeks

* seeds scratched with sandpaper prior to sterilization

** seeds soaked in water, lemma and husk removed using forceps prior to sterilization

*** germinated on separate plates for 3 days before growth period

**** (Broughton and Dilworth 1971).

Supplementary Reference

Broughton, W. J. and Dilworth, M. J. (1971). Control of leghaemoglobin synthesis in snake beans. *Biochem J* **125**, 1075-1080.

Appendix 3.2 Plants recruit peptides and micro RNAs to regulate nutrient acquisition from soil and symbiosis.

plants

MDPI

Review

Plants Recruit Peptides and Micro RNAs to Regulate Nutrient Acquisition from Soil and Symbiosis

Marios I. Valmas [1], Moritz Sexauer [2], Katharina Markmann [2] and Daniela Tsikou [1,*]

[1] Department of Biochemistry and Biotechnology, University of Thessaly, Biopolis, 41500 Larissa, Greece
[2] Julius-von-Sachs-Institute for Biosciences, Würzburg University, Julius-von-Sachs-Platz 3, 97082 Würzburg, Germany
* Correspondence: dtsikou@uth.gr

Abstract: Plants engage in symbiotic relationships with soil microorganisms to overcome nutrient limitations in their environment. Among the best studied endosymbiotic interactions in plants are those with arbuscular mycorrhizal (AM) fungi and N-fixing bacteria called rhizobia. The mechanisms regulating plant nutrient homeostasis and acquisition involve small mobile molecules such as peptides and micro RNAs (miRNAs). A large number of CLE (CLAVATA3/EMBRYO SURROUNDING REGION-RELATED) and CEP (C-TERMINALLY ENCODED PEPTIDE) peptide hormones as well as certain miRNAs have been reported to differentially respond to the availability of essential nutrients such as nitrogen (N) and phosphorus (P). Interestingly, a partially overlapping pool of these molecules is involved in plant responses to root colonization by rhizobia and AM fungi, as well as mineral nutrition. The crosstalk between root endosymbiosis and nutrient availability has been subject of intense investigations, and new insights in locally or systemically mobile molecules in nutrient- as well as symbiosis-related signaling continue to arise. Focusing on the key roles of peptides and miRNAs, we review the mechanisms that shape plant responses to nutrient limitation and regulate the establishment of symbiotic associations with beneficial soil microorganisms.

Keywords: CEP/CLE peptide hormones; mobile miRNAs; nutrient homeostasis; root symbiosis

Citation: Valmas, M.I.; Sexauer, M.; Markmann, K.; Tsikou, D. Plants Recruit Peptides and Micro RNAs to Regulate Nutrient Acquisition from Soil and Symbiosis. *Plants* **2023**, *12*, 187. https://doi.org/10.3390/plants12010187

Academic Editor: Ping Lan

Received: 6 December 2022
Revised: 24 December 2022
Accepted: 27 December 2022
Published: 2 January 2023

1. Introduction

Plant growth and development depend on the acquisition of a number of mineral nutrients from the soil. Essential nutrients such as nitrogen (N) and phosphorus (P) have key roles in agriculture, as their limitation is considered a frequent cause of reduced crop productivity. Most land plants meet nutrient limitation in terrestrial environments by associating with beneficial microorganisms. Arbuscular mycorrhizal (AM) associations with fungi and N-fixing root nodulation of legume plants with rhizobial bacteria improve the acquisition of mineral elements, such as P and N. Microbial inoculants are increasingly used as biofertilizers, and tested for their potential to replace cost-intensive and environmentally harmful synthetic P and N fertilizers in agricultural settings.

This review discusses the role of peptides and micro RNAs (miRNAs) in mediating the plant responses to N and P availability and the establishment and control of symbiotic relationships improving N and P acquisition.

2. Plants Associate with Soil Microorganisms to Access Essential Nutrients

Root nodule symbiosis is an endosymbiotic association formed between legumes and rhizobial bacteria. Under symbiotic conditions, the latter fix aerial N_2 through the enzyme nitrogenase, converting it to ammonia (NH_3) (reviewed in [1]). Upon release to the peribacteroid space that separates symbiotic bacteria from the infected host cell, NH_3 is converted to ammonium (NH_4^+), which is then released to the plant cytosol [2]. NH_4^+ transporters have been characterized in legumes, as in soybean (*Glycine max*) [3] and *Lotus*

japonicus [4]. In return for fixed N, plants provide rhizobia with branched amino acids, sugars and micronutrients essential for bacterial development. Besides that, dicarboxylic acids, mainly malate, are also provided to bacteria by the plant, and are essential for N fixation [1].

During the establishment of the symbiotic relationship, communication signals are exchanged between rhizobia and legumes, involving flavonoids, which are released into the rhizosphere by the plant root [5,6] and trigger the production of lipochitooligosaccharide (LCO) nodulation factors (Nod factors) in compatible rhizobia (reviewed in [7]). Nod factor signaling triggers a response cascade resulting in rhizobial entry into the root epidermis and cortex, paralleled by the formation of a nodule primordium. Nodules are lateral root organs where rhizobia are hosted intracellularly and develop into N-fixing bacteroids surrounded by a plant-derived membrane individually or in small groups, forming organelle-like symbiosomes (reviewed in [8]).

Arbuscular mycorrhizal symbiosis, the association formed between plants and fungi of the phylum Glomeromycota, plays a critical role in nutrient acquisition by providing access predominantly to P, but also to N and other mineral nutrients. AM fungi were found to possess high-affinity transporters of inorganic phosphate (P) [9], which accumulates as polyphosphate within arbuscules and is then rapidly translocated to the host plant [10]. N is also taken up by AM fungi from the substrate, and genes involved in the transfer of NH_4^+ and amino acids to host plants have been identified [11,12]. AM fungi receive photosynthetic carbon in the form of sugars and lipids (reviewed in [13]) and are obligate biotrophs, strictly relying on host plant resources for growth and reproduction.

Early chemical communication between AM fungi and host plants involves strigolactones released by plant roots [14], and a cocktail of fungal chitooligosaccharides (COs) and lipochitooligosaccharides (LCOs) [15,16]. AM fungal entry into the root is achieved through appressoria that develop on the root epidermal surface [17]. Following hyphal entry, highly branched fungal arbuscules are formed within cells of the inner root cortex. Like symbiosomes in nodules, these are surrounded by a plant plasmalemma-derived membrane and represent the major sites of nutrient exchange between micro- and macrosymbiont [18]. Arbuscules have a limited lifetime, and following their collapse and digestion by the host cell, the latter can be re-colonized by a new arbuscule (reviewed in [19]).

3. Plant Responses to N Availability and Rhizobial Symbiosis Involve CEP and CLE Peptide Regulation

Peptide hormones facilitate both cell-to-cell signaling in plant tissues and systemic communication between organs by long-distance mobility through the vascular system. Plant genomes encode a variety of small signaling peptides (SSPs), which in their mature state are post-translationally modified, small (<20 amino acids) peptides cleaved from a longer precursor protein, and are involved in developmental and physiological processes and mediating plant responses to environmental stimuli. Several SSP gene families show differential abundances in response to changes in plant nutrient status, and have roles in processes controlling root morphogenesis and physiology, as well as macronutrient uptake [20,21]. The CLE (CLAVATA3/EMBRYO SURROUNDING REGION-RELATED) and CEP (C-TERMINALLY ENCODED PEPTIDES) families have been studied extensively in relation to their roles in systemic N signaling. Members of other SSP gene families including CAPE (CAP-DERIVED PEPTIDE), GLV (GOLVEN/ROOT GROWTH FACTOR), IDA (INFLORESCENCE DEFICIENT IN ABCISSION), PIP (PAMP-INDUCED SECRETED PEPTIDE) and TAX (TAXIMIN) encoding genes were similarly suggested to play roles in nutrient-status-related signaling [20]. In the following paragraphs we discuss the roles of CLE and CEP peptides in N deficiency and nodulation symbiosis signaling.

3.1. Roles of CLE Peptides in N Homeostasis and Symbiosis Regulation

CLE peptides are 12 to 13 amino acids long and function as secreted peptide ligands that bind to plasma membrane-localized receptor-like proteins, thereby triggering down-

stream signaling events. The CLE gene family encodes small proteins with a conserved CLE domain at the C-terminus, generating the mature CLE peptide following proteolytic processing [22]. CLE peptides regulate various physiological and developmental processes, and a number of CLEs were reported to be involved in nutrient homeostasis and to respond to symbiotic interactions with microorganisms [23].

The *Arabidopsis thaliana* genome harbors 32 *CLE* genes [22]. Among them, *CLE1*, *-3*, *-4* and *-7* show increased activity in N-deficient compared to sufficient roots and were suggested to regulate lateral root primordia formation through binding to the CLAVATA1 (CLV1) leucine-rich repeat-receptor-like kinase [24]. These CLE genes are expressed in the root pericycle, and the corresponding CLE peptides are hypothesized to be secreted from pericycle cells and transported through the apoplastic continuum within the central cylinder to reach phloem companion cells where CLV1 is localized. The CLE-CLV1 signaling pathway is a key mechanism regulating the outgrowth of lateral roots and the expansion of the root system when *A. thaliana* plants grow under N-deficient conditions, enhancing the plant survival in N-poor environments [24].

In legume plants, multiple *CLE* genes have been proposed to be involved in nodulation control. Some legume *CLE* genes are specifically linked to the rhizobial symbiosis, while others are regulated by both rhizobia and N availability. A number of CLE peptides have been reported to negatively regulate nodulation, acting as essential components of a plant mechanism called autoregulation of nodulation (AON) which balances nodule numbers with plant needs and resource availability (for a recent review see [25]). *CLE* genes related to rhizobial infection or symbiosis include *L. japonicus LjCLE-RS1*, *-2*, *-3* and *LjCLE40* [26,27], *M. truncatula MtCLE12*, *-13* and *-35* [28–30], *Glycine max GmRIC1* and *-2* [31] and *Phaseolus vulgaris PvRIC1* and *-2* [32] (Figure 1, Table 1). Among them, *LjCLE-RS1*, *MtCLE12*, *MtCLE13*, *GmRIC1* and *GmRIC2* were reported to specifically show increased expression activity in roots upon rhizobial infection compared to mock treated roots [27,28,31]. Consistent with root–shoot mobility, *LjCLE-RS2* derived peptides, though specifically expressed in roots, were found in xylem sap collected from shoot tissue of infected plants [26]. *Lj*CLE-RS2 peptides were further found to directly bind to the shoot-localized CLV1-type leucine-rich repeat receptor-like kinase (LRR-RLK) *Lj*HAR1 (HYPERNODULATION ABERRANT ROOT FORMATION 1) [33], a negative regulator of symbiosis [34,35]. Putative orthologues of *Lj*HAR1 in other legumes, the symbiosis regulators *Mt*SUNN, *Gm*NARK [36] and *Pv*NARK [32] are likely to similarly act as receptors of rhizobia-induced, xylem-mobile CLE peptides.

In a process analogous to AON, root nodulation symbiosis is inhibited by high nitrate concentrations in the environment. *LjCLE-RS2* expression is induced by both rhizobial inoculation and nitrate supply, implying a dual role in rhizobia-induced autoregulation and nitrate-mediated inhibition of nodulation [26]. Studies on CLE35 in *M. truncatula* offer further evidence for an involvement of AON components in nitrate inhibition of nodulation. *MtCLE35* is a nitrate-responsive gene, which is also expressed during nodulation [29]. Overexpression of *MtCLE35* in transgenic roots of *M. truncatula* led to reduced root nodule numbers, in a *SUNN*- dependent manner [30]. Additionally, downregulation of *MtCLE35* through RNAi resulted in increased nodule numbers, even under nitrate conditions where nodulation was inhibited in wild-type plants [37]. *MtCLE34* was also co-induced by nitrate and rhizobia but turned out to be a pseudogene lacking a functional CLE domain [30]. It was thus proposed that *MtCLE34* might have had a role in nodulation, before it was mutated and lost its function [30].

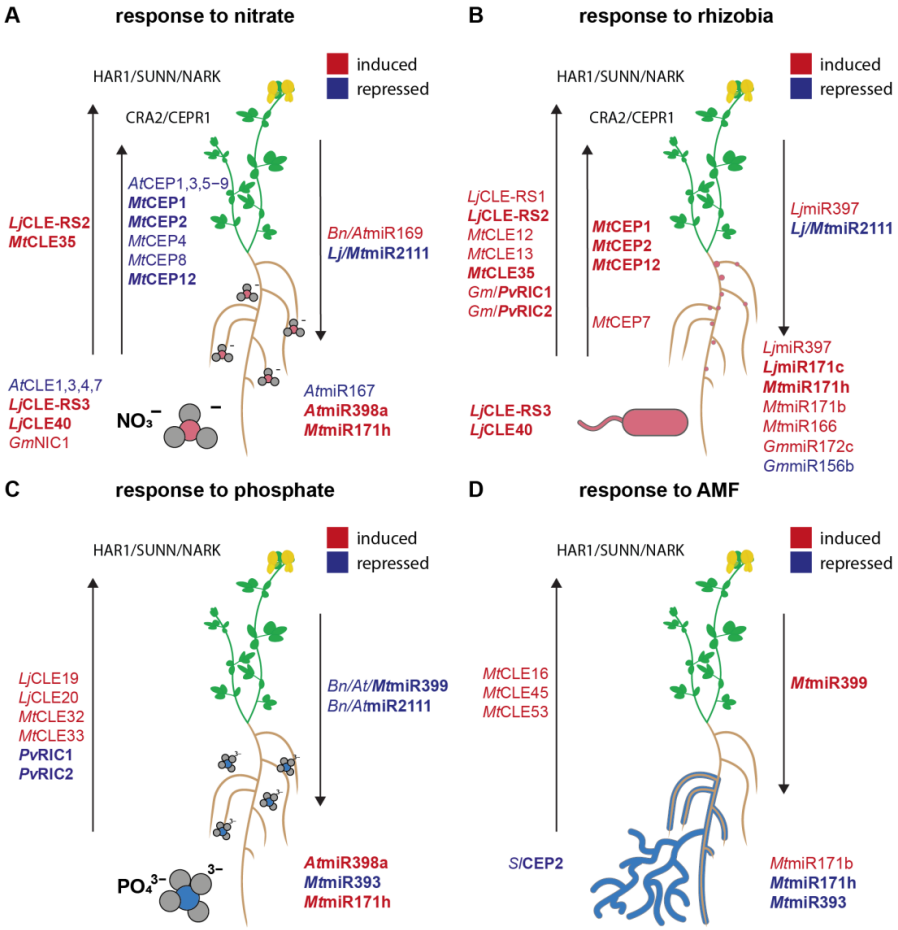

Figure 1. Nutrient homeostasis and acquisition mechanisms involve regulation by peptide hormones and miRNAs. CLE and CEP peptides and miRNAs responding to (**A**) N availability, (**B**) rhizobia , (**C**) P availability and (**D**) arbuscular mycorrhizal fungi. Molecules that are induced or repressed by a respective stimulus are displayed in red or blue, respectively. Molecules that are responsive to more than one stimulus are in bold. Arrows indicate shoot-to-root or root-to-shoot translocation of mobile molecules. Specific responses are mediated by the shoot localized leucine-rich repeat receptor-like kinases HAR1/SUNN/NARK and CRA2/CEPR1. *Lj*, *Lotus japonicus*; *Mt*, *Medicago truncatula*; *At*, *A. thaliana*; *Bn*, *Brassica napus*; *Gm*, *Glycine max*; *Pv*, *Phaseolus vulgaris*; *Sl*, *Solanum lycopersicum*.

Biochemical studies revealed that CLE peptides are post-translationally modified. In the well-studied CLV3 peptide of *A. thaliana*, a proline residue at position 7 is hydroxylated and subsequently arabinosylated, a prerequisite for its biological activity and high-affinity binding to its receptor CLV1 [38]. Hydroxyproline *O*-arabinosylation is widely observed in secreted *A. thaliana* peptides, and Golgi-localized enzymes encoded by three *AtHPAT* genes mediate this process [39]. CLE arabinosylation was similarly reported in other plants, such as *L. japonicus* [33], *M. truncatula* [40,41] and *P. sativum* [42], suggesting that this modification may be a requirement for receptor binding and functionality in general. In *M. truncatula*, the rhizobium-induced *MtCLE12* was suggested to be arabinosylated by the Golgi-localized hydroxyproline *O*-arabinosyltransferase ROOT DETERMINED NODULATION1 (RDN1), as *MtCLE12* overexpression did not affect root nodule numbers in *rdn1* loss-of-function mutants [40,41]. Interestingly, in contrast to *MtCLE12*, tri-arabinosylation of *MtCLE13* was *RDN1*-independent, suggesting that other enzymes are also involved in

CLE peptide arabinosylation in this species [41]. In *L. japonicus*, CLE-RS1 and CLE-RS2 tri-arabinosylation was shown to be critical for HAR1 binding and activity in AON [33]. While the enzyme catalyzing glycosylation of these peptides is unclear, a third CLE mediating HAR1-dependent AON in *L. japonicus*, *Lj*CLE-RS3, was shown to be arabinosylated through *LjPLENTY*, a putative ortholog of *MtRDN1*/*Pisum sativum NOD3*, which are all homologs of *AtHPAT* genes [43]. Consistently, PLENTY also localizes to the Golgi complex. Overexpression of *LjCLE-RS1* and *-2* in a *plenty* mutant background retained AON activity, whereas *LjCLE-RS3* mediated repression of nodulation was abolished in *plenty* mutants [43]. *LjCLE-RS1* and *-2* are thus likely arabinosylated at least in part by enzymes other than PLENTY [43].

Table 1. List of selected CLE and CEP peptides responding to nitrogen (N), phosphorus (P) and microsymbionts (rhizobium and AM fungi).

	Stimuli	Organism	Influence Range	Predominant Expression (Tissue)	Refs
AtCLE1 *AtCLE3* *AtCLE4* *AtCLE7*	N-deficiency induced	*A. thaliana*	systemic	roots	[24]
LjCLE-RS1	Rhizobium-induced	*L. japonicus*	systemic	roots	[26]
LjCLE-RS2	Rhizobium- and N-induced	*L. japonicus*	local and systemic	roots	[26]
LjCLE-RS3 *LjCLE40*	Rhizobium- and N-induced	*L. japonicus*		roots, nodule primordia	[27]
LjCLE19 *LjCLE20*	P-induced	*L. japonicus*		roots	[44]
MtCLE12	Rhizobium-induced	*M. truncatula*	local and systemic	nodules	[28]
MtCLE13	Rhizobium- and nod factor-induced, cytokinin-induced	*M. truncatula*	local and systemic	roots (symbiosis susceptible zone), inner cortical cells, nodules	[28] [45]
MtCLE35	Rhizobium- and N-induced	*M. truncatula*	systemic	roots, nodules	[29] [30]
MtCLE32	Pi-induced	*M. truncatula*		roots	[46]
MtCLE33	Pi-induced	*M. truncatula*		root vascular tissue	[46] [47]
MtCLE16 MtCLE45	AM-induced	*M. truncatula*		roots	[46] [47]
MtCLE53	AM-induced	*M. truncatula*		root vascular tissue near colonized regions	[46] [47]
GmRIC1 *GmRIC2*	Rhizobium-induced	*G. max*	systemic	roots	[31]
GmNIC1	N-induced	*G. max*	local	roots	[31]
PvRIC1 *PvRIC2*	Rhizobium-induced, P-deficiency increased	*P. vulgaris*	systemic	roots, pericycle cells of Pi-deficient roots	[32] [48]
AtCEP1 *AtCEP3* *AtCEP5* *AtCEP6* *AtCEP7* *AtCEP8* *AtCEP9*	N starvation-induced	*A. thaliana*	systemic	mainly roots (but also in aerial tissues)	[49]

Table 1. *Cont.*

	Stimuli	Organism	Influence Range	Predominant Expression (Tissue)	Refs
MtCEP1	Rhizobium-induced, N starvation-induced	*M. truncatula*	local and systemic	roots, shoots	[50–52]
MtCEP2 *MtCEP12*	Rhizobium-induced, N starvation-induced	*M. truncatula*		mainly roots, shoots	[52]
MtCEP4 *MtCEP5* *MtCEP6* *MtCEP8*	N starvation-induced	*M. truncatula*		mainly roots, shoots	[52]
MtCEP7	Rhizobium- and nod factors-induced, cytokinin-induced	*M. truncatula*	systemic	roots, epidermal cells in colonized roots, nodule primordia, mature nodules	[45]
SlCEP2	AM-reduced	*S. lycopersicum*	local	roots	[53]

3.2. Roles of CEP Peptides in N Homeostasis and Symbiosis Regulation

CEP peptides are a family of SSPs which are 15 amino acids long, secreted peptides released from a C-terminal conserved domain (the CEP domain) of precursor proteins through proteolytic processing. Similarly to CLEs, CEPs are also post-translationally modified by proline hydroxylation and arabinosylation [54]. The accumulation of CEPs was observed to be highly correlated with plant responses to N starvation. The *A. thaliana* genome includes 11 *CEP* genes, 7 of which have been shown to be up-regulated specifically in response to N starvation [49]. Moreover, 10 out of the 11 *CEP* genes led to enhanced expression of the nitrate transporter gene *NRT2.1* when overexpressed in *A. thaliana* seedlings [49].

The well-studied *At*CEP1 peptide in *A. thaliana* was shown to undergo long-distance root-to-shoot translocation and proposed to mediate plant adaptations to low environmental N availability [49]. CEP1 directly binds to the leucine-rich repeat receptor kinases CEPR1 and CEPR2, found to locate in both shoots and roots [49]. The systemic nature of this mechanism was shown via grafting (*cepr1-1 cepr2-1* mutant scions were grafted onto wild-type rootstocks by hypocotyl-to-hypocotyl grafting) and split root (the root system of a plant was separated into two parts exposed to different nutrient conditions) studies, and the translocation of CEP1 was verified by its detection in the xylem sap [49]. Exogenous application of CEP1 and CEPR1/2 loss of function studies showed that the CEP1-CEPR1/2 signaling pathway regulates N uptake by affecting the expression of genes encoding for the nitrate transporters NRT1.1, NRT2.1 and NRT3.1 [49].

Similarly to CLE peptides, CEP peptides have been reported to be involved not only in N-deficiency responses but also nodulation control in legumes. In contrast to the repressive role of CLE peptides on symbiotic nodule numbers, CEPs have been attributed a positive regulatory role in nodulation. *Mt*CEP1 in *M. truncatula* was shown to enhance nodulation when overexpressed or externally applied to *Sinorhizobium meliloti*-infected roots [50]. Exogenous application of *Mt*CEP1 to *M. truncatula* roots led to significantly decreased lateral root numbers, while nodule numbers increased [50]. Both effects were mediated by the LRR-RLK CRA2 (COMPACT ROOT ARCHITECTURE 2), the putative orthologue of *At*CEPR1 in *M. truncatula*, as they were abolished in *cra2* loss-of-function mutants [51]. In addition to *MtCEP1*, *MtCEP2* and *MtCEP12* were N-starvation induced, and co-regulated lateral root and nodule numbers [52] (Table 1). Grafting studies revealed that the CRA2-mediated signaling pathway affecting root architecture is locally active in roots, whereas CRA2-mediated nodulation control is an independent process which is systemically regulated through shoot-localized CRA2 [55]. The systemic *Mt*CEP1-CRA2 node promotes nodulation under low N conditions by regulating the downstream signaling components miR2111 and *TML* (see below) [56].

*Mt*CEP7, which was reported to be induced by rhizobia, Nod factors and cytokinin [45], seems to function as positive regulators of symbiosis, as exogenous CEP7 application reinforced nodulation, whereas *CEP7* downregulation led to reduced nodule numbers [45]. Similarly to *Mt*CEP1, *Mt*CEP7 was also seen to control nodulation through a systemic signaling pathway mediated by the shoot-localized population of the CRA2 receptor [45].

In summary, downstream effects of rhizobium or nitrate-induced CLE and CEP peptides are antagonistic, with CLE peptides mediating restriction, and CEP peptides promoting nodulation. These opposite responses are mediated by partially overlapping signaling pathways sharing common components. Chromatin immunoprecipitation studies revealed that the transcription factor NIN co-regulates the expression of *MtCLE13* and *MtCEP7*, and ectopic expression of *MtNIN* induced the expression of *MtCLE13* and *MtCEP7* in the absence of external stimuli [45]. Moreover, both *MtCLE13* and *MtCEP7* were induced by cytokinin, and the effects of both peptides on nodulation were mediated by the cytokinin receptor gene *MtCRE1* [45]. Studies on the crosstalk between peptide and classical hormones provide evidence that peptide signaling is interlinked with signaling through cytokinin, auxin, ethylene and strigolactones (for a recent review see [57]). The concurrent induction of the antagonistic CLE and CEP pathways may be part of a mechanism that enables the plant to flexibly adjust rhizobial infection events and the nodule numbers to its needs based on the endogenous supply status of various nutrients, photosynthetic capacity and environmental conditions.

4. CLEs and CEPs Respond to Both P and AM Fungal Infection

In contrast to root nodulation symbiosis, where host plants are supplied with bacterially fixed aerial N, AM fungi predominantly deliver phosphate extracted from the surrounding substrate to the host. It was shown that high exogenous phosphate supply restricts the initiation and development of AM symbiosis. P acts systemically to repress symbiotic gene expression and AM fungal root colonization [58].

Analogous to CLE-mediated regulation of nodulation symbiosis, this regulation of AM involves CLE peptides (Table 1, Figure 1). In *M. truncatula*, expression of *MtCLE32* and *MtCLE33* was significantly induced in roots grown under high (2 mM) P conditions compared to P-starved roots [46]. Further, ectopic overexpression of the *MtCLE33* in *M. truncatula* transgenic roots resulted in reduced AM root colonization [46]. Apart from peptides, phytohormones and miRNAs have been reported to have key roles in P starvation and AM symbiosis signaling, regulating the initiation, maintenance, and extent of AM root colonization (reviewed in [59]).

The development of AM fungi within the root is regulated by the host plant through a genetic mechanism termed autoregulation of mycorrhizal symbiosis (AOM) [60], a systemic signaling cascade sharing common elements with AON [61]. Along this line, it was shown that root-derived CLE peptides and a CLV1-type shoot-localized receptor regulate the colonization of roots by AM fungi [46,47]. Transcript abundance of specific *CLE* genes was found to increase upon AM fungal root colonization [46,47,62]. Certain *CLE* genes responding to AM symbiosis were also shown to respond to phosphate availability [47] (Table 1, Figure 1), reminiscent of the dual regulation of *CLE* genes by rhizobial infection and nitrate [26,27]. Ectopic overexpression of the AM-induced *MtCLE53* in the roots of *M. truncatula* resulted in reduced fungal colonization compared to control roots [46,47], whereas *cle53* mutants showed higher colonization levels than wild-type plants [47]. Interestingly, the nodulation-induced *MtCLE13* [28] was not induced by AM symbiosis, and ectopic overexpression of *MtCLE13* seems not to have an effect on fungal colonization levels, implying specificity of the respective *CLEs* [46].

Similarly to AON, arabinosylation of CLE peptides may also be a requirement for receptor binding and functionality in AOM. Karlo et al. [47] showed that the hydroxyproline *O*-arabinosyltransferase RDN1 has a role in the control of fungal colonization in *M. truncatula*. Mycorrhized roots of *rdn1* mutants contained more vesicles and arbuscules than wild-type roots. In line with a requirement for RDN1-mediated arabinosylation of

*Mt*CLE53, overexpression of the latter in an *rdn1* genetic background did not reduce AM fungal colonization as in wild-type plants [47].

Although CLE peptides may respond to diverse stimuli, the shoot-localized receptor *Lj*HAR1/*Mt*SUNN/*Gm*NARK/*Ps*SYM29, may be a common component of the respective signaling mechanisms (discussed in [57]). In *M. truncatula*, downstream signaling of the AM-induced *MtCLE53*, the rhizobium-induced *MtCLE13* or the P-responsive *MtCLE33* was dependent on SUNN in overexpression assays, implying SUNN as a common receptor for all three CLE peptides [45,46]. Components acting downstream of the shoot receptor in AOM are still unknown, except that it was shown that the control of fungal root colonization in *M. truncatula* seems mediated by regulation of strigolactone biosynthesis via *M. truncatula DWARF27* (*MtD27*) expression [63]. This regulation was shown to be dependent on P levels and AM signaling, and was mediated by SUNN and CLEs [46].

In addition to CLE peptides, a genome-wide investigation of SSPs in *M. truncatula* found CEPs to be responsive to P deficiency [21]. Further, recent findings showed *CEP2* to be downregulated in AM-inoculated *S. lycopersicum* roots. *Sl*CEP2 was proposed to promote lateral root formation in tomato plants through an auxin-related pathway, which might be CEPR1-mediated [53]. However, so far, no direct evidence of a functional involvement of CEPs in AOM has been reported, and a putative function in AM control will be an interesting subject of future studies.

5. miRNAs Respond to N and P Availability and Symbiosis-Mediated Nutrient Acquisition

MicroRNAs are small, non-coding RNA molecules, typically 21–24 nucleotides in length, that exert post-transcriptional gene regulation by homology-based pairing to target mRNAs, inducing their degradation or translational inhibition.

Several miRNAs have been associated with responses to N availability in different plant species (Table 2, Figure 1). In *A. thaliana*, upon N starvation, the expression of one or more miRNAs of the miR169, miR171 and miR395 families was repressed, while miR160 and miR780 expression was induced [64]. In addition, an *A. thaliana* miR167 isoform was the first miRNA to be linked to plant N-responses, and was shown to mediate N dependent lateral root outgrowth [65]. More studies in *A. thaliana*, but also other plants, have shown that the regulation of the plant root architecture is a major function of N-responsive miRNAs. Interestingly, both miR167 and miR393 influence root architecture by interfering with auxin signaling through targeting the AUXIN RESPONSE FACTOR 8 (ARF8) [65] and the AUXIN-SIGNALING F-BOX PROTEIN 3 (AFB3) [66], respectively. Further, miR169 targets the transcript of *NFYA5*, which encodes a transcription factor suggested to regulate N-starvation responses in plants by affecting the expression of the nitrate transporters *AtNRT1.1* and *AtNRT2.1* [67]. Interestingly, apart from miRNAs, also long non-coding RNAs (lncRNAs) have been found to respond to the N status in different plants (for a recent review see [68]).

Consistent with a general role of miRNAs in maintaining plant nutrient homeostasis, several miRNAs have further been reported to respond to P availability (Table 2, Figure 1). Among them, miR399, miR827 and miR2111 isoforms were found to accumulate under P-starvation conditions in different plant species including *A. thaliana* and *N. benthamiana*. These miRNAs were present in the phloem sap of P-starved *B. napus* plants, suggesting organ-to-organ mobility along with long-distance regulation of gene expression [69–71]. A well-studied P-responsive miRNA is miR399, which undergoes long-distance shoot-to-root allocation during the onset of P deficiency [69] and is suggested to mediate enhanced P uptake and translocation [72]. miR399 post-transcriptionally regulates PHO2 (PHOSPHATE 2), a ubiquitin-conjugating E2 enzyme that targets members of the PHT1 (PHOSPHATE TRANSPORTER 1) family for ubiquitin-mediated degradation [69,72–74].

Phosphate starvation and AM-symbiosis-related signaling networks interlink, and miRNAs are among the shared components. For example, the miR399-*PHO2* node-regulating P-homeostasis in non-mycorrhizal plants was shown to be acting in AM-

colonized roots of *M. truncatula* [75]. Studies in different symbiotic plants have identified miRNAs that dually respond to P availability and AM fungal infection. For example, miR393, shown to restrict arbuscule development by targeting auxin receptors involved in arbuscule formation, is induced by low P-concentrations and repressed by AM [76]. The responsiveness of different miRNAs in the environmental P conditions and their roles in AM symbiosis are reviewed in [59]. A particularly interesting antagonistic role is reported for miR171 isoforms in *M. truncatula* AM symbiosis control. Several miR171 family members negatively regulate root invasion by AM fungi via post-transcriptional control of the GRAS-type transcription factor LOM (LOST MERISTEMS 1), a positive regulator of AM [77]. In contrast, miR171b, which specifically accumulates in arbuscule-containing plant cells, displays a mismatched cleavage site and prevents cleavage of *LOM1* transcripts by other members of the miR171 family [77].

M. truncatula miR171h (*L. japonicus* miR171c), which targets the GRAS-type transcription factor *NODULATION SIGNALLING PATHWAY2 (NSP2)* transcripts [78,79], accumulates under both N and P sufficiency and has been reported to be involved in both rhizobial nodulation and AM symbioses. NSP2 is essential for nodulation in legumes [80,81], and positively regulates AM fungal colonization [15]. It is further involved in strigolactone biosynthesis [82]. In line with its roles in symbiosis development, *M. truncatula* miR171h accumulation is not only nutrient-status-dependent, but also induced by myc-LCO and nod factor signaling during AM and nodulation symbioses [78,79,83]. Ectopic overexpression of pri-miR171h in *M. truncatula* roots resulted in reduced mycorrhizal root colonization and nodule numbers compared to controls, when plants were inoculated with AM fungi and rhizobia, respectively [83]. Thus miR171h seems to have a central role in integrating plant responses to the essential nutrients N and P, and the acquisition of these nutrients through symbiotic associations.

Several miRNAs have been reported to respond to rhizobial inoculation (Table 2, Figure 1) and are presumed to play roles during early stages of the symbiotic interaction, mostly by targeting transcripts of genes encoding transcription factors. Apart from miR171 family members, these include miR319d in common beans and miR172 in many plant species (reviewed in [84]). The sequencing of sRNA libraries from nodules alongside a degradome analysis identified several miRNA-target pairs that show activity in nodules. In soybeans, combined sRNA and degradome sequencing revealed miR167 targeting the 5′UTR of the nuclear cation channel CYCLOPS as well as miR393j-3p targeting of *ENOD93* (*EARLY NODULIN 93*) [85]. The overexpression of miR393 in soybean roots significantly reduced nodulation [85]. *M. truncatula* miR167 family members further target auxin response factors [86], and *L. japonicus* miR397 targets a Cu^{2+}-containing LACCASE [79]. The regulation of some miRNAs has been linked to auxin and cytokinin action in the legume–rhizobium symbiosis, however there are only a few studies on this topic (reviewed in [84]). Interestingly, in line with an adaptation of conserved developmental mechanisms in the genetic regulation of symbiosis, *M. truncatula* miR166 has a dual role regulating root and nodule development. miR166 isoforms target *HD-ZIPIII* (*CLASS-III HOMEODOMAIN-LEUCINE ZIPPER*) genes, a family of transcription factors associated with nodule development, and overexpression of *MtMIR166* affected both nodule and lateral root numbers as well as vascular bundle development [87].

Over the last years, miR2111 has emerged as a key component of root nodulation control via the AON mechanism (discussed in Section 6 of the current article). miR2111 is a mobile signal undergoing shoot-to-root translocation. It accumulates in shoots under low N conditions and acts as a positive regulator of nodulation by targeting root-localized transcripts encoding the F-Box Kelch-repeat protein TML (TOO MUCH LOVE) [88], an inhibitor of rhizobial infection and nodulation [89,90].

A second miRNA implemented in AON is soybean miR172c [91,92]. miR172c strongly accumulates in the vicinity of rhizobial invasion and in nodules [91,93] and acts as a positive regulator of rhizobial infection and nodule formation through regulation of AP2/ERF transcription factor mRNAs [91,93]. In soybeans, the transcriptional repressor NNC1

(NODULE NUMBER CONTROL 1) is assumed to be the primary miR172 target [91,92]. NNC1 is a negative regulator of nodulation and was shown to bind to the promoters of the early nodulin genes *ENOD40-1* and -2, inhibiting their expression. NNC1 further interacts with NIN (NODULE INCEPTION), inhibiting the transcription of downstream genes encoding *Gm*RIC1 and *Gm*RIC2 peptides, linking it to AON. Using a *nark* loss-of-function mutant, it was shown that miR172c is negatively regulated by NARK, an observation providing additional evidence for the involvement of the miR172c-*NNC1* node in AON in soybeans [91,92].

Table 2. List of selected miRNAs responding to nitrogen (N), phosphorus (P) and microsymbionts (rhizobium and AM fungi).

	Stimuli	Organism	Influence	Tissue	Target	Refs
miR167	N-repressed	*A. thaliana*	local	root pericycle cells	*ARF8*	[65]
miR169	N-limitation repressed	*A. thaliana and B. napus*	systemic	shoots, roots, phloem sap	*NFYA5*	[67] [70]
miR398a	N-limitation and P-limitation repressed	*A. thaliana*				[70]
miR399	P-limitation induced	*A. thaliana and B. napus*	systemic	vascular tissues, phloem sap	*PHO2*	[70] [72]
miR2111	P-limitation induced N-repressed, rhizobium-repressed	*A. thaliana and B. napus* *L. japonicus*	systemic	phloem sap leaves phloem, phloem sap	*E3 ligase TML*	[76] [88]
miR397	nodulation-induced	*L. japonicus*	local and systemic	nodules, leaves	*LACCASE10*	[79]
miR171c	nodulation-induced	*L. japonicus*		nodules	*NSP2*	[79]
miR171h	expressed in high P and N, AM-repressed, nodulation-induced	*M. truncatula*		roots, arbuscule-containing cells, nodules	*NSP2*	[83]
miR171b	AM-specific	*M. truncatula*	local	colonized root cells	*LOM1*	[77]
miR393	low-P expressed, AM-repressed	*M. truncatula*	local	roots	*auxin receptors*	[76]
miR399	low P-induced, AM-induced	*M. truncatula*	systemic	leaves and roots	*PHO2*	[75]
miR166	nodulation induced	*M. truncatula*	local	vascular bundles, roots, nodules	*HD-ZIP III*	[87]
miR172c	rhizobium-induced, nod factors-induced	*G. max*	local	rhizobium-inoculated roots and nodules	*NNC1*	[91]
miR156b	rhizobium-repressed	*G. max*	local	roots	*GmSPL9d*	[94]

In a recent report, Yun et al. [94] showed that overexpression of miR156b in soybean roots resulted in reduced expression of *NINa*, *ENOD40-1* and *MIR172c*. The main target of miR156b is the *GmSPL9d* (*SQUAMOSA PROMOTER-BINDING LIKE 9d*) gene, a positive regulator of symbiosis that accumulates upon infection. *Gm*SPL9d affects the expression of *NINa*, *ENOD40-1* and *MIR172c* by direct promoter binding [94]. Similarly, in *L. japonicus*, ectopic overexpression of miR156a reduced nodulation and affected the expression of early nodulation genes such as *ENOD* genes, *NFR1*, *CYCLOPS* and *NSP1* [95]. These data suggest that the miR156-SPL node has a key regulatory role in nodulation by directly activating the expression of core genes in the early stages of nodulation signaling.

6. CEPs and CLEs and miR2111 Jointly Orchestrate Plant Responses to N and Rhizobia

AON controls rhizobial infection and nodule numbers to ensure a viable balance between ammonia uptake and carbohydrate as well as nutrient costs. This feedback loop has been well-described in different plant species and was shown to be systemic, involving CLE and CEP peptides as root-derived signals moving to the shoot through the xylem, and micro RNA miR2111 as well as CEPD peptides as shoot-derived, root-active signals navigating through the phloem [56,88]. miR2111 is mainly expressed in shoot tissues, more precisely in leaf vein phloem [88,96]. Leaf phloem expression was postulated as prerequisite for systemic mobility of small RNAs [97], and indeed, miR2111 was shown to translocate from shoot to root [88,96]. Shoot-derived miR2111 effectively reduces root transcript levels of *TML* via endonucleolytic cleavage [88].

The miR2111-*TML* node is responsive to both soil nitrate levels and rhizobial signaling, suggesting a role in balancing nodulation symbiosis with N availability. Nitrate fertilization or rhizobial inoculation led to decreased miR2111 levels, and accordingly, *TML* transcript abundance increased [56,88].

miR2111 expression depends on two peptide receptors, the LRR-RLKs *Lj*HAR1/*Mt*SUNN/*Gm*NARK and *Mt*CRA2 [37,56,88,96]. Both factors are expressed in the whole plant, however the regulation of symbiosis is mainly achieved by the shoot fraction. HAR1, a negative regulator of symbiosis, represses miR2111 levels in rhizobially infected plants, resulting in *TML* transcript accumulation and restriction of further infections [88,96]. The second regulator of miR2111, CRA2, is a positive regulator of symbiosis and promotes miR2111 accumulation under low N conditions [56]. The antagonistic regulation of infection through miR2111 underlines the biological relevance of this node. For the plant, both miR2111 promotion and repression, and a fast switch of these states, seem equally important, allowing the plant to quickly change from a susceptible status welcoming infection to restriction of the latter.

Consistent with the divergent effects of activated HAR1/SUNN/NARK and CRA2 on miR2111 regulation, these two shoot receptors differ in the groups of peptide ligands they perceive. HAR1/SUNN/NARK interacts with CLE peptides [29,33], and several studies suggest that the receptor regulates miR2111 depending on root-derived CLE peptide perception [37,88,96]. For example, nitrate induction of *MtCLE35* coincided with reduced miR2111 levels and, consistently, an accumulation of *MtTML2* transcripts downstream of the SUNN receptor [37]. CRA2, in contrast, perceives CEP peptide ligands, positively regulating miR2111 depending on the presence of CEPs [56]. Overexpression of *MtCEP1*, for example, resulted in increased miR2111 abundance and reduced transcript levels of both *M. truncatula TML1* and *TML2* in roots. This was dependent on CRA2, as those effects were not apparent in *cra2* mutants [56]. Both classes of peptides possess several members regulated by N and/or symbiosis signaling (see Section 3 of the current article) (Table 1, Figure 1). The combined results indicate that a multitude of CEP and CLE peptide signals triggering divergent responses converge in the miR2111-*TML* regulon, shaping a model of AON as a complex, multilayered network that dynamically integrates infection and symbiosis development with plant nutritional status and needs.

7. CLE Peptide Involvement in P-Dependent Control of Nodulation

P supply is well known to positively correlate with nodulation and symbiotic N fixation in legumes [98,99], and consistently, nodule fresh weight and activity are sensitive to P deficiency [100]. A study in the actinorhizal plant *Alnus incana* showed that a high phosphate concentration can reverse the nitrate-induced inhibition of nodulation, leading to an increase of nodules. The positive effect of P on nodule numbers was found to be systemically regulated and independent of overall plant growth and development [101]. In common beans, P deficiency reduced the numbers of the bacterially induced root hair deformations during the initial steps of rhizobial infection [102]. Although a negative effect of P deficiency on nodulation has been clearly documented, the underlying molecular mechanisms were unknown until recently.

In the roots of common beans, P deficiency induced the expression of genes encoding the AON-related root-to-shoot signals RIC1 and RIC2 in the absence of symbiosis [48] (Table 1). Moreover, it was shown that, under P deficiency, RIC1 and RIC2 led to a systemic restriction of nodulation, through the HAR1/SUNN/NARK receptor in both common beans and soybeans. This effect seems to be mediated by TML, as *TML* transcripts accumulated in the roots of both plants [48]. These data suggest that CLE peptides negatively regulate nodule formation under P deficiency conditions via the AON genetic network.

8. Conclusions

Plants have adopted different strategies to control nutrient homeostasis and overcome nutrient limitation in their environment, such as the adaptation of root system architecture and the establishment of root symbiotic relationships.

The molecular basis of these response systems has been the subject of intense interest by the scientific community in the light of reducing dependence on inorganic fertilizers while securing global food supplies. Studies in model plants revealed conserved processes that ensure survival and productivity under nutrient deprivation, and there is an increasing host of knowledge on how plants cope with fluctuations in the availability of important nutrients such as N and P in the soil. However, more research to this field is not only important for transferring the knowledge acquired in model systems to a wider range of species including crop plants, but also to grasp the relevance of these processes in natural communities, and in adapting plant populations to increasingly challenging environmental conditions in the face of climate change.

Author Contributions: Conceptualization, D.T.; writing—original draft preparation, M.I.V. and M.S.; writing—review and editing, D.T. and K.M.; supervision, D.T. and K.M. All authors have read and agreed to the published version of the manuscript.

Funding: This work received no external funding.

Data Availability Statement: Not applicable.

Conflicts of Interest: The authors declare no conflict of interest.

References

1. Udvardi, M.; Poole, P.S. Transport and Metabolism in Legume-Rhizobia Symbioses. *Annu. Rev. Plant Biol.* **2013**, *64*, 781–805. [CrossRef] [PubMed]
2. Patriarca, E.J.; Tatè, R.; Iaccarino, M. Key Role of Bacterial NH_4^+ Metabolism in Rhizobium-Plant Symbiosis. *Microbiol. Mol. Biol. Rev.* **2002**, *66*, 203–222. [CrossRef] [PubMed]
3. Kaiser, B.N.; Finnegan, P.M.; Tyerman, S.D.; Whitehead, L.F.; Bergersen, F.J.; Day, D.A.; Udvardi, M.K. Characterization of an Ammonium Transport Protein from the Peribacteroid Membrane of Soybean Nodules. *Science* **1998**, *281*, 1202–1206. [CrossRef] [PubMed]
4. Salvemini, F.; Marini, A.; Riccio, A.; Patriarca, E.J.; Chiurazzi, M. Functional Characterization of an Ammonium Transporter Gene from *Lotus japonicus*. *Gene* **2001**, *270*, 237–243. [CrossRef]
5. Maxwell, C.A.; Hartwig, U.A.; Joseph, C.M.; Phillips, D.A. A Chalcone and Two Related Flavonoids Released from Alfalfa Roots Induce Nod Genes of Rhizobium Meliloti. *Plant Physiol.* **1989**, *91*, 842–847. [CrossRef]
6. Long, S.R.; Staskawicz, B.J. Prokaryotic Plant Parasites. *Cell* **1993**, *73*, 921–935. [CrossRef]
7. Dénarié, J.; Debellé, F.; Promé, J.C. Rhizobium Lipo-Chitooligosaccharide Nodulation Factors: Signaling Molecules Mediating Recognition and Morphogenesis. *Annu. Rev. Biochem.* **1996**, *65*, 503–535. [CrossRef]
8. Oldroyd, G.E.D.; Murray, J.D.; Poole, P.S.; Downie, J.A. The Rules of Engagement in the Legume-Rhizobial Symbiosis. *Annu. Rev. Genet.* **2011**, *45*, 119–144. [CrossRef]
9. Harrison, M.J.; van Buuren, M.L. A Phosphate Transporter from the Mycorrhizal Fungus Glomus Versiforme. *Nature* **1995**, *378*, 626–629. [CrossRef]
10. Hijikata, N.; Murase, M.; Tani, C.; Ohtomo, R.; Osaki, M.; Ezawa, T. Polyphosphate Has a Central Role in the Rapid and Massive Accumulation of Phosphorus in Extraradical Mycelium of an Arbuscular Mycorrhizal Fungus. *New Phytol.* **2010**, *186*, 285–289. [CrossRef]
11. López-Pedrosa, A.; González-Guerrero, M.; Valderas, A.; Azcón-Aguilar, C.; Ferrol, N. GintAMT1 Encodes a Functional High-Affinity Ammonium Transporter That Is Expressed in the Extraradical Mycelium of Glomus Intraradices. *Fungal Genet. Biol.* **2006**, *43*, 102–110. [CrossRef] [PubMed]

12. Cappellazzo, G.; Lanfranco, L.; Fitz, M.; Wipf, D.; Bonfante, P. Characterization of an Amino Acid Permease from the Endomycorrhizal Fungus Glomus Mosseae. *Plant Physiol.* **2008**, *147*, 429–437. [CrossRef] [PubMed]
13. MacLean, A.M.; Bravo, A.; Harrison, M.J. Plant Signaling and Metabolic Pathways Enabling Arbuscular Mycorrhizal Symbiosis. *Plant Cell* **2017**, *29*, 2319–2335. [CrossRef] [PubMed]
14. Akiyama, K.; Matsuzaki, K.; Hayashi, H. Plant Sesquiterpenes Induce Hyphal Branching in Arbuscular Mycorrhizal Fungi. *Nature* **2005**, *435*, 824–827. [CrossRef]
15. Maillet, F.; Poinsot, V.; André, O.; Puech-Pagès, V.; Haouy, A.; Gueunier, M.; Cromer, L.; Giraudet, D.; Formey, D.; Niebel, A.; et al. Fungal Lipochitooligosaccharide Symbiotic Signals in Arbuscular Mycorrhiza. *Nature* **2011**, *469*, 58–63. [CrossRef]
16. Genre, A.; Chabaud, M.; Balzergue, C.; Puech-Pagès, V.; Novero, M.; Rey, T.; Fournier, J.; Rochange, S.; Bécard, G.; Bonfante, P.; et al. Short-Chain Chitin Oligomers from Arbuscular Mycorrhizal Fungi Trigger Nuclear Ca^{2+} Spiking in *Medicago truncatula* Roots and Their Production Is Enhanced by Strigolactone. *New Phytol.* **2013**, *198*, 190–202. [CrossRef]
17. Nagahashi, G.; Douds, D.D., Jr. Appressorium Formation by AM Fungi on Isolated Cell Walls of Carrot Roots. *New Phytol.* **1997**, *136*, 299–304. [CrossRef]
18. Bonfante, P.; Genre, A. Mechanisms Underlying Beneficial Plant–Fungus Interactions in Mycorrhizal Symbiosis. *Nat. Commun.* **2010**, *1*, 48. [CrossRef]
19. Gutjahr, C.; Parniske, M. Cell Biology: Control of Partner Lifetime in a Plant–Fungus Relationship. *Curr. Biol.* **2017**, *27*, R420–R423. [CrossRef]
20. de Bang, T.C.; Lay, K.S.; Scheible, W.-R.; Takahashi, H. Small Peptide Signaling Pathways Modulating Macronutrient Utilization in Plants. *Curr. Opin. Plant Biol.* **2017**, *39*, 31–39. [CrossRef]
21. de Bang, T.C.; Lundquist, P.K.; Dai, X.; Boschiero, C.; Zhuang, Z.; Pant, P.; Torres-Jerez, I.; Roy, S.; Nogales, J.; Veerappan, V.; et al. Genome-Wide Identification of Medicago Peptides Involved in Macronutrient Responses and Nodulation. *Plant Physiol.* **2017**, *175*, 1669–1689. [CrossRef] [PubMed]
22. Betsuyaku, S.; Sawa, S.; Yamada, M. The Function of the CLE Peptides in Plant Development and Plant-Microbe Interactions. *Arab. Book* **2011**, *9*, e0149. [CrossRef]
23. Yamaguchi, Y.L.; Ishida, T.; Sawa, S. CLE Peptides and Their Signaling Pathways in Plant Development. *J. Exp. Bot.* **2016**, *67*, 4813–4826. [CrossRef] [PubMed]
24. Araya, T.; Miyamoto, M.; Wibowo, J.; Suzuki, A.; Kojima, S.; Tsuchiya, Y.N.; Sawa, S.; Fukuda, H.; von Wirén, N.; Takahashi, H. CLE-CLAVATA1 Peptide-Receptor Signaling Module Regulates the Expansion of Plant Root Systems in a Nitrogen-Dependent Manner. *Proc. Natl. Acad. Sci. USA* **2014**, *111*, 2029–2034. [CrossRef] [PubMed]
25. Chaulagain, D.; Frugoli, J. The Regulation of Nodule Number in Legumes Is a Balance of Three Signal Transduction Pathways. *Int. J. Mol. Sci.* **2021**, *22*, 1117. [CrossRef]
26. Okamoto, S.; Ohnishi, E.; Sato, S.; Takahashi, H.; Nakazono, M.; Tabata, S.; Kawaguchi, M. Nod Factor/Nitrate-Induced CLE Genes That Drive HAR1-Mediated Systemic Regulation of Nodulation. *Plant Cell Physiol.* **2009**, *50*, 67–77. [CrossRef]
27. Nishida, H.; Handa, Y.; Tanaka, S.; Suzaki, T.; Kawaguchi, M. Expression of the CLE-RS3 Gene Suppresses Root Nodulation in *Lotus japonicus*. *J. Plant Res.* **2016**, *129*, 909–919. [CrossRef]
28. Mortier, V.; Den Herder, G.; Whitford, R.; Van de Velde, W.; Rombauts, S.; D'Haeseleer, K.; Holsters, M.; Goormachtig, S. CLE Peptides Control *Medicago truncatula* Nodulation Locally and Systemically. *Plant Physiol.* **2010**, *153*, 222–237. [CrossRef]
29. Lebedeva, M.; Azarakhsh, M.; Yashenkova, Y.; Lutova, L. Nitrate-Induced CLE Peptide Systemically Inhibits Nodulation in *Medicago truncatula*. *Plants* **2020**, *9*, 1456. [CrossRef]
30. Mens, C.; Hastwell, A.H.; Su, H.; Gresshoff, P.M.; Mathesius, U.; Ferguson, B.J. Characterisation of *Medicago truncatula* CLE34 and CLE35 in Nitrate and Rhizobia Regulation of Nodulation. *New Phytol.* **2021**, *229*, 2525–2534. [CrossRef]
31. Reid, D.E.; Ferguson, B.J.; Gresshoff, P.M. Inoculation- and Nitrate-Induced CLE Peptides of Soybean Control NARK-Dependent Nodule Formation. *Mol. Plant-Microbe Interact.* **2011**, *24*, 606–618. [CrossRef] [PubMed]
32. Ferguson, B.J.; Li, D.; Hastwell, A.H.; Reid, D.E.; Li, Y.; Jackson, S.A.; Gresshoff, P.M. The Soybean (*Glycine max*) Nodulation-Suppressive CLE Peptide, GmRIC1, Functions Interspecifically in Common White Bean (*Phaseolus vulgaris*), but Not in a Supernodulating Line Mutated in the Receptor PvNARK. *Plant Biotechnol. J.* **2014**, *12*, 1085–1097. [CrossRef] [PubMed]
33. Okamoto, S.; Shinohara, H.; Mori, T.; Matsubayashi, Y.; Kawaguchi, M. Root-Derived CLE Glycopeptides Control Nodulation by Direct Binding to HAR1 Receptor Kinase. *Nat. Commun.* **2013**, *4*, 2191. [CrossRef] [PubMed]
34. Krusell, L.; Madsen, L.H.; Sato, S.; Aubert, G.; Genua, A.; Szczyglowski, K.; Duc, G.; Kaneko, T.; Tabata, S.; de Bruijn, F.; et al. Shoot Control of Root Development and Nodulation Is Mediated by a Receptor-like Kinase. *Nature* **2002**, *420*, 422–426. [CrossRef]
35. Nishimura, R.; Hayashi, M.; Wu, G.-J.; Kouchi, H.; Imaizumi-Anraku, H.; Murakami, Y.; Kawasaki, S.; Akao, S.; Ohmori, M.; Nagasawa, M.; et al. HAR1 Mediates Systemic Regulation of Symbiotic Organ Development. *Nature* **2002**, *420*, 426–429. [CrossRef]
36. Searle, I.R.; Men, A.E.; Laniya, T.S.; Buzas, D.M.; Iturbe-Ormaetxe, I.; Carroll, B.J.; Gresshoff, P.M. Long-Distance Signaling in Nodulation Directed by a CLAVATA1-like Receptor Kinase. *Science* **2003**, *299*, 109–112. [CrossRef]
37. Moreau, C.; Gautrat, P.; Frugier, F. Nitrate-Induced CLE35 Signaling Peptides Inhibit Nodulation through the SUNN Receptor and MiR2111 Repression. *Plant Physiol.* **2021**, *185*, 1216–1228. [CrossRef]
38. Ohyama, K.; Shinohara, H.; Ogawa-Ohnishi, M.; Matsubayashi, Y. A Glycopeptide Regulating Stem Cell Fate in Arabidopsis Thaliana. *Nat. Chem. Biol.* **2009**, *5*, 578–580. [CrossRef]

39. Ogawa-Ohnishi, M.; Matsushita, W.; Matsubayashi, Y. Identification of Three Hydroxyproline O-Arabinosyltransferases in Arabidopsis Thaliana. *Nat. Chem. Biol.* **2013**, *9*, 726–730. [CrossRef]
40. Kassaw, T.; Nowak, S.; Schnabel, E.; Frugoli, J. ROOT DETERMINED NODULATION1 Is Required for M. Truncatula CLE12, But Not CLE13, Peptide Signaling through the SUNN Receptor Kinase. *Plant Physiol.* **2017**, *174*, 2445–2456. [CrossRef]
41. Imin, N.; Patel, N.; Corcilius, L.; Payne, R.J.; Djordjevic, M.A. CLE Peptide Tri-Arabinosylation and Peptide Domain Sequence Composition Are Essential for SUNN-Dependent Autoregulation of Nodulation in *Medicago truncatula*. *New Phytol.* **2018**, *218*, 73–80. [CrossRef] [PubMed]
42. Hastwell, A.H.; Corcilius, L.; Williams, J.T.; Gresshoff, P.M.; Payne, R.J.; Ferguson, B.J. Triarabinosylation Is Required for Nodulation-Suppressive CLE Peptides to Systemically Inhibit Nodulation in Pisum Sativum. *Plant Cell Environ.* **2019**, *42*, 188–197. [CrossRef] [PubMed]
43. Yoro, E.; Nishida, H.; Ogawa-Ohnishi, M.; Yoshida, C.; Suzaki, T.; Matsubayashi, Y.; Kawaguchi, M. PLENTY, a Hydroxyproline O-Arabinosyltransferase, Negatively Regulates Root Nodule Symbiosis in *Lotus japonicus*. *J. Exp. Bot.* **2019**, *70*, 507–517. [CrossRef] [PubMed]
44. Funayama-Noguchi, S.; Noguchi, K.; Yoshida, C.; Kawaguchi, M. Two CLE Genes Are Induced by Phosphate in Roots of *Lotus japonicus*. *J. Plant Res.* **2011**, *124*, 155–163. [CrossRef] [PubMed]
45. Laffont, C.; Ivanovici, A.; Gautrat, P.; Brault, M.; Djordjevic, M.A.; Frugier, F. The NIN Transcription Factor Coordinates CEP and CLE Signaling Peptides That Regulate Nodulation Antagonistically. *Nat. Commun.* **2020**, *11*, 3167. [CrossRef] [PubMed]
46. Müller, L.M.; Flokova, K.; Schnabel, E.; Sun, X.; Fei, Z.; Frugoli, J.; Bouwmeester, H.J.; Harrison, M.J. A CLE-SUNN Module Regulates Strigolactone Content and Fungal Colonization in Arbuscular Mycorrhiza. *Nat. Plants* **2019**, *5*, 933–939. [CrossRef] [PubMed]
47. Karlo, M.; Boschiero, C.; Landerslev, K.G.; Blanco, G.S.; Wen, J.; Mysore, K.S.; Dai, X.; Zhao, P.X.; de Bang, T.C. The CLE53-SUNN Genetic Pathway Negatively Regulates Arbuscular Mycorrhiza Root Colonization in *Medicago truncatula*. *J. Exp. Bot.* **2020**, *71*, 4972–4984. [CrossRef] [PubMed]
48. Isidra-Arellano, M.C.; Pozas-Rodríguez, E.A.; Del Rocío Reyero-Saavedra, M.; Arroyo-Canales, J.; Ferrer-Orgaz, S.; Del Socorro Sánchez-Correa, M.; Cardenas, L.; Covarrubias, A.A.; Valdés-López, O. Inhibition of Legume Nodulation by Pi Deficiency Is Dependent on the Autoregulation of Nodulation (AON) Pathway. *Plant J.* **2020**, *103*, 1125–1139. [CrossRef] [PubMed]
49. Tabata, R.; Sumida, K.; Yoshii, T.; Ohyama, K.; Shinohara, H.; Matsubayashi, Y. Perception of Root-Derived Peptides by Shoot LRR-RKs Mediates Systemic N-Demand Signaling. *Science* **2014**, *346*, 343–346. [CrossRef]
50. Imin, N.; Mohd-Radzman, N.A.; Ogilvie, H.A.; Djordjevic, M.A. The Peptide-Encoding CEP1 Gene Modulates Lateral Root and Nodule Numbers in *Medicago truncatula*. *J. Exp. Bot.* **2013**, *64*, 5395–5409. [CrossRef]
51. Laffont, C.; Huault, E.; Gautrat, P.; Endre, G.; Kalo, P.; Bourion, V.; Duc, G.; Frugier, F. Independent Regulation of Symbiotic Nodulation by the SUNN Negative and CRA2 Positive Systemic Pathways. *Plant Physiol.* **2019**, *180*, 559–570. [CrossRef] [PubMed]
52. Zhu, F.; Ye, Q.; Chen, H.; Dong, J.; Wang, T. Multigene Editing Reveals That MtCEP1/2/12 Redundantly Control Lateral Root and Nodule Number in *Medicago truncatula*. *J. Exp. Bot.* **2021**, *72*, 3661–3676. [CrossRef] [PubMed]
53. Hsieh, Y.-H.; Wei, Y.-H.; Lo, J.-C.; Pan, H.-Y.; Yang, S.-Y. Arbuscular Mycorrhizal Symbiosis Enhances Tomato Lateral Root Formation by Modulating CEP2 Peptide Expression. *New Phytol.* **2022**, *235*, 292–305. [CrossRef] [PubMed]
54. Ohyama, K.; Ogawa, M.; Matsubayashi, Y. Identification of a Biologically Active, Small, Secreted Peptide in Arabidopsis by in Silico Gene Screening, Followed by LC-MS-Based Structure Analysis. *Plant J.* **2008**, *55*, 152–160. [CrossRef]
55. Huault, E.; Laffont, C.; Wen, J.; Mysore, K.S.; Ratet, P.; Duc, G.; Frugier, F. Local and Systemic Regulation of Plant Root System Architecture and Symbiotic Nodulation by a Receptor-like Kinase. *PLoS Genet.* **2014**, *10*, e1004891. [CrossRef]
56. Gautrat, P.; Laffont, C.; Frugier, F. Compact Root Architecture 2 Promotes Root Competence for Nodulation through the MiR2111 Systemic Effector. *Curr. Biol.* **2020**, *30*, 1339–1345. [CrossRef]
57. Roy, S.; Müller, L.M. A Rulebook for Peptide Control of Legume-Microbe Endosymbioses. *Trends Plant Sci* **2022**, *27*, 870–889. [CrossRef]
58. Breuillin, F.; Schramm, J.; Hajirezaei, M.; Ahkami, A.; Favre, P.; Druege, U.; Hause, B.; Bucher, M.; Kretzschmar, T.; Bossolini, E.; et al. Phosphate Systemically Inhibits Development of Arbuscular Mycorrhiza in *Petunia hybrida* and Represses Genes Involved in Mycorrhizal Functioning. *Plant J.* **2010**, *64*, 1002–1017. [CrossRef]
59. Müller, L.M.; Harrison, M.J. Phytohormones, MiRNAs, and Peptide Signals Integrate Plant Phosphorus Status with Arbuscular Mycorrhizal Symbiosis. *Curr. Opin. Plant Biol.* **2019**, *50*, 132–139. [CrossRef]
60. Meixner, C.; Ludwig-Müller, J.; Miersch, O.; Gresshoff, P.; Staehelin, C.; Vierheilig, H. Lack of Mycorrhizal Autoregulation and Phytohormonal Changes in the Supernodulating Soybean Mutant Nts1007. *Planta* **2005**, *222*, 709–715. [CrossRef]
61. Wang, C.; Reid, J.B.; Foo, E. The Art of Self-Control—Autoregulation of Plant–Microbe Symbioses. *Front. Plant Sci.* **2018**, *9*, 988. [CrossRef] [PubMed]
62. Handa, Y.; Nishide, H.; Takeda, N.; Suzuki, Y.; Kawaguchi, M.; Saito, K. RNA-Seq Transcriptional Profiling of an Arbuscular Mycorrhiza Provides Insights into Regulated and Coordinated Gene Expression in *Lotus japonicus* and *Rhizophagus irregularis*. *Plant Cell Physiol.* **2015**, *56*, 1490–1511. [CrossRef] [PubMed]
63. van Zeijl, A.; Liu, W.; Xiao, T.T.; Kohlen, W.; Yang, W.-C.; Bisseling, T.; Geurts, R. The Strigolactone Biosynthesis Gene DWARF27 Is Co-Opted in Rhizobium Symbiosis. *BMC Plant Biol.* **2015**, *15*, 260. [CrossRef]

64. Liang, G.; He, H.; Yu, D. Identification of Nitrogen Starvation-Responsive MicroRNAs in Arabidopsis Thaliana. *PLoS ONE* **2012**, *7*, e48951. [CrossRef] [PubMed]
65. Gifford, M.L.; Dean, A.; Gutierrez, R.A.; Coruzzi, G.M.; Birnbaum, K.D. Cell-Specific Nitrogen Responses Mediate Developmental Plasticity. *Proc. Natl. Acad. Sci. USA* **2008**, *105*, 803–808. [CrossRef] [PubMed]
66. Vidal, E.A.; Araus, V.; Lu, C.; Parry, G.; Green, P.J.; Coruzzi, G.M.; Gutiérrez, R.A. Nitrate-Responsive MiR393/AFB3 Regulatory Module Controls Root System Architecture in Arabidopsis Thaliana. *Proc. Natl. Acad. Sci. USA* **2010**, *107*, 4477–4482. [CrossRef]
67. Zhao, M.; Ding, H.; Zhu, J.-K.; Zhang, F.; Li, W.-X. Involvement of MiR169 in the Nitrogen-Starvation Responses in Arabidopsis. *New Phytol.* **2011**, *190*, 906–915. [CrossRef]
68. Fukuda, M.; Fujiwara, T.; Nishida, S. Roles of Non-Coding RNAs in Response to Nitrogen Availability in Plants. *Int. J. Mol. Sci.* **2020**, *21*, 8508. [CrossRef]
69. Pant, B.D.; Buhtz, A.; Kehr, J.; Scheible, W.-R. MicroRNA399 Is a Long-Distance Signal for the Regulation of Plant Phosphate Homeostasis. *Plant J.* **2008**, *53*, 731–738. [CrossRef]
70. Pant, B.D.; Musialak-Lange, M.; Nuc, P.; May, P.; Buhtz, A.; Kehr, J.; Walther, D.; Scheible, W.-R. Identification of Nutrient-Responsive Arabidopsis and Rapeseed MicroRNAs by Comprehensive Real-Time Polymerase Chain Reaction Profiling and Small RNA Sequencing. *Plant Physiol.* **2009**, *150*, 1541–1555. [CrossRef]
71. Huen, A.; Bally, J.; Smith, P. Identification and Characterisation of MicroRNAs and Their Target Genes in Phosphate-Starved Nicotiana Benthamiana by Small RNA Deep Sequencing and 5′RACE Analysis. *BMC Genom.* **2018**, *19*, 940. [CrossRef] [PubMed]
72. Lin, S.-I.; Chiang, S.-F.; Lin, W.-Y.; Chen, J.-W.; Tseng, C.-Y.; Wu, P.-C.; Chiou, T.-J. Regulatory Network of MicroRNA399 and PHO2 by Systemic Signaling. *Plant Physiol.* **2008**, *147*, 732–746. [CrossRef] [PubMed]
73. Aung, K.; Lin, S.-I.; Wu, C.-C.; Huang, Y.-T.; Su, C.-L.; Chiou, T.-J. Pho2, a Phosphate Overaccumulator, Is Caused by a Nonsense Mutation in a MicroRNA399 Target Gene. *Plant Physiol.* **2006**, *141*, 1000–1011. [CrossRef] [PubMed]
74. Huang, T.-K.; Han, C.-L.; Lin, S.-I.; Chen, Y.-J.; Tsai, Y.-C.; Chen, Y.-R.; Chen, J.-W.; Lin, W.-Y.; Chen, P.-M.; Liu, T.-Y.; et al. Identification of Downstream Components of Ubiquitin-Conjugating Enzyme PHOSPHATE2 by Quantitative Membrane Proteomics in Arabidopsis Roots. *Plant Cell* **2013**, *25*, 4044–4060. [CrossRef]
75. Branscheid, A.; Sieh, D.; Pant, B.D.; May, P.; Devers, E.A.; Elkrog, A.; Schauser, L.; Scheible, W.-R.; Krajinski, F. Expression Pattern Suggests a Role of MiR399 in the Regulation of the Cellular Response to Local Pi Increase during Arbuscular Mycorrhizal Symbiosis. *Mol. Plant-Microbe Interact.* **2010**, *23*, 915–926. [CrossRef]
76. Etemadi, M.; Gutjahr, C.; Couzigou, J.-M.; Zouine, M.; Lauressergues, D.; Timmers, A.; Audran, C.; Bouzayen, M.; Bécard, G.; Combier, J.-P. Auxin Perception Is Required for Arbuscule Development in Arbuscular Mycorrhizal Symbiosis. *Plant Physiol.* **2014**, *166*, 281–292. [CrossRef]
77. Couzigou, J.-M.; Lauressergues, D.; André, O.; Gutjahr, C.; Guillotin, B.; Bécard, G.; Combier, J.-P. Positive Gene Regulation by a Natural Protective MiRNA Enables Arbuscular Mycorrhizal Symbiosis. *Cell Host Microbe* **2017**, *21*, 106–112. [CrossRef]
78. Lauressergues, D.; Delaux, P.-M.; Formey, D.; Lelandais-Brière, C.; Fort, S.; Cottaz, S.; Bécard, G.; Niebel, A.; Roux, C.; Combier, J.-P. The MicroRNA MiR171h Modulates Arbuscular Mycorrhizal Colonization of *Medicago truncatula* by Targeting NSP2. *Plant J.* **2012**, *72*, 512–522. [CrossRef]
79. De Luis, A.; Markmann, K.; Cognat, V.; Holt, D.B.; Charpentier, M.; Parniske, M.; Stougaard, J.; Voinnet, O. Two MicroRNAs Linked to Nodule Infection and Nitrogen-Fixing Ability in the Legume *Lotus japonicus*. *Plant Physiol.* **2012**, *160*, 2137–2154. [CrossRef]
80. Kaló, P.; Gleason, C.; Edwards, A.; Marsh, J.; Mitra, R.M.; Hirsch, S.; Jakab, J.; Sims, S.; Long, S.R.; Rogers, J.; et al. Nodulation Signaling in Legumes Requires NSP2, a Member of the GRAS Family of Transcriptional Regulators. *Science* **2005**, *308*, 1786–1789. [CrossRef]
81. Heckmann, A.B.; Lombardo, F.; Miwa, H.; Perry, J.A.; Bunnewell, S.; Parniske, M.; Wang, T.L.; Downie, J.A. *Lotus japonicus* Nodulation Requires Two GRAS Domain Regulators, One of Which Is Functionally Conserved in a Non-Legume. *Plant Physiol.* **2006**, *142*, 1739–1750. [CrossRef] [PubMed]
82. Liu, W.; Kohlen, W.; Lillo, A.; Op den Camp, R.; Ivanov, S.; Hartog, M.; Limpens, E.; Jamil, M.; Smaczniak, C.; Kaufmann, K.; et al. Strigolactone Biosynthesis in *Medicago truncatula* and Rice Requires the Symbiotic GRAS-Type Transcription Factors NSP1 and NSP2. *Plant Cell* **2011**, *23*, 3853–3865. [CrossRef] [PubMed]
83. Hofferek, V.; Mendrinna, A.; Gaude, N.; Krajinski, F.; Devers, E.A. MiR171h Restricts Root Symbioses and Shows like Its Target NSP2 a Complex Transcriptional Regulation in *Medicago truncatula*. *BMC Plant Biol.* **2014**, *14*, 199. [CrossRef] [PubMed]
84. Hoang, N.T.; Tóth, K.; Stacey, G. The Role of MicroRNAs in the Legume-Rhizobium Nitrogen-Fixing Symbiosis. *J. Exp. Bot.* **2020**, *71*, 1668–1680. [CrossRef] [PubMed]
85. Yan, Z.; Hossain, M.S.; Arikit, S.; Valdés-López, O.; Zhai, J.; Wang, J.; Libault, M.; Ji, T.; Qiu, L.; Meyers, B.C.; et al. Identification of MicroRNAs and Their MRNA Targets during Soybean Nodule Development: Functional Analysis of the Role of MiR393j-3p in Soybean Nodulation. *New Phytol.* **2015**, *207*, 748–759. [CrossRef] [PubMed]
86. Lelandais-Brière, C.; Naya, L.; Sallet, E.; Calenge, F.; Frugier, F.; Hartmann, C.; Gouzy, J.; Crespi, M. Genome-Wide *Medicago truncatula* Small RNA Analysis Revealed Novel MicroRNAs and Isoforms Differentially Regulated in Roots and Nodules. *Plant Cell* **2009**, *21*, 2780–2796. [CrossRef]
87. Boualem, A.; Laporte, P.; Jovanovic, M.; Laffont, C.; Plet, J.; Combier, J.-P.; Niebel, A.; Crespi, M.; Frugier, F. MicroRNA166 Controls Root and Nodule Development in *Medicago truncatula*. *Plant J.* **2008**, *54*, 876–887. [CrossRef]

88. Tsikou, D.; Yan, Z.; Holt, D.B.; Abel, N.B.; Reid, D.E.; Madsen, L.H.; Bhasin, H.; Sexauer, M.; Stougaard, J.; Markmann, K. Systemic Control of Legume Susceptibility to Rhizobial Infection by a Mobile MicroRNA. *Science* **2018**, *362*, 233–236. [CrossRef]
89. Magori, S.; Oka-Kira, E.; Shibata, S.; Umehara, Y.; Kouchi, H.; Hase, Y.; Tanaka, A.; Sato, S.; Tabata, S.; Kawaguchi, M. Too Much Love, a Root Regulator Associated with the Long-Distance Control of Nodulation in *Lotus japonicus*. *Mol. Plant-Microbe Interact.* **2009**, *22*, 259–268. [CrossRef]
90. Takahara, M.; Magori, S.; Soyano, T.; Okamoto, S.; Yoshida, C.; Yano, K.; Sato, S.; Tabata, S.; Yamaguchi, K.; Shigenobu, S.; et al. Too Much Love, a Novel Kelch Repeat-Containing F-Box Protein, Functions in the Long-Distance Regulation of the Legume–*Rhizobium* Symbiosis. *Plant Cell Physiol.* **2013**, *54*, 433–447. [CrossRef]
91. Wang, Y.; Wang, L.; Zou, Y.; Chen, L.; Cai, Z.; Zhang, S.; Zhao, F.; Tian, Y.; Jiang, Q.; Ferguson, B.J.; et al. Soybean MiR172c Targets the Repressive AP2 Transcription Factor NNC1 to Activate ENOD40 Expression and Regulate Nodule Initiation. *Plant Cell* **2014**, *26*, 4782–4801. [CrossRef] [PubMed]
92. Wang, L.; Sun, Z.; Su, C.; Wang, Y.; Yan, Q.; Chen, J.; Ott, T.; Li, X. A GmNINa-MiR172c-NNC1 Regulatory Network Coordinates the Nodulation and Autoregulation of Nodulation Pathways in Soybean. *Mol. Plant* **2019**, *12*, 1211–1226. [CrossRef] [PubMed]
93. Holt, D.B.; Gupta, V.; Meyer, D.; Abel, N.B.; Andersen, S.U.; Stougaard, J.; Markmann, K. Micro RNA 172 (MiR172) Signals Epidermal Infection and Is Expressed in Cells Primed for Bacterial Invasion in *Lotus japonicus* Roots and Nodules. *New Phytol.* **2015**, *208*, 241–256. [CrossRef] [PubMed]
94. Yun, J.; Sun, Z.; Jiang, Q.; Wang, Y.; Wang, C.; Luo, Y.; Zhang, F.; Li, X. The MiR156b-GmSPL9d Module Modulates Nodulation by Targeting Multiple Core Nodulation Genes in Soybean. *New Phytol.* **2022**, *233*, 1881–1899. [CrossRef]
95. Wang, Y.; Wang, Z.; Amyot, L.; Tian, L.; Xu, Z.; Gruber, M.Y.; Hannoufa, A. Ectopic Expression of MiR156 Represses Nodulation and Causes Morphological and Developmental Changes in *Lotus japonicus*. *Mol. Genet. Genom.* **2015**, *290*, 471–484. [CrossRef] [PubMed]
96. Okuma, N.; Soyano, T.; Suzaki, T.; Kawaguchi, M. MIR2111-5 Locus and Shoot-Accumulated Mature MiR2111 Systemically Enhance Nodulation Depending on HAR1 in *Lotus japonicus*. *Nat. Commun.* **2020**, *11*, 5192. [CrossRef]
97. Skopelitis, D.S.; Hill, K.; Klesen, S.; Marco, C.F.; von Born, P.; Chitwood, D.H.; Timmermans, M.C.P. Gating of MiRNA Movement at Defined Cell-Cell Interfaces Governs Their Impact as Positional Signals. *Nat. Commun.* **2018**, *9*, 3107. [CrossRef]
98. Jakobsen, I. The Role of Phosphorus in Nitrogen Fixation by Young Pea Plants (*Pisum sativum*). *Physiol. Plant.* **1985**, *64*, 190–196. [CrossRef]
99. Kuang, R.-B.; Liao, H.; Yan, X.-L.; Dong, Y.-S. Phosphorus and Nitrogen Interactions in Field-Grown Soybean as Related to Genetic Attributes of Root Morphological and Nodular Traits. *J. Integr. Plant Biol.* **2005**, *47*, 549–559. [CrossRef]
100. Divito, G.A.; Sadras, V.O. How Do Phosphorus, Potassium and Sulphur Affect Plant Growth and Biological Nitrogen Fixation in Crop and Pasture Legumes? A Meta-Analysis. *Field Crops Res.* **2014**, *156*, 161–171. [CrossRef]
101. Gentili, F.; Huss-Danell, K. Local and Systemic Effects of Phosphorus and Nitrogen on Nodulation and Nodule Function in *Alnus incana*. *J. Exp. Bot.* **2003**, *54*, 2757–2767. [CrossRef] [PubMed]
102. Isidra-Arellano, M.C.; Reyero-Saavedra, M.D.R.; Sánchez-Correa, M.D.S.; Pingault, L.; Sen, S.; Joshi, T.; Girard, L.; Castro-Guerrero, N.A.; Mendoza-Cozatl, D.G.; Libault, M.; et al. Phosphate Deficiency Negatively Affects Early Steps of the Symbiosis between Common Bean and Rhizobia. *Genes* **2018**, *9*, 498. [CrossRef] [PubMed]

Appendix 3.3 A micro RNA mediates shoot control of root branching.

nature communications

Article

https://doi.org/10.1038/s41467-023-43738-6

A micro RNA mediates shoot control of root branching

Received: 22 January 2022

Accepted: 18 November 2023

Published online: 06 December 2023

Check for updates

Moritz Sexauer[1,3,5], Hemal Bhasin[1,4,5], Maria Schön[1], Elena Roitsch[1,2], Caroline Wall[1], Ulrike Herzog[1] & Katharina Markmann[1,2,3]

Plants extract mineral nutrients from the soil, or from interactions with mutualistic soil microbes via their root systems. Adapting root architecture to nutrient availability enables efficient resource utilization, particularly in patchy and dynamic environments. Root growth responses to soil nitrogen levels are shoot-mediated, but the identity of shoot-derived mobile signals regulating root growth responses has remained enigmatic. Here we show that a shoot-derived micro RNA, miR2111, systemically steers lateral root initiation and nitrogen responsiveness through its root target *TML* (*TOO MUCH LOVE*) in the legume *Lotus japonicus*, where miR2111 and *TML* were previously shown to regulate symbiotic infections with nitrogen fixing bacteria. Intriguingly, systemic control of lateral root initiation by miR2111 and *TML/HOLT* (*HOMOLOGUE OF LEGUME TML*) was conserved in the nonsymbiotic ruderal *Arabidopsis thaliana*, which follows a distinct ecological strategy. Thus, the miR2111-*TML/HOLT* regulon emerges as an essential, conserved factor in adaptive shoot control of root architecture in dicots.

Root systems are the main contact point of land plants with soluble nutrients. Adapting the root surface area to nutrient availability in the substrate is thus a key aspect of endogenous resource management in land plants.

Consistently, the perception of both restrictive and sufficient levels of nitrate, a frequently limiting macronutrient, induces root architectural adaptations. To this end, plants can enhance lateral root growth, and thus root surface area, either under deficient nitrate conditions or within local, nitrogen-rich patches. This process is termed foraging[1]. Within a given root segment, several factors have been suggested to be involved in regulating nitrate foraging locally. In *Arabidopsis thaliana* (Arabidopsis), the nitrate transceptor protein NRT1.1 controls biosynthesis and transport of auxin, thereby mediating local repression of lateral root development where perceived nitrate levels are low[2]. Downstream of *NRT1.1*, the GRAS transcription factor NIN LIKE PROTEIN 7 (NLP7) was shown to induce expression of the MADS-box gene *ANR1*, mediating further transcriptional changes that specifically promote lateral root elongation in nitrate rich soil patches[3]. Signalling via CLE (CLAVATA3/ESR) peptides and the leucine-rich repeat receptor kinase CLAVATA1 (CLV1) was further shown to be involved in nitrate-dependent local regulation of lateral root emergence in Arabidopsis[4]. A similar role has been assigned to the putative CLV1-ortholog *HYPERNODULATION ABERRANT ROOT FORMATION1* (*HAR1*) in *Lotus japonicus* (Lotus)[5]. Balancing need and availability of nutrients is a challenge concerning the plant as a whole. Adaptations to nutrient stress thus require communication not only within, but also across plant organs, suggesting that they involve systemic signalling circuits linking above- and belowground tissues. Grafting experiments demonstrated that both shoot and root expression of *HAR1* is required for nitrate-dependent adaptation of lateral root growth in Lotus[5]. This suggests a dual root-specific as well as systemic role of the CLE-HAR1 signalling node. Consistently, Lotus CLE-RS peptides were shown to be competent of xylem-based root-shoot mobility following arabinosylation, and can directly bind to HAR1[6]. In addition, both C-terminally encoded peptide

[1]Eberhard-Karls-University, Centre for Molecular Biology of Plants, Tübingen, Germany. [2]Martin-Luther-University Halle-Wittenberg, Institute for Genetics, Halle/Saale, Germany. [3]Present address: Julius-Maximilians-University, Julius-von-Sachs Institute for Biosciences, Würzburg, Germany. [4]Present address: University of Toronto – Scarborough, Department of Biological Sciences, Toronto, ON, Canada. [5]These authors contributed equally: Moritz Sexauer, Hemal Bhasin. e-mail: katharina.markmann@uni-wuerzburg.de

(CEP) hormones[1,2] as well as cytokinins[3,4] act as systemic root-shoot factors signalling low or high root nitrate content, respectively. In Arabidopsis, upon CEP perception by the CEP receptors CEPR1/2, shoot-produced CEP Downstream (CEPD) and CEPD LIKE (CEPDL) peptides translocate to roots to regulate nitrate uptake via transcriptional as well as post-translational regulation of *NRT2.1*[7,8]. In the legume *Medicago truncatula* (Medicago), the putative CEPR1 orthologue *COMPACT ROOT ARCHITECTURE 2* (*CRA2*) similarly steers *NRT2.1* dependent nitrate uptake by mediating *CEP1* dependent expression regulation[9,10].

While shoot-root mobile CEPD and CEPDL signals systemically regulate root nitrate uptake, systemic shoot factors mediating nitrate-dependent root growth adaptations are so far unknown. We previously observed that a shoot-derived, phloem-mobile micro RNA, miR2111, regulates the formation of symbiotic infections and nitrogen-fixing nodule organs in *Lotus japonicus* (Lotus) roots inoculated with rhizobial bacteria[11]. miR2111 post-transcriptionally targets the root-expressed F-Box Kelch-repeat gene *TOO MUCH LOVE* (*TML*), which represses symbiosis[11,12]. Both CLE-RS/HAR1[11] and CEP/CRA2 signalling nodes[12] regulate miR2111 abundance. Shoot miR2111 accumulation is repressed in the presence of sufficient nitrate as well as of compatible rhizobia[11], releasing *TML* mRNA from posttranscriptional regulation and restricting symbiosis progression. Interestingly, miR2111 and *TML* are not restricted to plants establishing root nodule symbiosis, but are conserved across dicot lineages. The Arabidopsis genome contains two *MIR2111* precursor gene loci[13], both encoding a single miR2111 isoform that specifically targets the F-box Kelch-repeat gene At3g27150[13], a *TML* homolog[14] of unknown function. In comparison, the Lotus genome contains seven *MIR2111* loci encoding three different isoforms[11,15]. On this basis, we hypothesized that miR2111 may have a conserved role in regulating lateral organ formation in roots also in nonsymbiotic settings, and have undergone functional diversification in nodulating lineages. Our work identifies miR2111 as a missing link signalling shoot nitrogen status to root organs and regulating adaptive root growth responses in a nitrate-dependent manner.

Results and discussion

miR2111 is a shoot factor regulating root architecture

To investigate possible conserved, symbiosis-independent functions of miR2111 in root system architecture control, we analysed root systems of plants mis-expressing the miRNA. Indeed, Lotus plants expressing a *pUBQ1::MIR2111-3* transgene resulting in overabundance of mature miR2111 (Fig. 1a) generated less lateral roots than wild type plants (Fig. 1b). miR2111 is produced primarily in shoots, and is proposed to translocate to roots via the phloem[11,15]. Phloem-mobile miRNAs were recently suggested to translocate as fully processed duplices, rather than as pri- or pre-miRNA precursors[16]. Consistently, we could trace plant specific mature miR2111 transcripts in aphids (*Planococcus citri*) feeding on Lotus, indicating its presence in the phloem sap (Supplementary Fig. 1a–c). To investigate whether shoot-derived miR2111 is indeed functional in Lotus roots and sufficient to regulate lateral root number, we grafted *pUBQ1::MIR2111-3* expressing shoots onto wild type root stocks (Fig. 1c). Roots of chimeric plants showed enhanced levels of miR2111 (Fig. 1d), and fewer emerged lateral roots compared to control grafts (Fig. 1c, e), confirming that shoot miR2111 indeed translocates to roots to steer lateral root numbers.

miR2111 regulates lateral root initiation through its target *TML*

miR2111 was proposed to directly target *TML* for posttranscriptional regulation in Lotus as well as Medicago[11,12]. Consistently, roots of *pUBQ1::MIR2111-3*/wild type (shoot/root) grafts had significantly lower *TML* levels than wild type/wild type controls (Fig. 1f). *tml* knockout mutants developed less lateral roots than wild type plants (Fig. 2a, b), and were phenotypically indistinguishable from *pUBQ1::MIR2111-3* plants (Fig. 2a, b), suggesting that *TML* is the main target of miR2111 activity in lateral root control. Interestingly, this was equally the case when all initiated lateral roots, including pre-emerged root primordia as well as emerged lateral roots, were considered (Fig. 2c, Supplementary Fig. 2). Lateral root initiations were also reduced in grafted plants expressing *pUBQ1::MIR2111-3* in their shoots compared to wild type/wild type control grafts (Fig. 2d). Using Crispr-CAS9 technology, we generated line *mir2111-3-1*, which possesses a 12 bp deletion in the stem-loop region of the *MIR2111-3* locus in immediate proximity to the mature miRNA2111a sequence (Supplementary Fig. 3a–c). *mir2111-3-1* plants showed significantly lower miR2111 abundance than wild type plants (Supplementary Fig. 4a) and, consistently, higher *TML* transcript levels (Supplementary Fig. 4b). In line with the observed reduced primordium formation in miR2111 overexpressors (Fig. 2c, d), lateral root

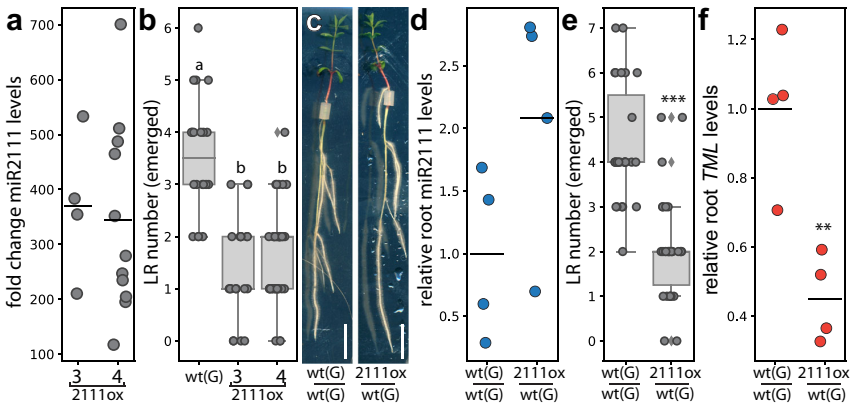

Fig. 1 | Shoot-derived miR2111 regulates lateral root (LR) numbers in *L. japonicus* (Lotus). a miR2111 abundance fold change compared to Gifu wild type (wt(G)) plants, and (**b**) LR count in transgenic *pUBQ1::MIR2111-3* (2111ox) expressing lines (#3, 4) compared to wt(G). Line #3 was used for further analysis. **c**–**f** 2111ox / wt(G) (shoot / root) grafts compared to wt(G) / wt(G) control grafts. **c** Example of grafted plants. Scale bars equal 1 cm. **d** miR2111 levels, (**e**) LR numbers and (**f**) *TML* levels in roots of respective grafts. **a**, **d**, **f** qRT-PCR analyses. RNA levels are relative to those of two reference genes. RNA was extracted from root (**d**, **f**) or shoot samples (**a**). **a** Adult plants grown in soil. **b**–**g** Plants were grown at 0 mM nitrate and evaluated or harvested after two weeks of cultivation. Student's *t*-test (**$p \le 0.01$; ***$p \le 0.001$) (**d**–**f**) or analysis of variance (ANOVA) and post-hoc Tukey testing ($p \le 0.05$) (**b**), with distinct letters indicating significant differences. All experiments were in ecotype Gifu B-129 (wt(G)). Sample size, replicates and exact *p*-values are listed in the Source Data file. Dotplots show individual data points and a line indicating their average value. Boxplot central line shows median value, box limits indicate the 25th and 75th percentile. Whiskers extend 1.5 times the interquartile range, or to the last datapoint. Individual datapoints are represented by dots.

https://doi.org/10.1038/s41467-023-43738-6

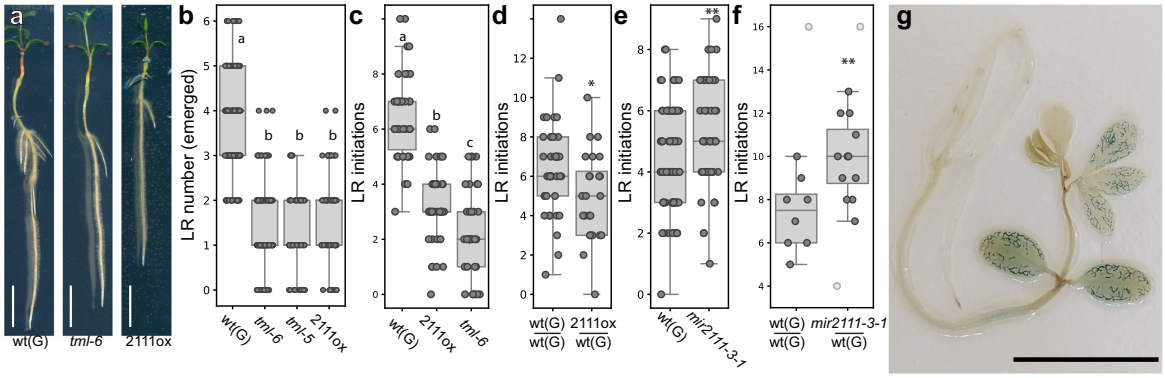

Fig. 2 | *TML* mediates miR2111 control of *L. japonicus* (Lotus) lateral root (LR) initiation. a Root phenotype of Gifu wild type (wt(G)), *tml-6* and *pUBQ1::MIR2111-3* plants (2111ox). Scale bars equal 1 cm. **b** Emerged LR numbers in wt, *tml-6*, *tml-5* and 2111ox plants. **c**–**e** Number of LR initiations (emerged and primordial stages combined) in wt(G), 2111ox and *tml-6* plants (**c**), on 2111ox / wt(G) (shoot / root) grafts compared to wt(G) / wt(G) control grafts (**d**), in *mir2111-3-1* compared to wt(G) plants (**e**) and on *mir2111-3-1* / wt(G) (shoot / root) grafts compared to wt(G) / wt(G) control grafts (**f**). **f** light grey dots represent data points not considered in the statistical analysis due to strong divergence of primary root length in the respective plants from the mean. **g** Plants expressing *pMIR2111-3:GUS* show pronounced GUS activity in leaf veins, while roots are free of visually traceable activity. Scale bar equals 1 cm. A total of 30 tested plants showed a similar expression pattern. **b** Datapoints are identical to datapoints at 0 mM nitrate in Fig. 3a. **a**–**e** Plants grown at 0 mM nitrate. Comparisons used Student's *t*-test (*$p \leq 0.05$; **$p \leq 0.01$) (**d**, **e**) or analysis of variance (ANOVA) and post-hoc Tukey testing ($p \leq 0.05$) (**b**, **c**), with distinct letters indicating significant differences. All experiments were in ecotype Gifu B-129 (wt(G)). **a**–**g** Plants were evaluated or harvested after two weeks of cultivation (**a**–**c**, **e** & **g**) or grafting (**d**, **f**). Sample size, replicates and exact *p*-values are listed in the Source Data file. Boxplot central line shows median value, box limits indicate the 25th and 75th percentile. Whiskers extend 1.5 times the interquartile range, or to the last datapoint. Individual datapoints are represented by dots.

initiation numbers were higher in *mir2111-3-1* plants compared to wild type plants (Fig. 2e), and grafts of *mir2111-3-1* shoots on wild type root stocks equally showed an enhanced lateral root initiation compared to control grafts. This is consistent with a shoot specific expression pattern of the *MIR2111-3* locus (Fig. 2f, g), and confirms that shoot miR2111 is required for lateral root initiation control. Taken together, these data suggest that shoot-derived miR2111 is both sufficient and necessary for modulating lateral root initiations via *TML* (Fig. 2c–e, Supplementary Fig. 3a–c). Interestingly, this is in addition to the described function of shoot-derived miR2111 in systemic nodule number control in the context of symbiosis autoregulation (Supplementary Fig. 4c)[11,15].

The miR2111/*TML* regulon controls root branching in response to nitrate levels

Since root nodulation symbiosis, a known activity context of miR2111-*TML*, is an adaptation to nitrogen limitation, we hypothesized that this regulon may also help adapting root architecture to nitrogen availability.

Lotus showed enhanced lateral root numbers under nitrogen starvation (Fig. 3a). This was ecotype-independent (Fig. 3a, b) and is consistent with the nitrate foraging responses reported in other plants[17]. Notably, this trend was only apparent for emerged lateral roots. Lateral root primordia, on the contrary, were more abundant under nitrate sufficient conditions compared to deficiency. This results in a positively nitrate-correlated (Fig. 3c, d) or nitrate-independent (Supplementary Fig. 5a) sum of initiated roots.

Following a likewise trend, mature miR2111 levels were negatively correlated with nitrate availability in a dosage-dependent manner in both shoots and roots (Fig. 3e, f), indicating an involvement in systemic nitrogen response signalling. The levels of *TML* transcripts, which were only detected in roots, showed a complementary, inverse pattern (Fig. 3g), suggesting *TML* suppression by systemic miR2111 under nitrogen starvation conditions. Indicating ecotype specific differences, this pattern was particularly apparent in the Lotus ecotype MG-20, consistent with a more pronounced responsiveness of lateral root initiations to nitrate availability compared to Gifu B-129 (Supplementary Fig. 5a–d).

Compared to wild type plants, both miR2111 overexpressors and *tml* mutants had a consistently lower number of lateral roots, and emerged lateral root number was independent of nitrate availability (Fig. 3a, b). The same was true for lateral root initiation, not only in the ecotype Gifu B-129, but also in MG-20, where a nitrate-dependent increase in lateral root primordia is more strongly pronounced than in Gifu B-129 (Fig. 3c, d and Supplementary Fig. 5a). Shoot specific overexpression of *MIR2111-3* using heterografting experiments induced a loss of nitrate responsive lateral root initiation in chimeric plants with MG-20 root stocks (Supplementary Fig. 6a, b), suggesting that shoot-derived miR2111 efficiently represses this response. On this basis, we predicted that nitrate-independent *TML* transcript levels in Gifu B-129 (Supplementary Fig. 5d) may prevent adaptive primordia formation in this ecotype. Indeed, increased *TML* transcript levels in *mir2111-3-1* compared to wild type plants (Supplementary Fig. 4b) resulted in a positive nitrate response of lateral root initiation numbers in the ecotype Gifu B-129 as well (Supplementary Fig. 6c), indicating that miR2111 mediated *TML* control is necessary for the ecotype-specific attenuation of root system response to nitrate observed in Gifu B-129. The combined phenotypic and molecular data suggests a role of the miR2111-*TML* regulon in lateral root initiation and adaptive emergence in response to nitrate, with miR2111 systemically repressing *TML*. Contrasting with their respective roles in symbiosis, our data identify miR2111, a positive regulator of nodule numbers, as a repressor of root primordia, and *TML* as a root primordial activator (Fig. 3h). The data further reveal that nitrate dependent regulation of primordia emergence into full lateral roots strictly requires the presence of functional *TML* (Fig. 3a–c), but does not correlate with *TML* transcript abundance (Fig. 3g, h, Supplementary Fig. 5d). This suggests involvement of additional factors in regulating nitrate responsive emergence of *TML*-dependent lateral root primordia.

Nitrate perception and nitrogen starvation have been found to trigger local and systemic responses involving physiological and morphological adaptations[17]. We thus performed split root assays to identify the trigger underlying miR2111 regulation under asymbiotic conditions. Roots growing on nitrogen starvation medium contained low miR2111 levels if other roots of the same plant experienced nitrate sufficiency (Fig. 3i). This suggests that miR2111 accumulation is not

https://doi.org/10.1038/s41467-023-43738-6

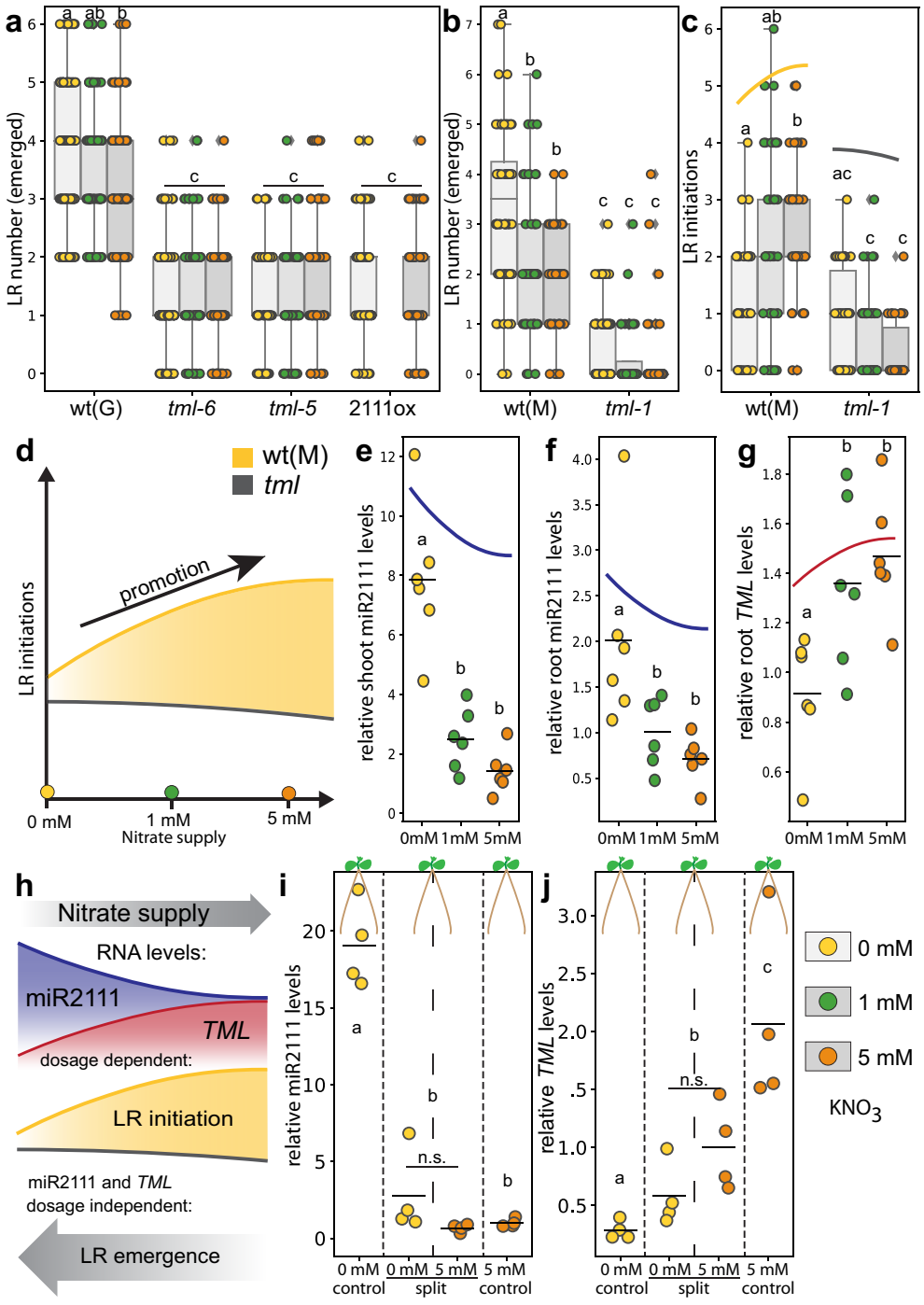

triggered by roots experiencing nitrate starvation, but rather is systemically repressed by roots exposed to nitrate sufficiency (Fig. 3i), implying that miR2111 levels are regulated through nitrate supply rather than deficiency. *TML* levels in these roots were complementary yet intermediate (Fig. 3j). Consistent with previous observations, *TML* abundance is thus likely subject to additional regulatory factors[11].

Apart from nitrate, rhizobial infection triggers changes in miR2111 and *TML* transcript abundance (ref. 11; Supplementary Fig. 7 a–c), and miR2111 acts as a positive regulator of nodule organogenesis by repressing the nodulation inhibitor *TML*[11]. We thus wondered how miR2111-*TML* dynamics affect lateral root formation under symbiotic conditions. Interestingly, in both wild type and *tml-6* mutant plants, symbiotic infection led to a decrease of lateral root initiations (Supplementary Fig. 7d), implying that an additional *TML*-independent regulation of lateral root initiation overlays miR2111-*TML* dependent primordium control under symbiotic conditions.

https://doi.org/10.1038/s41467-023-43738-6

Fig. 3 | Systemic N status controls lateral root (LR) initiations via the miR2111-*TML* regulon in *L. japonicus* (Lotus). **a**, **b** Emerged LRs in (**a**) Gifu B-129 wild type (wt(G)), *tml-6*, *tml-5* and *pUBQ1::MIR2111-3* (2111ox), and in (**b**) MG20 wildtype (wt(M)) and *tml-1* plants. **c** Number of LR initiations (emerged plus primordial stages) in wt(M) and *tml-1* plants. **d** Simplified model of nitrate dependency of LR initiations in wt and *tml* mutant plants. **e**, **f** Relative mature miR2111 levels in shoots (**e**) and roots (**f**). **g** Relative *TML* levels in same wild type root systems as in (**f**). **h** Simplified model outlining nitrate dependency of miR2111 and *TML* levels, and root architectural responses. **I**, **j** Split root experiments. Relative miR2111 (**i**) and *TML* (**j**) levels in secondary roots of wt(M) plants. **e**–**g**, **i**, **j** qRT-PCR analyses. RNA levels are relative to those of two reference genes. **a**, **b**, **e**–**g**, **i**, **j** Tissue harvest / analysis after two weeks and (**c**) 10 days of cultivation. Comparisons used analysis of variance (ANOVA) and post-hoc Tukey. testing ($p \leq 0.05$), with distinct letters indicating significant differences and additional Student's *t*-test (**i**, **j**) comparing only the split roots (n.s. $p > 0.05$). **c**–**h** Trendlines are simplified and not to scale. Plants grown at indicated nitrate concentrations. Sample size, replicates and exact p-values are listed in the Source Data file. Dotplots show individual data points and a line indicating their average value. Boxplot central line shows median value, box limits indicate the 25th and 75th percentile. Whiskers extend 1.5 times the interquartile range, or to the last datapoint. Individual datapoints are represented by dots.

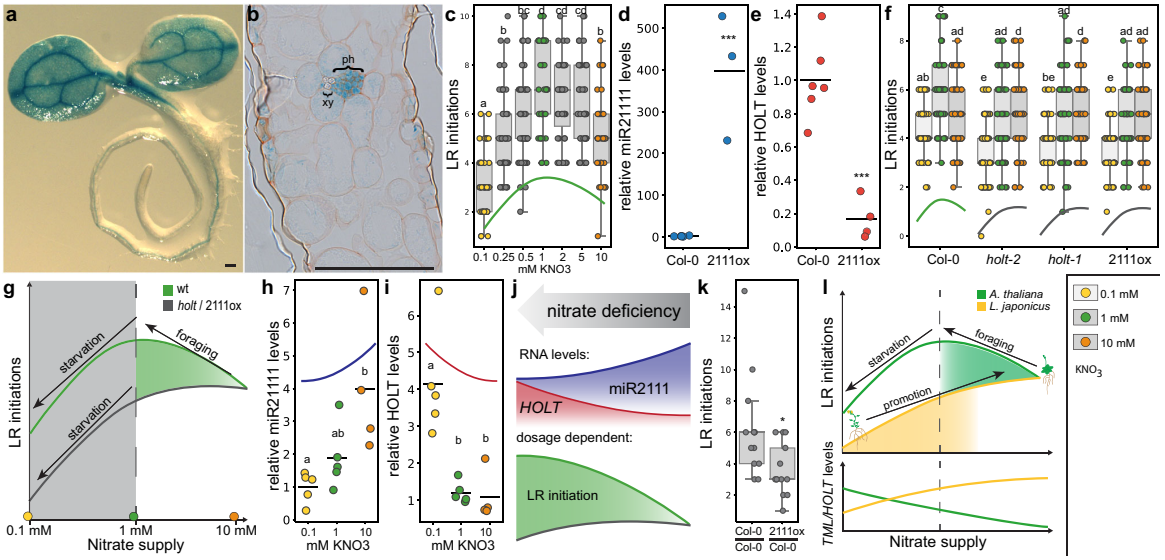

Fig. 4 | The *A. thaliana* (Arabidopsis) miR2111-*HOLT* regulon controls lateral root (LR) initiation at moderate nitrate starvation. **a**, **b** Stably transformed *A. thaliana* (Arabidopsis) plants expressing *pMIR2111b:GUS* show predominant GUS activity in the phloem of leaf veins. **b** Leaf cross section of *pMIR2111b:GUS* plants. ph, phloem and xy, xylem. **c** Numbers of LR initiations at different nitrate concentration in Arabidopsis wild type (Col-0) plants. **d**, **e** miR2111 (**d**) and *HOLT* (**e**) levels in Col-0 and *p35s::MIR2111b* expressing plants (2111ox) at 1 mM nitrate. **f** LR initiations in *holt-1*, *holt-2* and 2111ox plants compared to Col-0. **g** Schematic model of nitrate responsiveness of Arabidopsis lateral root initiations. *holt-1* and 2111ox plants lack a foraging response at moderate nitrate starvation. **h**, **i** miR2111 (**h**) and *HOLT* (**i**) levels of Col-0 at varying nitrate concentrations. **j** Simplified model outlining nitrate dependency of miR2111 and *HOLT* levels, and of root architectural responses in Arabidopsis between 1 and 10 mM nitrate. **k** Number of LR initiations on 2111ox / Col-0 (shoot / root) grafts compared to Col-0 / Col-0 control grafts at 1 mM KNO_3. **l** Combined simplified model of Arabidopsis and *L. japonicus* (Lotus) root responses to varying nitrate supply. *HOLT* positively correlates with LR initiations in both species, but nitrate dependent abundance patterns of both LR initiations and *TML*/*HOLT* levels are opposite. **d**, **e**, **h**, **i** qRT-PCR analyses. RNA levels are relative to those of two reference genes, whole plant tissue harvested 10 days after germination. **c**, **f**, **k** Analysis seven days after germination (**c**, **f**) or after graft regeneration (**k**). Comparisons used analysis of variance (ANOVA) and post-hoc Tukey testing ($p \leq 0.05$), with distinct letters indicating significant differences (**c**, **f**, **h**, **i**) or Student's *t*-test (*$p \leq 0.05$) (**d**, **e**, **k**). **a**, **b** Scale bars equal 200 μm (**a**) or 100 μm (**b**). **a**, **b** all 21 tested plants of 3 independent lines showed a similar expression pattern. Analysis of three independent lines showed similar results. **c**, **f**, **h**, **i** Plants were grown at indicated nitrate concentrations using ½ strength MS media free of other nitrogen sources. **c**, **f**–**j**, **l** Trendlines are simplified and not to scale. Sample size, replicates and exact *p*-values are listed in the Source Data file. Dotplots show individual data points and a line indicating their average value. Boxplot central line shows median value, box limits indicate the 25th and 75th percentile. Whiskers extend 1.5 times the interquartile range, or to the last datapoint. Individual datapoints are represented by dots.

Systemic root control by miR2111/*TML* is phylogenetically conserved

Root architecture adaptation to abiotic stimuli is an ancient necessity and a core developmental feature of land plants that is phylogenetically widespread[17] and thus precedes the evolution of nitrogen-fixing nodulation symbiosis. Consistently, the miR2111-*TML* regulon is conserved in non-nodulating plants, including the nonsymbiotic plant *Arabidopsis thaliana* (Arabidopsis)[11,14]. Arabidopsis possesses two *MIR2111* precursor loci generating a single isoform identical to *Lj*miR2111a (Supplementary Fig. 8a, b)[11]. Phylogenetic analysis revealed one putative *TML* orthologue, which we named *HOMOLOGUE OF LEGUME TML (HOLT)*, featuring a miR2111 complementary site in the coding sequence[11,14] (Supplementary Fig. 9a, b). Consistent with the expression pattern of *MIR2111* loci in Lotus, Arabidopsis *pMIR2111a/b:GUS* expressing lines showed predominant GUS activity in leaf vein phloem cells (Fig. 4a, b and Supplementary Fig. 10a, b), suggesting systemic mobility[18]. These observations are in line with organ specific expression data[19] (Supplementary Table 1). Similar to what has been previously observed for selected Lotus *MIR2111* precursor genes[15], moderate *pMIR2111a/b:GUS* activity was evident in mature root parts of Arabidopsis as well (Fig. 4a and Supplementary Fig. 10a), although *MIR2111a/b* precursor transcripts were not traceable in publicly available RNAseq datasets[19] (Supplementary Table 1). Like in Lotus, Arabidopsis lateral root initiation numbers depend on nitrogen supply, peaking around 1 mM nitrate under long day conditions in plate-grown wild type plants (Fig. 4c). In comparison, plants grown

under starvation or saturating conditions show reduced numbers of lateral root initiations (Fig. 4c). The observed increase of lateral root numbers under moderately deficient (1 mM nitrate) as compared to sufficient (10 mM nitrate) nitrogen supply has previously been associated with nitrogen dependent root architectural adaptations commonly referred to as foraging response[1]. To evaluate a possible role of the miR2111/*HOLT* regulon in nitrogen foraging related lateral root initiation in Arabidopsis, we generated transgenic lines overexpressing miR2111 under the control of a Cauliflower Mosaic Virus 35 s promoter fragment, showing a concomitant reduction in *HOLT* levels (Supplementary Fig. 11a, b). All tested lines showed reduced lateral root initiation compared to wild type plants in the T2 generation (Supplementary Fig. 11c). We chose a representative line, #3, for further propagation, as it showed stable overabundance of miR2111 and a corresponding reduction of *TML* transcript abundance in the T3 generation (Fig. 4d, e). We further isolated Arabidopsis *holt-1* and *holt-2* mutants lacking a traceable full-length *HOLT* transcript (Supplementary Fig. 12a, b). *holt-1*, *holt-2* and *p35s::MIR2111b* plants showed significantly reduced lateral root initiations at low and moderate nitrate concentrations compared to wild type plants (Fig. 4f). Notably, they failed to show a traceable foraging response (Fig. 4f,g). Wild type plants exposed to severe nitrogen limitation repress lateral root development, a response known as a survival strategy[1], which is thought to involve the nitrate transporter NRT1.1[20] as well as locally induced lateral root inhibition through the CLAVATA3/CLAVATA1 signalling module[4]. Transcript abundance of *NRT1.1* and other *NRTs* was not significantly altered in *holt-1* or *p35s::MIR2111b* as compared to wild type plants (Supplementary Fig. 13a–d). Consistent with a *HOLT* independent mechanism, a successive reduction in lateral root initiation numbers at nitrate levels <1 mM was retained in *holt-1*, *holt-2* and *p35s::MIR2111b* in a similar way as in wild type plants (Fig. 4f, g). In wild type plants, miR2111 levels correlate positively with nitrate concentration (Fig. 4h), consistent with low *HOLT* levels at high nitrate supply (Fig. 4i). The integration of phenotypic and molecular data reveals that, in line with observations in Lotus, *HOLT* levels positively correlate with lateral root initiations (Fig. 4j). To investigate whether shoot-derived miR2111 is sufficient to regulate root architecture in Arabidopsis as observed in Lotus, we analysed *p35s::MIR2111b*/Col-0 (shoot/root) grafts. These had significantly less lateral root initiations than Col-0/Col-0 control grafts (Fig. 4k), confirming miR2111 as a systemically acting, mobile regulator of lateral root initiation across dicot plant lineages.

In line with divergent habitat requirements and ecological strategies of the symbiotic Lotus[21,22] and the asymbiotic ruderal Arabidopsis[23], abundance patterns of lateral root primordia with respect to external nitrogen supply were distinct in these two species (Fig. 4l). Yet, consistent with a conserved positive role of *TML*/*HOLT* in nitrate-dependent lateral root initiation, *TML*/*HOLT* RNA levels were upregulated in both species under nitrate conditions triggering abundant lateral root primordia. Accordingly, in either species, miR2111 levels were low under such conditions, in line with a negative effect on *TML*/*HOLT* levels and lateral root initiation. The dynamic response pattern of the Arabidopsis root system reflected in integrating distinct and functionally overlapping regulatory nodes (refs. 4,20, this study) indicates its capacity to populate a wide variety of soils[23]. Our data suggests that Lotus, as a pioneer lineage that is primarily competitive on nitrogen poor soils[24], initiates additional root primordia under starvation conditions that have a limiting effect on Arabidopsis root architecture (Fig. 4l). The lack of a strong nitrogen starvation response in Lotus could be explained by the formation of nitrogen fixing symbiosis, which prevents nitrogen starvation even on nitrogen poor soils.

An important role of the miR2111-*TML*/*HOLT* regulon in adapting plant root systems to their natural habitat is in line with the observed differences in lateral root abundance patterns between Lotus MG-20 and Gifu ecotypes (Fig. 3a–c, Supplementary Fig. 5a, Supplementary Fig. 6a–c). *Lotus japonicus* underwent intense diversification during evolution and encompasses more than 130 ecotypes that have adapted to a wide range of environmental conditions on the Japanese Islands[21]. A time course experiment revealed an increasing difference between wild type and *tml-1* in lateral root numbers over time. Here, *tml-1* plants showed significantly less biomass production in both below- and aboveground tissues compared to wild type (Supplementary Fig. 14a, b), suggesting that root architecture adaption plays an important role in plant productivity and fitness. We have no evidence for a direct involvement of the miR2111-*TML*/*HOLT* regulon in nitrate uptake, and mRNA levels of nitrate transporter genes *NRT1.1*, *NRT1.5*, *NRT2.1* and *NRT3.1* are unaltered in *holt-1* and *p35s::MIR2111b* lines compared to wild type controls (Supplementary Fig. 13). This is in contrast to *CEP*/*CEPD*/*CEPDL2* mediated regulation of nitrate uptake via *NRT2.1*regulation[7,8], and suggests an indirect role of the miR2111-*TML*/*HOLT* regulon in nutrient uptake regulation by altering the extent of the root surface area (Supplementary Fig. 13).

Alteration of the root depletion zone also affects the uptake of other nutrients. Interestingly, in Arabidopsis, miR2111 was shown to be induced by phosphate starvation[25], and Arabidopsis is known to adapt its root architecture to phosphate availability[26]. This could hint to a more general role of miR2111 in adapting root architecture to nutrient availability.

The presented data identify miR2111 and *TML*/*HOLT* as conserved factors in root architectural control, suggesting that they were evolutionarily co-opted by rhizobial nodulation symbiosis to regulate root responses to symbiotic bacteria, and organogenesis of nodule organs[11]. Consistent with this hypothesis, the transcription factors *SCARECROW* and *SHORTROOT*[27], as well as *ASYMMETRIC LEAVES2-LIKE18*[28,29] and *STYLISH*[30] mediating auxin signalling hold dual roles in nodule organogenesis and root development, and comparative transcriptome analysis of lateral root and nodule primordia further supports generic ties between these organs[28].

Our data reveal the miR2111-*TML*/*HOLT* regulon as a key factor in systemic control of root system architecture and lateral root organ number. An exciting future challenge will be determining the molecular activity of the TML/HOLT protein, a proposed component of the E3 Ubiquitin ligase complex in Arabidopsis[31] with a possible role in mediating degradation of target transcription factors[31]. Determining downstream effectors will help us better understand how the miR2111-*TML*/*HOLT* regulon functionally integrates with hormonal networks and other regulators of root growth.

Methods

Plant and bacterial resources

Plants for root architecture analyses, qPCR assays and GUS stainings were *Lotus japonicus* L. ecotype Gifu B-129 (wild type, *tml-5* (line ID 30013998), *tml-6* (line ID 30086992) and *pMIR2111-3:GUS*[11,32]) and ecotype MG-20 (wild type and *tml-1*[33]). Generation of stable transgenic plants expressing *pUBQ1:MIR2111-3*[34] and *MIR2111-3* knockout lines followed a published procedure based on callus regeneration[11,35] and made use of *Agrobacterium tumefaciens* AGL1 and *L. japonicus* ecotype Gifu B-129.

Further, *A. thaliana* Col-0 wild type, *holt-1* (line ID SALK_044075.49.80.x) and *holt-2* (line ID SALK_140092.27.55.x) were used. Generation of *p35::MiR2111b* expressing plants as well as *pMIR2111a/b:GUS lines* was done via floral dipping using *A. tumefaciens* GV3101. Cloning approaches made use of *E. coli* strains TOP10 or DB3.1. Plants were infected with *M. loti* MAFF303099[36] expressing *DsRED* bacteria.

Construct generation

For *p35s* driven miRNA overexpression, the transcription start site upstream of the *MIR2111b* stemloop was predicted using the publicly

available Softberry toolset with standard settings (http://www.softberry.com/berry.phtml?topic=tssplant&group=programs&subgroup=promoter). The entire precursor gene, including 80–100 bp downstream of the miRNA stem loop, was amplified from *A. thaliana* Col-0 genomic DNA using primers carrying overhangs for subsequent cloning into the gateway vector PGWB602. For the *pMIR2111a/b:GUS* lines, a three kb region upstream of the precited stem loop was cloned into the vector PMDC163 using gateway cloning. For Golden Gate technology-based generation of CRISPR/Cas9 constructs targeting the *MIR2111-3* locus a codon optimized Cas9 endonuclease from the *Streptococcus pyogenes* containing the potato IV2 intron driven by a minimal 35 s promotor was used. Two gRNAs GGTAATCTGCATCCTG and GAGTCGGTATATATTGGGTC were predicted using CLC Main Workbench 8 (Qiagen). Primers can be found in Supplementary Table 2.

Lotus plant growth

For plant growth and phenotyping, *L. japonicus* seeds were surface scarified, sterilized using sodium hypochloride solution containing 1 g/l NaClO, imbibed in ddH_2O and transferred to sterile ¼-strength B&D medium[37] with 1% (w/v) phyto agar (Duchefa Biochemie). Following stratification for three days at 4 °C, seeds were germinated at 21 °C in constant darkness for two (MG-20) or three (Gifu B-129) days. For growth on plates, seedlings were transferred to 12 × 12 cm square plastic dishes containing 50 ml ¼-strength B&D / 1% (w/v) phyto agar medium supplemented with KNO_3 at indicated concentrations. Plants were grown at long day conditions (16 h light, 21 °C / 8 h dark, 17 °C). Roots were shaded from direct light. For root architecture evaluation and quantification of molecular miR2111 and *TML* levels, plants were grown for twoweeks. For quantification of lateral root initiations plants were grown for ten days.

Arabidopsis plant growth

For plant growth and phenotyping, *A. thaliana* seeds were sterilized by 30 minutes incubation in a solution of 70% (v/v) ethanol and 0.05% (v/v) Triton X-100. Sterile seeds were transferred to 12×12 cm square plastic dishes containing 50 ml ½-strength MS medium[38] without nitrogen / 1% (w/v) phyto agar medium supplemented with KNO_3 at indicated concentrations and stratified for three days at 4 °C. Plants were grown at long day conditions (16 h light, 21 °C / 8 h dark, 17 °C). Roots were shaded from direct light. For quantification of molecular *miR2111* and *HOLT* levels, plants were grown for ten days. For quantification of lateral root initiations plants were grown for seven days.

Lotus grafting

Plants were treated and germinated as described above. After germination plants were transferred to ¼-strength B&D / 1 mM KNO_3 / 1% (w/v) phyto agar medium. Plates were kept in darkness for two days, then eight days in long day conditions. For graftings, seedlings were cut near the lower end of the hypocotyl, and immediately submerged in water. New shoots were transplanted onto root stocks and arrested using silicone tubing (Ø 0.64 mm). Grafted plants were transferred to fresh medium and covered with filter paper soaked in ddH_2O, then grown at long day conditions for two to three weeks. Prior to phenotyping or tissue harvest, tubing was removed from chimeric plants to determine grafting success. Lotus hetero-grafting involving two distinct ecotypes followed a different procedure.

Lotus hetero grafting

Plants were treated and germinated as described above. After germination plants were transferred to ¼-strength B&D / 1 mM KNO_3 / 1% (w/v) phyto agar medium. Plates were kept three days in long day conditions. For graftings, seedlings were cut near the middle of the hypocotyl, and immediately submerged in water. New shoots were transplanted onto root stocks and arrested using silicone tubing (Ø 0.5 mm, ~3 mm long). Grafted plants were transferred to fresh medium, then kept at 26 °C 22 h light for five days to enable graft site regeneration. Afterwards grafted plants were incubated for two more weeks at long day conditions (16 h light, 21 °C / 8 h dark, 17 °C). Prior to phenotyping or tissue harvest, tubing was removed from chimeric plants to determine grafting success.

Arabidopsis grafting

Plants were treated and germinated as described above (section 'Arabidopsis plant growth'), and grown for five days on ½-strength MS / 1% (w/v) phyto agar medium medium with full nitrogen content[38]. Grafting followed a published protocol, utilizing sterile precision forceps and a sapphire blade[39]. For grafting one cotyledon of Arabidopsis plants was removed and cut at the hypocotyl. Cut Arabidopsis plants were reassembled on a sterile nitrocellulose membrane on sterile water soaked Whatman paper. After grafting, plants left to recover at 26 °C for four days, then grown for seven more days on ½-strength MS medium containing 100 μM KNO_3 at long day conditions before evaluation.

Split root assay

Plants were treated and germinated as described above (section 'Lotus plant growth'). After germination, root tips were cut off and plants transferred to ¼-strength B&D/0.5 mM KNO_3/1% (w/v) phyto agar medium. After 10 days at long day conditions, plants which had generated two secondary roots were selected for onward processing and transferred to plates containing slices of ¼-strength B&D/1.5% (w/v) phyto agar medium. Plants were positioned in a way that secondary roots were placed on separate agar patches not in physical contact with each other and containing KNO_3 concentrations as indicated. Plants were grown for 13 more days under long day conditions until phenotypic evaluation or tissue collection.

Root phenotypic analysis

Plate grown plants were scanned using a conventional scanning system (CanoScan 8800 F, Canon). Image processing made use of OpenCV (https://opencv.org/) functions. Root architectural traits were measured using an in-house Python script. The script was optimized to recognize Lotus roots by color contrast and relied on manual confirmation.

RNA extraction and quantitative PCR (qRT-PCR) assays

For total RNA extractions, plant or aphid tissue was shock frozen in liquid N. Total RNA was extracted by a modified Lithium Chloride-TRIzol LS (ThermoFisher) protocol[40]. Plant RNA was extracted from tissue of at least ten independent plants per biological replicate. RNA was eluted in DEPC-treated water, RNA concentration was determined using a Nanodrop device (ThermoFisher). RNA was DNAse treated using DNAseI (ThermoFisher) according to manufacturer guidelines. cDNA was prepared using SuperScriptIV (ThermoFisher) or RevertAid (ThermoFisher) reverse transcriptase following a previously optimized pulsed protocol[11,41]. Briefly, RNA and primers (2 μM odT, 0,5 μM specific primers) were mixed and incubated for 5 min at 65 °C. The remaining reaction mix was assembled and incubated at 16 °C for 30 mins followed by 60 cycles (30 °C for 30 s, 42 °C for 30 s and 50 °C for 1 s) and 5 min at 85 °C for enzyme inactivation. Stemloop primers for reverse transcription of small RNAs were designed such that the six basepairs at the 5′ end of the stemloop primer were complementary to six nucleotides at the 3′ end of the small RNA, for reverse transcription of Lotus mRNAs oligo dT primer was used, for *A. thaliana* RNA only locus specific primers were used for reverse transcription (Supplementary Table 3). The RT-reaction was assembled according to manufacturer's guidelines using 500 ng of total RNA. qRT-PCRs were assembled using SensiFAST™ SYBR® No-ROX mastermix (Bioline) at 10 μl reaction size and 500 nM primer concentration. Levels of target genes were

normalized to levels of two independent reference genes, Lotus *ATP SYNTHASE2* and Lotus *PROTEIN PHOSPHATASE2a* or Arabidopsis *PROTEIN PHOSPHATASE2a* and Arabidopsis *UBIQUITIN EXTENSION PROTEIN 2* or U6 (Supplementary Fig. 11a). qRT-PCR reactions were executed in a BioRad CFX384 lightcycler (BioRad). Primers are listed in Supplementary Table 4. Data analysis made use of LinRegPCR[42].

Aphids

For aphid experiments, we used *Planococcus citri*[43], which could be propagated on *L. japonicus* as sole host plant. Lotus plants were infected with aphids by placing an infested host stem with a small aphid population onto young, four week-old plants growing in a 3:1 clay granule (2–5 mm, Lamstedt): vermiculite (3–6 mm, Isola Vermiculite GmbH) mixture saturated with ¼-strength B&D medium. After two weeks, aphids were collected and snap frozen in liquid nitrogen. RNA extraction, as well as DNAse treatment, cDNA synthesis and qRT-PCRs, were performed as described. For qRT-PCR experiments on aphid RNA extracts we used aphid α-Tubulin as normalization reference[44].

Staining and microscopic analysis

GUS staining and fixation was performed as described[11]. Plants were fixed by incubation in 1x phosphate buffer (50 mM NaH_2PO_4, 50 mM Na_2HPO_4, pH 7.0) supplemented with 4% Paraformaldehyde, followed by 3 washing steps using 1x phosphate buffer. For GUS staining, samples were incubated overnight at 37 °C in X-Gluc buffer (0.5 mg/ml X-Gluc, 1 mM $K_4(Fe(CN)_6)$, 1 mM $K_3(Fe(CN)_6)$, 0,05% Triton X-100 in 1x phosphate buffer). After 3 more washing steps in 1x phosphate buffer, plants were incubated in a buffer containing acetic acid, glycerol and ethanol (ratio 1:1:3) at 60 °C until tissue was cleared from chlorophyll.

Whole plant phenotypes were monitored, and photographs taken using a Leica MZ FLIII stereomicroscope. For analysis of semithin sections, fixed, GUS-stained roots or leaves were further dehydrated and embedded in resin (Kulzer Technovit 7100). Sections were prepared using a Leica RM2065 microtome, then analyzed and documented using a Zeiss Imager M2 microscope. For quantification of lateral root initiations, roots were separated from shoots and fixed using 4% Paraformaldehyde in 1x PBS buffer, cleared using ClearSee (10% Xylitol, 15% sodium deoxycholate and 25% Urea in ddH_2O) and stained with Fluorol Yellow (0.01% in 96% Ethanol) as described[45]. Stained roots were scanned using a Leica SP8 confocal microscope, and images were used for phenotypic analysis. Fluorol yellow was imaged at $\lambda = 488$ nm excitation and $\lambda = 520–588$ nm emission, and additionally, transmission white light was observed. The resulting integrated images of whole roots allowed quantification of lateral root primordia at early, pre-emergence stages. Lateral root initiations include pre-emergence primordia as well as emerged lateral roots irrespective of the developmental stage (Supplementary Fig. 2).

Data analysis and graphical representation

Data analysis made use of Python 3.7.x using the libraries Statsmodels and Pandas. Plots were generated with the python libraries Matplotlib and Seaborn. Boxplot center lines show the medians, outer box limits indicate the 25th and 75th percentiles. Whiskers extend 1.5 times the interquartile range from the 25th and 75th percentiles, or the last data point. Data points are represented as dot. Dotplots center lines indicate the average value of all data points. All statistical tests used were two-sided. For pairwise comparison we used *t*-tests for multicomparison we used ANOVA and post hoc Tukey-HSD testing. Results of ANOVA or t-test analyses, biological replicate numbers and individual datapoints are listed in the Source Data file.

Reporting summary

Further information on research design is available in the Nature Portfolio Reporting Summary linked to this article.

Data availability

All primary data and images analysed in the context of this study are available from the corresponding author upon request. Source data are provided with this paper.

References

1. Giehl, R. F. & von Wiren, N. Root nutrient foraging. *Plant Physiol.* **166**, 509–517 (2014).
2. Maghiaoui, A. et al. The Arabidopsis NRT1.1 transceptor coordinately controls auxin biosynthesis and transport to regulate root branching in response to nitrate. *J. Exp. Bot.* **71**, 4480–4494 (2020).
3. Marchive, C. et al. Nuclear retention of the transcription factor NLP7 orchestrates the early response to nitrate in plants. *Nat. Commun.* **4**, 1713 (2013).
4. Araya, T. et al. CLE-CLAVATA1 peptide-receptor signaling module regulates the expansion of plant root systems in a nitrogen-dependent manner. *Proc. Natl Acad. Sci. USA* **111**, 2029–2034 (2014).
5. Hayashi-Tsugane, M. & Kawaguchi, M. Lotus japonicus HAR1 regulates root morphology locally and systemically under a moderate nitrate condition in the absence of rhizobia. *Planta* **255**, 95 (2022).
6. Okamoto, S., Shinohara, H., Mori, T., Matsubayashi, Y. & Kawaguchi, M. Root-derived CLE glycopeptides control nodulation by direct binding to HAR1 receptor kinase. *Nat. Commun.* **4**, 2191 (2013).
7. Ohkubo, Y., Kuwata, K. & Matsubayashi, Y. A type 2C protein phosphatase activates high-affinity nitrate uptake by dephosphorylating NRT2.1. *Nat. Plants* **7**, 310–316 (2021).
8. Ota, R., Ohkubo, Y., Yamashita, Y., Ogawa-Ohnishi, M. & Matsubayashi, Y. Shoot-to-root mobile CEPD-like 2 integrates shoot nitrogen status to systemically regulate nitrate uptake in Arabidopsis. *Nat. Commun.* **11**, 641 (2020).
9. Luo, Z. et al. *NLP1* reciprocally regulates nitrate inhibition of nodulation through *SUNN-CRA2* signaling in *Medicago truncatula*. *Plant Commun.* **2**, 100183 (2021).
10. Luo, Z. et al. The small peptide CEP1 and the NIN-like protein NLP1 regulate NRT2.1 to mediate root nodule formation across nitrate concentrations. *Plant Cell* **35**, 776–794 (2023).
11. Tsikou, D. et al. Systemic control of legume susceptibility to rhizobial infection by a mobile microRNA. *Science* **362**, 233–236 (2018).
12. Gautrat, P., Laffont, C. & Frugier, F. *Compact Root Architecture 2* promotes root competence for nodulation through the miR2111 systemic effector. *Curr. Biol.* **30**, 1339–1345.e1333 (2020).
13. Pant, B. D. et al. Identification of nutrient-responsive Arabidopsis and rapeseed microRNAs by comprehensive real-time polymerase chain reaction profiling and small RNA sequencing. *Plant Physiol.* **150**, 1541–1555 (2009).
14. Takahara, M. et al. Too much love, a novel Kelch repeat-containing F-box protein, functions in the long-distance regulation of the legume-Rhizobium symbiosis. *Plant Cell Physiol.* **54**, 433–447 (2013).
15. Okuma, N., Soyano, T., Suzaki, T. & Kawaguchi, M. *MIR2111-5* locus and shoot-accumulated mature miR2111 systemically enhance nodulation depending on *HAR1* in *Lotus japonicus*. *Nat. Commun.* **11**, 5192 (2020).
16. Devers, E. A. et al. Movement and differential consumption of short interfering RNA duplexes underlie mobile RNA interference. *Nat. Plants* **6**, 789–799 (2020).
17. Oldroyd, G. E. D. & Leyser, O. A plant's diet, surviving in a variable nutrient environment. *Science* **368**, eaba0196 (2020).
18. Skopelitis, D. S. et al. Gating of miRNA movement at defined cell-cell interfaces governs their impact as positional signals. *Nat. Commun.* **9**, 3107 (2018).
19. Klepikova, A. V., Kasianov, A. S., Gerasimov, E. S., Logacheva, M. D. & Penin, A. A. A high resolution map of the *Arabidopsis thaliana* developmental transcriptome based on RNA-seq profiling. *Plant J.* **88**, 1058–1070 (2016).

20. Krouk, G. et al. Nitrate-regulated auxin transport by *NRT1.1* defines a mechanism for nutrient sensing in plants. *Dev. Cell* **18**, 927–937 (2010).
21. Shah, N. et al. Extreme genetic signatures of local adaptation during *Lotus japonicus* colonization of Japan. *Nat. Commun.* **11**, 253 (2020).
22. Szczyglowski, K. & Stougaard, J. *Lotus* genome: pod of gold for legume research. *Trends Plant Sci.* **13**, 515–517 (2008).
23. Pigliucci, M. Ecology and evolutionary biology of Arabidopsis. *Arabidopsis Book* **1**, e0003 (2002).
24. Griesmann, M. et al. Phylogenomics reveals multiple losses of nitrogen-fixing root nodule symbiosis. *Science* **361**, eaat1743 (2018).
25. Hsieh, L. C. et al. Uncovering small RNA-mediated responses to phosphate deficiency. *Arabidopsis Deep Seq. Plant Physiol.* **151**, 2120–2132 (2009).
26. Williamson, L. C., Ribrioux, S. P., Fitter, A. H. & Leyser, H. M. Phosphate availability regulates root system architecture in Arabidopsis. *Plant Physiol.* **126**, 875–882 (2001).
27. Dong, W. et al. An SHR-SCR module specifies legume cortical cell fate to enable nodulation. *Nature*, https://doi.org/10.1038/s41586-020-3016-z (2020).
28. Schiessl, K. et al. *NODULE INCEPTION* recruits the lateral root developmental program for symbiotic nodule organogenesis in *Medicago truncatula*. *Curr. Biol.* **29**, 3657–3668 e3655 (2019).
29. Soyano, T., Shimoda, Y., Kawaguchi, M. & Hayashi, M. A shared gene drives lateral root development and root nodule symbiosis pathways in *Lotus*. *Science* **366**, 1021–1023 (2019).
30. Shrestha, A. et al. *Lotus japonicus Nuclear Factor YA1*, a nodule emergence stage-specific regulator of auxin signalling. *N. Phytol.* **229**, 1535–1552 (2021).
31. Schumann, N., Navarro-Quezada, A., Ullrich, K., Kuhl, C. & Quint, M. Molecular evolution and selection patterns of plant F-box proteins with C-terminal kelch repeats. *Plant Physiol.* **155**, 835–850 (2011).
32. Malolepszy, A. et al. The LORE1 insertion mutant resource. *Plant J.* **88**, 306–317 (2016).
33. Magori, S. et al. Too much love, a root regulator associated with the long-distance control of nodulation in Lotus japonicus. *Mol. Plant Microbe Interact.* **22**, 259–268 (2009).
34. Lazo, G. R., Stein, P. A. & Ludwig, R. A. A DNA transformation-competent Arabidopsis genomic library in *Agrobacterium*. *Biotechnol. (N. Y)* **9**, 963–967 (1991).
35. Thykaer, T., Schauser, L., Danielsen, D., Finneman, J. & Stougaard, J. in *Cell Biology: A laboratory handbook* Vol. 3 518–525 (Academic Press, 1998).
36. Maekawa, T. et al. Gibberellin controls the nodulation signaling pathway in *Lotus japonicus*. *Plant J.* **58**, 183–194 (2009).
37. Broughton, W. J. & Dilworth, M. J. Control of leghaemoglobin synthesis in snake beans. *Biochem J.* **125**, 1075–1080 (1971).
38. Murashige, T. & Skoog, F. A revised medium for rapid growth and bio assays with tobacco tissue cultures. *Physiologica Plant.* **15**, 473–497 (1962).
39. Melnyk, C. W. In *Plant* Hormones. Me*thods in Molecular Biology* Vol. 1497 (eds J. Kleine-Vehn & M. Sauer) 9-18 (Humana Press, 2017).
40. Holt, D. B. et al. micro RNA 172 (miR172) signals epidermal infection and is expressed in cells primed for bacterial invasion in *Lotus japonicus* roots and nodules. *N. Phytol.* **208**, 241–256 (2015).
41. Varkonyi-Gasic, E., Wu, R., Wood, M., Walton, E. F. & Hellens, R. P. Protocol: a highly sensitive RT-PCR method for detection and quantification of microRNAs. *Plant Methods* **3**, 12 (2007).
42. Ruijter, J. M. et al. Amplification efficiency: linking baseline and bias in the analysis of quantitative PCR data. *Nucleic Acids Res.* **37**, e45 (2009).
43. Danzig, E. M. & Gavrilov, I. A. Mealybugs of the genera Planococcus and Crisicoccus (Sternorrhyncha: Pseudococcidae) of Russia and adjacent countries. *Zoosystematica Rossica* **19**, 39–49 (2010).
44. Zheng, L. et al. Selection of reference genes for RT-qPCR analysis of *Phenacoccus solenopsis* (Hemiptera: Pseudococcidae) sexdimorphic development. *J. Integr. Agric.* **18**, 854–864 (2019).
45. Sexauer, M., Shen, D., Schön, M., Andersen, T. G. & Markmann, K. Visualizing polymeric components that define distinct root barriers across plant lineages. *Development* **148**, dev199820 (2021).

Acknowledgements

We thank Johanna Schröter and the ZMBP gardening team for dedicated plant care, Caterina Brancato for help with plant transformations, Dugald Reid for help with construct generation, Angela Fischer for designing Supplementary Figure 1b, and Laura Ragni for discussions. Our thanks further go to Christoph Weiste, Wolfgang Dröge-Laser and Arthur Korte for critical reading of the manuscript. We apologize to authors whose work could not be cited due to space limitations. This research was supported by the German Research Foundation (grant CRC1101, project C07), Ministry of Science, Research and Art of Baden-Wuerttemberg (Az:7533-30-20/1).

Author contributions

M.Se., H.B., M.Sch., E.R., C.W. and U.H. performed experiments and analyzed data; K.M., M.Se. and H.B. conceived and designed research; K.M. and M.Se. wrote the paper.

Funding

Open Access funding enabled and organized by Projekt DEAL.

Competing interests

The authors declare no competing interests.

Additional information

Supplementary information The online version contains supplementary material available at https://doi.org/10.1038/s41467-023-43738-6.

Correspondence and requests for materials should be addressed to Katharina Markmann.

Peer review information *Nature Communications* thanks Takuya Suzaki and the other, anonymous, reviewer(s) for their contribution to the peer review of this work. A peer review file is available.

A micro RNA mediates shoot control of root branching

SUPPLEMENTARY INFORMATION

Moritz Sexauer[1,4,5], Hemal Bhasin[1,2,5], Maria Schön[1], Elena Roitsch[1,3], Caroline Wall[1], Ulrike Herzog[1] and Katharina Markmann[1,3,4] *

Supplementary Tables

Supplementary Table 1. Relative transcript abundances of *MIR21111a/b* and *HOLT* in *A. thaliana* tissues. Data retrieved from RNAseq based developmental transcript profiling using two biological replicates[1]. Numbers represent relative expression values, with the maximum normalized read number observed for a particular locus set =1. Only an excerpt of the original dataset is represented. Expression foci are in bold.

	MIR2111a (AT3G09285)	*MIR2111b (AT5G02035)*	*HOLT (AT3G27150)*
***root** apex*	0	0	**0.5**
***root** without apex*	0	0	**1**
mature leaf, blade	0	0.11	0.01
*mature leaf, **petiole***	**0.45**	0.11	0
*mature leaf, **vein***	0	**0.21**	0
senescent leaf, petiole	0	0.13	0
*senescent leaf, **vein***	**1**	**0.36**	0.01
dry seeds	0	**1**	0

Supplementary Table 2. Oligonucleotide sequences used in cloning and genotyping.

Target	Orientation	Sequence (5'-3')
Gateway cloning of *At MIR2111b* overexpression fragment	forward	GGGGACAAGTTTGTACAAAAAAGCAGGCTCATAACCTTTCCCTCTCATG
Gateway cloning of *At MIR2111b* overexpression fragment	reverse	GGGGACCACTTTGTACAAGAAAGCTGGGTTGGTTTTCGTTAACCAAAGG
Gateway cloning of *At MIR2111a* promoter fragment	forward	GGGGACAAGTTTGTACAAAAAAGCAGGCTGTTAATGGAGTTATTTATAG
Gateway cloning of *At MIR2111a* promoter fragment	reverse	GGGGACCACTTTGTACAAGAAAGCTGGGTTCACCCCCCATAATGCGCGC
Gateway cloning of *At MIR2111b* promoter fragment	forward	GGGGACAAGTTTGTACAAAAAAGCAGGCTCATAACCTTTCCCTCTCATG
Gateway cloning of *At MIR2111b* promoter fragment	reverse	GGGGACCACTTTGTACAAGAAAGCTGGGTTTGTTTTATGTTAATGGTGA
Genotyping holt-1	forward	CTTCCAAGAGTTTGCATTTGC
Genotyping holt-1	reverse	ATCAAATCGGTAGAATTGGGG
Genotyping holt-2	forward	TTTTTAGCCTCTCAAGAATTTGG
Genotyping holt-2	reverse	TAGCTGGTGGGTTGAAAATTG
Genotyping holt-1/2 insertion	reverse	ATTTTGCCGATTTCGGAAC

Supplementary Table 3. Oligonucleotide sequences used in reverse transcription.
Nucleotides complementary or reverse complementary to small RNA sequences are in bold.

Target	Orientation	Sequence (5'-3')
PolyA signal	reverse	TTTTTTTTTTTTTTTV
Lj miR2111a/b	reverse	GTCGTATCCAGTGCAGGGTCCGAGGTATTCGCACTGGATACGAC**TACACC**
At miR2111	reverse	GTCGTATCCAGTGCAGGGTCCGAGGTATTCGCACTGGATACGAC**TAAACC**
AtHOLT	reverse	TAACCCACAATAGCACCGT
AtUBQ2	reverse	CAGATGAATAATGGGGCTC
AtPP2A	reverse	CGCCCAACGAACAAATCACA
U6	reverse	GTGCAGGGTCCGAGGTTTTGGACCATTTCTCGAT

Supplementary Table 4. Oligonucleotide sequences used in quantitative PCR.
Nucleotides complementary or reverse complementary to small RNA sequences are in bold.

Target	Orientation	Sequence (5'-3')
miR2111a/b stemloop primers	reverse	AGTGCAGGGTCCGAGGTATTC
Lj miR2111a/b and *At* miR2111	forward	GCGCG**TAATCTGCATCCTGAG**
LjTML	forward	GCCAACAATTGCCTGAAACCAGATG
	reverse	CTTTATGGTGTTTCTCTCTATGAATGCTG
LjPP2α	forward	GTAAATGCGTCTAAAGATAGGGTCC
	reverse	ACTAGACTGTAGTGCTTGAGAGGC
LjATPs	forward	CAATGTCGCCAAGGCCCATGGTG
	reverse	AACACCACTCTCGATCATTTCTCTG
AtPP2A	forward	GGTAATAACTGCATCTAAAGACAGAGTTCC
	reverse	CCACAACCGCTTGGTCG
AtUBQ2	forward	CCAAGATCCAGGACAAAGAAGGA
	reverse	TGGAGACGAGCATAACACTTGC
AtHOLT	forward	TTCTGTCCAATCTCCACCGCTC
	reverse	ACTTAAACGCAACGCCCCATC
AtNRT1.1	forward	GAGAGGCTGACGACGTTAGGT
	reverse	ATTGCGGCGAATATAGCAATCG
AtNRT1.5	forward	CGCAAAATGTCTTGCCTAGAG
	reverse	CATAGTAATCCACTGTCCCATCTCTT
AtNRT2.1	forward	GAAATCGAGCTACCTTGGAGAA
	reverse	TTGTAACGGCATACCACAGAA
AtNRT3.1	forward	TGGGTCTAAAAGAGAGGCTGA
	reverse	GCCATGGTCGGTCAACTT
αTubulin	forward	GGTTCGACAACAGCGGTAGA
	reverse	GTGGCACCGGATCAGGATTT
U6	forward	GGAACGATACAGAGAAGATTAGCA
	reverse	GTGCAGGGTCCGAGGT

Supplementary Table 5. Oligonucleotide sequences used in mutant characterization.

Target	Orientation	Sequence (5'-3')
HOLT 3' of holt-1 insertion	forward	ATGTTGACGCTAGGAGAAGA
	reverse	ATAGTCCGCGTCTTTCGGCTTCAAACATGTACTGCTCAGAGCCTTAG
HOLT full length	forward	ATGTTGACGCTAGGAGAAGA
	reverse	TTACGCAATCATTACACAACAG

Supplementary Figures

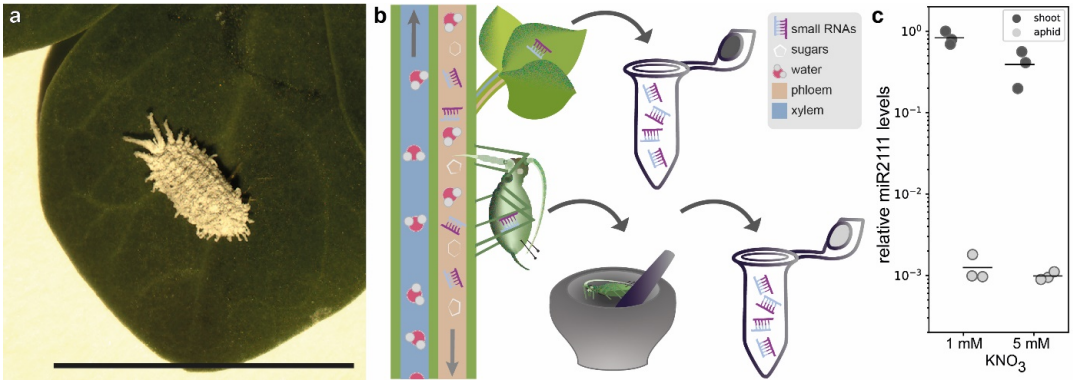

Supplementary Fig. 1. Mature miR2111 can be traced in aphids feeding on *L. japonicus* (Lotus) phloem sap. **a** *Planococcus citri* on Lotus leaf, scalebar equals 1 cm. **b** Simplified sketch of experimental procedure of an aphid feeding experiment. Plants are grown for four weeks in absence of aphids, then colonized by a small aphid population, which propagates for two weeks while feeding on phloem sap. During feeding, aphids ingest mobile small RNAs, which have been suggested to travel through the phloem as mature duplices[2]. Possible association of miRNAs with proteins during phloem transfer is not considered here. Aphids and plant material are harvested separately for RNA extraction and qRT-PCR based detection of mature plant miR2111. **c** miR2111 levels in shoot tissue of Lotus ecotype Gifu wild type plants and aphids (*Planococcus citri*) after feeding on respective plants grown at indicated nitrate conditions. qRT-PCR analyses. miR2111 levels from Lotus shoot RNA extracts are relative to two endogenous reference genes, miR2111 levels from aphid RNA extracts are relative to one aphid reference gene. Host and aphid tissues were harvested after two weeks of aphid feeding and six weeks after plant germination. Sample size, replicates and exact p-values are listed in Supplementary Data 1. Dotplots show individual data points and a line indicating their average value.

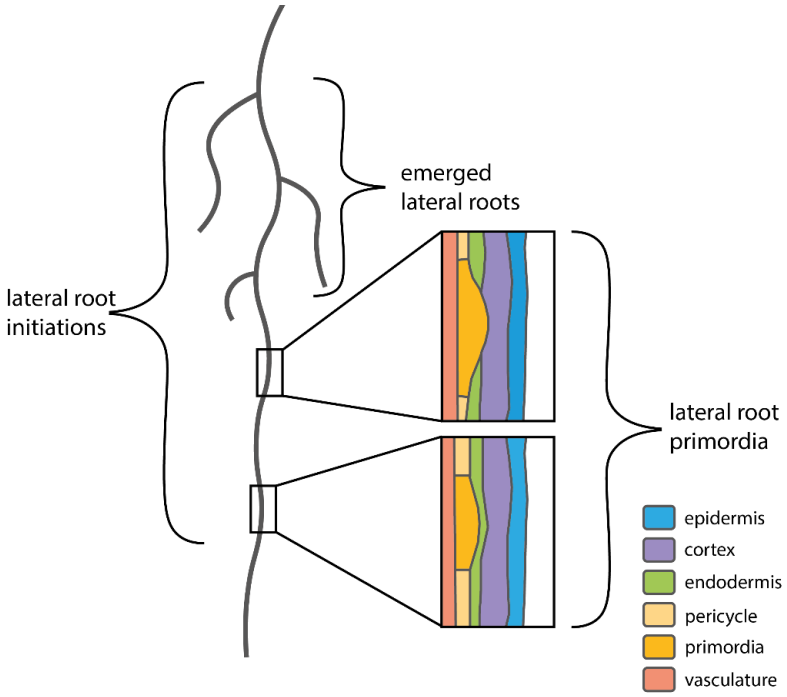

Supplementary Fig. 2. Schematic representation of lateral root initiations encompassing both emerged lateral roots and lateral root primordia. Insets show schematic representation of lateral root primordia, with different colors indicating root cell types as indicated.

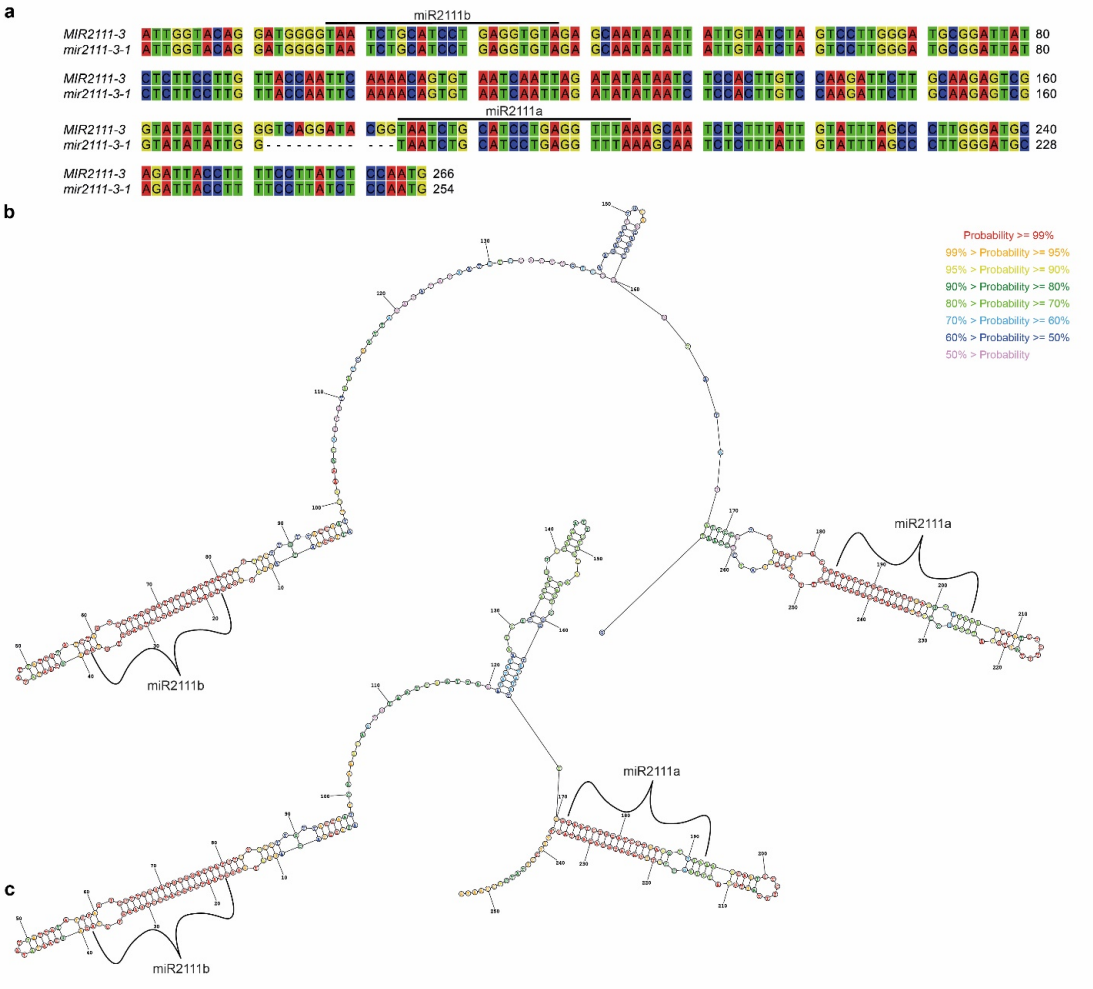

Supplementary Fig. 3. Characterization of the *L. japonicus MIR2111-3* CRISPR/Cas9-mediated knockout deletion. a Alignment of the *MIR2111-3* sequence and the 12 bp deletion in the *mir2111-3-1* allele. **b-c** Predicted hairpin structures of *MIR2111-3* without (**b**) and with the deletion indicated in **a** (**c**). **b-c** Secondary structure was modelled using the MaxExpect algorithm with default settings[3].

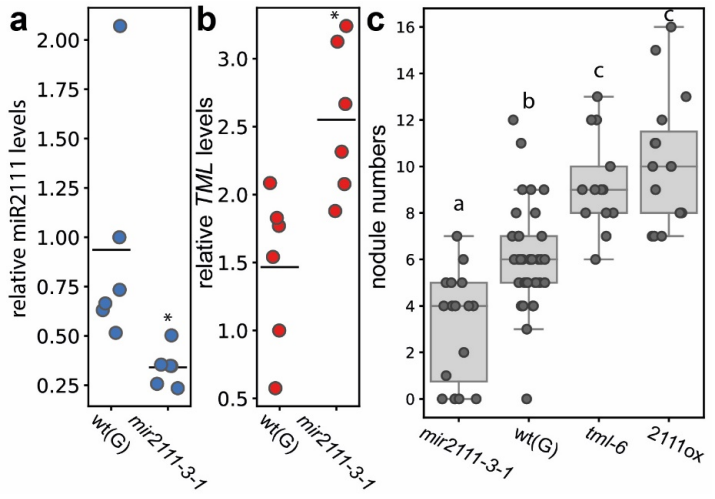

Supplementary Fig. 4. Alterations of miR2111 and *TML* levels influence nodule numbers in *L. japonicus* (Lotus). a, b miR2111 (**a**) and *TML* levels (**b**) in roots of Lotus ecotype Gifu wild type (wt(G)) and *mir2111-3-1* plants. **c** Nodule numbers of wt(G), *tml-6*, *MIR2111-3* ox (2111ox) and *mir2111-3-1* mutants, *tml-6* and 2111ox plants. **a-b** qRT-PCR analyses. Root RNA levels are relative to those of two reference genes. Tissue was harvested 14 days after transfer. Plants were grown at 5 mM nitrate. **a-c** Comparisons used Student's *t*-test (*=$p<0.05$) (**a-b**) or (**c**) analysis of variance (ANOVA) and post-hoc Tukey testing ($p\leq0.05$), with distinct letters indicating significant differences. **c** plants evaluated three weeks after inoculation with *M. loti*, plants grown at 0 mM nitrate. Sample size, replicates and exact p-values are listed in Supplementary Data 1. Dotplots show individual data points and a line indicating their average value. Boxplot central line shows median value, box limits indicate the 25th and 75th percentile. Whiskers extend 1.5 times the interquartile range, or to the last datapoint. Individual datapoints are represented by dots.

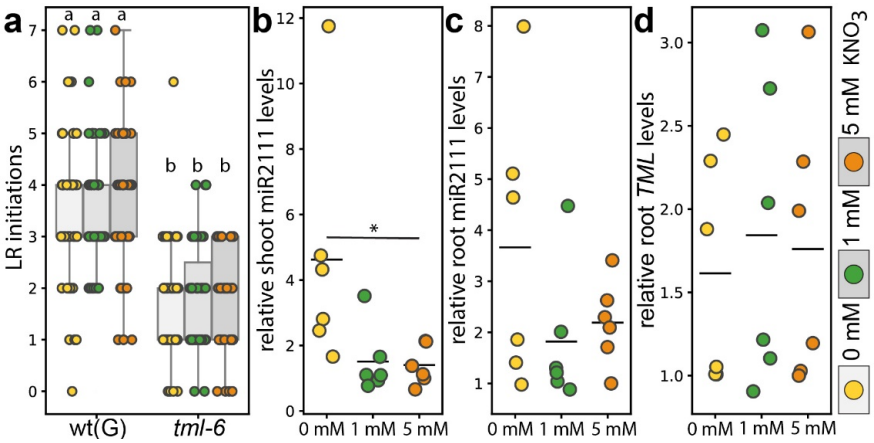

Supplementary Fig. 5. *L. japonicus* (Lotus) ecotype Gifu lateral root (LR) initiation numbers and *TML* levels are nitrate independent. a LR initiations in wild type Gifu (wt(G)) and *tml-6* plants 10 days post transfer. **b-d** Relative mature miR2111 levels in shoots (**b**) and roots (**c**) and relative *TML* levels in the same root systems (**d**) of ecotype Gifu B-129 wild type plants after 14 days of cultivation. **b-d** qRT-PCR analyses. RNA levels are relative to those of two reference genes. Comparisons used analysis of variance (ANOVA) and post-hoc Tukey testing ($p \leq 0.05$), with distinct letters indicating significant differences (**a**) or Student's t-test (*=$p<0.05$) (**b**). Sample size, replicates and exact p-values are listed in Supplementary Data 1. Dotplots show individual data points and a line indicating their average value. Boxplot central line shows median value, box limits indicate the 25th and 75th percentile. Whiskers extend 1.5 times the interquartile range, or to the last datapoint. Individual datapoints are represented by dots.

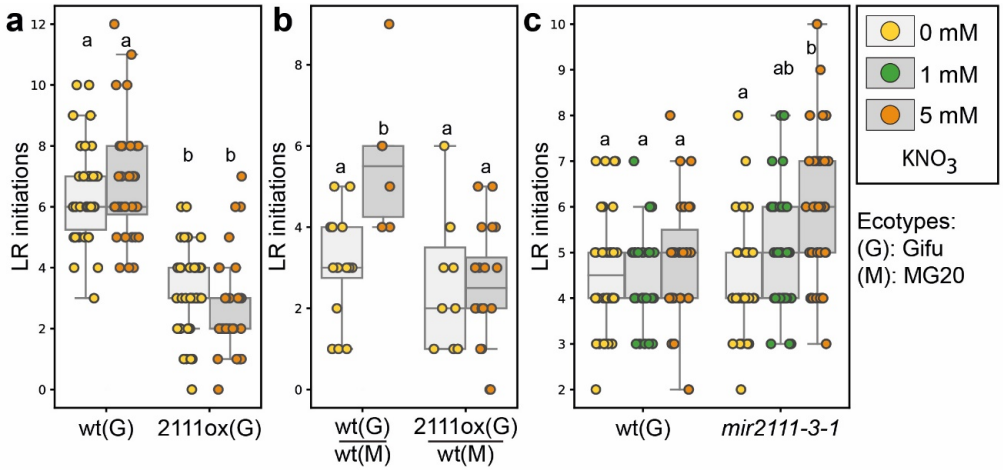

Supplementary Fig. 6. Low miR2111 levels are required and sufficient for enhanced lateral root (LR) initiation under high nitrate conditions in *L. japonicus* (Lotus). a-c LR initiations of Lotus ecotype Gifu wild type (wt(G)) and *mir2111-3-1* plants (**a**), heterografted plants assembled of Lotus ecotype MG20 wild type (wt(M)) root stocks and ecotype Gifu wild type or *MIR2111-3* overexpression (2111ox) shoots (**b**), and ecotype Gifu wild type and *mir2111-3-1* plants (**c**). **a-b** Plants were grown at indicated nitrate concentrations and analyzed after two weeks of cultivation (**a, b**) or graft regeneration (**c**), respectively. Comparisons used analysis of variance (ANOVA) and post-hoc Tukey testing ($p \leq 0.05$), with distinct letters indicating significant differences. Sample size, replicates and exact p-values are listed in Supplementary Data 1. Boxplot central line shows median value, box limits indicate the 25th and 75th percentile. Whiskers extend 1.5 times the interquartile range, or to the last datapoint. Individual datapoints are represented by dots.

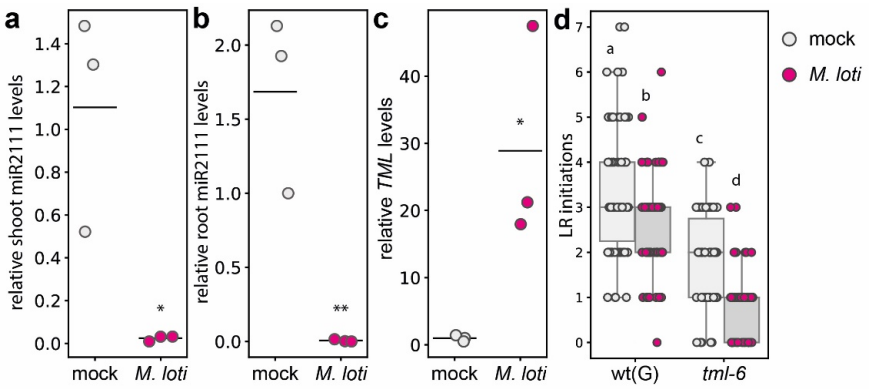

Supplementary Fig. 7. Symbiosis restricts lateral root (LR) initiation in a *TML*-independent manner in *L. japonicus* (Lotus). a-c Relative mature miR2111 levels in shoots (**a**) and roots (**b**) and relative *TML* levels (**c**) in the same Lotus plants (ecotype Gifu wild type (wt(G))) at 21 days post inoculation. Plant were cultivated for 3 weeks. **d** LR initiations in symbiotic and non-symbiotic wild type and *tml-6* plants at 10 days post inoculation. **a-c** qRT-PCR analyses. RNA levels are relative to those of two reference genes. Plants were inoculated with *Mesorhizobium loti*, or treated with water (mock control). Comparisons used analysis of variance (ANOVA) and post-hoc Tukey testing ($p \leq 0.05$) (**d**), with distinct letters indicating significant differences or Student's *t*-test (*=$p<0.05$) (**a-c**). Sample size, replicates and exact p-values are listed in Supplementary Data 1. Dotplots show individual data points and a line indicating their average value. Boxplot central line shows median value, box limits indicate the 25th and 75th percentile. Whiskers extend 1.5 times the interquartile range, or to the last datapoint. Individual datapoints are represented by dots.

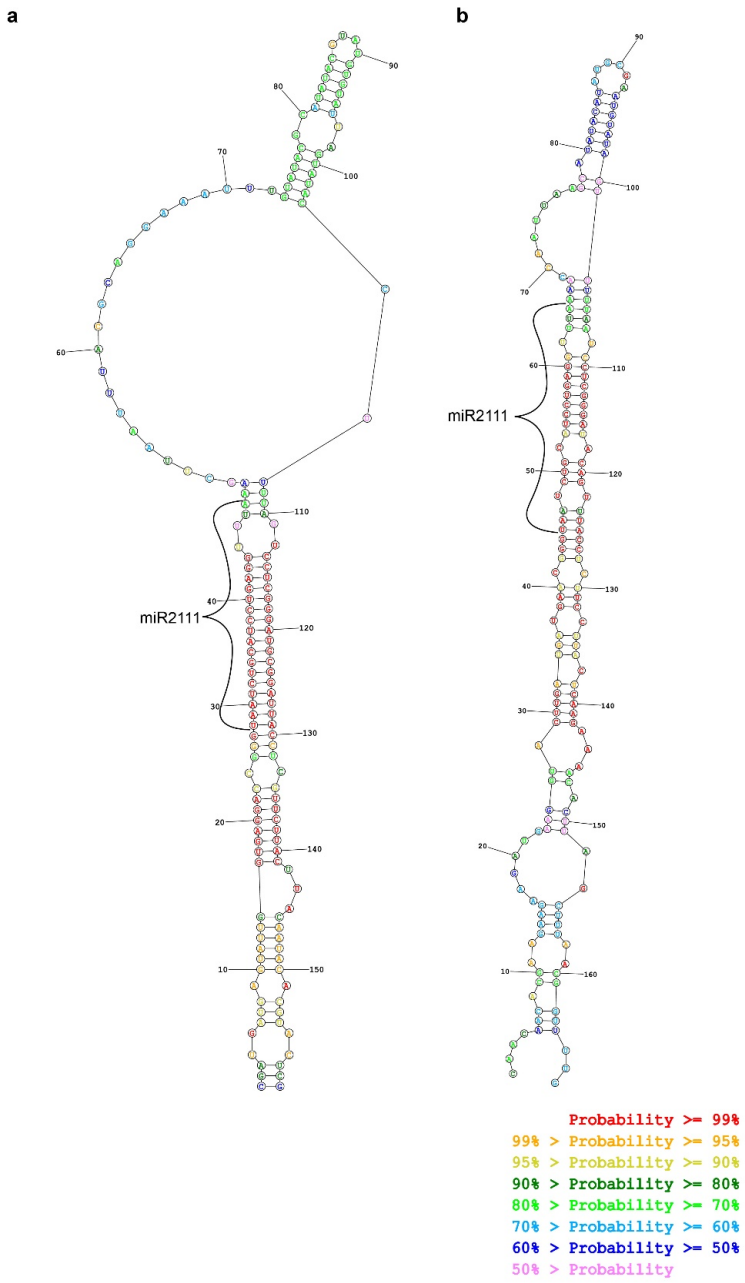

Supplementary Fig. 8. The *A. thaliana* genome contains one miR2111 isoform at two distinct loci. a-b, *MIR2111a* (**a**) and *MIR2111b* (**b**) transcripts are predicted to form hairpin structures. Secondary structure was modelled using the MaxExpect algorithm with default settings[3].

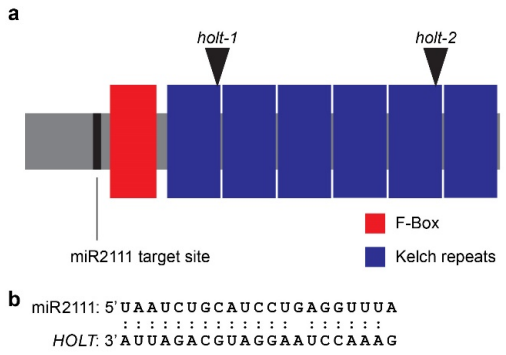

Supplementary Fig. 9. *A. thaliana HOLT* is an F-Box Kelch Repeat protein with a conserved miR2111 complementary site. a *HOLT* gene and predicted protein features including the miR2111 target site as indicated, and position of the t-DNA insertion in *holt-1*and *holt-2* (black arrowheads). The t-DNA insertion positions were confirmed by Sanger sequencing. Red and blue boxes indicate predicted protein domains as indicated. **b** Alignment of miR2111 and *HOLT* mRNA at the target site. Colons indicate A/U and G/C base pairing.

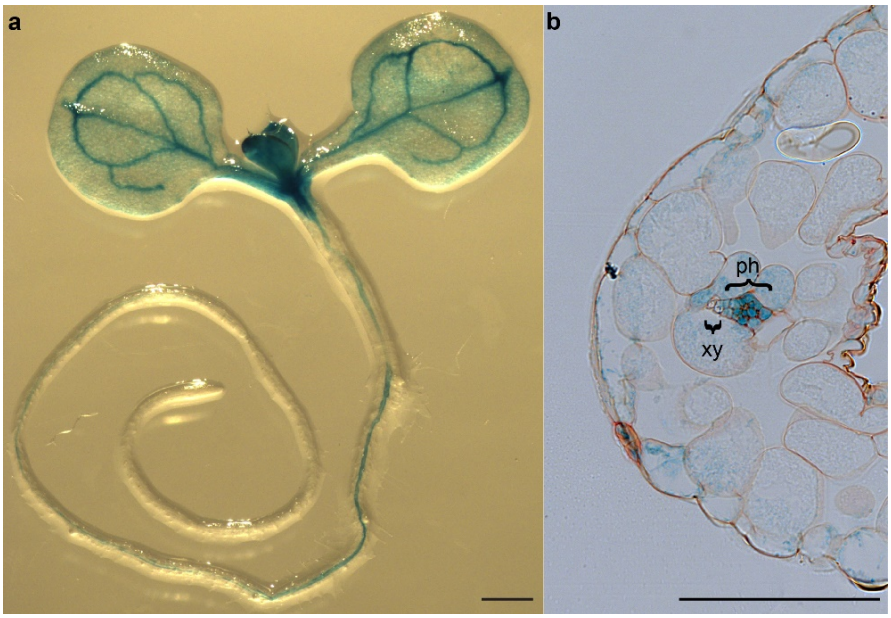

Supplementary Fig. 10. ***A. thaliana MIR2111a*** **is predominantly expressed in leaf vein phloem.**

a Five day-old stably transformed *A. thaliana* seedlings expressing *pMIR2111a:GUS* show GUS activity in leaf veins and root vasculature. **b** *GUS* expression is strongest in leaf phloem. **a**,**b** Scale bar equals 500 µm (**a**) or 100 µm (**b**). **a-b** Analysis of three independent lines showed similar results. All 34 tested plants of 3 independent lines showed a likewise expression pattern.

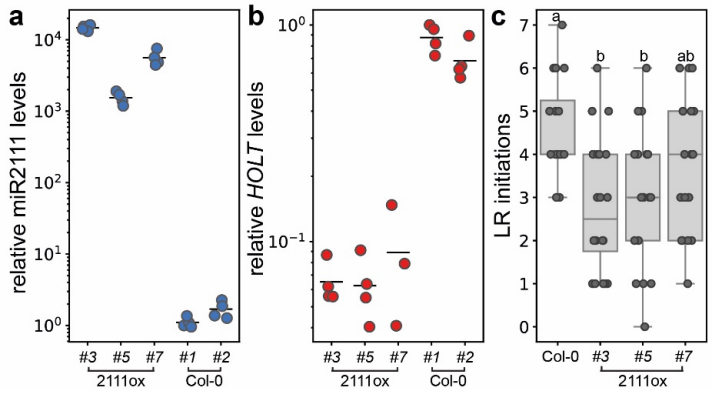

Supplementary Fig. 11. ***A. thaliana p35s::MIR2111b*** **(2111ox) lines show strongly reduced** ***HOLT*** **levels compared to wild type plants. a-c** miR2111 (**a**) and *HOLT* (**b**) levels and lateral root initiation (**c**) of independent 2111ox lines. Line #3 was selected for further propagation and experiments. **c** Plants were grown for seven days on 1 mM nitrate. **a**, **b** qRT-PCR analyses. RNA levels are relative to those of two reference genes (**b**) or relative to U6 (**a**). **c** Comparisons used analysis of variance (ANOVA) and post-hoc Tukey testing ($p \leq 0.05$). Sample size, replicates and exact p-values are listed in Supplementary Data 1. Dotplots show individual data points and a line indicating their average value. Boxplot central line shows median value, box limits indicate the 25th and 75th percentile. Whiskers extend 1.5 times the interquartile range, or to the last datapoint. Individual datapoints are represented by dots

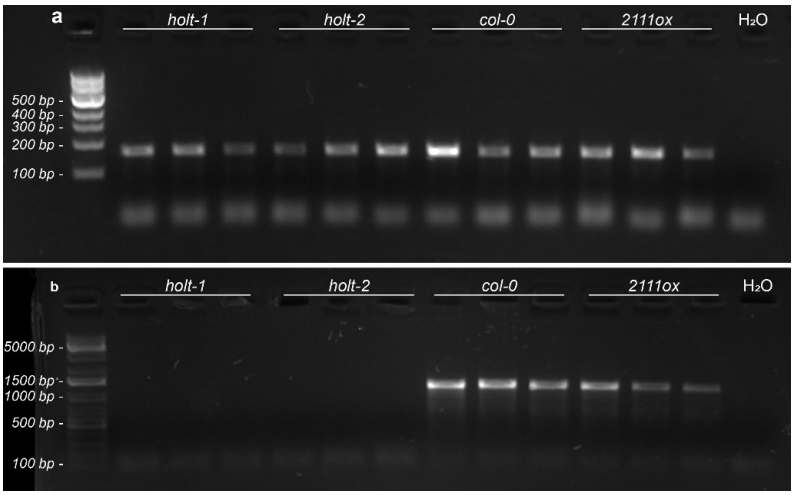

Supplementary Fig. 12. *A. thaliana holt-1* and *holt-2* are putative knockout mutant lines showing no full-length *HOLT* transcript. a,**b** Molecular characterization of the *holt-1* and *holt-2* mutants. **a** Amplicon of *HOLT* truncated transcript fragment 3' of the respective insertions, and 3' of F-Box as well as part of the Kelch-Repeat domain (Supplementary Fig. 8). **b** Fragments 5' of the insertion in *holt-1* cannot be generated from cDNA either of the *holt-1* or *holt-2* mutant lines, indicating absence of full-length *HOLT* transcripts in these mutants. **a-b**, Agarose gel electrophoresis of RT-PCR reactions. Col-0, wild type DNA positive control (ecotype Col-0); H_2O, negative control with water instead of DNA template added to reaction; 2111ox, *p35s::MIR2111b* plants. Two independent replicates showed the same results. All primers used for amplification are listed in Supplementary Table 5.

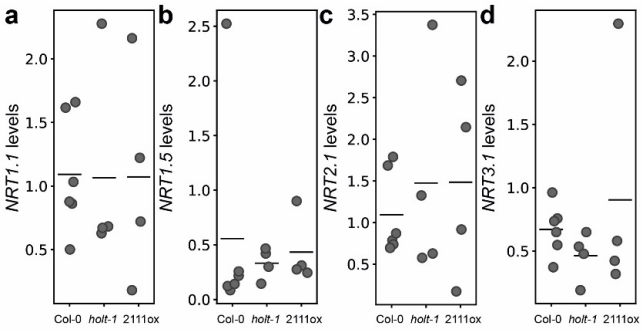

Supplementary Fig. 13. mRNA abundance of *A. thaliana NRT* genes is wild type-like in *holt-1* or *MIR2111b* overexpression plants. a-d Relative levels of *NRT1.1* (**a**), *NRT1.5* (**b**), *NRT2.1* (**c**) and *NRT3.1* (**d**) in *holt-1* and *p35s::MIR2111b* (2111ox) plants compared to ecotype col-0 wild type plants. Plants grown for ten days on 1 mM nitrate. **a-d** qRT-PCR analyses. RNA levels are relative to those of two reference genes. Comparisons using analysis of variance (ANOVA) identified no significant differences of mRNA abundances between lines. Sample size, replicates and exact p-values are listed in Supplementary Data 1. Dotplots show individual data points and a line indicating their average value.

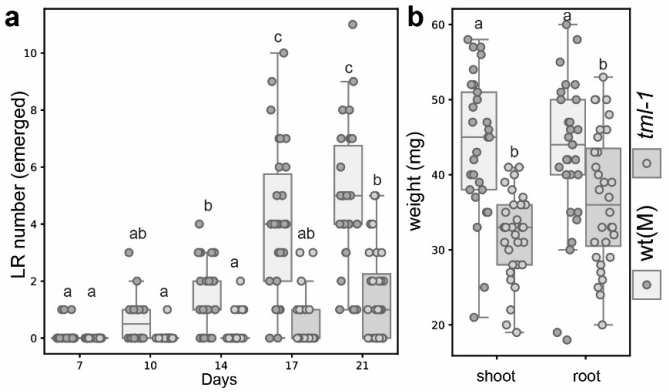

Supplementary Fig. 14. Root growth differences between *L. japonicus* (Lotus) *tml-1* and wild type increase over time. a Lateral root (LR) numbers of Lotus *tml-1* and wild type (ecotype MG20; wt(M)) plants at different timepoints between 7 and 21 days of cultivation. **b** Shoot and root weight of the same plants after four weeks of cultivation. Plants were grown at 1 mM nitrate. Comparisons used analysis of variance (ANOVA) and post-hoc Tukey testing ($p \leq 0.05$), with distinct letters indicating significant differences. Sample size, replicates and exact p-values are listed in Supplementary Data 1. Boxplot central line shows median value, box limits indicate the 25th and 75th percentile. Whiskers extend 1.5 times the interquartile range, or to the last datapoint. Individual datapoints are represented by dots.

Supplementary Information References

1 Klepikova, A. V., Kasianov, A. S., Gerasimov, E. S., Logacheva, M. D. & Penin, A. A. A high resolution map of the *Arabidopsis thaliana* developmental transcriptome based on RNA-seq profiling. *Plant J* **88**, 1058-1070, doi:10.1111/tpj.13312 (2016).

2 Devers, E. A. *et al.* Movement and differential consumption of short interfering RNA duplexes underlie mobile RNA interference. *Nat Plants* **6**, 789-799, doi:10.1038/s41477-020-0687-2 (2020).

3 Lu, Z. J., Gloor, J. W. & Mathews, D. H. Improved RNA secondary structure prediction by maximizing expected pair accuracy. *RNA* **15**, 1805-1813, doi:10.1261/rna.1643609 (2009).

Appendix 4 Manuscripts in preparation

Appendix 4.1 To the roots of nodules: Nodule organogenesis utilizes lateral root development processes.

To the roots of nodules: Nodule organogenesis utilizes lateral root development processes.

RNS and AM symbiosis share a common set of genes involved in early symbiosis signaling and establishment of endosymbiont accommodation. These dually required genes are referred to as common symbiosis (Common Sym) genes (Kistner and Parniske, 2002; Markmann and Parniske, 2009; Genre and Russo, 2016). Relatively seen, RNS is phylogenetically young and only found in certain members of the FaFaCuRo (Soltis et al., 1995; Griesmann et al., 2018), whereas AM likely arose among the first land plants and is widespread in the plant kingdom. It was thus suggested that during the evolution of RNS, pre-existing symbiosis genes were adapted to mediate the recognition and accommodation of bacterial symbionts in addition to fungal ones. The recruitment of these symbiotic genes from AM can therefore be seen as a key step in evolution of rhizobial symbiosis, allowing intracellular infection (Markmann et al., 2008). The Common Sym genes are active in the early stages of symbiotic signaling immediately downstream of Nod/Myc factor perception, triggering transcriptional responses specific to the respective type of symbiosis mediated by *CYCLOPS* (Yano et al., 2008; Genre and Russo, 2016).

A gene directly regulated by *CYCLOPS* is the transcription factor *NODULE INCEPTION* (*NIN*) which has been intensely studied in legumes (Singh et al., 2014; Lin et al., 2018; Liu et al., 2019; Schiessl et al., 2019; Akamatsu et al., 2022; Cathebras et al., 2022). *NIN* is dually required for IT formation and nodule organogenesis during rhizobial infection. Interestingly, these functions can be linked to separate regulatory elements in the *NIN* promoter region and sequential, spatially distinct expression activities (Cathebras et al., 2022). IT formation depends on epidermal *NIN* expression (Schauser et al., 1999; Yoro et al., 2014; Akamatsu et al., 2022; Cathebras et al., 2022), whereas nodule organogenesis relies on the cortical and, in case of indetermined nodules, pericyclic expression of *NIN* (Yoro et al., 2014; Liu et al., 2019).

While *NIN* is not exclusively present in the nitrogen fixing clade, the presence of an intact copy of the gene is crucial for successful RNS formation. Notably, the *NIN* promoter of RNS forming species features a *CYCLOPS* binding element (PACE), which is involved in

NIN regulation following Nod factor signaling (Griesmann et al., 2018; Cathebras et al., 2022). *NIN* is a homologue of the widely conserved *NLPs*, which in contrast to *NIN* are regulated in a nitrate dependent manner (Suzuki et al., 2013).

Much like during lateral root growth, nodule organogenesis follows a developmental chronology that in its early phase can be divided in the stages of priming, initiation, outgrowth and emergence. Legume root nodules which maintain a persistent apical meristem are termed indeterminate, while determinate nodules only have an active meristem during their early development (Hirsch, 1992). Like LRs, indeterminate nodules emerge from pericycle cells (Xiao et al., 2014), while determinate nodule initiation takes place in the root cortex (Hirsch, 1992). Cytokinin signaling and *NIN* expression precede and accompany nodule primordium initiation in either nodule type and may represent the onset of nodule initiation (Liu et al., 2019; Miri et al., 2019; Cathebras et al., 2022) (**Figure 6A,B**).

Recent transcriptome analyses suggest that during nodule organogenesis, *NIN* recruits various genes associated with lateral root development (Schiessl et al., 2019). This was experimentally verified for the transcription factor *LOB-DOMAIN PROTEIN 16* (*LBD16*)/*ASYMMETRIC LEAVES 2-LIKE 18* (*ASL18*), which is directly regulated by *NIN* through an intronic *NIN* responsive element (Schiessl et al., 2019; Soyano et al., 2019). In Arabidopsis, *LBD16* expression is induced by *IAA14-ARF7-ARF19* dependent auxin signaling in LR founder cells (Okushima et al., 2007; Goh et al., 2012; Lavenus et al., 2013). The presence of a functional *LBD16* gene is required for both LR and adventious root initiation in this species (Goh et al., 2012; Lee et al., 2019), and was further shown to be involved in the initiation of other root-derived structures such as nematode feeding galls (Liu et al., 2018).

In both Medicago and Lotus, *LBD16/ASL18* was shown to be involved in nodule formation in addition to a conserved role in LR initiation (Schiessl et al., 2019; Soyano et al., 2019). In both legume species, *LBD16/ASL18* expression is enhanced upon infection and can be traced in both early stage LR- and nodule primordia (Schiessl et al., 2019; Soyano et al., 2019). *lbd16* mutants showed reduced and delayed formation of nodule primordia, suggesting a role during initiation of nodules (Schiessl et al., 2019; Soyano et al., 2019). In Lotus, this function was also dependent on *NF-YA* & *NF-YB* , while *LBD16s* function in LR initiation was not (Soyano et al., 2019). Like lateral root development, nodule

organogenesis requires and is paralleled by auxin signaling (reviewed in (Du and Scheres, 2017a; Lin et al., 2020). The initiation of lateral roots was intensely studied in Arabidopsis and was shown to involve auxin maxima dependent priming of pericycle cells, which then develop into LR founder cells (De Smet et al., 2007; De Smet, 2012). In these cells, LR initiation can occur via asymmetric anticlinal cell division mediated by *LBD16*/*18* downstream of *ARF7*/*19* (Goh et al., 2012; Lee et al., 2017; Lee et al., 2019). After this initial cell division, the LRP grows by successive periclinal and anticlinal divisions of pericycle-derived cells. Likewise indetermined nodule primordium (NP) development is initiated with anticlinal divisions of the pericycle (Xiao et al., 2014). However, during NP development these are followed by further anticlinal and periclinal divisions in pericycle, inner cortex and the endodermis (Xiao et al., 2014).

The two transcription factors *SHORTROOT* (*SHR*) and *SCARECROW* (*SCR*) mediate the regulation of cell patterning and determination of endodermal identity in Arabidopsis (Helariutta et al., 2000; Nakajima et al., 2001; Cui et al., 2007). Notably, *SCR* is also active in LRPs, where it is proposed to induce periclinal cell divisions (Goh et al., 2016). Its expression focused in the outer layers of LRPs. This expression pattern was a prerequisite for the correct activity of the downstream acting transcription factor *WUSCHEL-RELATED HOMEOBOX 5* (*WOX5*), and specification of the QC during later stages of LRP development (Goh et al., 2016).

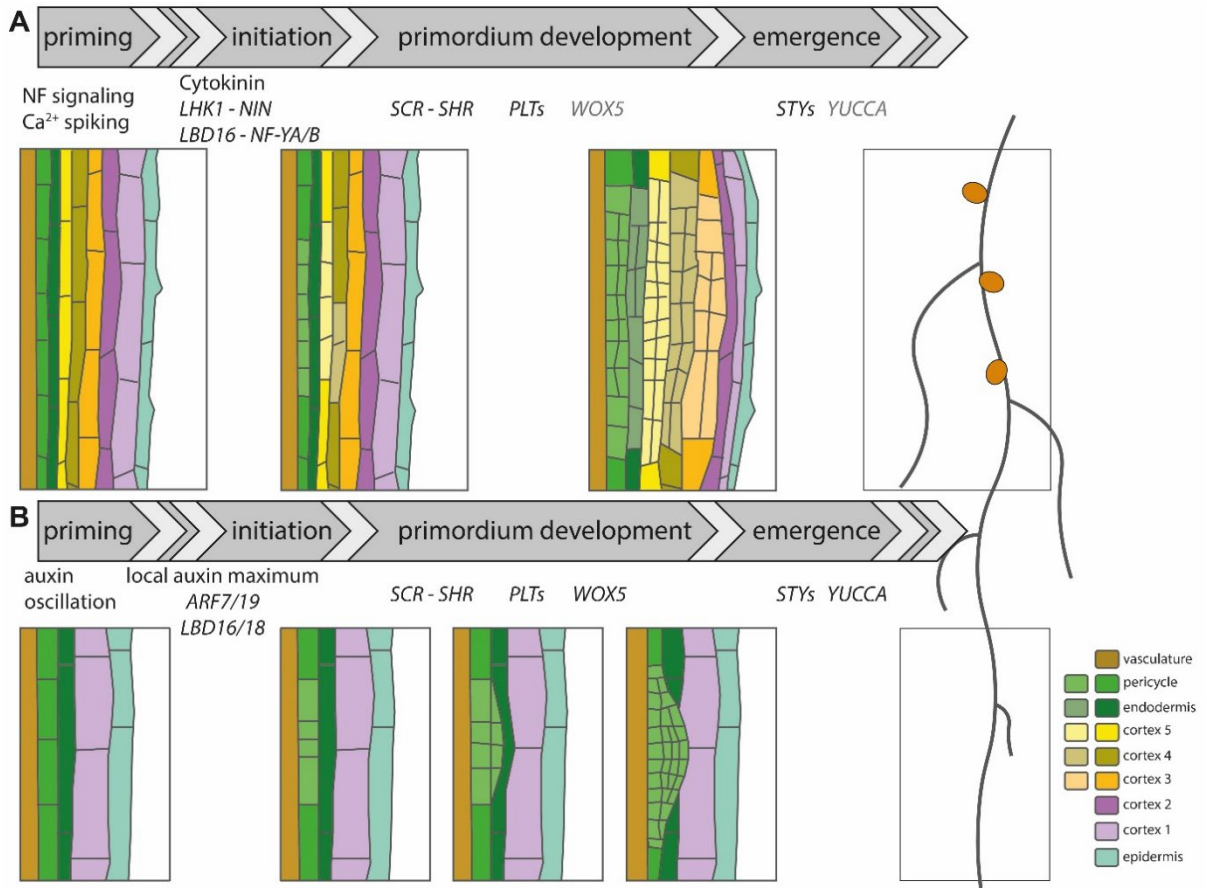

Figure 1 Nodule organogenesis and lateral root formation follow a similar pattern (Sexauer and Markmann, 2024). A, scheme of nodule development in Medicago based on (Xiao et al., 2014). **B**, scheme of LR development in Arabidopsis based on (Malamy and Benfey, 1997; Du and Scheres, 2017a). **A, B** The first step of both indeterminate nodule (**A**) and lateral root (**B**) organogenesis is priming, a transcriptional reprogramming of the founder cells, prior the first division. **B** In LR organogenesis, priming depends on auxin oscillation and downstream signaling. **A** As for nodule development, nod factor (NF) signaling and downstream Ca^{2+} spiking could be seen as priming step as they lead to transcriptional reprogramming of respective cells. **B** After priming, LR formation continues with *ARF7/19* and downstream *LBD16/18* dependent initiation, marked by the first asymmetric anticlinal division. Initiation is followed by primordial development involving further periclinal and anticlinal divisions. These following divisions and later primordium development depend on *SCR*, *SHR, PLTs* and *WOX5.* **A** Nodule initiation also starts with anticlinal divisions of pericycle cells followed by further divisions of the pericycle and cortex during NP development. **A** Initiation of primordia formation is dependent on cytokinin responsive *NIN* expression and downstream *LBD16* recruitment. *SHR*, *SCR* and *PLTs* appear to be involved during later cortical cell divisions. **A, B** The mature nodule and LR primordium emerge in a *STY* dependent manner. Black genes are placed based on functional data, grey genes are based on their expression and analogy to lateral development.

More recently, the *SHR-SCR* module was shown to mediate nodule organogenesis downstream of *NIN* in Medicago (Dong et al., 2020). The legume specific expression of *SCR* in cortical cells was shown to be crucial for cortical cell division during nodule primordia development (Dong et al., 2020). A role in LRP development in this species has

not yet been described, yet *scr-1* mutants showed decreased LR density (Dong et al., 2020). Beyond *SCR*, *PLETHORA* (*PLT*) transcription factors have been shown to be involved in QC definition and maintenance of stem cell identity in the root apical meristem in Arabidopsis (Aida et al., 2004; Shimotohno et al., 2018), and *plt1 plt2* double mutants show abnormal meristem patterning (Aida et al., 2004). These plants formed more lateral roots than wild type plants, but mutant roots displayed smaller apical meristems (Aida et al., 2004). *plt3 plt5 plt7* triple mutants showed delayed periclinal cell division during LR primordia development, which resulted in abnormal primordium patterning and reduced lateral root density (Du and Scheres, 2017b). Recently it was shown that during root stem cell maintenance, *PLTs* restrict *WOX5* expression to the QC while *WOX5* indirectly promotes *PLT* expression in surrounding cell layers (Burkart et al., 2022).

Differential expression of several *PLT* genes during LR and nodule formation in the legume Medicago (Franssen et al., 2015; Franssen et al., 2017) suggests a dual role in root lateral organ development. Indeed Medicago plants transiently expressing RNAi constructs targeting multiple *PLTs* showed, reduced nodule numbers and impaired nodule development (Franssen et al., 2015). Further, *WOX5* was also shown to be strongly expressed during early stages of Medicago nodule primordia development, however functional data of involvement in nodule formation is still lacking (Osipova et al., 2012).

The last step during both LR and nodule development is the emergence, a step which has been shown to be accompanied by auxin signaling (Ståldal et al., 2012; Singh et al., 2020; Shrestha et al., 2021).

In Arabidopsis, *STYLISH (STYs)/SHORT INTERNODES (SHIs)* regulate auxin biosynthesis (Sohlberg et al., 2006) which was shown for *STY1* to be achieved via YUCCA (*YUC)* induction (Eklund et al., 2010). *LATERAL ROOT PRIMORDIUM1 (LRP1),* a member of the *STY* family, was shown to be involved in lateral root emergence (Singh et al., 2020). In Lotus, plants stably expressing a dominant negative *STY3-SRDX* (*SUBERMAN REPRESSION DOMAIN X*) (Hiratsu et al., 2003) construct showed a slightly reduced number of nodule primordia and failed to produce mature nodules (Shrestha et al., 2021). Furthermore, Lotus *YUCCA* expression was shown to be partially dependent on *STY3* (Shrestha et al., 2021), indicating a possible role of *STY-YUCCA* signaling in nodule emergence. Functional involvement of *STY3* or other *STY* genes as well as *STY*-dependent

auxin signaling via *YUCCAs* in the regulation of lateral roots in legumes appears likely, as *STY* expression was shown for both nodule and LR primordia and plants transiently overexpressing *YUCCAs* show aberrant LR formation (Shrestha et al., 2021). However, a direct involvement of *STY* genes in LR formation in legumes has yet to be established.

Strikingly, the vast majority of previously discussed genes shows induced expression after inoculation with rhizobia, which was dependent on either *SCR*, or *LBD16* downstream of *NIN* (Schiessl et al., 2019; Dong et al., 2020). Transcriptome analysis by (Schiessl et al., 2019) revealed a major overlap of differentially regulated genes in *nin-1* and *lbd16-1* mutants compared to wild type plants, including *STY, YUC and PLT* genes. In addition, cell cycle associated genes display similar regulation patterns in these two mutant backgrounds. These observations allow interesting insights into the subset of *NIN*-dependent genes requiring downstream factors potentially co-involved in RNS and root architecture control. Interestingly, (Dong et al., 2020) proposed a feedforward loop between *SCR* and *LBD16*, as their expression depends on each other.

Comparing the regulation and function of previously discussed genes during both LR and NP development, it appears that LBD16 acts as a key transcription factor in lateral organ initiation and further recruits a common set of downstream genes involved in lateral organ development (**Figure 7A,B**). The transcriptional regulation of LBD16, however seems to differ between both functions, as during LR initiation LBD16 expression is induced via the auxin dependent IAA14-ARF7/ARF19 module (Okushima et al., 2007) (**Figure 7A**). During nodule formation LBD16 expression is controlled via cytokinin induced NIN expression (Schiessl et al., 2019; Soyano et al., 2019) (**Figure 7B**). Whether an ARF7/19 dependent recruitment of LBD16 is also involved in nodulation is so far unknown.

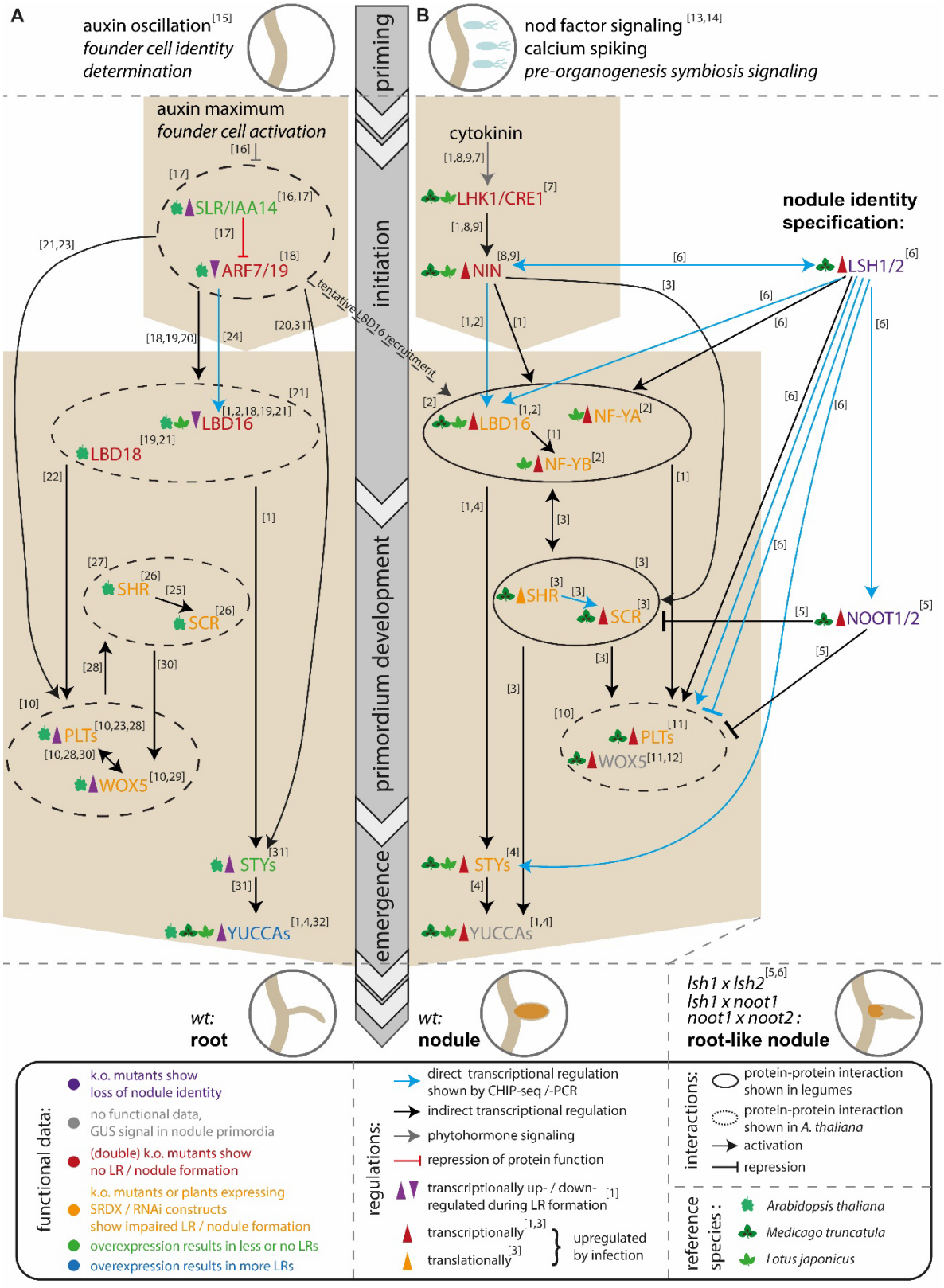

Figure 2 Genetic network involved in nodule and lateral root (LR) formation and nodule identity (Sexauer and Markmann, 2024). A, B schematic representation of dependencies between genes involved in nodule (**A**) and LR (**B**) formation. Circles indicate protein-protein interaction, gene color indicates functional data generated by mutant analysis. Arrows between genes indicate dependencies, colored triangles indicate transcriptional / translational regulation in response to rhizobial inoculation (**A**) or during LR formation (**B**). The Model is based on data

derived from *Medicago truncatula*, *Lotus japonicus* and *Arabidopsis thaliana*. leaves next to genes indicate species, in which analysis took place. Central arrow indicates during which stage of lateral organ formation each gene is active. Pictograms indicate which lateral organ is produced by the genetic network. **A** double knock out (k.o.) of the nodule identity genes *NOOT1/2* and *LSH1/2* leads to formation of root like nodules. Bracketed numbers indicate respective citations: [1](Schiessl et al., 2019),[2] (Soyano et al., 2019),[3](Dong et al., 2020),[4](Shrestha et al., 2021),[5](Magne et al., 2018),[6] (T. Lee et al., 2024),[7](Miri et al., 2019),[8](Yoro et al., 2014),[9](J. Liu et al., 2019),[10](Burkart et al., 2022),[11](Franssen et al., 2015),[12](Osipova et al., 2012),[13](Hayashi et al., 2010),[14](Liu et al., 2022),[15](Laskowski and Ten Tusscher, 2017),[16](Fukaki et al., 2002),[17](Fukaki et al., 2005),[18](Okushima et al., 2007),[19](Lee et al., 2019),[20](Okushima et al., 2005)[21](Vanneste et al., 2005),[21](Lee et al., 2017)[22](Fan et al., 2012),[23](Hofhuis et al., 2013)[24] (Lavenus et al., 2015),[25](Levesque et al., 2006),[26](Goh et al., 2016),[27](Cui et al., 2007),[28](Du and Scheres, 2017b),[29](Tian et al., 2014),[30](Shimotohno et al., 2018),[31](Singh et al., 2020),[32](Munguía-Rodríguez et al., 2020).

Even though many similarities between lateral root and nodule development exist, they represent distinct organs. Lateral roots and actinorhiza nodules share the most features, as actinorhiza nodules resembling lateral root by both having a central vasculature as well as an apical meristem (Huss-Danell, 1997). Determined and indetermined nodules differ from LRs as they possess a peripheral vasculature and in case of determined nodules lack a persistent meristem (Hirsch, 1992). This raises the question how nodule identity is distinguished from LRs on a genetic basis. In Medicago *MtNODULE ROOT1* (*NOOT1*) and *NOOT2* were described as essential factors for maintaining nodule identity (Magne et al., 2018). Double mutants of *noot1 noot2* showed only few functional nodules, instead a high percentage of the nodules showed a root-like conversion (Magne et al., 2018). More recently in Medicago the expression of *LIGHT SENSITIVE HYPOCOTYL1/2* (*LSH1/2*) was shown to be strongly induced during nodule formation (Lee et al., 2024). (Lee et al., 2024) could further show that overexpression of *LSH1* lead to a reduction in LR numbers, while *lsh1* knock out plants showed less functional, and more deformed nodules than wt, which was at least partially dependent on *NOOT1*. Further they could show that induction of *NOOT1/2* expression upon rhizobial inoculation is impaired in *lsh1/2* mutants (Lee et al., 2024). In both *noot1/2* and *lsh1/2* mutants the expression of *PLTs* among other factors associated with nodule and or lateral root primordia development was deregulated (Magne et al., 2018; Lee et al., 2024). This suggests that *LSH1/2* may act as positive regulators of nodule identity by promoting the expression of *NOOT1/2* and downstream factors like *PLTs* (**Figure 7B**).

Comparing the genetic bases of nodule organogenesis and root branching reveals commonalities consistent with the hypothesis that during RLS evolution, existing genetic pathways of conserved developmental processes were co-opted. This hypothesis is further backed by a recent study which utilizes a comparative phylotranscriptomic approach to identify a set of differentially expressed orthogroups (DEOGs) shared by 9 species of the FaFaCuRo, in response to RLS or actinorhiza (Libourel et al., 2023). These DEOGs are hypothesized to have evolved RNS-dependent expression patterns in the most recent common ancestor of all RNS species (Libourel et al., 2023). Notably, these DEOGs include several genes showing activity patterns depending on AM or LR formation including *SHR*, *LBDs*, *STYs*, *ARFs*, *YUCCAs*, *PLTs* and *WOX* all of which are involved in LR formation (Libourel et al., 2023).

The successful establishment of RNS requires 4 major steps: 1. symbiont recognition 2. intracellular symbiont accommodation 3. lateral organ formation 4. autoregulation of nodulation. Taken together, it appears that during evolution of RNS, plants adapted genes for symbiont recognition and intracellular infection from AM (Markmann et al., 2008; Libourel et al., 2023), and further co-opted genes involved in LR development to establish a new lateral organ, the nodule (Schiessl et al., 2019; Libourel et al., 2023).

Literature:

Aida, M., Beis, D., Heidstra, R., Willemsen, V., Blilou, I., Galinha, C., Nussaume, L., Noh, Y.S., Amasino, R., and Scheres, B. (2004). The *PLETHORA* genes mediate patterning of the Arabidopsis root stem cell niche. Cell **119,** 109-120.

Akamatsu, A., Nagae, M., and Takeda, N. (2022). The CYCLOPS response element in the *NIN* promoter is important but not essential for infection thread formation during *Lotus japonicus*–rhizobia symbiosis. Molecular Plant-Microbe Interactions **35,** 650-658.

Burkart, R.C., Strotmann, V.I., Kirschner, G.K., Akinci, A., Czempik, L., Dolata, A., Maizel, A., Weidtkamp-Peters, S., and Stahl, Y. (2022). PLETHORA-WOX5 interaction and subnuclear localization control *Arabidopsis* root stem cell maintenance. EMBO reports **23,** e54105.

Cathebras, C., Gong, X., Andrade, R.E., Vondenhoff, K., Keller, J., Delaux, P.-M., Hayashi, M., Griesmann, M., and Parniske, M. (2022). A novel *cis*-element enabled bacterial uptake by plant cells. pre-print bioRxiv, 2022.2003.2028.486070.

Cui, H., Levesque, M.P., Vernoux, T., Jung, J.W., Paquette, A.J., Gallagher, K.L., Wang, J.Y., Blilou, I., Scheres, B., and Benfey, P.N. (2007). An evolutionarily conserved mechanism delimiting SHR movement defines a single layer of endodermis in plants. Science **316,** 421-425.

De Smet, I. (2012). Lateral root initiation: one step at a time. New Phytologist **193,** 867-873.

De Smet, I., Tetsumura, T., De Rybel, B., Frey, N.F.d., Laplaze, L., Casimiro, I., Swarup, R., Naudts, M., Vanneste, S., Audenaert, D., Inzé, D., Bennett, M.J., and Beeckman, T. (2007). Auxin-dependent regulation of lateral root positioning in the basal meristem of Arabidopsis. Development **134,** 681-690.

Dong, W., Zhu, Y., Chang, H., Wang, C., Yang, J., Shi, J., Gao, J., Yang, W., Lan, L., Wang, Y., Zhang, X., Dai, H., Miao, Y., Xu, L., He, Z., Song, C., Wu, S., Wang, D., Yu, N., and Wang, E. (2020). An SHR-SCR module specifies legume cortical cell fate to enable nodulation. Nature.

Du, Y., and Scheres, B. (2017a). Lateral root formation and the multiple roles of auxin. J Exp Bot **69,** 155-167.

Du, Y., and Scheres, B. (2017b). PLETHORA transcription factors orchestrate de novo organ patterning during Arabidopsis lateral root outgrowth. Proc Natl Acad Sci U S A **114,** 11709-11714.

Eklund, D.M., Ståldal, V., Valsecchi, I., Cierlik, I., Eriksson, C., Hiratsu, K., Ohme-Takagi, M., Sundström, J.F., Thelander, M., Ezcurra, I., and Sundberg, E. (2010). The *Arabidopsis thaliana* STYLISH1 protein acts as a transcriptional activator regulating auxin biosynthesis The Plant Cell **22,** 349-363.

Fan, M., Xu, C., Xu, K., and Hu, Y. (2012). *LATERAL ORGAN BOUNDARIES DOMAIN* transcription factors direct callus formation in Arabidopsis regeneration. Cell Research **22,** 1169-1180.

Franssen, H.J., Kulikova, O., Willemsen, V., and Heidstra, R. (2017). Cis-regulatory *PLETHORA* promoter elements directing root and nodule expression are conserved between *Arabidopsis thaliana* and *Medicago truncatula*. Plant Signal Behav **12,** e1278102.

Franssen, H.J., Xiao, T.T., Kulikova, O., Wan, X., Bisseling, T., Scheres, B., and Heidstra, R. (2015). Root developmental programs shape the *Medicago truncatula* nodule meristem. Development **142,** 2941-2950.

Fukaki, H., Tameda, S., Masuda, H., and Tasaka, M. (2002). Lateral root formation is blocked by a gain-of-function mutation in the *SOLITARY-ROOT/IAA14* gene of Arabidopsis. The Plant Journal **29,** 153-168.

Fukaki, H., Nakao, Y., Okushima, Y., Theologis, A., and Tasaka, M. (2005). Tissue-specific expression of stabilized *SOLITARY-ROOT/IAA14* alters lateral root development in Arabidopsis. The Plant Journal **44,** 382-395.

Genre, A., and Russo, G. (2016). Does a common pathway transduce symbiotic signals in plant-microbe interactions? Frontiers in plant science **7,** 96.

Goh, T., Joi, S., Mimura, T., and Fukaki, H. (2012). The establishment of asymmetry in Arabidopsis lateral root founder cells is regulated by LBD16/ASL18 and related LBD/ASL proteins. Development **139,** 883-893.

Goh, T., Toyokura, K., Wells, D.M., Swarup, K., Yamamoto, M., Mimura, T., Weijers, D., Fukaki, H., Laplaze, L., Bennett, M.J., and Guyomarc'h, S. (2016). Quiescent center initiation in the Arabidopsis lateral root primordia is dependent on the SCARECROW transcription factor. Development **143,** 3363-3371.

Griesmann, M., Chang, Y., Liu, X., Song, Y., Haberer, G., Crook, M.B., Billault-Penneteau, B., Lauressergues, D., Keller, J., Imanishi, L., Roswanjaya, Y.P., Kohlen, W., Pujic, P., Battenberg, K., Alloisio, N., Liang, Y., Hilhorst, H., Salgado, M.G., Hocher, V., Gherbi, H., Svistoonoff, S., Doyle, J.J., He, S., Xu, Y., Xu, S., Qu, J., Gao, Q., Fang, X., Fu, Y., Normand, P., Berry, A.M., Wall, L.G., Ané, J.-M., Pawlowski, K., Xu, X., Yang, H., Spannagl, M., Mayer, K.F.X., Wong, G.K.-S., Parniske, M., Delaux, P.-M., and Cheng, S. (2018). Phylogenomics reveals multiple losses of nitrogen-fixing root nodule symbiosis. Science **361,** eaat1743.

Hayashi, T., Banba, M., Shimoda, Y., Kouchi, H., Hayashi, M., and Imaizumi-Anraku, H. (2010). A dominant function of *CCaMK* in intracellular accommodation of bacterial and fungal endosymbionts. The Plant Journal **63,** 141-154.

Helariutta, Y., Fukaki, H., Wysocka-Diller, J., Nakajima, K., Jung, J., Sena, G., Hauser, M.-T., and Benfey, P.N. (2000). The *SHORT-ROOT* gene controls radial patterning of the Arabidopsis root through radial signaling. Cell **101,** 555-567.

Hiratsu, K., Matsui, K., Koyama, T., and Ohme-Takagi, M. (2003). Dominant repression of target genes by chimeric repressors that include the EAR motif, a repression domain, in Arabidopsis. The Plant Journal **34,** 733-739.

Hirsch, A. (1992). Developmental biology of legume nodulation. New Phytologist **122,** 211-237.

Hofhuis, H., Laskowski, M., Du, Y., Prasad, K., Grigg, S., Pinon, V., and Scheres, B. (2013). Phyllotaxis and rhizotaxis in Arabidopsis are modified by three *PLETHORA* transcription factors. Current Biology **23,** 956-962.

Huss-Danell, K. (1997). Actinorhizal symbioses and their N_2 fixation. New Phytologist **136,** 375-405.

Kistner, C., and Parniske, M. (2002). Evolution of signal transduction in intracellular symbiosis. Trends in Plant Science **7,** 511-518.

Laskowski, M., and Ten Tusscher, K.H. (2017). Periodic lateral root priming: What makes it tick? The Plant Cell **29,** 432-444.

Lavenus, J., Goh, T., Roberts, I., Guyomarc'h, S., Lucas, M., De Smet, I., Fukaki, H., Beeckman, T., Bennett, M., and Laplaze, L. (2013). Lateral root development in Arabidopsis: fifty shades of auxin. Trends in Plant Science **18,** 450-458.

Lavenus, J., Goh, T., Guyomarc'h, S., Hill, K., Lucas, M., Voß, U., Kenobi, K., Wilson, M.H., Farcot, E., Hagen, G., Guilfoyle, T.J., Fukaki, H., Laplaze, L., and Bennett, M.J. (2015). Inference of the Arabidopsis lateral root gene regulatory network suggests a bifurcation mechanism that defines primordia flanking and central zones. The Plant Cell **27,** 1368-1388.

Lee, H.W., Kang, N.Y., Pandey, S.K., Cho, C., Lee, S.H., and Kim, J. (2017). Dimerization in LBD16 and LBD18 transcription factors is critical for lateral root formation. Plant Physiology **174,** 301-311.

Lee, H.W., Cho, C., Pandey, S.K., Park, Y., Kim, M.-J., and Kim, J. (2019). *LBD16* and *LBD18* acting downstream of *ARF7* and *ARF19* are involved in adventitious root formation in Arabidopsis. BMC Plant Biology **19,** 46.

Lee, T., Orvosova, M., Batzenschlager, M., Bueno Batista, M., Bailey, P.C., Mohd-Radzman, N.A., Gurzadyan, A., Stuer, N., Mysore, K.S., Wen, J., Ott, T., Oldroyd, G.E.D., and Schiessl, K. (2024). *Light-sensitive short hypocotyl* genes confer symbiotic nodule identity in the legume *Medicago truncatula*. Current Biology **34,** 825-840.e827.

Levesque, M.P., Vernoux, T., Busch, W., Cui, H., Wang, J.Y., Blilou, I., Hassan, H., Nakajima, K., Matsumoto, N., Lohmann, J.U., Scheres, B., and Benfey, P.N. (2006). Whole-genome analysis of the *SHORT-ROOT* developmental pathway in Arabidopsis. PLOS Biology **4,** e143.

Libourel, C., Keller, J., Brichet, L., Cazalé, A.-C., Carrère, S., Vernié, T., Couzigou, J.-M., Callot, C., Dufau, I., Cauet, S., Marande, W., Bulach, T., Suin, A., Masson-Boivin, C., Remigi, P., Delaux, P.-M., and Capela, D. (2023). Comparative phylotranscriptomics reveals ancestral and derived root nodule symbiosis programmes. Nature Plants.

Lin, J.-s., Li, X., Luo, Z., Mysore, K.S., Wen, J., and Xie, F. (2018). NIN interacts with NLPs to mediate nitrate inhibition of nodulation in *Medicago truncatula*. Nature Plants **4,** 942-952.

Lin, J., Frank, M., and Reid, D. (2020). No home without hormones: How plant hormones control legume nodule organogenesis. Plant Communications **1,** 100104.

Liu, H., Lin, J.S., Luo, Z., Sun, J., Huang, X., Yang, Y., Xu, J., Wang, Y.F., Zhang, P., Oldroyd, G.E.D., and Xie, F. (2022). Constitutive activation of a nuclear-localized calcium channel complex in *Medicago truncatula*. Proceedings of the National Academy of Sciences **119,** e2205920119.

Liu, J., Rutten, L., Limpens, E., van der Molen, T., van Velzen, R., Chen, R., Chen, Y., Geurts, R., Kohlen, W., Kulikova, O., and Bisseling, T. (2019). A remote cis-regulatory region is required for *NIN* expression in the pericycle to initiate nodule primordium formation in *Medicago truncatula*. The Plant Cell **31,** 68-83.

Liu, W., Yu, J., Ge, Y., Qin, P., and Xu, L. (2018). Pivotal role of LBD16 in root and root-like organ initiation. Cellular and molecular life sciences **75,** 3329-3338.

Magne, K., Couzigou, J.M., Schiessl, K., Liu, S., George, J., Zhukov, V., Sahl, L., Boyer, F., Iantcheva, A., Mysore, K.S., Wen, J., Citerne, S., Oldroyd, G.E.D., and Ratet, P. (2018). *MtNODULE ROOT1* and *MtNODULE ROOT2* are essential for indeterminate nodule identity. Plant Physiology **178,** 295-316.

Malamy, J.E., and Benfey, P.N. (1997). Organization and cell differentiation in lateral roots of *Arabidopsis thaliana*. Development **124,** 33-44.

Markmann, K., and Parniske, M. (2009). Evolution of root endosymbiosis with bacteria: how novel are nodules? Trends in Plant Science **14,** 77-86.

Markmann, K., Giczey, G., and Parniske, M. (2008). Functional adaptation of a plant receptor-kinase paved the way for the evolution of intracellular root symbioses with bacteria. PLoS biology **6,** e68.

Miri, M., Janakirama, P., Huebert, T., Ross, L., McDowell, T., Orosz, K., Markmann, K., and Szczyglowski, K. (2019). Inside out: root cortex-localized *LHK1* cytokinin receptor limits epidermal infection of *Lotus japonicus* roots by *Mesorhizobium loti*. New Phytologist **0**.

Munguía-Rodríguez, A.G., López-Bucio, J.S., Ruiz-Herrera, L.F., Ortiz-Castro, R., Guevara-García Á, A., Marsch-Martínez, N., Carreón-Abud, Y., López-Bucio, J., and Martínez-Trujillo, M. (2020). *YUCCA4* overexpression modulates auxin biosynthesis and transport and influences plant growth and development via crosstalk with abscisic acid in *Arabidopsis thaliana*. Genetics and molecular biology **43,** e20190221.

Nakajima, K., Sena, G., Nawy, T., and Benfey, P.N. (2001). Intercellular movement of the putative transcription factor *SHR* in root patterning. Nature **413,** 307-311.

Okushima, Y., Fukaki, H., Onoda, M., Theologis, A., and Tasaka, M. (2007). ARF7 and ARF19 regulate lateral root formation via direct activation of *LBD/ASL* genes in Arabidopsis. The Plant Cell **19,** 118-130.

Okushima, Y., Overvoorde, P.J., Arima, K., Alonso, J.M., Chan, A., Chang, C., Ecker, J.R., Hughes, B., Lui, A., Nguyen, D., Onodera, C., Quach, H., Smith, A., Yu, G., and Theologis, A. (2005). Functional genomic analysis of the *AUXIN RESPONSE FACTOR* gene family members in *Arabidopsis thaliana*: Unique and overlapping functions of *ARF7* and *ARF19* The Plant Cell **17,** 444-463.

Osipova, M.A., Mortier, V., Demchenko, K.N., Tsyganov, V.E., Tikhonovich, I.A., Lutova, L.A., Dolgikh, E.A., and Goormachtig, S. (2012). *Wuschel-related homeobox5* gene expression and interaction of CLE peptides with components of the systemic control add two pieces to the puzzle of Autoregulation of Nodulation. Plant physiology **158,** 1329-1341.

Schauser, L., Roussis, A., Stiller, J., and Stougaard, J. (1999). A plant regulator controlling development of symbiotic root nodules. Nature **402,** 191-195.

Schiessl, K., Lilley, J.L.S., Lee, T., Tamvakis, I., Kohlen, W., Bailey, P.C., Thomas, A., Luptak, J., Ramakrishnan, K., Carpenter, M.D., Mysore, K.S., Wen, J., Ahnert, S., Grieneisen, V.A., and Oldroyd, G.E.D. (2019). *NODULE INCEPTION* recruits the lateral root developmental program for symbiotic nodule organogenesis in *Medicago truncatula*. Current Biology **29,** 3657-3668.e3655.

Sexauer, M., and Markmann, K. (2024). To the roots of nodules: Nodule organogenesis utilizes lateral root development processes. . Manuscript in preparation.

Shimotohno, A., Heidstra, R., Blilou, I., and Scheres, B. (2018). Root stem cell niche organizer specification by molecular convergence of *PLETHORA* and *SCARECROW* transcription factor modules. Genes & development **32,** 1085-1100.

Shrestha, A., Zhong, S., Therrien, J., Huebert, T., Sato, S., Mun, T., Andersen, S.U., Stougaard, J., Lepage, A., Niebel, A., Ross, L., and Szczyglowski, K. (2021). *Lotus japonicus Nuclear Factor YA1*, a nodule emergence stage-specific regulator of auxin signalling. New Phytologist **229,** 1535-1552.

Singh, S., Katzer, K., Lambert, J., Cerri, M., and Parniske, M. (2014). CYCLOPS, a DNA-binding transcriptional activator, orchestrates symbiotic root nodule development. Cell Host & Microbe **15,** 139-152.

Singh, S., Yadav, S., Singh, A., Mahima, M., Singh, A., Gautam, V., and Sarkar, A.K. (2020). Auxin signaling modulates *LATERAL ROOT PRIMORDIUM1* (*LRP1*) expression during lateral root development in Arabidopsis. The Plant Journal **101,** 87-100.

Sohlberg, J.J., Myrenås, M., Kuusk, S., Lagercrantz, U., Kowalczyk, M., Sandberg, G., and Sundberg, E. (2006). *STY1* regulates auxin homeostasis and affects apical–basal patterning of the Arabidopsis gynoecium. The Plant Journal **47,** 112-123.

Soltis, D.E., Soltis, P.S., Morgan, D.R., Swensen, S.M., Mullin, B.C., Dowd, J.M., and Martin, P.G. (1995). Chloroplast gene sequence data suggest a single origin of the predisposition for symbiotic nitrogen fixation in angiosperms. Proc Natl Acad Sci U S A **92,** 2647-2651.

Soyano, T., Shimoda, Y., Kawaguchi, M., and Hayashi, M. (2019). A shared gene drives lateral root development and root nodule symbiosis pathways in *Lotus*. Science **366,** 1021-1023.

Ståldal, V., Cierlik, I., Chen, S., Landberg, K., Baylis, T., Myrenås, M., Sundström, J.F., Eklund, D.M., Ljung, K., and Sundberg, E. (2012). The *Arabidopsis thaliana* transcriptional activator *STYLISH1* regulates genes affecting stamen development, cell expansion and timing of flowering. Plant Molecular Biology **78,** 545-559.

Suzuki, W., Konishi, M., and Yanagisawa, S. (2013). The evolutionary events necessary for the emergence of symbiotic nitrogen fixation in legumes may involve a loss of nitrate responsiveness of the *NIN* transcription factor. Plant Signal Behav **8**.

Tian, H., Jia, Y., Niu, T., Yu, Q., and Ding, Z. (2014). The key players of the primary root growth and development also function in lateral roots in Arabidopsis. Plant Cell Reports **33,** 745-753.

Vanneste, S., De Rybel, B., Beemster, G.T.S., Ljung, K., De Smet, I., Van Isterdael, G., Naudts, M., Iida, R., Gruissem, W., Tasaka, M., Inzé, D., Fukaki, H., and Beeckman, T. (2005). Cell cycle progression in the pericycle is not sufficient for *SOLITARY ROOT/IAA14*-mediated lateral root initiation in *Arabidopsis thaliana*. The Plant Cell **17,** 3035-3050.

Xiao, T.T., Schilderink, S., Moling, S., Deinum, E.E., Kondorosi, E., Franssen, H., Kulikova, O., Niebel, A., and Bisseling, T. (2014). Fate map of *Medicago truncatula* root nodules. Development **141,** 3517-3528.

Yano, K., Yoshida, S., Müller, J., Singh, S., Banba, M., Vickers, K., Markmann, K., White, C., Schuller, B., Sato, S., Asamizu, E., Tabata, S., Murooka, Y., Perry, J., Wang, T.L., Kawaguchi, M., Imaizumi-Anraku, H., Hayashi, M., and Parniske, M. (2008). *CYCLOPS*, a mediator of symbiotic intracellular accommodation. Proc Natl Acad Sci U S A **105,** 20540-20545.

Yoro, E., Suzaki, T., Toyokura, K., Miyazawa, H., Fukaki, H., and Kawaguchi, M. (2014). A positive regulator of nodule organogenesis, *NODULE INCEPTION*, acts as a negative regulator of rhizobial infection in *Lotus japonicus*. Plant physiology **165,** 747-758.